UNIVERSITÀ DI PARMA

UNIVERSITA' DEGLI STUDI DI PARMA

Corso di dottorato di Ricerca in

"BIOLOGIA EVOLUZIONISTICA ED ECOLOGIA"

CICLO XXXVI

Climate change impacts on nutrient load generation, nitrogen cycling, and self-purification capacity of a large temperate river, the Po (Italy)

Coordinatore

Prof. Pierluigi Viaroli

Candidata

Dott.ssa Maria Pia Gervasio

Tutori:

Prof. Giuseppe Castaldelli

Dott.ssa Elisa Soana

Anni Accademici 2020/2021 – 2022/2023

Il dottorato in Biologia Evoluzionistica ed Ecologia – Ciclo XXXVI è in convenzione tra le Università di Ferrara, Firenze e Parma (sede amministrativa)

Contents

Italian extended abstract 5

Abstract 9

List of publications 11

List of figures 15

Chapter 1: Introduction 17

1.1. Nitrogen cycling in river sediments 18

1.2. Climate Change in the Po River basin and its delta 20

Chapter 2: Materials and methods 22

2.1. Annual and seasonal historical data of temperature, discharge, and riverine nutrient loads…. 22

2.2. Measurements of N processing in river sediments 22

2.2.1. Seasonal effect of water warming on denitrification and DNRA processes 23

2.2.2. Impact of saline intrusion on denitrification and DNRA processes in summer 23

Chapter 3: Main results and discussion 24

Chapter 4: General conclusions 36

References 38

Appendix I: Two published articles on the effect of temperature rise on the Po River nutrients loads in the last thirty years

Appendix II: One submitted article entitled: "*Contrasting effects of climate change on denitrification and nitrogen load reduction in the Po River (Northern Italy)*"

Appendix III: Two published articles on the impact of saline intrusion in the Po Delta on nitrogen metabolism and N loads dissipation

Italian extended abstract

Il bacino del Po è una delle aree più produttive e densamente popolate d'Europa, indicato come hotspot di inquinamento da nitrati. Gli elevati carichi di nutrienti, azoto nitrico in particolare, condizionano lo stato trofico degli ambienti di transizione e delle acque costiere dal Delta all'intera costa emiliano-romagnola.

La disponibilità di studi pregressi, riguardanti i carichi dei nutrienti e di serie storiche di misure di portata costituiscono un'importante base di informazioni che può essere utilizzata per indagare l'impatto dei cambiamenti climatici sui processi di generazione, trasformazione e recapito verso le zone costiere.

Ad oggi gli effetti dei cambiamenti climatici nel bacino del fiume Po sono già evidenti. L'aumento della frequenza delle anomalie climatiche, le alterazioni dell'intensità e della distribuzione temporale delle precipitazioni, da cui dipendono le variazioni repentine dei deflussi registrate negli ultimi anni, l'aumento della temperatura dell'aria e della frequenza e severità dei periodi di siccità e stress idrico, l'espansione spaziale e temporale del cuneo salino nell'area deltizia sono solo alcuni dei fenomeni emersi negli ultimi anni. D'altro canto, i possibili effetti di questi fenomeni, determinati dal cambiamento climatico, sulla trasformazione e sull'export dei carichi azotati nel Mar Adriatico non sono stati ancora indagati.

La tesi qui discussa presenta due obiettivi principali. Il primo è stato la valutazione dell'incremento di temperatura del fiume Po e del suo effetto sulla rimozione dei carichi di azoto, attraverso la denitrificazione. A questo scopo, l'area di studio interessata è stata la chiusura di bacino, Pontelagoscuro (Ferrara), dove sono state analizzate le serie storiche di temperatura e carichi di azoto e sono state effettuate misure stagionali del metabolismo sedimentario, dei tassi di denitrificazione e di DNRA (Dissimilatory Nitrate Reduction to Ammonium). Il secondo obiettivo è stato quello di valutare l'effetto del cambiamento climatico sull'intrusione salina nel Delta del Po. Tramite misure di campo e di laboratorio sono stati studiati, anche in questo caso, il metabolismo sedimentario, la denitrificazione e la DNRA, ma incubando i sedimenti campionati lungo il gradiente salino registrato in un ramo del delta, il Po di Goro.

I risultati hanno evidenziato il graduale aumento delle temperature del Po da inizio anni '90 (circa 0.11 °C anno^{-1}) e un parallelo aumento della frequenza dei giorni caldi, soprattutto in estate e in primavera (+50%), cioè del numero di giorni con temperatura dell'acqua superiore alla media di lungo periodo. Negli stessi anni è stata evidenziata una riduzione dei carichi annuali di azoto, costituiti in prevalenza da nitrato (NO_3^-), alla sezione di chiusura bacino. Si è osservato che la riduzione dei carichi azotati è avvenuta in corrispondenza dell'aumento della temperatura media di quasi 3 °C, soprattutto in primavera ed estate che sono indicate anche come i periodi più sensibili alle crisi distrofiche nel Mar Adriatico. Ad un aumento di 1°C di temperatura del fiume Po è corrisposta una riduzione dei carichi azotati di circa il 7% in primavera e di circa il 4% in estate.

La relazione inversa tra temperatura e carichi di azoto è la risultante di un effetto temperatura dipendente dell'attività dei batteri denitrificanti a livello sedimentario. Ciò è stato evidenziato tramite prove sperimentali effettuate in laboratorio su sedimenti fluviali campionati stagionalmente alla sezione di Pontelagoscuro nel corso dell'anno 2022, identificato come uno dei più siccitosi dagli anni '60, in cui la portata del fiume è andata al di sotto dei minimi storici (< 150 m^3 s^{-1}). Attraverso l'incubazione di carote di sedimento sono stati misurati i flussi di ossigeno, i tassi di denitrificazione e di DNRA. In ogni stagione sono stati applicati diversi gradienti di temperatura basati sui dati storici e sulle previsioni future relative al riscaldamento del Bacino del Po. I risultati hanno confermato che entrambi i processi sono temperatura dipendenti, secondo una correlazione positiva in ogni stagione. In particolare, durante la primavera sono stati misurati i tassi più alti (591 ± 29 µmol N m^{-2} h^{-1} per il processo di denitrificazione e 53 ± 24 µmol N m^{-2} h^{-1} per la DNRA a 22 °C), in quanto la disponibilità di NO_3^- era ai massimi annuali. Dai risultati si è evidenziato come la denitrificazione sia il principale processo responsabile della rimozione di NO_3^- in ogni stagione, con tassi mediamente superiori di un ordine di grandezza rispetto ai tassi della DNRA.

Per ottenere un riscontro sulla rappresentatività dei tassi misurati in termini di macro-scala, i tassi di denitrificazione ottenuti nella stagione primaverile sono stati estesi ad un tratto del medio-basso corso (per una superficie complessiva di 45 km^2 compresa tra Borgoforte, provincia di Mantova, e Pontelagoscuro), in cui le incubazioni effettuate a Pontelagoscuro possono essere considerate rappresentative per le caratteristiche simili dei sedimenti

campionati. L'up-scale dei tassi all'intera area ha fornito un valore coerente con la riduzione dei carichi calcolata tra le due sezioni, in base ai dati di portata, monitorati dall'Autorità di Bacino del Po, e di concentrazione, misurati dalle Agenzia Regionale per la Protezione Ambientale (ARPA). Questo ha confermato che la riduzione dei carichi di nitrato verificata negli ultimi decenni è imputabile soprattutto al processo di denitrificazione sedimentaria.

Un ulteriore conseguenza del cambiamento climatico, verificatasi nel delta a seguito delle eccezionali condizioni di scarsità idrica e ridotte portate del 2022, è stata l'incremento della estensione del cuneo salino a partire dalla tarda primavera. Per valutare gli effetti di questo fenomeno sul ciclo dell'azoto e sulla capacità del Delta del Po di abbattere una quota dei carichi in transito, carote intatte di sedimento sono state prelevante in estate, in tre siti nel ramo del Po di Goro disposti lungo un gradiente di salinità, e incubate in laboratorio per misurare i tassi di denitrificazione e DNRA. La denitrificazione è risultata essere il principale processo responsabile della rimozione del nitrato nei siti d'acqua dolce e leggermente salini (368 ± 45 µmol N m^{-2} h^{-1} e 274 ± 19 µmol N m^{-2} h^{-1}, rispettivamente), con tassi di un ordine di grandezza superiore a quelli di DNRA (55 ± 9 and 27 ± 8 µmol N m^{-2} h^{-1}, rispettivamente). Al contrario, la DNRA ha mostrato i tassi più alti nel sito più salino (116 ± 29 µmol N m^{-2} h−1), in accordo con quanto riportato in letteratura, secondo cui le condizioni saline favoriscono la DNRA rispetto alla denitrificazione. I risultati ottenuti mostrano come l'incremento della salinità negli ambienti di transizione, in conseguenza al cambiamento climatico, sia un fattore chiave nella regolazione del metabolismo bentonico dell'azoto. In uno scenario di cambiamento climatico, una sempre maggiore intrusione salina potrebbe decrementare la capacità di rimozione di azoto tramite denitrificazione nelle zone di transizione e aumentarne il ricircolo tramite DNRA, incrementando l'eutrofizzazione costiera.

Complessivamente i risultati di questa tesi hanno evidenziato come due conseguenze del cambiamento climatico, il riscaldamento delle acque del Po e l'aumento dell'intrusione salina nel suo Delta, influenzino in modo inverso la capacità dissipativa dei carichi di nitrati lungo il continuum acque interne-acque costiere.

Come emerso dalla sperimentazione, ulteriori sviluppi di questa ricerca dovrebbero mirare ad indagare altri aspetti sinora non studiati, come l'effetto del cambiamento climatico sulle

tempistiche di recapito dei nutrienti alle sezioni fluviali terminali ed il ruolo delle variazioni stagionali della quantità e qualità della sostanza organica sedimentaria.

Abstract

The Po River basin is one of the most productive and densely populated areas in Europe and a hot-spot for nitrate pollution. In recent years, the effects of climate change (CC) have been observed in the Po River basin, e.g. the increase in the frequency of climatic anomalies, the intensity and temporal distribution of rainfall and, consequently, variations in runoff, the increase in air temperature and in the frequency of prolonged drought periods, leading to the increase in saline intrusion in the Po River Delta. However, these impacts on transport and export of nitrogen loads in the Adriatic Sea are unexplored. The aims of this thesis were to assess: (i) the increase in the Po River water temperature and its effect on the removal of nitrogen loads via denitrification; (ii) the effect of saline intrusion on the dissimulative capacity of nitrogen loads in the Po River Delta.

The study area was Pontelagoscuro (Ferrara province), the closing section of the Po River basin, where the time series of temperature and nitrogen loads were analyzed and seasonal measurements of sediment metabolism, denitrification and dissimilatory nitrate reduction to ammonium (DNRA) were carried out. At the same time, the extension of the saline wedge was monitored during the summer in the Po di Goro, one branch of the Po River Delta, where measurements of sediment metabolism, denitrification and DNRA rates were applied. Laboratory incubations of intact cores were carried out in both cases, but different temperature gradients were applied to the sediments of the Po River, based on the historical data and future predictions of warming, while the sediments of the Po di Goro River were sampled along a salinity gradient.

The results showed a gradual increase of the Po River temperature from the '90s and of the frequency of warm days, in particular during summers and springs. At the same time, there was a decrease in the total nitrogen loads, mainly nitrate (NO_3^-), transported to the basin closing section. Over the last three decades, nitrogen loads have declined by a third, while average water temperature have increased by 3°C. The 1°C increase in temperature was associated with a reduction in nitrogen loads around 7% and 4% in spring and summer, respectively. The inverse relationship between temperature and nitrogen loads is the result of the effect of temperature on denitrification activity in the sediment. The evidence was tested and confirmed by laboratory experiments on river sediments sampled seasonally at the

Pontelagoascuro section during 2022, the driest year since 1960s. The results showed that denitrification and DNRA process are temperature dependent. In particular, the rates increased along the temperature gradients in each season, with denitrification being higher than DNRA by an order of magnitude. The up-scale of denitrification rates along a section from Borgoforte (Mantua province) to Pontelagoscuro, for an overall surface of 45 km^2, showed that the measured values corresponded to the calculated load reduction between the two sections. The obtained results confirmed that the reduction in nitrate loads, monitored in the last decades in the Po River basin, was mainly attributable to the denitrification process in river sediments.

The saline wedge in the Po River Delta increased its extension during the droughts of the 2022, due to the low flow of the Po River, starting in the late spring. The sediment incubations showed that denitrification was the main process to NO_3^- removal at the freshwater and slightly saline sites, while DNRA had the highest rates in the saline site, highlighting that the saline intrusion in transitional areas, due to the climate change, is a key factor in regulating benthic N metabolism. In a CC scenario, the saline intrusion may reduce the N removal capacity of the transitional areas, inhibiting denitrification and increasing N recycling via DNRA.

In conclusion, the results highlighted that two of the most important impacts of CC in rivers, i.e. the warming and the increase of the saline wedge, may have an inverse effect on the dissimilative capacity towards NO_3^- loads along the continuum from the freshwater to the coastal zones. However, further research should address other aspects that are not investigated, such as the effect of CC on the nutrient availability and the role of organic matter content in river sediments, in terms of seasonal quantity and quality.

List of publications

This thesis is based on the following publications, that at the time of the thesis submission, 4 papers were published and one is under review (submitted in January 2024):

[1] Soana, E., **Gervasio, M. P.**, Granata, T., Colombo, D., & Castaldelli, G. (2024). Climate change impacts on eutrophication in the Po River (Italy): Temperature-mediated reduction in nitrogen export but no effect on phosphorus. *Journal of Environmental Sciences,* 143, 148–163. https://doi.org/10.1016/j.jes.2023.07.008

Contributions: conceptualization, methodology, data curation, writing-original draft was provided by Dr. Elisa Soana; investigation, formal analysis and writing-original draft by **Maria Pia Gervasio**; conceptualization, writing-review and editing, supervision were undertaken by Professor Giuseppe Castaldelli.

[2] **Gervasio, M. P.**, Soana, E., Granata, T., Colombo, D., & Castaldelli, G. (2022). An unexpected negative feedback between climate change and eutrophication: higher temperatures increase denitrification and buffer nitrogen loads in the Po River (Northern Italy). *Environmental Research Letters*, 17(8), 084031. 10.1088/1748-9326/ac8497

Contributions: investigation, formal analysis, writing−original draft preparation, visualization were undertaken by **Maria Pia Gervasio**; conceptualization, methodology, writing-review and editing by Dr. Elisa Soana; review and final editing, supervision were provided by Professor Giuseppe Castaldelli.

[3] **Gervasio, M. P.***, Soana, E., Gavioli, A., Vincenzi, F., & Castaldelli, G. (under review). Contrasting effects of climate change on denitrification and nitrogen load reduction in the Po River (Northern Italy). Submitted to *Science of The Total Environment* (STOTEN-D-24-03466).

Contributions: investigation, formal analysis, writing original draft preparation by **Maria Pia Gervasio**; methodology, conceptualization, writing review and editing, supervisor were provided by Dr. Elisa Soana; formal analysis were provided by Dr. Anna Gavioli; investigation by Fabio Vincenzi; conceptualization, writing review and editing, funding acquisition, supervision by Professor Giuseppe Castaldelli.

[4] Gervasio, M. P., Soana, E., Vincenzi, F., & Castaldelli, G. (2022). An Underestimated Contribution of Deltaic Denitrification in Reducing Nitrate Export to the Coastal Zone (Po River–Adriatic Sea, Northern Italy). *Water*, 14(3), 501. https://doi.org/10.3390/w14030501

Contributions: conceptualization, writing-original draft, formal analysis were undertaken by **Maria Pia Gervasio**; writing-original draft and editing, conceptualization, methodology by Dr. Elisa Soana; resources by Fabio Vincenzi; conceptualization, methodology and supervision were provided by Professor Giuseppe Castaldelli.

[5] Gervasio, M. P., Soana, E., Vincenzi, F., Magri, M., & Castaldelli, G. (2023). Drought-Induced Salinity Intrusion Affects Nitrogen Removal in a Deltaic Ecosystem (Po River Delta, Northern Italy). *Water*, 15(13), 2405. https://doi.org/10.3390/w15132405

Contributions: conceptualization, writing-original draft, and formal analysis were undertaken by **Maria Pia Gervasio**; writing-original draft and editing, conceptualization, methodology by Dr. Elisa Soana; resources by Fabio Vincenzi; conceptualization, methodology and supervision were provided by Professor Giuseppe Castaldelli.

*corresponding author

Other papers not included in the main thesis project:

[1] Gavioli, A., Soana, E., Trasforini, S., Puzzi, C., **Gervasio, M.P.**, Granata, T., Colombo, D., Castaldelli, G (under review). Effects of global warming on the decline of native and increase of non-native fish species in the Po River (Northern Italy). Submitted to Climatic Change (CLIM-D-23-00707).

Contributions: investigation and data curation by **Maria Pia Gervasio**; conceptualization, writing-original draft, methodology and formal analysis were undertaken by Dr. Anna Gavioli; conceptualization, writing review and editing, supervisor were provided by Dr. Elisa Soana; writing review and editing, supervision by Professor Giuseppe Castaldelli.

[2] Mastrocicco, M., **Gervasio, M. P.**, Busico, G., & Colombani, N. (2021). Natural and anthropogenic factors driving groundwater resources salinization for agriculture use in the Campania plains (Southern Italy). *Science of the Total Environment*, 758, 144033. https://doi.org/10.1016/j.scitotenv.2020.144033

Contributions: conceptualization, methodology, data curation, writing - original draft and editing, supervision were undertaken by Professor Micòl Mastrocicco; validation, formal analysis, visualisation by **Maria Pia Gervasio**; methodology, software, validation, formal analysis, visualization were provided by Dr. Gianluigi Busico; methodology, software, formal analysis, data curation, writing - review and editing by Dr. Nicolò Colombani.

[3] Alessandrino, L., **Gervasio, M. P.**, Vincenzi, F., Colombani, N., Castaldelli, G., & Mastrocicco, M. (2021). Nutrients and carbon fate in two lowland contrasting soils amended with compost. *Catena*, 206, 105493. https://doi.org/10.1016/j.catena.2021.105493

Contributions: conceptualization, data curation, writing - original draft and editing, formal analysis, visualisation by Dr. Luigi Alessandrino; writing - original draft and editing, data

curation, formal analysis, visualisation were undertaken by **Maria Pia Gervasio**; conceptualization, methodology, writing review and editing, supervisor were provided by Dr. Nicolò Colombani; conceptualization, writing review and editing, supervisor by Professor Micòl Mastrocicco.

[4] Colombani, N., Fronzi, D., Palpacelli, S., Gaiolini, M., **Gervasio, M. P.**, Marcellini, M., Mastrocicco, M., & Tazioli, A. (2021). Modelling Shallow Groundwater Evaporation Rates from a Large Tank Experiment. *Water Resources Management*, 35, 3339-3354.https://doi.org/10.1007/s11269-021-02896-2

Contributions: model conceptualization, methodology, data curation, writing – original draft were undertaken by Dr. Nicolò Colombani; validation, data curation by Dr. Davide Fronzi and Dr. Stefano Palpacelli; visualization, software, formal analysis by Mattia Gaiolini; formal analysis by **Maria Pia Gervasio**; data curation by Mirco Marcellini; writing – review and editing, methodology were undertaken by Professor Micòl Mastrocicco; supervision and methodology by Professor Alberto Tazioli.

List of figures

Figure 1: Predicted changes in maximum daily temperature (°C) and maximum daily precipitation (%) at the 4 levels of global warming (+1.5, +2, +3, +4 °C) compared to the period 1850-1900 (modified from IPCC report, 2023).

Figure 2: Nitrogen cycle diagram with the main N transformations: nitrification (nitr), denitrification (den), anammox (anam) and dissimilatory nitrate reduction to ammonium (DNRA), that occur in water column, river sediments and the water-sediment interface.

Figure 3: Temporal trend of annual average of water temperature (°C) of the Po River since 1992. Black lines show statistically significant trends.

Figure 4: Temporal trend of seasonal minimum, average and maximum water temperature (°C) of the Po River since 1992. Black lines show statistically significant trends.

Figure 5: Daily water temperature of the Po River at the closing section of basin in the last 30 years.

Figure 6: Average daily discharge ($m^3 s^{-1}$) of the Po River in 2022 compared to the average daily discharge of the drought year 2006 and to the minimum and average monthly discharge over the last 30 years.

Figure 7: Temporal trend in flow-normalised NO_3^- loads measured at the closing section of the Po River basin on an annual basis (on the left; t N yr^{-1}) and during winter, spring, summer and autumn (on the right; t N $seasonal^{-1}$) since 1992. Dashed lines show statistically significant trends.

Figure 8: Correlation between flow-normalised NO_3^- (t N $month^{-1}$) and average water temperature (°C) measured at the closing section of the Po River basin in spring (on the left) and in the summer (on the right). Black lines show statistically significant trends.

Figure 9: Total denitrification rates (µmol N $m^{-2} h^{-1}$) splitted into Dw and Dn measured along the temperature gradients in the four seasons (note the different scale of the y-axis) in the Po River. Average values ± standard deviations are reported.

Figure 10: Total dissimilatory nitrate reduction to ammonium (DNRA) rates (µmol N $m^{-2} h^{-1}$) splitted into DNRAw e DNRAn, measured along the temperature gradients in the four seasons

(note the different scale of the y-axis) in the Po River. Average values ± standard deviations are reported.

Figure 11: Denitrification and DNRA rates measured along the salinity gradient in the Po di Goro River. The rates are splitted in Dw and DNRAw, and Dn and DNRAn, indicated the rates supported by NO_3^- from the water column and the rates coupled to nitrification, respectively. Average values ± standard deviations are reported.

Chapter 1: Introduction

Climate Change (CC) is defined by NASA as a wide range of phenomena caused mainly by the combustion of fossil fuels, which release gases such as carbon dioxide (CO_2) and nitrous oxide (N_2O) into the atmosphere. Over time, major impacts have been identified. These include effects on the hydrological cycle in terms of rainfall and the flow of river systems, global warming with the raise of air and surface water temperatures and the increase in frequency of extreme events, such as droughts and heatwaves, the raise of sea levels as the saline intrusion into coastal areas. According to the IPCC report (2022; 2023), CC has been identified as one of the major challenges of the 21st century. It is expected to reduce precipitation by 20%, increase droughts and lead to a more frequent alternation between warmer days and extreme rainfall, as has already occurred in the Mediterranean over the last decade (Fig.1; Gao & Giorgi, 2008; Carvalho et al., 2022).

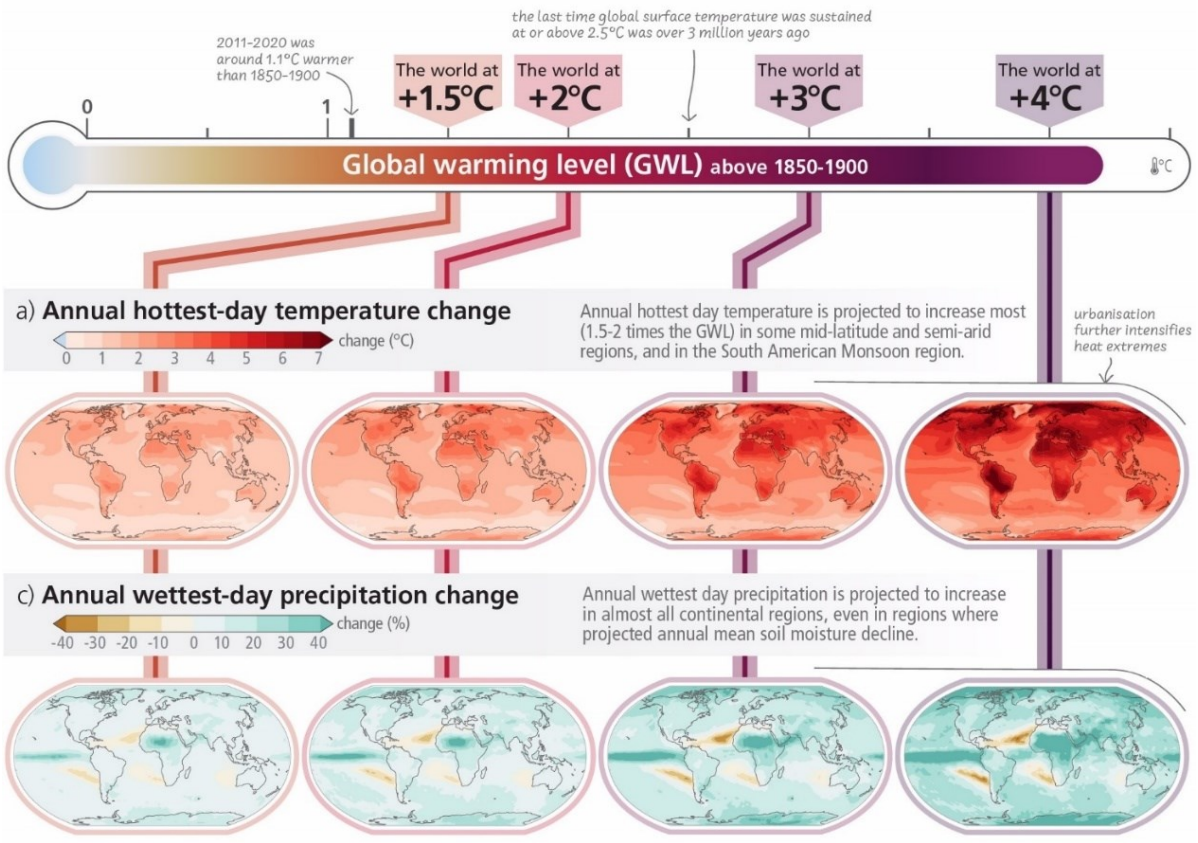

Figure 1: Predicted changes in maximum daily temperature (°C) and maximum daily precipitation (%) at the 4 levels of global warming (+1.5, +2, +3, +4 °C) compared to the period 1850-1900 (modified from IPCC report, 2023).

CC have many negative implications in aquatic ecosystems. The warmer climate can result in greater evapo-transpiration at the scale of the entire basin which turns out in a lower water surface and ground water availability and thus in a decrease in water quality due to the loss of dilution capacity of freshwater (Luo et al., 2023). The reduced dilution capacity may also lead to an increase of biological oxygen demand, and as a consequence to lower dissolved oxygen (O_2) concentrations in the water column with a cascade of effects on river biological community (Whitehead et al., 2009). Moreover, the increase of extreme events may enhance erosive events and so the transport and the deposit of fine sediments in rivers (Glavan et al., 2015) with several potential effects on biotic components and metabolism (Kemp et al., 2011). In particular, river sediments are active sites for biogeochemical reactions (Triska & Higler, 2009), both aerobic and anaerobic, which may be influenced by the CC driven increase in water temperature.

1.1. Nitrogen cycling in river sediments

The water-sediment interface in large rivers is characterised by O_2 penetration by molecular diffusion to a depth of only a few millimetres. Dissolved O_2 diffusion is driven by temperature, whose increase reduces O_2 solubility in the water column, further increasing O_2 consumption and sediment deoxygenation state, i.e. the vertical extension of the anoxic zone in surface sediments (de Klein et al., 2017). Consequently, the increase in water temperature and the extension of the anoxic layer in river sediments favours the activity of anaerobic bacteria in the lower layer of sediments (Rajesh & Rehana, 2022; Veraart et al., 2011). However, in the uppermost oxic sediments layer nitrification may occur, with the oxidation of ammonium (NH_4^+) to nitrite (NO_2^-) and to final nitrate (NO_3^-). Produced NO_3^- may diffuse back to the water column or deeper into the anoxic subsurface sediments, where anaerobic N transformations occur, such as denitrification, dissimilatory nitrate reduction to ammonium (DNRA) and anammox (Thamdrup & Dalsgaard, 2008; Reddy et al., 1984) (Fig.2).

Denitrification is considered to be the most important process for the permanent removal of reactive N in aquatic ecosystems, particularly in rivers and transitional ecosystems, because of their role in processing anthropogenic N inputs (Tiedje, 1983; Burgin & Hamilton, 2007; Pina-Ochoa & Àlvarez-Cobelas, 2006). It is the stepwise reduction of NO_3^- to di-nitrogen gas (N_2) as

final product, and NO_2^- and N_2O as intermediate products, with concomitant oxidation of organic carbon. Denitrification is distinguished in two terms, Dw and Dn, according to the source of NO_3^- substrate, from the water column or from the sediment nitrification, respectively (Seitzinger et al., 1988). DNRA, namely the dissimilatory NO_3^- reduction to ammonium, is another bacterial dissimilatory process using the same substrates of denitrification (NO_3^- and organic carbon), and could be an alternative pathway of NO_3^- reduction. Unlike denitrification, DNRA converts NO_3^- to NH_4^+, recycling N and making it available to primary producers rather than removing it from the aquatic ecosystem (Scott et al., 2008). Both denitrification and DNRA are favoured by the availability of NO_3^- in the water column and labile organic matter in the sediments.

In riverine anoxic sediments, another anaerobic process of the nitrogen cycle may occur, anammox, literally anaerobic NH_4^+ oxidation. It consists in the oxidation of NH_4^+ by NO_2^- with release of N_2 as final product, and with NO as the intermediate product. Availability of sediment biodegradable organic matter in river sediments is an important factor to control anammox (Hu et al., 2011), as NH_4^+ is mostly released by organic matter mineralization. Anammox is also favoured by denitrification, as NO_2^- deriving from incomplete denitrification is a substrate of the process (Risgaard-Petersen et al., 2004; Trimmer & Nicholls, 2009). Anammox rates in rivers are usually very low and nearly negligible if compared to denitrification and DNRA (Zhou et al., 2014; Li et al., 2021).

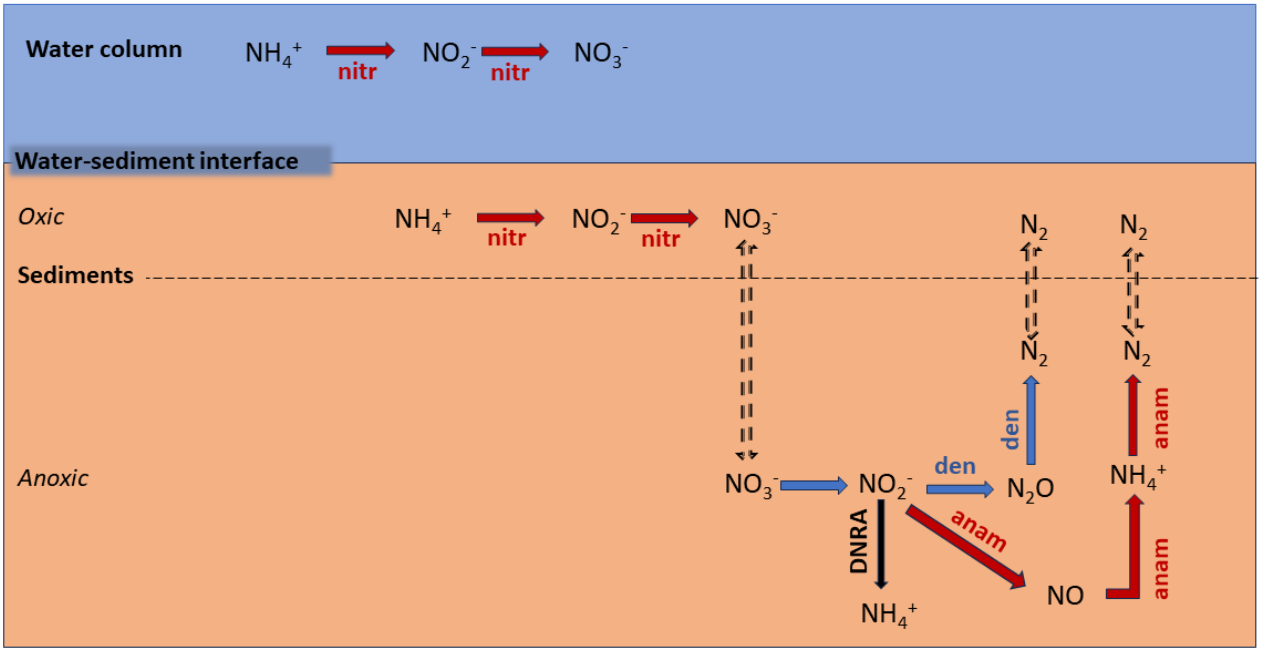

Figure 2: Nitrogen cycle diagram with the main N transformations: nitrification (nitr), denitrification (den), anammox (anam) and dissimilatory nitrate reduction to ammonium (DNRA), that occur in water column, river sediments and at the water-sediment interface.

1.2. Climate Change in the Po River basin and its delta

Climate change could affect the biogeochemical dynamics and the capacity of river ecosystems to act as natural N filters (Abily et al., 2021), by affecting the ability of rivers to actively transform, temporarily store and remove nutrients. The potential effects of climate change on the nutrient metabolism and self-depuration capacity of the Po River and the transitional ecosystems of the Po River delta (Italy) are currently unknown. The Po River basin already suffers from many climate impacts, such as a decrease of precipitation and river flow, and an increase of air temperature anomalies (Appiotti et al., 2014; Coppola et al., 2014; Marchina et al., 2017; Montanari et al., 2023). Moreover, the Po River basin is the most densely populated and agriculturally exploited area of Italy and it is considered a hotspot for NO_3^- pollution (Viaroli et al., 2018). Diffuse nutrient runoff has caused recurrent and intense algal blooms, in particular, during spring and summer, leading to dystrophy in the coastal lagoons and extensive anoxia in coastal waters (Viaroli et al., 2001; Marini et al., 2010; Viaroli et al., 2015). In addition,

the CC related reduction of Po River discharge in summer in the Delta, in the recent years (Marchina et al., 2015; Bonaldo et al., 2022; Toreti et al., 2022), favoured higher saline intrusion, which determined a more stable vertical water stratification and lack of mixing, leading to bottom hypoxia and anoxia and related effects on the N cycling (Rysgaard et al., 1999; Giblin et al., 2010; Pinardi et al., 2011; Cornwell et al., 2014).

The main hypothesis of this thesis is that CC has increased water temperature in the Po River and that this, together with CC-induced changes in river discharge, has had significant effects on the magnitude and seasonality of N export to the Adriatic coastal zone in recent years. The aim of the present study was to assess the extent to which the two CC drivers, the seasonal increase in the temperature of the Po River and the deltaic saline intrusion during the summer, may affect the self-depuration capacity of the lowland reach of the river and the ability of the delta to buffer the N loads before it reaches the coast. All of the above parameters and their effects on benthic N metabolism and N cycling in the Po River were analysed at the catchment scale and tested in the laboratory.

In fact, the thesis is divided into three main sections according to the three topics:

1) Analysis of the long-term trends of nutrient export from the Po River by studying the seasonal patterns in relation to water temperature and discharge variations;

2) laboratory experiments to assess the effect of water warming on bacterial denitrification and DNRA processes in the lower reach of the Po River, in order to evaluate the response of river self-depuration capacity to CC;

3) laboratory experiments to assess the impact of saline intrusion in the Po River Delta on denitrification and DNRA processes during summer and the capacity of the delta to dissipate N loads before they reach the Adriatic Sea.

The results are presented in chapters that consist of research articles, most of which have already been published, that present the sequence of hypotheses and the evidence produced to support them.

Chapter 2: Materials and methods

2.1. Annual and seasonal historical data of temperature, discharge, and riverine nutrient loads

The water temperature datasets since 1992 were collected from monitoring stations located along the Po River lowland reach. The daily data were used to obtain the average of the annual and seasonal water temperature trends of the Po River over the last three decades. The seasonal trends were determined according to the following seasonal breakdowns: winter (from January to March), spring (from April to June), summer (from July to September) and autumn (from October to December). Concentrations of nitrogen nutrients (NO_3^-, NH_4^+ and total nitrogen, TN) were monitored at the river closing section (Pontelagoscuro gauging station, 44°53'19.34'' N, 11°36'29.60'' E, province of Ferrara), sourced by the Environmental Agency of the Emilia-Romagna Region (ARPAE). Nitrogen concentrations were derived from monthly and/or fortnightly samples taken by APRAE as part of the official surface water monitoring programme, while daily discharge data were derived from permanent records of a gauge operated by ARPAE.

Daily loads were calculated as the product of the measured daily discharge and nutrients concentration, that were measured or interpolated to daily intervals. The product results were aggregated into monthly values, according to the equation reported in Papers I and II (Appendix I). Moreover, monthly flow was normalised to remove the effect of varying inter-annual hydrological conditions in the trend assessment of annual and seasonal nutrient export, according to the procedure described in the above-mentioned papers. The annual and seasonal normalised loads were calculated by the summing up the normalised monthly loads.

2.2. Measurements of N processing in river sediments

The experimental procedure included the collection of intact sediment cores at each sampling site used for benthic dark flux, denitrification and DNRA measurements and for sediment characterization, according to the standard protocols (Dalsgaard et al., 2000; Owens et al., 2016). Details of the experimental design, the incubation procedure to determine gas and nutrient fluxes, the application of the Isotope Pairing Technique (IPT) to measure

denitrification and DNRA rates (Nielsen, 1992), and the calculation of rates are described in Papers III, IV and V (Appendix II and III, respectively). The adopted approach consisted of both manipulative experiments and incubations mimicking the *in situ* conditions.

2.2.1. Seasonal effect of water warming on denitrification and DNRA processes

The sediment cores were collected at the closing section of the Po River Basin (Pontelagoscuro, province of Ferrara) during four seasons in 2022: winter (February sampling), spring (May sampling), summer (July sampling) and autumn (November sampling). The work consisted of applying a temperature gradient in each seasonal incubation with the aim of assessing how benthic N processes were affected by temperature. The temperature ranges were different in the four seasons, as follow: 5-14 °C in winter, 13-22 °C in spring, 21-30 °C in summer and 9-18 °C in autumn. The minimum of each seasonal temperature range corresponded to the current minimal temperature recorded during the last three decade, while the warming manipulations were the expected values in the near future owing to climate warming (Vezzoli et al., 2015). The experimental design is described in detail in Paper III (Appendix II).

2.2.2. Impact of saline intrusion on denitrification and DNRA processes in summer

Sediment cores were incubated at three sites in the Po di Goro branch along the salinity gradient during summers 2021 and 2022 to assess the impact of saline intrusion on the self-depuration capacity of the Po Delta. Sampling was carried out at three locations along the river, with salinity being the discriminating factor. The experiments were carried out in the laboratory by maintaining the *situ* conditions to assess how the benthic N processes changed in freshwater, slightly saline and saline sites. The *in situ* conditions were different in the two summers, particularly the summer 2022 was warmer than the previous one and the saline wedge was more extended than in the previous years (Po River District Authority, 2022). The experimental design is described in detail in Paper IV and V (Appendix III).

Chapter 3: Main results and discussion

The increase of temperature appeared from the historical data, monitored near the city of Piacenza (Emilia-Romagna Region), representative of the middle-lower reach of the Po River. The increase of average annual temperature was ∼3 ◦C, resulting in a warming rate of 0.11 ◦C yr−1, with the change point in 2002 (Fig. 3). The highest annual temperatures were recorded since 2003, with a slight decrease a few years later and then a gradual increase until the year 2022, when the maximum temperature appeared (Brunetti et al., 2006; Marchina et al., 2017; Po River District Authority, 2022).

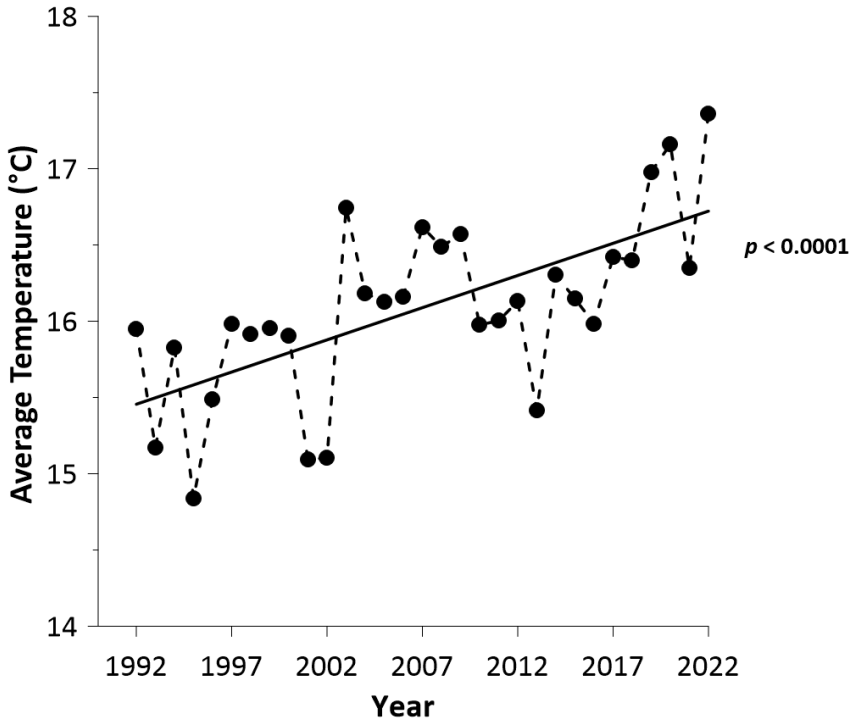

Figure 3: Temporal trend of annual average of water temperature (°C) of the Po River since 1992. Black lines show the statistically significant trend.

Seasonally, the upward trend was particularly marked in summer and autumn (nearly +5°C; fig. 4), while a slightly lower increase was observed in the other seasons (~ +3°C; fig.4). The extreme temperatures showed a significant increase, in particular temporal trends in the

minimum Po River water temperature were significant in all seasons except autumn. Summer minima showed the most pronounced warming signal (0.25 °C yr^{-1}; around 6 °C).

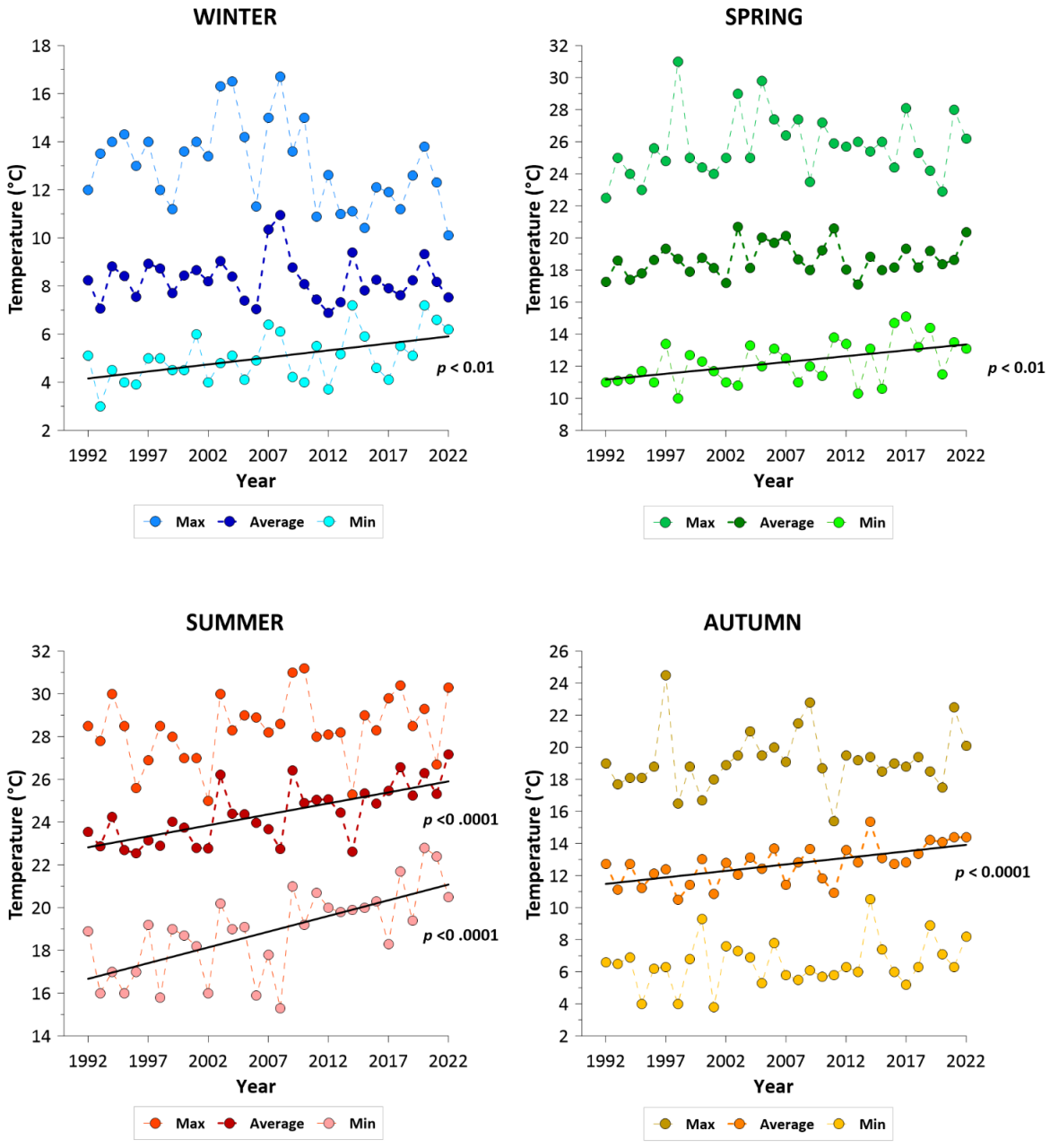

Figure 4: Temporal trend of seasonal minimum, average and maximum water temperature (°C) of the Po River since 1992. Black lines show statistically significant trends.

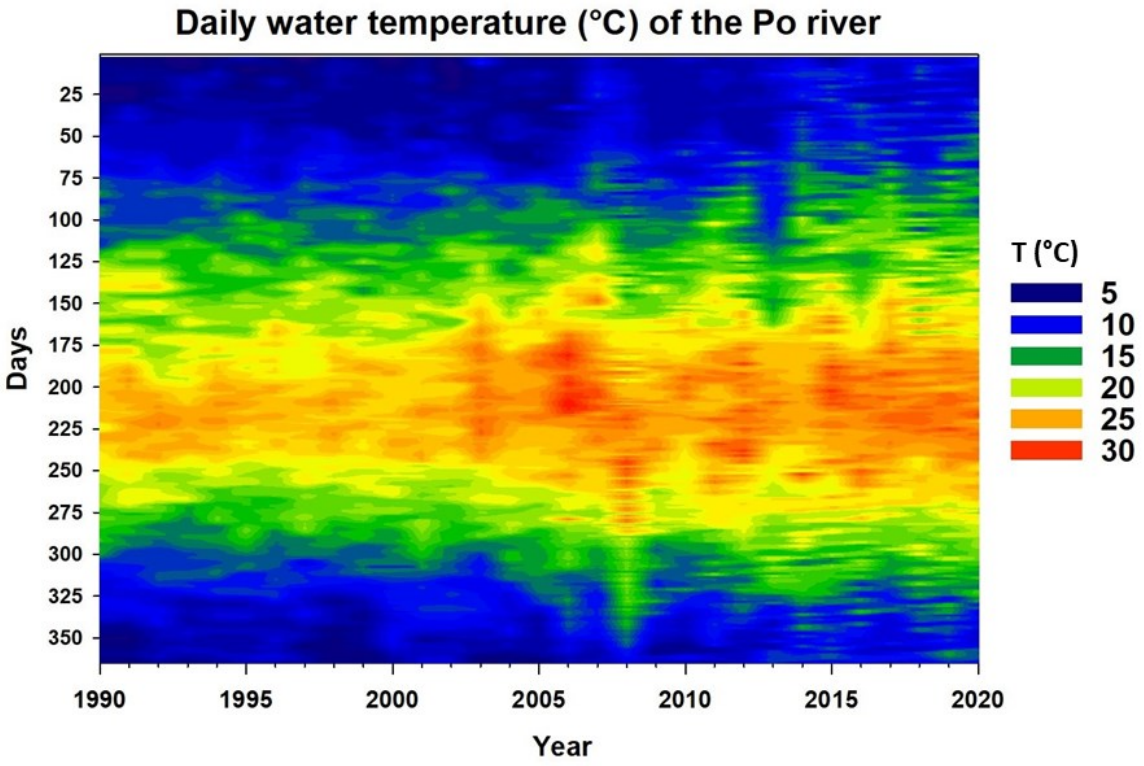

Figure 5: Daily water temperature of the Po River at the closing section of basin in the last 30 years.

The warming of the Po River water was observed with the increase of the occurrence of warm days, which appeared mostly during the summer, when the maximum temperature reached and/or exceed 30°C (Fig.5). This was related to low-flow conditions, as in the case of the period 2003- 2007, which was characterized by prolonged drought in the Po River basin (Ferrara Land Reclamation Consortium, 2022). Over the last decade, the Po River has become increasingly sensitive and vulnerable to such extreme temperature events with ongoing climate change (Markovic et al., 2013). In particular, the year 2022 showed the extreme conditions, with large areas of Europe, including Italy (Toreti et al., 2022) affected by extreme and prolonged drought. In the Northern Italy, the dry conditions were a result of low snow accumulation in the Alps during the winter and early spring of 2021–2022, similar to the year 2015 (Marchina et al., 2017), combined with the lack of precipitation from the late spring until early summer (Bonaldo et al., 2022). The emergency was manifested in the exceptional hydrological drought of the Po River in 2022, which the average annual discharge was 60% lower than the annual

average of the last 30 years (Fig. 6). The daily river discharge was constantly near or below the historical minimum, in fact the worst anomaly was monitored in July, when discharge was 30% below the historical minimum for 1990–2021, which occurred in July 2006 (Montanari et al., 2023).

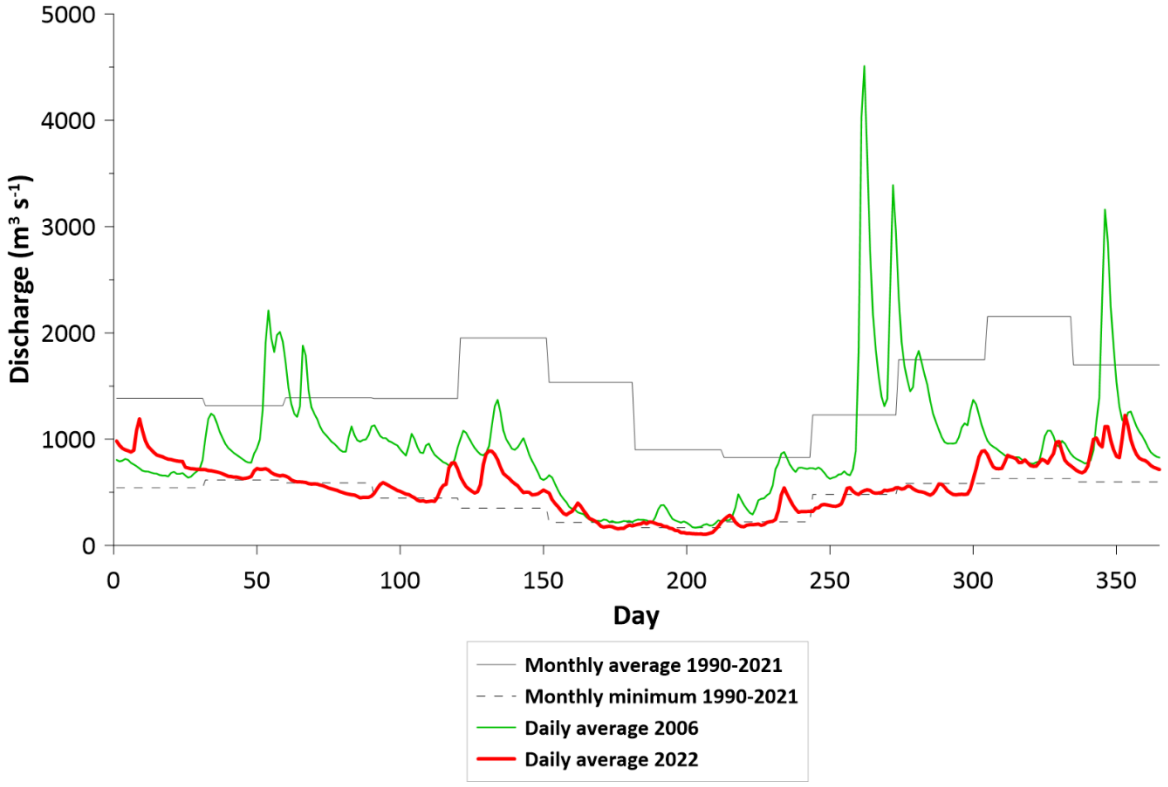

Figure 6: Average daily discharge ($m^3 s^{-1}$) of the Po River in 2022 compared to the average daily discharge of the drought year 2006 and to the minimum and average monthly discharge over the last 30 years.

The critical reduction in the river discharge led to a significant intrusion of the deep and persistent saline wedge during late spring and summer in the Po Delta, extending along the Po di Goro branch for a maximum length of 35-40 km from the mouth (Tarolli et al., 2023; Po River District Authority, 2022), more than about 15 km longer than the saline intrusion recorded during the summer of 2006 for 33 days (Tarolli et al., 2023; Luo et al., 2023).

In terms of nutrient loads, in particular N loads, the Climate Change affected their export to the Adriatic Sea from the Po River basin. In the last decades, the decrease of N export was not

related to changes in anthropogenic pressures in the catchment area or nutrient loads from diffuse (agriculture) and point sources (sewage) (Viaroli et al., 2018). Total nitrogen is mainly NO_3^- (62-86% of the annual total nitrogen load), a common feature of agriculture-dominated waterheads (Pina-Ochoa and Álvarez-Cobelas, 2006; Hill, 2023; Li et al., 2023). The time series of flow-normalized NO_3^- loads showed that the annual transport at the Po River closing section decreased by 23% since 1992 (Fig. 7) and the downward trend was evident in all seasons, except in summer (Fig. 7), highlighting that load decline was related to a discharge decrease. In fact, drought events have been exacerbated during the more recent decades and the Po River experienced temporary phases of low regime during 2003–2007, 2015–2017 and 2022 (Zanchettin et al., 2008; Montanari et al., 2012; Marchina et al., 2019; Montanari et al., 2023).

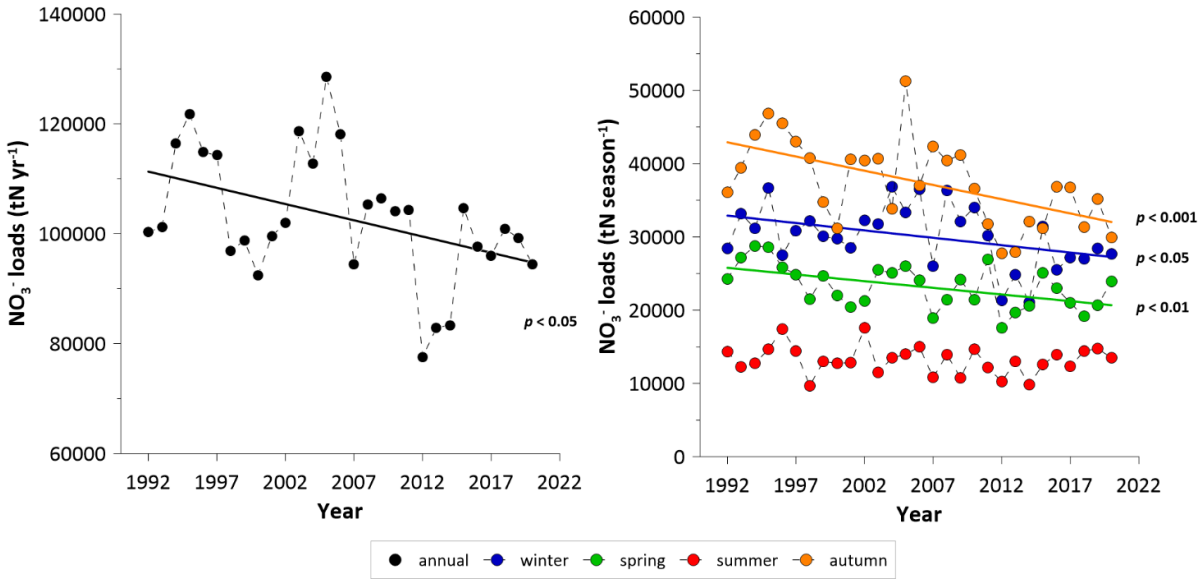

Figure 7: Temporal trend in flow-normalised NO_3^- loads measured at the closing section of the Po River basin on an annual basis (on the left; t N yr^{-1}) and during winter, spring, summer and autumn (on the right; t N $season^{-1}$) since 1992. Lines show statistically significant trends.

The link between climate change and N export into the Adriatic Sea appeared during the warmer periods, as springs and summers. There is an inverse correlation between the nitrogen load and the temperature, in fact when the water temperature of the Po River increased by 1 °C, NO_3^- loads decreased by approximately 7% and 4% in summer and spring, respectively (Fig. 8). The strong negative relationship indicate that the warming of the Po River may could have

stimulated the NO_3^- removal and/or reduction thought N biogeochemical process, decreasing the export to the Adriatic Sea and likely contributing to a partial mitigation of the eutrophication phenomena in the coastal waters.

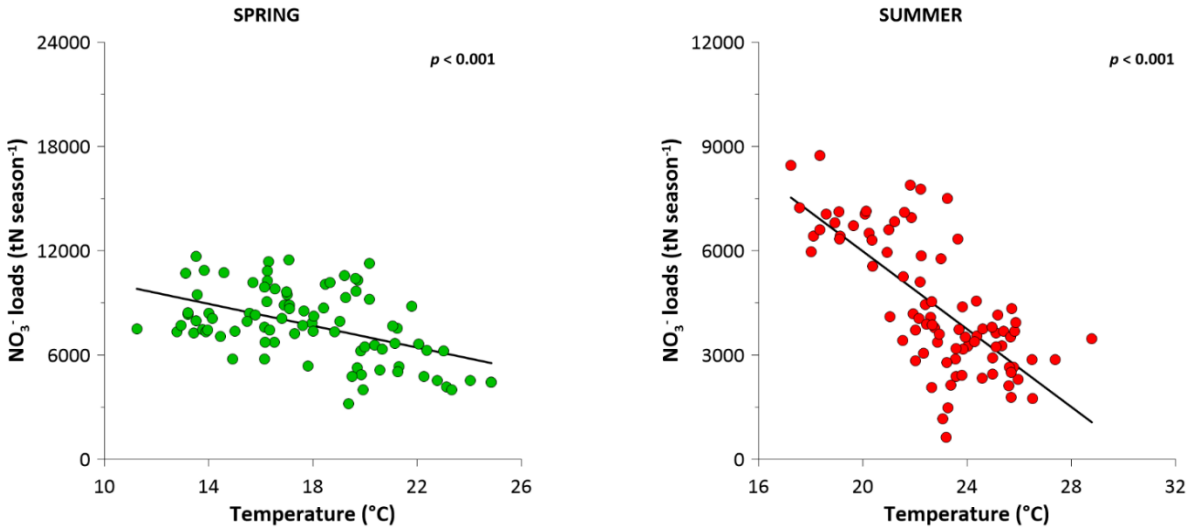

Figure 8: Correlation between flow-normalised NO_3^- (t N $month^{-1}$) and average water temperature (°C) measured at the closing section of the Po River basin in spring (on the left) and in the summer (on the right). Black lines show statistically significant trends.

Direct confirmation of this conclusion was sought through seasonal controlled laboratory incubations of intact sediment cores, aimed at (1) determining the relative contribution of denitrification and DNRA to riverine NO_3^- removal, and (2) quantifying the effects of water temperature on the rates of aerobic respiration and of dissimilatory nitrogen processes in river sediments. Manipulative laboratory experiments demonstrated the denitrification and DNRA process responded positively to water warming, increasing along the gradient temperature in each season (Fig. 9 and 10). Results showed that the denitrification rates were one order of magnitude higher than DNRA rates in the terminal section of Po River during each season and both processes were strongly correlated to the increase of water temperature. The activity of DNRA bacteria, favoured in highly reducing conditions, was likely limited to micro-niches (Kraft et al., 2014), due to the high oxygen availability, combined with low sediment organic carbon in Po River sediments and low sediments oxygen demand (SOD), resulting in the almost complete oxidation of the sandy sediments.

In general, total denitrification rates increased along the experimental temperature gradient that was set in each season ($p < 0.001$), with the denitrification rates of NO_3^- present in water column (Dw) higher than the denitrification coupled to nitrification (Dn), except in the summer, when Dw was systematically lower than Dn, representing an average of 31% of Dtot, due to the low NO_3^- availability (Fig. 9). Similar to the denitrification, the DNRA rates increased along the temperature gradient in each season, with the highest rates measured in the order of spring, winter, autumn, and summer. However, in winter the rates remained constant at the first three temperatures of the series, increasing at the last one (14 °C). The DNRA rates, splitted in DNRAw, the direct DNRA of NO_3^- from the water column, and DNRAn, that is the DNRA rate coupled with nitrification, showed that DNRAw was higher than DNRAn in all seasons, except in summer (around 30% of DNRAtot), due to the low water NO_3^- availability. The exceptionally low discharges that characterize the Po River in the year 2022 (Montanari et al., 2023) led to a reduction in nutrient runoff from the basin (Cozzi et al., 2018; Viaroli et al., 2018) and consequently limited NO_3^- availability in water, resulting in a greater relevance of Dn and DNRAn compared to Dw and DNRAw, respectively. These conditions confirmed that N processes are strongly correlated with temperature, but they are also dependent on other factors such as NO_3^- availability which change with the seasons, in fact the highest processes rates appeared during spring period at the highest NO_3^- concentration in sampling site.

Consequently, denitrification can be considered as the main process responsible for the removal of NO_3^- from the Po River water, in fact the Dw contributed on average >85% of the total NO_3^- removal, in contrast to <15% of the total NO_3^- dissimilatory reduction by DNRAw.

In order to obtain macroscale feedback on the representativeness of laboratory measurements, in spring, when the eutrophication effect of riverine N loads on coastal zones is greatest, denitrification rates were scaled-up to a lowland reach of the Po, where laboratory incubations can be considered representative of sediment features and processes. The studied stretch (length around 90 km, area 45 km^2) is located between Borgoforte (province of Mantua) and Pontelagoscuro (province of Ferrara), two sections where N loads can be estimated on the basis of monthly samples taken by ARPAE and flow measurements carried out by the Po River Authority (AdBPo). The calculated NO_3^- load reduction between the two sections during the last two decades was in the same order of magnitude as the NO_3^- removal

calculated by upscaling the measured denitrification rates to the whole river bed between the same two sections.

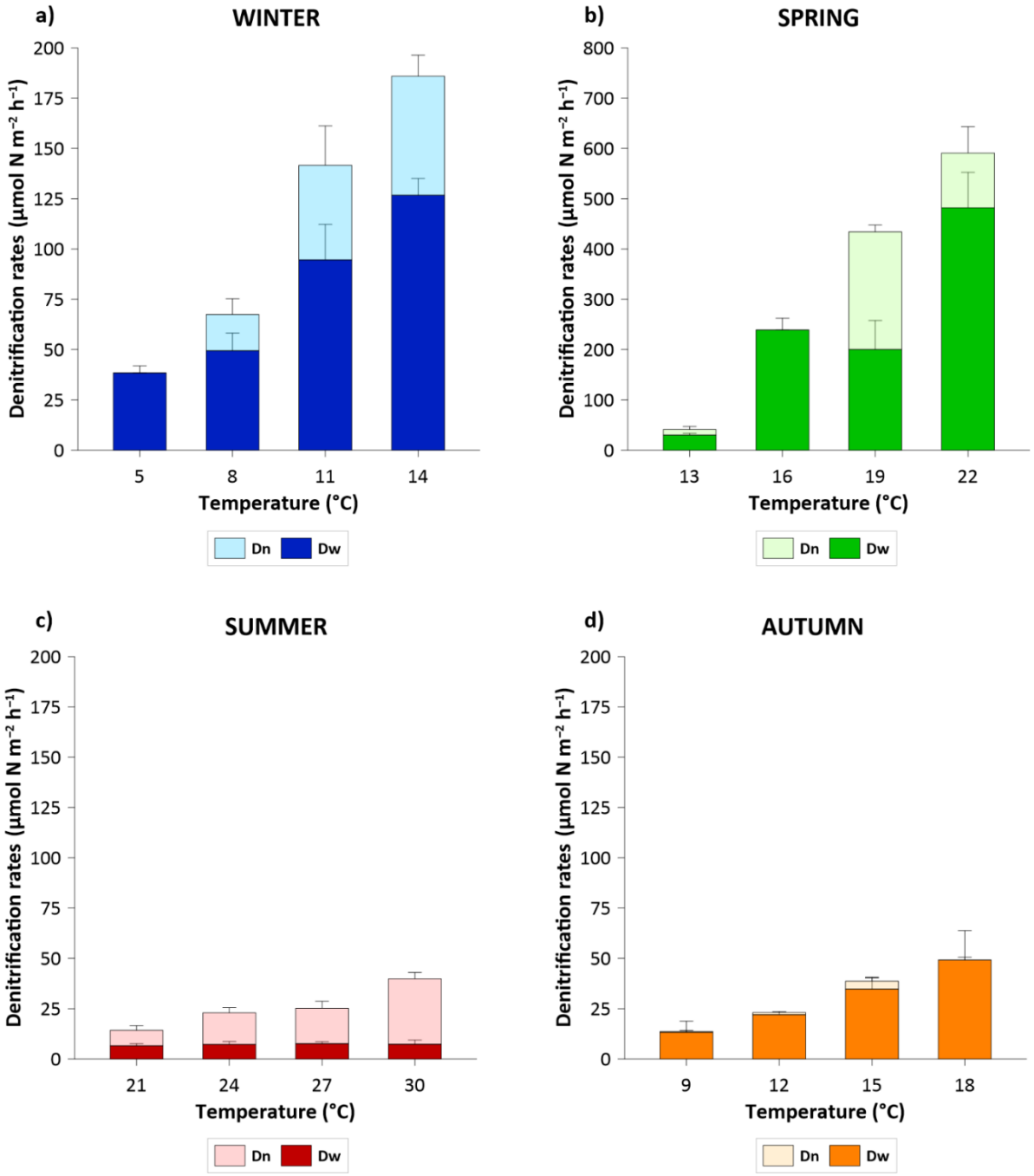

Figure 9: Total denitrification rates (µmol N m^{-2} h^{-1}) splitted into Dw and Dn measured along the temperature gradients in the four seasons (note the different scale of the y-axis) in the Po River. Average values ± standard deviations are reported.

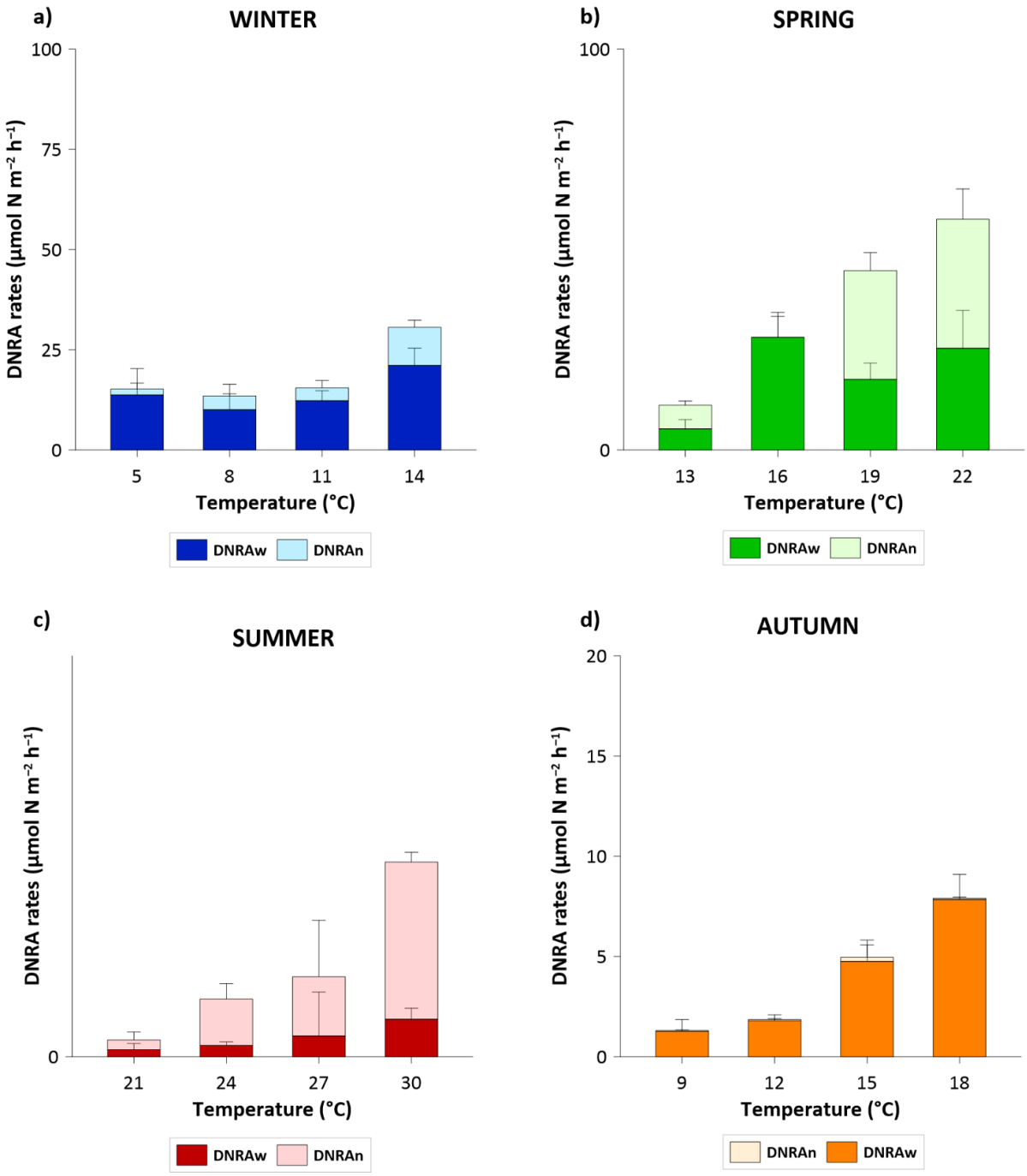

Figure 10: Total dissimilatory nitrate reduction to ammonium (DNRA) rates (µmol N m^{-2} h^{-1}) splitted into DNRAw e DNRAn, measured along the temperature gradients in the four seasons (note the different scale of the y-axis) in the Po River. Average values ± standard deviations are reported.

In addition to the calculations and experiments carried out on the freshwater lower reaches of the river, the study was extended to include the impact of saline intrusion in the Po Delta

on the nitrogen loads exported to the coastal areas of the Adriatic Sea. In particular, in 2022, the extreme drought of the Po River and low river discharge (Bonaldo et al., 2022) led to a significant saline intrusion during the late spring and summer, extending along the Po di Goro branch for a maximum of 35 km from the mouth (Po River District Authority, 2022), more than 10 km than in the summer of 2021. The hypothesis, whether these conditions have an effect on the self-depuration capacity of the Po delta on NO_3^- loads, was tested by incubations targeting benthic N metabolism. N processes were found to be strongly influenced by salinity conditions, which tended to favour recycling of N nutrients via DNRA rather than permanent removal via denitrification (Fig. 11). However, denitrification consistently outperformed DNRA along the salinity gradient, resulting in a factor of 7 of magnitude higher in freshwater and slightly saline sites, in fact the consumption of NO_3^- by denitrification 86% and 89%, respectively. In contrast to the saline site the DNRA rates were slightly higher than the denitrification rates, in fact DNRA was responsible to the 74% of NO_3^- recycled in NH_4^+, due to the salinity induced sulphidic conditions, inhibiting the nitrification process (Æsøy et al., 1998; Bonaldo et al., 2022) and the loss of NO_3^- via coupled nitrification–denitrification (Joye & Hollybaugh, 1995). The results showed the contributions of Dw and DNRAw were higher than those of Dn and DNRAn, respectively; except that the split DNRAn and DNRAw were different, in fact DNRAn (56% of total DNRA) was higher than the DNRAw. These results, due to the drought conditions of 2022, measured in the Po di Goro arm of the delta, can be extended to the NO_3^- loads carried through the whole the Po River delta.

In this second case study, represented by the southernmost branch of the Po Delta, the Po di Goro, it was not possible to verify the representativeness of the experimental measurements by referring them to transited loads, as both flow and concentration measurements of nitrogen species entering and leaving the Po Delta are not available. This lack should be taken into account at the institutional level in order to assess the role of the Po Delta in reducing nitrogen loads in the current climate change scenario.

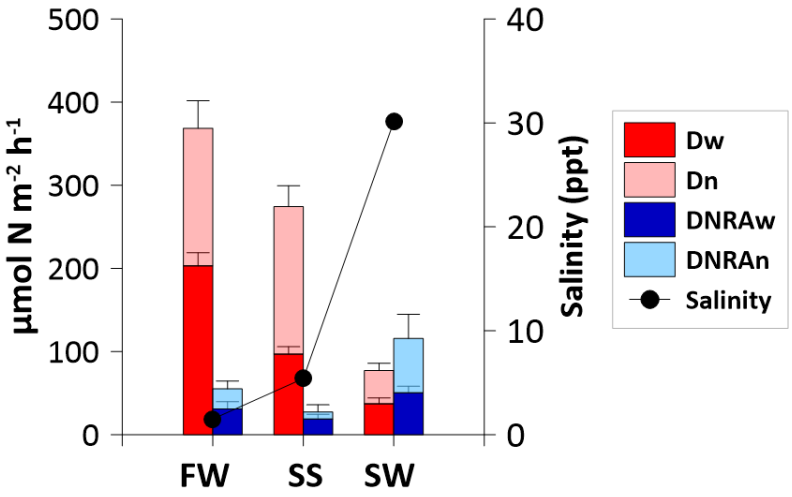

Figure 11: Denitrification and DNRA rates measured along the salinity gradient in the Po di Goro River. The rates are splitted in Dw and DNRAw, and Dn and DNRAn, indicated the rates supported by NO_3^- from the water column and the rates coupled to nitrification, respectively. Average values ± standard deviations are reported.

Chapter 4: General conclusions

The present study demonstrates that climate change may have a critical impact on the biogeochemical dynamics of N in large lowland rivers and deltas. The model chosen, i.e. the Po River, the largest river in Italy and one of the most important in the Mediterranean area, is fully representative as a hot-spot of nitrogen pollution and eutrophication and of the consequences of increasing water temperature and saline intrusion in a delta.

A decreasing trend in N export from the Po has been observed over the last three decades, which is related to the increase in water temperature. The increase in water temperature has been associated with higher rates of microbial processes, especially denitrification. The results of this study are relevant for the eutrophication state and secondary productivity of the Adriatic Sea. The study of the effect of temperature increase on the river N metabolic capacity should also be studied in the middle reaches of the Po, especially in spring, when NO_3^- loads are generally higher and more effective in triggering algal blooms and dystrophic crises in the coastal areas.

In transitional waters such as the Po Delta, low freshwater river flow favours saltwater intrusion and reduces the dissipative capacity of the transitional area. Under these conditions, which were made even more extreme in 2022 by an exceptionally low rainfall and river flow, the capacity of the Po Delta to remove NO_3^- was reduced by recycling nitrogen through DNRA. This unexpected positive feedback of climate change on eutrophication contrasts with the negative feedback observed in the upstream freshwater sections of the Po in the same year, as described above.

The multiple functions of the different drivers of climate change make the river system and the associated deltaic areas complex to analyse and difficult to predict. Future investigation should clarify the specific role of extreme weather conditions on aquatic ecosystems and biogeochemical processes and on the river self-depuration capacity, including the relative effect of multiple stressors. To address the dynamics of NO_3^- removal in rivers more comprehensively, the role of rising water temperatures should be considered as together with other effects of climate change, such as reduced nutrient runoff due to prolonged low rainfall or nutrient peaks after extreme rainfall events. These large-scale phenomena affecting NO_3^-

availability for denitrification should be considered together with other local drivers of sediment nitrogen biogeochemistry (i.e., sediment organic matter quality and sulphide concentrations, the latter especially in transitional waters) or the effect of higher temperatures on phytoplankton uptake rates and hence N processing in the water column. In addition, further research is needed to extend the experimental results to the ecosystem scale, both in terms of nutrient load generation and nutrient export to coastal zones. This is a key issue for the effective implementation of environmental policies to control eutrophication and protect coastal zones.

References

Abily, M., Acuña, V., Gernjak, W., Rodríguez-Roda, I., Poch, M., & Corominas, L. (2021). Climate change impact on EU rivers' dilution capacity and ecological status. Water Research, 199, 117166. https://doi.org/10.1016/j.watres.2021.117166

Æsøy, A., Ødegaard, H., & Bentzen, G. (1998). The effect of sulphide and organic matter on the nitrification activity in a biofilm process. Water Science and Technology, 37(1), 115-122. https://doi.org/10.1016/S0273-1223(97)00760-9

Appiotti, F., Krželj, M., Russo, A., Ferretti, M., Bastianini, M., & Marincioni, F. (2014). A multidisciplinary study on the effects of climate change in the northern Adriatic Sea and the Marche region (central Italy). Regional environmental change, 14, 2007-2024. https://doi.org/10.1007/s10113-013-0451-5

Autorità di Bacino Distrettuale del Fiume Po. Osservatorio Permanente Sugli Utilizzi Idrici Del Distretto Idrografico Del Fiume Po; Autorità di Bacino Distrettuale del Fiume Po: Parma, Italy, 2022. https://www.adbpo.it/osservatorio-permanente/

Bonaldo, D., Bellafiore, D., Ferrarin, C. et al. The summer 2022 drought: a taste of future climate for the Po valley (Italy)?. Reg Environ Change 23, 1 (2023). https://doi.org/10.1007/s10113-022-02004-z

Brunetti, M., Maugeri, M., Nanni, T., Auer, I., Böhm, R., & Schöner, W. (2006). Precipitation variability and changes in the greater Alpine region over the 1800–2003 period. Journal of Geophysical Research: Atmospheres, 111(D11). https://doi.org/10.1029/2005JD006674

Burgin, A. J., & Hamilton, S. K. (2007). Have we overemphasized the role of denitrification in aquatic ecosystems? A review of nitrate removal pathways. Frontiers in Ecology and the Environment, 5(2), 89-96. https://doi.org/10.1890/1540-9295(2007)5[89:HWOTRO]2.0.CO;2

Carvalho, D., Pereira, S. C., Silva, R., & Rocha, A. (2022). Aridity and desertification in the Mediterranean under EURO-CORDEX future climate change scenarios. Climatic Change, 174(3-4), 28. https://doi.org/10.1007/s10584-022-03454-4

Coppola, E., Verdecchia, M., Giorgi, F., Colaiuda, V., Tomassetti, B., Lombardi, A., 2014. Changing hydrological conditions in the Po basin under global warming. Science of The Total Environment 493, 1183–1196. https://doi.org/10.1016/j.scitotenv.2014.03.003

Cornwell, J. C., Glibert, P. M., & Owens, M. S. (2014). Nutrient fluxes from sediments in the San Francisco Bay Delta. Estuaries and coasts, 37, 1120-1133. https://doi.org/10.1007/s12237-013-9755-4

Cozzi, S., Ibáñez, C., Lazar, L., Raimbault, P., Giani, M., 2018. Flow Regime and Nutrient-Loading Trends from the Largest South European Watersheds: Implications for the Productivity of Mediterranean and Black Sea's Coastal Areas. Water 11, 1. https://doi.org/10.3390/w11010001

Dalsgaard, T., 2000. Protocol handbook for nitrogen cycling in estuaries: A project under the EU research programme: Marine Science and Technology (MAST III). Ministry of Environment and Energy,. Protocol handbook for nitrogen cycling in estuaries: A project under the EU research programme: Marine Science and Technology (MAST III). ISBN: 9788777725357.

de Klein, J. J., Overbeek, C. C., Juncher Jørgensen, C., & Veraart, A. J. (2017). Effect of temperature on oxygen profiles and denitrification rates in freshwater sediments. Wetlands, 37, 975-983. https://doi.org/10.1007/s13157-017-0933-1

Ferrara Land Reclamation Consortium (2022). Focus: La siccità del 2022. Ferrara, Italy, 2022.

Gao, X., & Giorgi, F. (2008). Increased aridity in the Mediterranean region under greenhouse gas forcing estimated from high resolution simulations with a regional climate model. Global and Planetary Change, 62(3-4), 195-209. https://doi.org/10.1016/j.gloplacha.2008.02.002

Giblin, A., Tobias, C., Song, B., Weston, N., Banta, G., Rivera-Monroy, V., (2013). The Importance of Dissimilatory Nitrate Reduction to Ammonium (DNRA) in the Nitrogen Cycle of Coastal Ecosystems. oceanog 26, 124–131. https://doi.org/10.5670/oceanog.2013.54

Glavan, M., Ceglar, A., & Pintar, M. (2015). Assessing the impacts of climate change on water quantity and quality modelling in small Slovenian Mediterranean catchment–lesson for

policy and decision makers. Hydrological Processes, 29(14), 3124-3144. https://doi.org/10.1002/hyp.10429

Hill, A. R. (2023). Patterns of nitrate retention in agriculturally influenced streams and rivers. Biogeochemistry, 163(2), 155-183. https://doi.org/10.1007/s10533-023-01027-w

Hu, B. L., Shen, L. D., Xu, X. Y., & Zheng, P. (2011). Anaerobic ammonium oxidation (anammox) in different natural ecosystems. Biochemical Society Transactions, 39(6), 1811-1816. https://doi.org/10.1042/BST20110711

IPCC, 2022: Climate Change 2022: Impacts, Adaptation and Vulnerability. Contribution of Working Group II to the Sixth Assessment Report of the Intergovernmental Panel on Climate Change [H.-O. Pörtner, D.C. Roberts, M. Tignor, E.S. Poloczanska, K. Mintenbeck, A. Alegría, M. Craig, S. Langsdorf, S. Löschke, V. Möller, A. Okem, B. Rama (eds.)]. Cambridge University Press. Cambridge University Press, Cambridge, UK and New York, NY, USA, 3056 pp. 10.1017/9781009325844

IPCC, 2023: Summary for Policymakers. In: Climate Change 2023: Synthesis Report. Contribution of Working Groups I, II and III to the Sixth Assessment Report of the Intergovernmental Panel on Climate Change [Core Writing Team, H. Lee and J. Romero (eds.)]. IPCC, Geneva, Switzerland, pp. 1-34, 10.59327/IPCC/AR6-9789291691647.001

Joye, S. B., & Hollibaugh, J. T. (1995). Influence of sulfide inhibition of nitrification on nitrogen regeneration in sediments. Science, 270(5236), 623-625. 10.1126/science.270.5236.623

Kemp, P., Sear, D., Collins, A., Naden, P., & Jones, I. (2011). The impacts of fine sediment on riverine fish. Hydrological processes, 25(11), 1800-1821. https://doi.org/10.1002/hyp.7940

Kraft, B., Tegetmeyer, H.E., Sharma, R., Klotz, M.G., Ferdelman, T.G., Hettich, R.L., Geelhoed, J.S., Strous, M., 2014. The environmental controls that govern the end product of bacterial nitrate respiration. Science 345, 676–679. https://doi.org/10.1126/science.1254070

Li, X., Gao, D., Hou, L., Qian, W., Liu, M., Zeng, H., ... & Tong, C. (2021). Nitrogen loads alter the N2 production between denitrification and anammox in Min River Estuary, a highly impacted estuary in southeast China. Environmental Pollution, 277, 116757. https://doi.org/10.1016/j.envpol.2021.116757

Luo, J., Straffelini, E., Bozzolan, M., Zheng, Z., & Tarolli, P. (2023). Saltwater intrusion in the Po River Delta (Italy) during drought conditions: Analyzing its spatio-temporal evolution and potential impact on agriculture. International Soil and Water Conservation Research. https://doi.org/10.1016/j.iswcr.2023.09.009

Marchina, C., Bianchini, G., Natali, C., Pennisi, M., Colombani, N., Tassinari, R., & Knoeller, K. (2015). The Po river water from the Alps to the Adriatic Sea (Italy): New insights from geochemical and isotopic (δ 18 O-δD) data. Environmental Science and Pollution Research, 22, 5184-5203. https://doi.org/10.1007/s11356-014-3750-6

Marchina, C., Natali, C., & Bianchini, G. (2019). The Po River water isotopes during the drought condition of the year 2017. Water, 11(1), 150. https://doi.org/10.3390/w11010150

Marchina, C., Natali, C., Fazzini, M. et al. Extremely dry and warm conditions in northern Italy during the year 2015: effects on the Po river water. Rend. Fis. Acc. Lincei 28, 281–290 (2017). https://doi.org/10.1007/s12210-017-0596-0

Marini, M., Grilli, F., Guarnieri, A., Jones, B. H., Klajic, Z., Pinardi, N., & Sanxhaku, M. (2010). Is the southeastern Adriatic Sea coastal strip an eutrophic area?. Estuarine, Coastal and Shelf Science, 88(3), 395-406. https://doi.org/10.1016/j.ecss.2010.04.020

Markovic, D., Scharfenberger, U., Schmutz S., Pletterbauer, F., and Wolter, C. (2013). Variability and alterations of water temperatures across the Elbe and Danube River Basins. Clim. Change 119 375–89. https://doi.org/10.1007/s10584-013-0725-4

Montanari, A. (2012). Hydrology of the Po River: looking for changing patterns in river discharge. Hydrology and Earth System Sciences, 16(10), 3739-3747. https://doi.org/10.5194/hess-16-3739-2012, 2012.

Montanari, A., Nguyen, H., Rubinetti, S., Ceola, S., Galelli, S., Rubino, A., & Zanchettin, D. (2023). Why the 2022 Po River drought is the worst in the past two centuries. Science Advances, 9(32), eadg8304. 10.1126/sciadv.adg8304

Nielsen, L.P., (1992). Denitrification in sediment determined from nitrogen isotope pairing. FEMS Microbiology Letters 86, 357–362. https://doi.org/10.1111/j.1574-6968.1992.tb04828.x

Owens, M.S., Cornwell, J.C., (2016). The Benthic Exchange of O2, N2 and Dissolved Nutrients Using Small Core Incubations. JoVE 54098. https://doi.org/10.3791/54098

Pina-Ochoa, E., & Álvarez-Cobelas, M. (2006). Denitrification in aquatic environments: a cross-system analysis. Biogeochemistry, 81, 111-130. https://doi.org/10.1007/s10533-006-9033-7

Pinardi, M., Bartoli, M., Longhi, D., & Viaroli, P. (2011). Net autotrophy in a fluvial lake: the relative role of phytoplankton and floating-leaved macrophytes. Aquatic Sciences, 73, 389-403. https://doi.org/10.1007/s00027-011-0186-7

Rajesh, M., & Rehana, S. (2022). Impact of climate change on river water temperature and dissolved oxygen: Indian riverine thermal regimes. Scientific Reports, 12(1), 9222. https://doi.org/10.1038/s41598-022-12996-7

Reddy, K. R., Patrick, W. H., & Broadbent, F. E. (1984). Nitrogen transformations and loss in flooded soils and sediments. Critical Reviews in Environmental Science and Technology, 13(4), 273-309. https://doi.org/10.1080/10643388409381709

Risgaard-Petersen, N., Meyer, R. L., Schmid, M., Jetten, M. S., Enrich-Prast, A., Rysgaard, S., & Revsbech, N. P. (2004). Anaerobic ammonium oxidation in an estuarine sediment. Aquatic Microbial Ecology, 36(3), 293-304. 10.3354/ame036293

Rysgaard, S., Thastum, P., Dalsgaard, T., Christensen, P. B., & Sloth, N. P. (1999). Effects of salinity on NH 4+ adsorption capacity, nitrification, and denitrification in Danish estuarine sediments. Estuaries, 22, 21-30. https://doi.org/10.2307/1352923

Scott, J. T., McCarthy, M. J., Gardner, W. S., & Doyle, R. D. (2008). Denitrification, dissimilatory nitrate reduction to ammonium, and nitrogen fixation along a nitrate concentration

gradient in a created freshwater wetland. Biogeochemistry, 87, 99-111. https://doi.org/10.1007/s10533-007-9171-6

Seitzinger, S. P. (1988). Denitrification in freshwater and coastal marine ecosystems: ecological and geochemical significance. Limnology and oceanography, 33(4part2), 702-724. https://doi.org/10.4319/lo.1988.33.4part2.0702

Tarolli, P., Luo, J., Straffelini, E., Liou, Y. A., Nguyen, K. A., Laurenti, R., ... & D'Agostino, V. (2023). Saltwater intrusion and climate change impact on coastal agriculture. PLOS Water, 2(4), e0000121. https://doi.org/10.1371/journal.pwat.0000121

Thamdrup, B. O., & Dalsgaard, T. (2008). Nitrogen cycling in sediments. Microbial ecology of the oceans, 2, 527-568. 10.1002/9780470281840

Tiedje, J. M. (1983). Denitrification. Methods of Soil Analysis: Part 2 Chemical and Microbiological Properties, 9, 1011-1026. https://doi.org/10.2134/agronmonogr9.2.2ed.c47

Toreti, A., Masante, D., Acosta Navarro, J., Bavera, D., Cammalleri, C., De Jager, A., Di Ciollo, C., Hrast Essenfelder, A., Maetens, W., Magni, D., Mazzeschi, M., Spinoni, J. and De Felice, M., (2022). Drought in Europe July 2022, EUR 31147 EN, Publications Office of the European Union, Luxembourg, 2022, ISBN 978-92-76-54953-6, 10.2760/014884, JRC130253.

Trimmer, M., & Nicholls, J. C. (2009). Production of nitrogen gas via anammox and denitrification in intact sediment cores along a continental shelf to slope transect in the North Atlantic. Limnology and Oceanography, 54(2), 577-589. https://doi.org/10.4319/lo.2009.54.2.0577

Triska, F. J., & Higler, L. B. (2009). Biogeochemical processes in river systems. Fresh Surface Water, 2, 175.

Veraart, A. J., De Klein, J. J., & Scheffer, M. (2011). Warming can boost denitrification disproportionately due to altered oxygen dynamics. PLoS One, 6(3), e18508. https://doi.org/10.1371/journal.pone.0018508

Vezzoli, R., Mercogliano, P., Pecora, S., Zollo, A.L., Cacciamani, C., (2015). Hydrological simulation of Po River (North Italy) discharge under climate change scenarios using the RCM COSMO-CLM. Science of The Total Environment 521–522, 346–358. https://doi.org/10.1016/j.scitotenv.2015.03.096

Viaroli, P., Azzoni, R., Bartoli, M., Giordani, G., & Tajé, L. (2001). Evolution of the trophic conditions and dystrophic outbreaks in the Sacca di Goro lagoon (Northern Adriatic Sea). Mediterranean Ecosystems: Structures and Processes, 467-475. https://doi.org/10.1007/978-88-470-2105-1_59

Viaroli, P., Nizzoli, D., Pinardi, M., Soana, E., & Bartoli, M. (2015). Eutrophication of the Mediterranean Sea: a watershed—cascading aquatic filter approach. Rendiconti Lincei, 26, 13-23. https://doi.org/10.1007/s12210-014-0364-3

Viaroli, P., Soana, E., Pecora, S., Laini, A., Naldi, M., Fano, E. A., & Nizzoli, D. (2018). Space and time variations of watershed N and P budgets and their relationships with reactive N and P loadings in a heavily impacted river basin (Po river, Northern Italy). Science of the Total Environment, 639, 1574-1587. https://doi.org/10.1016/j.scitotenv.2018.05.233

Whitehead, P. G., Wilby, R. L., Battarbee, R. W., Kernan, M., & Wade, A. J. (2009). A review of the potential impacts of climate change on surface water quality. Hydrological sciences journal, 54(1), 101-123. https://doi.org/10.1623/hysj.54.1.101

Zanchettin, D., Traverso, P., & Tomasino, M. (2008). Po River discharges: a preliminary analysis of a 200-year time series. Climatic Change, 89(3-4), 411-433. https://doi.org/10.1007/s10584-008-9395-z

Zhou, S., Borjigin, S., Riya, S., Terada, A., & Hosomi, M. (2014). The relationship between anammox and denitrification in the sediment of an inland river. Science of the total environment, 490, 1029-1036. https://doi.org/10.1016/j.scitotenv.2014.05.096

Appendix I: The effect of the warming of the Po River on nutrients loads in recent decades

Paper I: Soana, E., Gervasio, M. P., Granata, T., Colombo, D., & Castaldelli, G. (2024). Climate change impacts on eutrophication in the Po River (Italy): Temperature-mediated reduction in nitrogen export but no effect on phosphorus. *Journal of Environmental Sciences*, 143, 148–163. https://doi.org/10.1016/j.jes.2023.07.008

JOURNAL OF ENVIRONMENTAL SCIENCES 143 (2024) 148–163

Available online at www.sciencedirect.com

ScienceDirect

www.elsevier.com/locate/jes

JES JOURNAL OF ENVIRONMENTAL SCIENCES

www.jesc.ac.cn

Research Article

Climate change impacts on eutrophication in the Po River (Italy): Temperature-mediated reduction in nitrogen export but no effect on phosphorus

Elisa Soana[1,*], *Maria Pia Gervasio*[1], *Tommaso Granata*[2], *Daniela Colombo*[2], *Giuseppe Castaldelli*[1]

[1] *Department of Environmental and Prevention Sciences, University of Ferrara, Via Luigi Borsari 46, 44121 Ferrara, Italy*

[2] *CESI - Italian Electrical and Technical Experimental Center, via Rubattino 54, 20134, Milano, Italy*

ARTICLE INFO

Article history:
Received 7 April 2023
Revised 4 July 2023
Accepted 4 July 2023
Available online 10 July 2023

Keywords:
Nutrient export
Eutrophication
Climate change
Water temperature
Denitrification
Po River

ABSTRACT

Rivers worldwide are under stress from eutrophication and nitrate pollution, but the ecological consequences overlap with climate change, and the resulting interactions may be unexpected and still unexplored. The Po River basin (northern Italy) is one of the most agriculturally productive and densely populated areas in Europe. It remains unclear whether the climate change impacts on the thermal and hydrological regimes are already affecting nutrient dynamics and transport to coastal areas. The present work addresses the long-term trends (1992–2020) of nitrogen and phosphorus export by investigating both the annual magnitude and the seasonal patterns and their relationship with water temperature and discharge trajectories. Despite the constant diffuse and point sources in the basin, a marked decrease (-20%) in nitrogen export, mostly as nitrate, was recorded in the last decade compared to the 1990s, while no significant downward trend was observed for phosphorus. The water temperature of the Po River has warmed, with the most pronounced signals in summer (+0.13°C/year) and autumn (+0.16°C/year), together with the strongest increase in the number of warm days (+70%–80%). An extended seasonal window of warm temperatures and the persistence of low flow periods are likely to create favorable conditions for permanent nitrate removal via denitrification, resulting in a lower delivery of reactive nitrogen to the sea. The present results show that climate change-driven warming may enhance nitrogen processing by increasing respiratory river metabolism, thereby reducing export from spring to early autumn, when the risk of eutrophication in coastal zones is higher.

* Corresponding author.
E-mail: elisa.soana@unife.it (E. Soana).

https://doi.org/10.1016/j.jes.2023.07.008

Introduction

Over the last century, nitrogen (N) and phosphorus (P) inputs have increased dramatically in human-impacted watersheds with a cascade of multiple negative impacts on aquatic environments in terms of water pollution, eutrophication, greenhouse gas emissions, ecosystem functioning, and biodiversity loss (Battye et al., 2017; Glibert, 2017; Yuan et al., 2018). Watershed nutrient budgets provide insight into the relative importance of anthropogenic sources, i.e., the main determinants of riverine loads (Romero et al., 2021), but the amounts of nutrients processed or transported downstream and ultimately exported are closely linked to hydrological dynamics and internal biogeochemical cycling. Several temperature-dependent (e.g., organic matter mineralisation and biogeochemical N pathways in soils and waters) or precipitation-dependent (e.g., runoff and erosion processes) processes occur across landscapes and shape the timing and the magnitude of nutrient mobilisation (Baron et al., 2013; Wagena et al., 2018; Goyette et al., 2019). Many rivers around the world are under stress due to eutrophication and nitrate (NO_3^-) pollution, but their ecological consequences overlap with the effects of climate change and the resulting interactions may be complex, unexpected not yet fully understood (Rozemeijer et al., 2021; Meerhoff et al., 2022; Costa et al., 2022). Climate change may affect the biogeochemical dynamics and the ecological functioning of rivers by influencing the amount and the timing of nutrient delivery from terrestrial ecosystems, and by altering the dilution capacity and the extent of internal dissipation and recycling processes (Goyette et al., 2019; Abily et al., 2021; Zheng et al., 2023).

River networks are disproportionately important relative to their surface areas for processing anthropogenic N inputs. On a global scale, more than 75% of the N load generated in the catchments and transferred to rivers is removed along the terrestrial-freshwater-marine continuum (Seitzinger et al., 2006; Howarth et al, 2012). In these systems, microbial denitrification is considered the main mechanism responsible for permanent N removal through the reduction of nitrate (NO_3^-) to nitrogen gas (N_2) under hypoxic-anoxic conditions (Birgand et al., 2007; Reisinger et al., 2016; Hill, 2023). Warming can affect denitrification both as a direct effect of enzyme activity and as an indirect effect of temperature upon redox conditions. Higher water temperature decreases oxygen solubility and enhances sediment oxygen respiration, limiting oxygen penetration depth and resulting in a synergistic effect that stimulates denitrification (de Klein et al., 2017; Velthuis and Veraart, 2022). In cases where denitrification is strongly dependent on NO_3^- supply from nitrifying bacteria, decreased oxygen at higher water temperatures may result in reduced nitrification, and consequently lower denitrification (Pina-Ochoa and Álvarez-Cobelas, 2006; Birgand et al., 2007).

Simultaneously, a wide range of abiotic and biotic processes (e.g., sorption, particulate sedimentation, periphyton, and phytoplankton uptake) are responsible for P retention in river sediments and account for the temporary storage of this element (Yuan et al., 2018; Goyette et al., 2019). Overall, rivers actively transform, temporarily store, and permanently remove nutrients in a highly dynamic environment largely controlled by microbial activity, which is temperature-dependent and thus sensitive to global warming (Salmon-Monviola et al., 2013; Velthuis and Veraart, 2022; Hill, 2023).

Nutrient transport and transformation are expected to change in response to changes in the seasonality of precipitation patterns and snow accumulation, intensified climatic variability, and increased frequency and severity of extreme thermal and hydrological (floods and droughts) events (Howarth et al, 2012; Baron et al., 2013; IPCC, 2021). A better understanding of the combined and simultaneous effects of hydrological variability and temperature warming on current and future nutrient export from watersheds is essential for defining and implementing policies to effectively tackle eutrophication in an era of climate change.

Nitrogen pollution is a priority challenge in the Po River basin (northern Italy), one of the most agriculturally exploited and densely populated areas in Europe, and eutrophication is a major concern, especially in the receiving coastal lagoons and the Adriatic Sea. Between the 1960s and the 1990s, the temporal trajectory of the input-output N and P budgets in the Po River watershed was deeply affected by changes in land use, agricultural and livestock practices, and wastewater treatment efficiency (e.g., de Wit and Bendoricchio, 2001; Artioli et al., 2008). In recent decades, the excess agricultural nutrients have remained stable (Viaroli et al., 2018; Gervasio et al., 2022a). Therefore, the basin can be considered as a case study to investigate the response of removal and recycling processes and downstream nutrient delivery to recent climatic anomalies. The effects of climate change in the Po River basin are already evident, as shown by alterations in precipitation intensity and patterns, temperature warming, increased evaporation, and frequency of droughts and water stress periods (Appiotti et al., 2014; Coppola et al., 2014; Formetta et al., 2022; Tarolli et al., 2023). Anyway, it is currently unclear whether climate change impacts on the hydrological cycle and temperature of the Po River are already affecting the river functioning in terms of nutrient removal, recycling, and delivery to the coastal zones and the Adriatic Sea. To fill this research gap, the present work addresses the long-term trends (1992–2020) of N and P export from the Po River basin by investigating both the annual magnitude and the seasonal patterns and their relationship with the trajectories of water temperature and discharge. The main hypothesis is that warming and an increase in the duration of low flow periods may enhance the rates of microbial processes and sustain more favorable conditions for denitrification and NO_3^- removal, resulting in a net decrease in N delivery to the Adriatic Sea. On the other hand, the increase in rainfall intensity and frequency may result in enhanced erosion processes and sediment yields, and downstream P delivery may eventually be favored over N.

1. Materials and methods

1.1. *Study area*

The Po River, with a length of 652 km from the Alps to the Adriatic Sea, is the longest river in Italy (Fig. 1) and the largest one with an average annual discharge of ~1,500 m^3/sec mea-

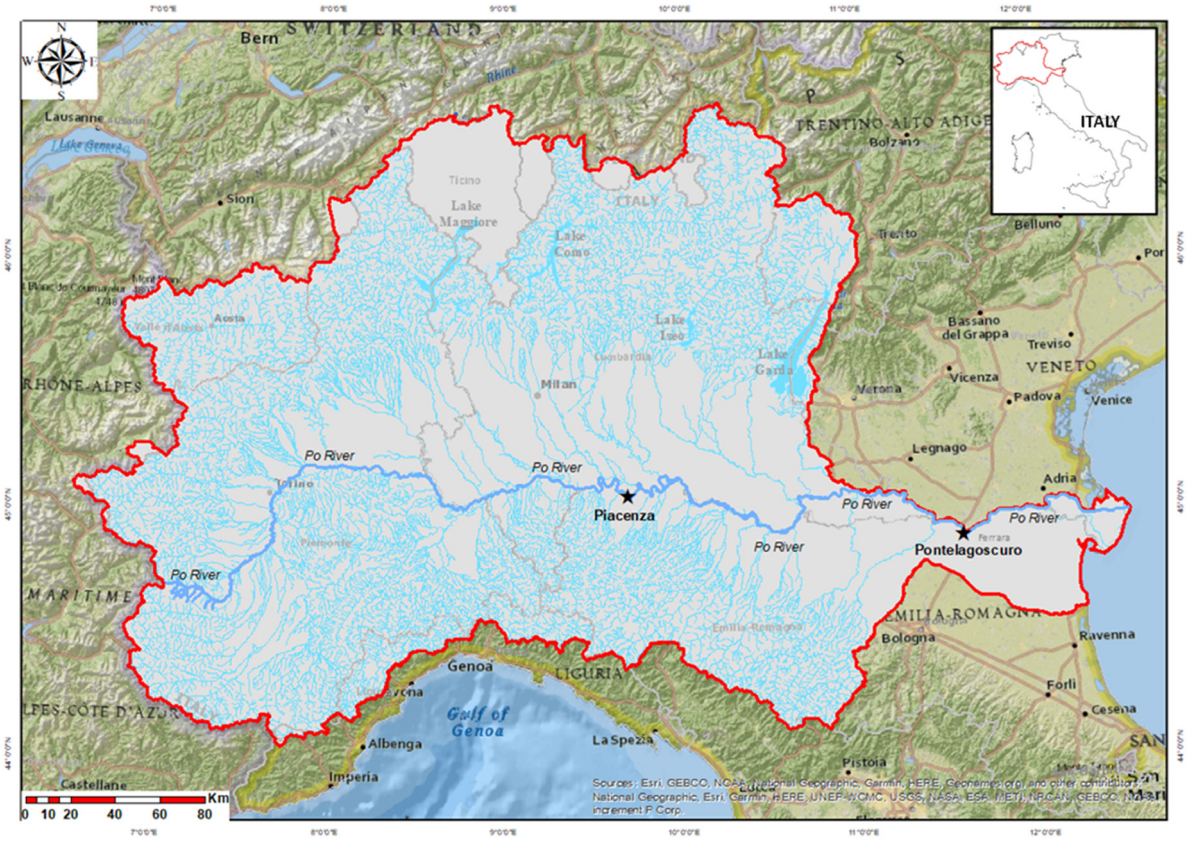

Fig. 1 – Map of the Po River basin (red line), its natural hydrological network (blue lines), and the administrative boundaries of the Northern Italy Regions (grey lines). The two monitoring stations (Piacenza and Pontelagoscuro) are indicated as black stars.

sured at the Pontelagoscuro gauging station, right upstream of the deltaic system (Zanchettin et al., 2008). The Po River basin extends over an area of ~75,000 km^2, from the headwaters on the northern slope of Monviso (3,841 m asl, Cottian Alps) to the delta, which projects into the northern Adriatic Sea. The river is fed from both the Alps and the Apennines by a network of more than 140 tributaries with a total length of over 6,700 km and a secondary network of artificial irrigation and drainage canals that is almost ten times larger (Soana et al., 2019). The hydrological regime is characterized by two periods of low flow (winter and summer) and two flood periods (spring and late autumn) associated with snowmelt and precipitation that feed the tributaries descending from the valleys of the Alps and the Apennines, respectively (Montanari, 2012; Coppola et al., 2014; Ravazzani et al., 2015). The basin crosses the transition zone between the subcontinental climate of Central Europe and the Mediterranean climate (warm-temperate climate). The average annual precipitation is 1,200 mm, varying from a maximum of 2,000 mm in the Alpine sector to less than 700 mm in the deltaic region (Vezzoli et al., 2015; Beck et al., 2018). Water resources in the basin are intensively exploited, particularly for irrigation, hydropower generation, domestic, and industrial purposes (Montanari et al., 2012).

The basin includes the area with the highest economic income in Italy, where approximately 40% of the gross domestic product is produced. Cropland accounts for more than half of the land use in the basin, which encompasses a large part of the Padano–Veneta plain, the widest and most fertile alluvial lowland in Italy (~47,000 km^2). The Po River lowland is the largest cultivated area in Italy and accounts for more than one-third of the national agricultural and livestock production. The Padano–Veneta plain is the most densely urbanized, industrialized, and agriculturally exploited area in Italy, resulting in one of the European regions with the highest N and P inputs to cropland and nutrient losses to surface and groundwater (Viaroli et al., 2018; Romero et al., 2021; Batool et al., 2022). The Po River accounts for approximately two-thirds of the total freshwater discharge and nutrient inputs to the northern Adriatic Sea, making it a well-known eutrophication hotspot (Ludwig et al., 2009; Blaas and Kroeze, 2016; Malone and Newton, 2020).

1.2. *Calculation of nutrient loads exported from the Po River basin*

Monthly, seasonal, and annual N and P loads exported to the Adriatic Sea were calculated using discharge and nutrient concentration datasets collected for the period 1992–2020 at the Pontelagoscuro gauging station (44°53'19.34"N, 11°36'29.60"E; Ferrara, river kilometer 586), which is conventionally considered the basin closing section (Fig. 1). Daily dis-

charge data were obtained from the Hydrological Annals published by the Environmental Protection Agency of the Emilia-Romagna Region (ARPAE), whose electronic versions are available on the ARPAE Open Data Portal (Dexter Portal, https://simc.arpae.it/dext3r/). Observed discharge data were derived from rating curves which convert river water levels, measured every 15 min at the gauged cross section of interest, into flow rates (rating curve uncertainty <10% of discharge value; Domeneghetti et al., 2012). Concentrations of total nitrogen (TN), total phosphorus (TP), NO_3^-, ammonium (NH_4^+), and PO_4^{3-} (reactive phosphorus) were obtained from monthly, and in some cases, fortnightly, samples taken by ARPAE as part of the official surface water monitoring programme (Regional Open Data Portal, https://dati.arpae.it/group/acqua). Dissolved inorganic nutrients were determined on filtered water samples (Whatman GF/F filters) by standard colorimetric methods based on the azo dye reaction for NO_3^- (detection limit >0.2 mg N/L), the indophenol reaction for NH_4^+ detection limit >0.02 mg N/L), and the molybdate reaction for PO_4^{3-} (detection limit >0.01 mg N/L). Precision ranged between ±3% and ±5% for the three nutrient analyses. Total nitrogen and total phosphorus were determined on unfiltered samples by the persulphate oxidation method followed by the colorimetric determinations of NO_3^- and PO_4^{3-}. Sample collection and analytical determinations were performed according to standard methods and analytical protocols outlined by national environmental regulations and adopted by the Regional Environmental Agencies in Italy (APAT—IRSA/CNR, 2003). The analytical methods were comparable to those applied in a wide range of environmental studies (e.g., APHA, 2005). When TN concentrations were not available, TN values were calculated from DIN ($NO_3^- + NH_4^+$) concentrations using the equation $TN = 0.93 \cdot DIN + 0.75$ ($r^2 = 0.54$; $p < 0.001$), previously obtained by plotting time series with simultaneous measurements of TN and DIN (Gervasio et al., 2022a).

The method used to calculate loads was based on linear interpolation of daily nutrient concentrations between two consecutive sampling events. Previous applications have shown that this method is accurate for large rivers with recurrent seasonal variations of nutrient concentrations (Moatar et al., 2005; Nava et al., 2019). Daily loads were calculated as the product of the measured daily discharge and nutrient concentration (measured or interpolated) and then aggregated monthly according to the following equation:

$$L = k \cdot \sum_{j}^{n} C_i \cdot Q_i \quad (1)$$

where L (tons/month) is the monthly load, C_i (mg/m^3) is the daily concentration on day i measured or linearly interpolated between two consecutive measurements to represent unsampled days, Q_i (m^3/sec) is the average daily discharge on day i, n is the number of days in each month, and k (86.4x10^{-6}, from mg/sec to tons/day) is the unit conversion factor.

Annual loads (tons N/year or tons P/year) were calculated by summing the monthly contributions. Trends in seasonal loads (tons N/season or tons P/season) were evaluated according to the following seasonal breakdowns: winter (January–March), spring (April–June), summer (July–September), and autumn (October–December).

The annual loads calculated by the interpolation concentration method were compared for consistency with those calculated by the flow-adjusted concentration method, previously used to estimate the long-term trajectories of the reactive nutrient loads exported from the Po River basin (Cozzi et al., 2018; Viaroli et al., 2018). The flow-adjusted concentration method is commonly adopted to assess annual loads as recommended by international conventions (e.g., OSPAR-Convention for the Protection of the Marine Environment of the North-East Atlantic; Lenhart et al., 2010) and regional guidelines for the implementation of River Basin Management Plans, as required by EU Directive 2000/60/EC (e.g., Po River District Authority, 2021). In fact, the method allows for the best weighting of the data when the chemical and flow data series have different temporal resolutions. However, this approach is not suitable for the calculation of monthly and seasonal loads because the Regional Environmental Agencies generally conduct only one sampling per month. A very good correlation was found between the annual values calculated using the two methods ($r^2 = 0.99$; $p < 0.001$), with an average discrepancy of less than 5% (Appendix A Fig. S1).

To remove the effect of varying inter-annual hydrological conditions in the trend assessment of annual and seasonal nutrient export, monthly flow-normalized loads (Ln) were calculated as follows (Sileika et al., 2006):

$$Ln = L \cdot Kh \quad (2)$$

where Kh is the hydrological coefficient. The hydrological coefficient was obtained as the ratio of the long-term (period 1992–2020) average outflow for a given month to the monthly outflow for a given year. The annual normalized loads were calculated by summing up the monthly flow-normalized loads.

1.3. *Datasets of Po River water temperature and air temperature*

Water temperature time series representative of the middle-lower reach of the Po River were collected at two monitoring stations located at the cooling water intakes of two thermoelectric power plants near the city of Piacenza (Emilia-Romagna Region, river kilometer 330) (Fig. 1). Daily average water temperature data were recorded at La Casella Power Station operated by the ENEL group (https://www.enel.com/it/media/esplora/ricerca-foto/photo/2020/03/italia-centrale-la-casella) and at Piacenza Power Station operated by the A2A Life Company Group (https://www.a2a.eu/en/group), and integrated to cover the period 1992–2020. Water temperature measurements were carried out using RTD probes with platinum Pt100 resistance thermometers with a nominal resistance of 100 Ω at 0°C, defined according to IEC 751 (EN 60751). Other sensor features: measuring range 0–40°C, accuracy ±0.1°C at 0°C, 4-wire connection, signal conversion electronics with 4-20 mA output in the range 0–40°C.

A validation procedure was applied to reconstruct a continuous three-decade time series from the daily water temperature values recorded at the two sites. The water temperature of the Po River was retrieved from the ARPAE database (https://dati.arpae.it/group/acqua) for the two stations in the

official monitoring network. The ARPAE Castel San Giovanni station (45°05'30.0"N, 9°26'44.2"E) is located close to the La Casella Power Station (<2 km), whereas the ARPAE Piacenza statio' (45"03′37.9'N, 9"42′19.9"E) is located close to the A2A Piacenza Power Station (<1.5 km). Water temperatures were obtained from monthly sampling campaigns conducted on the same day (within < 2 hr) for the two stations as part of the ARPAE environmental monitoring program. The observations made on the same day at the two ARPAE stations were consistent. Because of the very good correlation (Appendix A Fig. S2) and a discrepancy of less than 0.3°C, on average, between the observations, the merging of the two datasets was considered appropriate. Occasional missing data points (up to five consecutive days) owing to temporary maintenance operations of the thermoelectric power plants were linearly interpolated between two subsequent sampling events. From the daily temperature data, annual and seasonal trends in the average, minimum, and maximum values were analysed according to the monthly clustering previously described for nutrient loads. The occurrence of warm days (i.e., the number of days with water temperatures above the long-term average) was assessed on an annual and seasonal scales.

Nutrient loads transported seasonally and annually at the basin closing section (i.e., Pontelagoscuro) were related to the water temperature data recorded at the Piacenza section. Water temperature data that were both sufficiently detailed (daily) and recorded over the entire 1992–2020-time interval were not available for the Pontelagoscuro section. Although in the river reach between Piacenza and Pontelagoscuro the inflow of tributaries and groundwater does not substantially modify the thermal regime (data not shown), it should be noted that Pontelagoscuro is the most suitable section for calculating loads, as it is at the end of the basin before the delta, and Piacenza is the most suitable section for measuring temperature, as it is in the middle of the river, thus providing average values of all the hydrological situations that contribute to the overall nutrient metabolism and denitrification capacity expressed by the river .

Continuous air temperature measurements were obtained from a monitoring station located close to the course of the Po River, near the city of Piacenza (45"02′15.0'N, 9"42′03.5"E). Time series were retrieved from the ARPAE climate database (Antolini et al., 2016; https://dati.arpae.it/dataset/erg5-eraclito) and analysed as previously described for the water temperature datasets.

1.4. *Calculation of nutrient loads from diffuse and point sources in the basin*

Changes in anthropogenic pressures in the Po River basin and in nutrient loads from diffuse (agriculture) and point sources (urban areas) were assessed by collecting census data at 10-years intervals over the last three decades. N and P loads from diffuse sources were quantified by calculating the soil budget (SB), i.e., accounting for the difference between inputs (livestock manure, synthetic fertilizers, atmospheric deposition, and biological fixation in the case of N) and outputs via crop harvest (Romero et al., 2021). Point sources (PS) N and P loads were quantified using resident population data and the per capita nutrient production coefficients corrected for the percentage of sewerage systems connected to wastewater treatment plants and the depuration efficiency. The details of the calculation methods, sources of the census data and coefficients are presented in Appendix A Tables S1, S2 and S3).

1.5. *Statistical analyses*

Parametric (linear regression) and non-parametric (Mann-Kendall, Sens's slope and Pettitt's test) tests were applied to the annual and seasonal historical data of temperature, riverine nutrient loads, and discharge (Helsel et al., 2020). The Mann–Kendall test was used to verify the presence of a significant monotonic trend in the time series, whereas Sen's test quantified the magnitude of this change by calculating the slope of the linear interpolation model. The relationship between the water temperature and nutrient loads of the Po River (monthly values) was tested using Pearson's correlation analysis. Statistical analyses were performed using the XLSTAT (Addinsoft, 2022). In all cases, the trends and factors tested were considered to be statistically significant at $p < 0.05$.

2. Results and discussion

2.1. *Trajectories of annual and seasonal nutrient export from the Po River basin*

Over the last three decades, the annual TN load exported by the Po River to the Adriatic Sea showed high inter-annual variability, ranging from ~68,000 tons N/year (2017) to ~238,000 tons N/year (1996), while a significant negative trend was observed (Fig. 2a, Appendix A Table S4), with an average decrease of 20% in the last decade compared to the '90s. Nitrate was the most abundant form of N, accounting for 62%–86% of the annual TN load (Fig. 2a), a common feature of agriculture-dominated watersheds (Pina-Ochoa and Álvarez-Cobelas, 2006; Hill, 2023; Li et al., 2023). During the period 1992–2020, a significant load reduction was also observed for NO_3^- (23%), although the export varied greatly among years according to hydrological conditions, with the highest values occurring in 1996 and 2014 (+40%−54% of the long-term average annual discharge) and the lowest in 2007 and 2017 (−45% of the long-term average annual discharge). The annual NH_4^+ load was quantitatively much less relevant (1%−5% of TN load), but, similar to NO_3^-, reached a minimum in 2017 and a maximum in 1996. During the study period, annual NH_4^+ export decreased by more than 50%, from ~5,600 tons N/year in the early 1990s to less than 2,700 tons N/year in the last decade (Fig. 2a, Appendix A Table S4). The annual loads of TP and PO_4^{3-}, accounting for on average of 40%, were characterized by a high inter-annual variability, mainly due to the highly variable hydrological conditions; however, in contrast to the loads of TN and its dissolved inorganic forms, without a significant decreasing trend in recent years (Table 1, Fig. 3a).

The decrease in nitrogen export to the Adriatic Sea was not related to changes in anthropogenic pressures in the catchment area or nutrient loads from diffuse (agriculture) and point sources (sewage). The soil N budget in agricultural land showed a steady constant excess in the last three decades

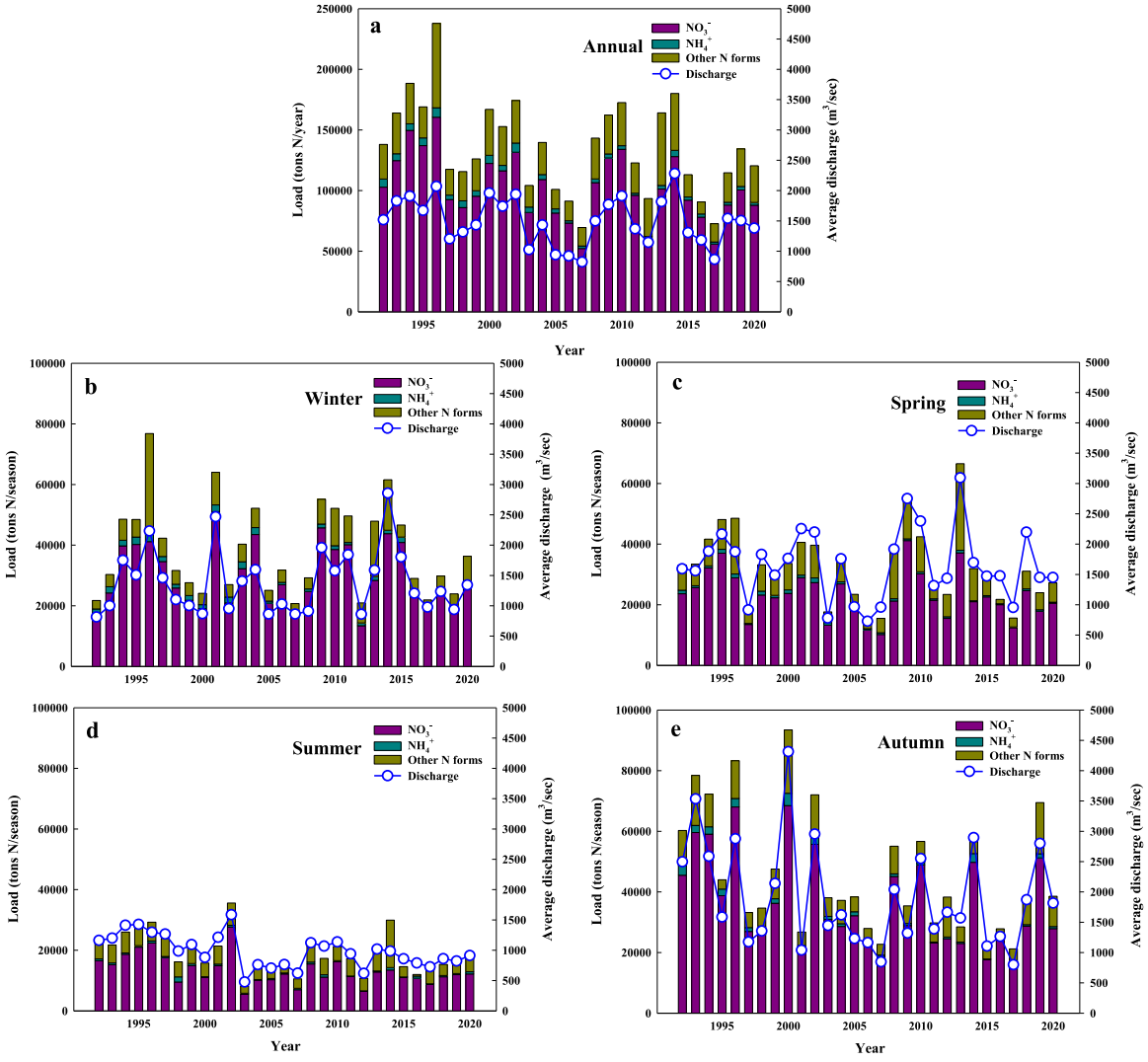

Fig. 2 – Trajectories of annual and seasonal N loads (TN, NO_3^-, and NH_4^+) and average discharge measured at the Po River closing section.

Table 1 – Decadal changes (1990–2020) of the soil N budget (SB-N) and the N load from point sources (PS-N) in the Po River basin. All budget terms are expressed as ktons N/year.

Year	N_{Man}	N_{Fert}	N_{Fix}	N_{Dep}	N_{Harv}	SB-N	PS-N
1990	214.1±30.6	231.0±3.2	194.3±33.3	31.9±4.7	336.8±22.3	**334.5±94.1**	**40.3±1.8**
2000	221.6±31.8	217.8±3.0	174.4±28.0	31.9±4.8	372.6±24.6	**273.1±92.2**	**22.1±2.2**
2010	221.9±29.4	170.9±2.3	149.7±25.5	24.3±3.7	290.8±22.3	**276.0±83.2**	**22.9±2.4**
2020	222.2±31.0	195.4±2.7	126.5±21.2	24.5±3.7	270.1±18.8	**298.4±77.4**	**23.4±2.5**

N_{Man} = N in livestock manure; N_{Fert} = synthetic N fertilizers; N_{Fix} = biological fixation; N_{Dep} = atmospheric N deposition; N_{Harv} = N export with crop harvest

(Table 1). Total N inputs showed a slight decrease in 2010 compared to the previous two decades, but this was also associated with a decrease in crop N harvest, resulting in a net surplus that was not significantly different between the two periods, taking into account the uncertainty associated with the budget terms. In contrast to N, there was a marked decrease in the soil P budget between 1990 and 2000, mainly due to the reduction in the use of synthetic fertilisers, which together with livestock manure are the main inputs to agricultural land (Table 1). While the resident population of the Po River basin has remained almost stable over the last three decades (~17 million), nutrient loads from point sources decreased by about 45% between 1990 and 2000, and then remained almost constant until today. The reduction in nutrient loads from urban areas occurred exclusively in the first decade of the study period and followed a significant abate-

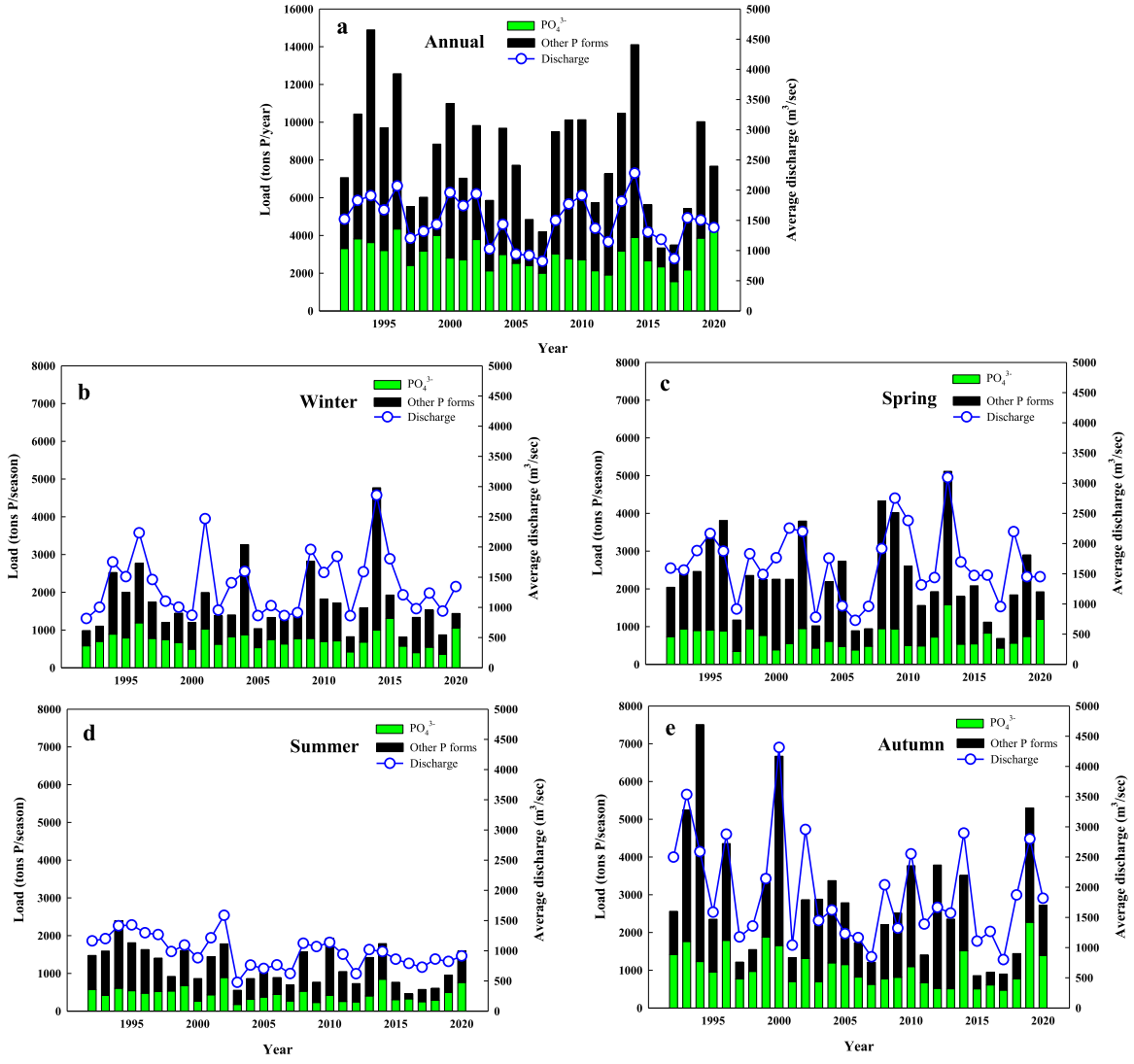

Fig. 3 – Trajectories of annual and seasonal P loads (TP and PO_4^{3-}) and average discharge measured at the Po River closing section.

ment in direct discharges of untreated or poorly treated domestic wastewater into surface waters. Indeed, the enforcement of environmental policies and legislative acts aimed at controlling nutrient emissions from point sources, such as the construction of wastewater treatment plants, the introduction of nitrification/denitrification processes, and the ban on polyphosphates in detergents in the early '90s, led to a marked reduction in N and P loads from domestic sources (de Wit and Bendoricchio, 2001; Palmeri et al., 2005). Nitrogen load decline from urban areas may have been partly responsible for the decrease of riverine NH_4^+ loads, but it was not in the order of magnitude to explain the decrease recorded for the riverine TN loads. Overall, nutrient loads from point sources have accounted for 3%–6% of the total nutrient inputs from diffuse agricultural sources over the last three decades (Tables 1 and 2).

Previous experimental and modelling studies have quantified the historical trajectories of annual nutrient export from the Po River basin (e.g., Cozzi et al., 2018; Viaroli et al., 2018), but none of them have isolated the seasonal contributions and analysed their temporal evolution, although a preliminary investigation of N export during the spring-summer months has been reported by Gervasio and co-authors (2022a). The present

Table 2 – Decadal changes (1990–2020) of the soil P budget (SB-P) and the P load from point sources (PS-P) in the Po River basin. All budget terms are expressed as ktons P/year.

Year	P_{Man}	P_{Fert}	P_{Dep}	P_{Harv}	SB-P	PS-P
1990	62.8±4.2	55.38±0.7	0.67±0.1	53.1±3.1	**65.8±8.1**	**6.5±0.3**
2000	57.4±3.2	37.95±0.5	0.67±0.1	63.36±4.0	**32.7±7.8**	**3.5±0.6**
2010	57.71±3.1	27.92±0.4	0.61±0.1	50.72±4.0	**35.5±7.5**	**3.6±0.6**
2020	49.9±2.7	27.1±0.4	0.50±0.1	51.70±4.0	**25.8±7.1**	**3.7±0.6**

P_{Man} = P in livestock manure; P_{Fert} = synthetic P fertilizers; P_{Dep} = atmospheric P deposition; P_{Harv} = P export with crop harvest

results clearly show that considering the overall decline in annual N loads may mask significant differences in the load trends at the seasonal scale. In the Po River, the main contributions to the annual TN loads were autumn (34% on average, range 17%–56%) and winter (29% on average, range 14%–42%), while spring and summer loads represented 15%–41% (23% on average) and 8%–21% (14% on average), of the corresponding annual values, respectively (Fig. 2). The analysis of the seasonal trends showed a significant decline in summer and autumn for TN loads (Fig. 2d, e, Appendix A Table S4), decreasing on average by 26% and 32%, respectively, in the last decade compared to the '90s, while this tendency was not detected in winter and spring when the temporal variation was more erratic (Fig. 2b, c, Appendix A Table S4). The seasonal distribution of NO_3^- and NH_4^+ overlapped with that of TN, with an average of two-thirds of the annual loads transported during the autumn-winter months. This is a common finding in watersheds with Mediterranean or temperate climates where most of the riverine N export occurs during the wet season, when hydrological processes overwhelm the in-stream N metabolism (McCrackin et al., 2014; Compton et al., 2020). The time series of NO_3^- loads exhibited a downward trend in summer and autumn (Fig. 2d, e, Appendix A Table S4), decreasing by 32%, whereas no significant decline was observed in spring and winter, although the annual NO_3^- loads were reduced by 12%–22% in the last five years compared to the previous decades. No tendency towards reduced export was observed for P forms, except in summer (Fig. 3d, Appendix A Table S4).

Over the last three decades, the hydrological conditions of the Po River have been characterized by large inter-annual oscillations, but without any significant downward or upward trend. On a seasonal scale, only summer discharge showed a highly significant decrease with a breakpoint in the time series observed in 2002, the same year when the decline in summer TN and NO_3^- loads started (Appendix A Table S4, Table 3). In fact, the Po River experienced temporary phases of low regime during 2003–2007 and 2015–2017 (Zanchettin et al., 2008; Montanari et al., 2012; Marchina et al., 2019), the periods most affected by prolonged droughts with a consequent strong reduction in nutrient loads transported to the coastal zones.

After the flow normalisation procedure, highly significant downward trends were detected for loads of TN and the two dissolved inorganic species, NO_3^- and NH_4^+, at both annual and seasonal scales, with the sole exception of summer (Appendix A Table S4, Fig. 3), highlighting that a considerable contribution to the variability in summer nutrient transport was undoubtedly due to variations in water flow. The most marked decline of TN and NO_3^- loads occurred in spring (15%–19%) and autumn (18%–21%), whereas for NH_4^+ the decrease was generalized and always >30% in the last decade compared to the '90s (Fig. 4). In contrast to N, no significant downward trends were detected for the flow-normalized P loads (Fig. 5).

Assessing the intra-annual dynamics of nutrient loads is crucial for identifying those periods when the risk of eutrophication is particularly high. Phytoplankton growth and coastal biogeochemical dynamics are constrained by environmental factors that follow seasonal cycles (Glibert, 2017; Cozzi et al., 2018; Ricci et al., 2022), but seasonal patterns of nutrient loads are rarely analysed (Gervasio et al., 2022a), and there is a lack of systematic research predicting the effects of climate change on river nutrient cycling alongside the expected intra-annual export variations. This study provides the first evidence of long-term changes in N export from the Po River, demonstrating a generalized decline over the years but with different extent at the seasonal scale: lower N loads are transported to the Adriatic Sea throughout the spring-summer-early autumn period, when the risk of eutrophication in the coastal lagoons is higher. Summer N loads declined owing to a reduction in water flow, while downward trends in the other seasons are likely to be related to other drivers that require further investigation.

2.2. *Water temperature trends*

Since 1992, the annual average water temperature of the Po River has increased by almost 3.5°C, corresponding to an overall rate of 0.12°C/year and the warming accelerated in 2004, when a breakpoint in the time series was detected (Table 3). The analysis of the daily river temperatures showed the existence of two phases: a condition of relative stability characterized the first decade of the series with an average value of 13.91±0.24°C and low inter-annual variability, then a marked increase occurred, and the temperature varied widely among the years with a mean value of 15.95±0.97°C (Fig. 6a). Highly significant upward trends were identified in all seasons, with the most pronounced warming signals in summer (0.13°C/year) and autumn (0.16°C/year) starting in 2002 and 2006, respectively (Table 3), while the spring and winter increases averaged at 0.10°C/year (Fig. 6a). The present outcomes were consistent with the analysis of the air temperature trends, which showed a significant warming in annual and seasonal values, with the highest slope in summer and the early 2000s as change point years in the time series (Appendix A, Fig. S3, Table S5). This is in agreement with previous long-term climate studies and model-based climate projections demonstrating that warming has occurred throughout the Po River basin since the '80s, with more pronounced changes in summer followed by spring and elevated temperatures maintained until the mid-autumn (Appiotti et al., 2014; Fioravanti et al., 2016; Vezzoli et al., 2015).

The temperature increase measured for the Po River was found to be almost an order of magnitude (or at the very least two times) faster than the increases observed in other large temperate European rivers over similar time periods (Hannah and Garner, 2015; Arora et al., 2016; Hardenbicker et al., 2017; Ptak et al., 2022), suggesting that Mediterranean watercourses may be among the most vulnerable worldwide to the impacts of climate change and require more research attention.

Similar to the trends observed for mean temperature, the minimum and maximum water temperature time series showed marked warming since the 2000s and an increased inter-annual variability for both annual and the seasonal values (Fig. 6b, c, Table 3). The highest annual temperature values (up to 29–31°C) were recorded in 2003–2007 and 2015–2017, two periods characterized by both climatic anomalies (reduced precipitation, high air temperature in summer) and hydrological extremes (phases of low flow regime in

Table 3 – Summary of statistical results from the trend analysis performed on water temperature and discharge datasets. Values in bold are statistically significant at p=0.05. Arrows indicate significant increasing or decreasing trends.

Variable	Period	Linear regression	Mann-Kendall				Pettitt test		
		p-value	Kendall's tau	p-value	Sen's slope	Trend	K	p-value	Change point year
Average water temperature	Annual	**<0.0001**	**0.695**	**<0.0001**	**0.124**	**↑**	**200**	**<0.0001**	**2004**
	Winter	**<0.0001**	**0.488**	**0.0002**	**0.103**	**↑**	**182**	**<0.0001**	**2006**
	Spring	**0.0019**	**0.453**	**0.0006**	**0.093**	**↑**	**152**	**0.004**	**2002**
	Summer	**<0.0001**	**0.567**	**<0.0001**	**0.134**	**↑**	**198**	**<0.0001**	**2002**
	Autumn	**<0.0001**	**0.700**	**<0.0001**	**0.160**	**↑**	**206**	**<0.0001**	**2005**
Minimum water temperature	Annual	**0.0001**	**0.545**	**<0.0001**	**0.120**	**↑**	**188**	**<0.0001**	**2005**
	Winter	**0.0001**	**0.441**	**0.0008**	**0.101**	**↑**	**170**	**0.0004**	**2006**
	Spring	**0.0025**	**0.385**	**0.0036**	**0.094**	**↑**	122	0.052	2003
	Summer	**<0.0001**	**0.647**	**<0.0001**	**0.157**	**↑**	**196**	**<0.0001**	**2002**
	Autumn	**0.0003**	**0.451**	**0.0006**	**0.120**	**↑**	**146**	**0.0062**	**2005**
Maximum water temperature	Annual	**<0.0001**	**0.527**	**<0.0001**	**0.162**	**↑**	**204**	**<0.0001**	**2004**
	Winter	**<0.0001**	**0.438**	**0.0009**	**0.147**	**↑**	**154**	**0.0024**	**2010**
	Spring	**0.0007**	**0.481**	**0.0003**	**0.160**	**↑**	**182**	**<0.0001**	**2001**
	Summer	**<0.0001**	**0.527**	**<0.0001**	**0.162**	**↑**	**204**	**<0.0001**	**2004**
	Autumn	**<0.0001**	**0.621**	**<0.0001**	**0.224**	**↑**	**210**	**<0.0001**	**2005**
Frequency of occurrence	Annual	**<0.0001**	**0.672**	**<0.0001**	**0.005**	**↑**	**195**	**<0.0001**	**2005**
	Winter	**0.0005**	**0.388**	**0.0034**	**0.013**	**↑**	**154**	**0.002**	**2006**
	Spring	**0.0068**	**0.410**	**0.0021**	**0.009**	**↑**	**143**	**0.0086**	**2002**
	Summer	**<0.0001**	**0.535**	**<0.0001**	**0.018**	**↑**	**181**	**<0.0001**	**2002**
	Autumn	**<0.0001**	**0.644**	**<0.0001**	**0.014**	**↑**	**208**	**<0.0001**	**2004**
Average discharge	Annual	0.2225	-0.172	0.196	-11.591		102	0.193	2002
	Winter	0.8338	0.020	0.8955	2.161		56	0.6352	2008
	Spring	0.9554	-0.074	0.5865	-4.158		64	0.9118	2002
	Summer	**0.0025**	**-0.379**	**0.0041**	**-17.511**	**↓**	**172**	**<0.0001**	**2002**
	Autumn	0.1210	-0.158	0.2373	-23.647		82	0.5262	2000

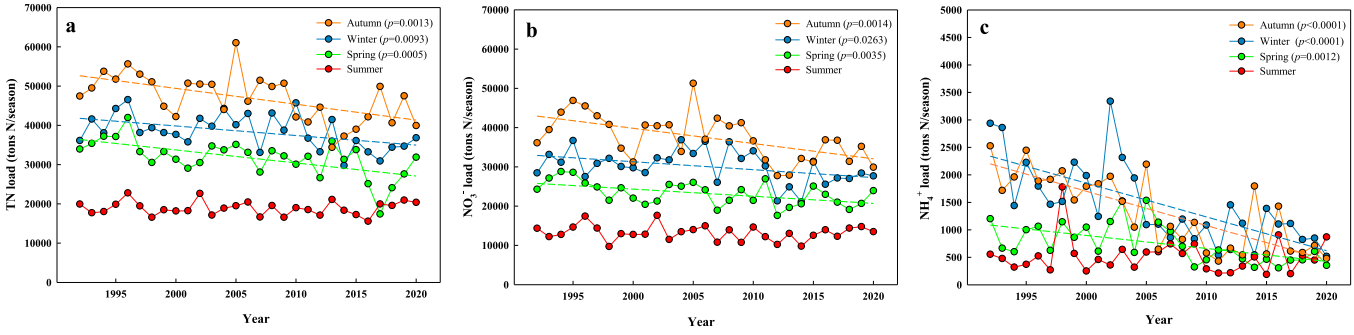

Fig. 4 – Trajectories of flow-normalized seasonal TN (panel a), NO_3^- (panel b), and NH_4^+ loads (panel c) measured at the Po River closing section.

the Po River) (Zanchettin et al., 2008; Appiotti et al., 2014; Marchina et al., 2019). The highest warming rates for the Po River water were observed for maximum temperatures in spring, summer (0.16°C/year) and autumn (0.22°C/year) (Fig. 6), together with the highest increase in the frequency of occurrence, i.e. the number of days in each season with water temperature above the long-term average, that passed from ~30% in the '90s to ~80% and ~70% in summer and autumn nowadays, respectively (Fig. 7). Summer and autumn were also characterised by the most pronounced increase in air temperature and frequency of occurrence of warm days (Appendix A, Fig. S3, Fig. S4, Table S5). In parallel with the positive trends in water temperature, the occurrence of warm days showed a noticeable increase at both the annual and the seasonal scales (Fig. 7; Table 3), suggesting an extension of the vegetative season length, as previously shown for the entire Mediterranean region (Efthymiadis et al., 2011) and other large European rivers (Hardenbicker et al., 2017). Water temperature trends were generally superimposed on air temperature trends, which is the main forcing factor explaining long-term river temperature trajectories and inter-annual variability. The coupled effect of air temperature warming, and reduced flow may explain why water temperature increased faster than air temperature, as found for

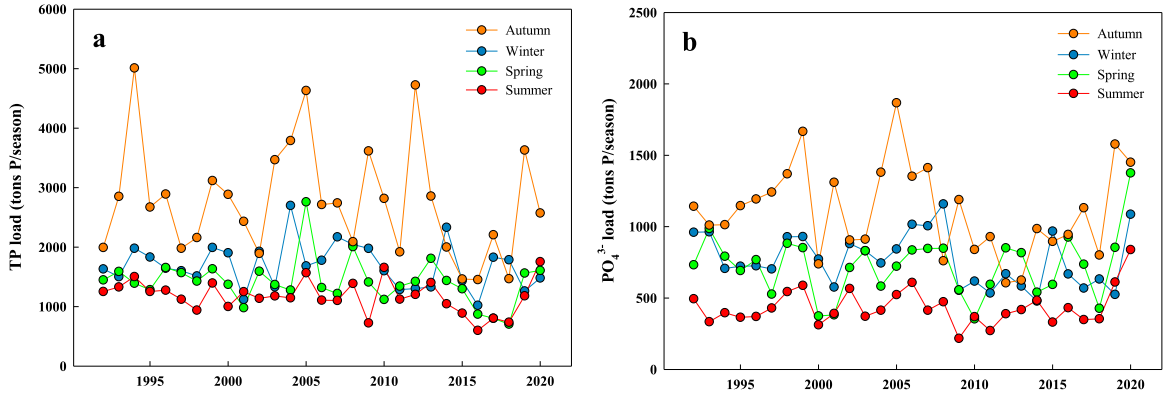

Fig. 5 – Trajectories of flow-normalized seasonal TP (panel a), and PO_4^{3-} loads (panel b) measured at the Po River closing section.

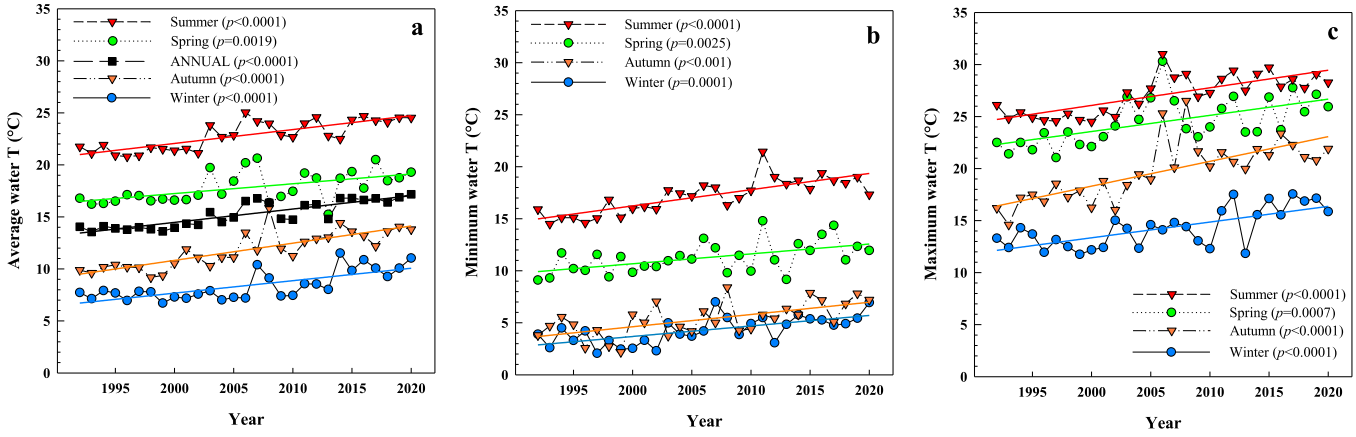

Fig. 6 – Temporal trends of average (panel a), minimum (panel b), and maximum (panel c) temperature of the Po River water.

other large European rivers (Seyedhashemi et al., 2022). This effect is likely to be exacerbated in the future, as the Po River is expected to experience lower flows and more severe summer droughts because of reduced rainfall (Vezzoli et al., 2015).

2.3. *Impact of water temperature warming on in-stream nutrient cycling*

The link between climate change and eutrophication is controversial and currently under discussion. Several previous studies have reported an increased risk of eutrophication due to warming in lentic water bodies (Jenny et al., 2016; Woolway et al., 2022). Although the scientific community has made remarkable progress in addressing the impacts of climate change in lakes and coastal zones (Glibert, 2017; Meerhoff et al., 2022), the potential feedbacks between climatic anomalies, river functioning, and water quality are still understudied and far from being evidenced and proven. Nevertheless, their understanding is crucial for the definition and implementation of effective watershed management strategies to counteract eutrophication in heavily exploited areas, such as the Po basin. The intensification of extreme climatic events causes sharp fluctuations in hydrological conditions, with marked alternation between flash floods and periods of minimum flow, thereby affecting the rates of nutrient export from agricultural soils to aquatic ecosystems, the water residence time and, consequently, the rates of permanent removal or temporary sequestration (Baron et al., 2013; Goyette et al., 2019; Costa et al., 2022). Climate change is generally expected to further delay European water quality goals by altering both the amount and timing of nutrient delivery from terrestrial ecosystems through changes in the magnitude and seasonal patterns of precipitation (Abily et al., 2021; Rozemeijer et al., 2021). Catchment-scale modelling studies developed for northern Europe have predicted boosted and accelerated annual riverine nutrient export in response to projected increase in precipitation and rising leaching effects of increased water flows, and further enhanced by temperature-induced nutrient mineralisation in soils (Øygarden et al., 2014; Plunge et al., 2022). In contrast, for the Mediterranean region, the climate models predicted a shift in the seasonal pattern of precipitation rather than a change in the total amount of precipitation, with more severe droughts in the summer and flash floods in the other seasons (Sperna Weiland et al., 2021). The alternation between large floods and droughts is likely to disrupt biogeochemical dynamics in rivers, resulting in reduced dilution effect during low flow periods and the rapid downstream delivery of large quantities of nutrients, particularly in particulate form, owing to the erosive power of intense

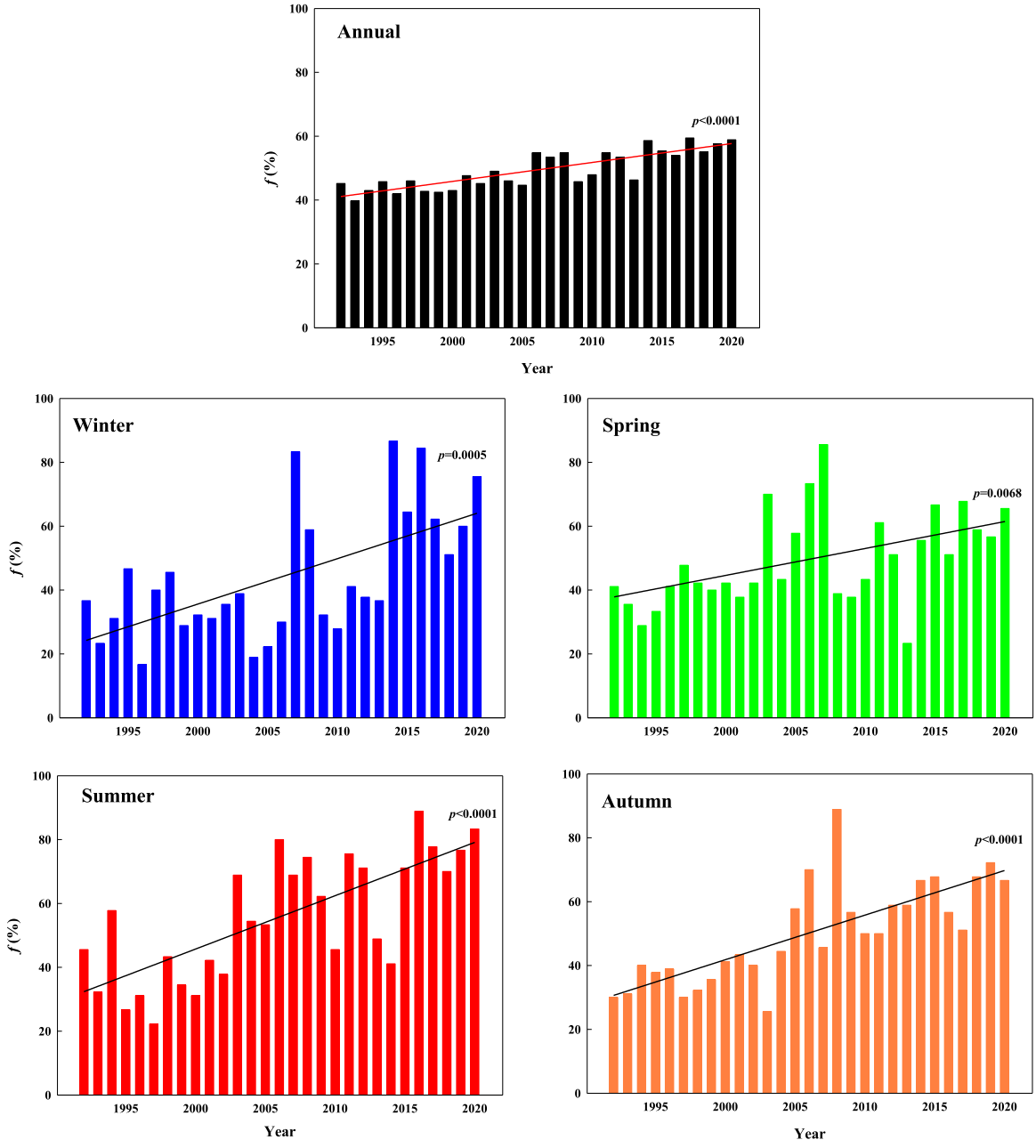

Fig. 7 – Frequency of occurrence of days with Po River water temperature above the long-term average (1992–2020). Long-term average values calculated from daily measurements were 15.2°C, 8.4°C, 17.8°C, 22.9°C, and 11.8°C for the annual, winter, spring, summer, autumn periods, respectively.

rainfall events (Withers and Jarvie, 2008; Goyette et al., 2019; Abily et al., 2021).

Contrary to previous studies in northern European catchments, a generalized negative trend in annual N loads was highlighted for the Po River, associated with a discharge reduction only for the summer season. No significant variations in annual P export were observed and this, together with the hydrological evidence, i.e., no significant long-term trend detected for the annual discharge, strongly supports the hypothesis that the riverine N load decline was not due to variations in load generation and transport but triggered by temperature-dependent effects increasing the river metabolic capacity. Highly significant negative seasonal correlations were found between monthly average water temperature and TN loads and of its main dissolved inorganic species, i.e., NO_3^- and NH_4^+ (Fig. 8). No significant relationship was found between water temperature and P export, highlighting that the main mechanisms responsible for P processing are not as strictly temperature dependent as N, which relies on key microbial processes such as nitrification and denitrification. In large turbid rivers, such as the Po, P cycling is likely less sensitive to temperature warming and the negative relationship found between water temperature and P loads only in summer (Fig. 9) likely reflects increased PO_4^{3-} uptake by

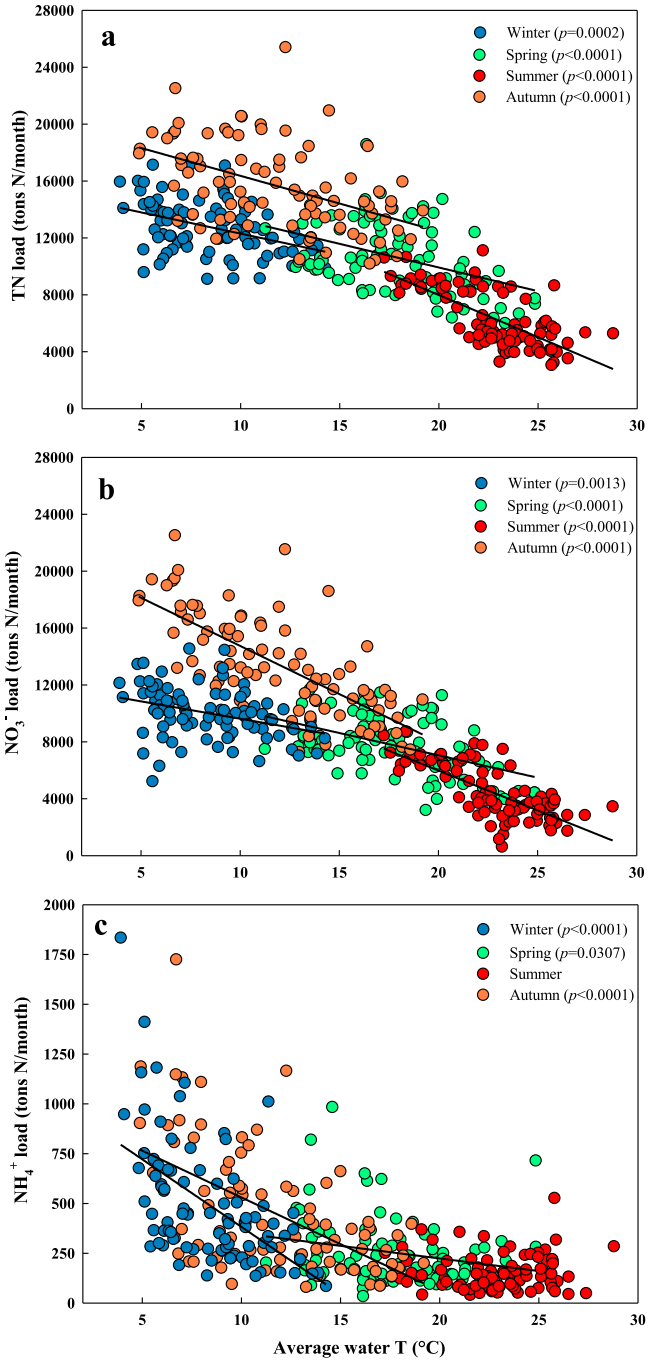

Fig. 8 – Correlations between monthly average water temperature and N loads measured at the Po River closing section.

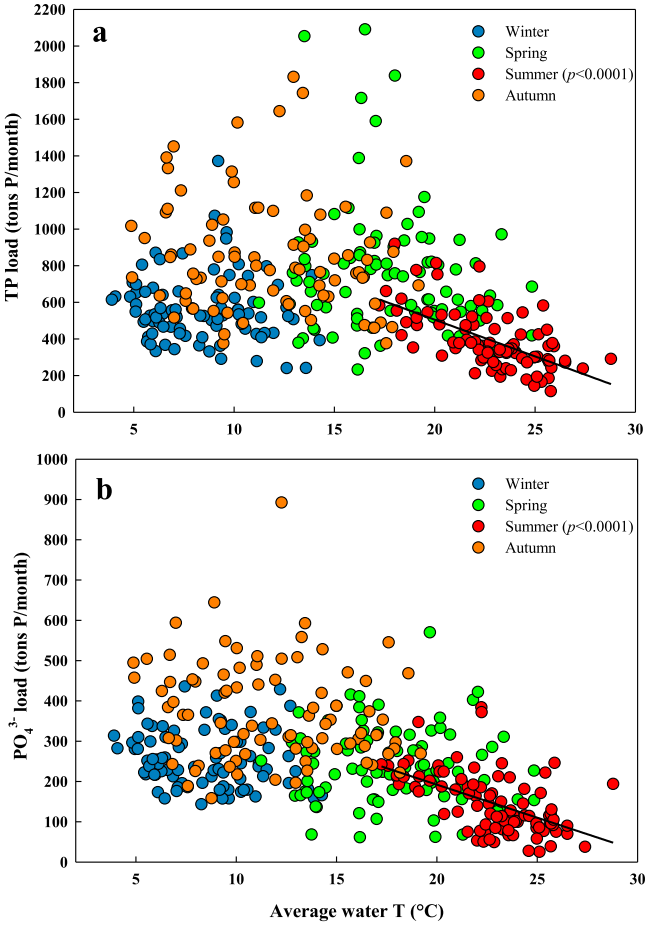

Fig. 9 – Correlations between monthly average water temperature and P loads measured at the Po River closing section.

phytoplankton (Withers and Jarvie, 2008). Differently to P, a 1°C increase in water temperature resulted in a 7% decrease of monthly TN and NO_3^- export in summer, almost 4% in spring and autumn, and about 2% in winter. Underlying biogeochemical processes support the observed inverse relationship between water temperature and N loads (Fig. 8). Water temperature warming is likely to stimulate heterotrophic activity, including denitrification, and create more favourable conditions for permanent NO_3^- removal (de Klein et al., 2017; Velthuis and Veraart, 2022), resulting in lower N delivery to the coastal zones.

The Po River basin is a global hotspot for NO_3^- pollution and eutrophication, and in recent years, denitrification rates have been widely measured in aquatic ecosystems within the basin (e.g., drainage canals, riverine wetlands, pit lakes and lagoons), as recently reviewed by Gervasio and co-authors (2022b). On the contrary, denitrification has been little documented in the riverbed sediments of the main channel. Evidence of riverine denitrification has been observed through the isotopic signature of river water collected from deltaic branches in summer (Marchina et al., 2016). Some preliminary measurements of denitrification were performed recently in the lowland reach in mid-summer by incubation of intact sediment cores. The good agreement between NO_3^- consumption and N_2 production proved that denitrification is the dominant mechanism driving NO_3^- removal from the water column, with rates among the highest found in freshwater and brackish environments (Pina-Ochoa and Álvarez-Cobelas, 2006; Reisinger et al., 2016; Gervasio et al., 2022b).

Data on dissolved organic carbon in the lowland reach of the Po River are scarce (Pettine et al., 1998) and its routine measurement has only recently been included in the institutional

monitoring programs. Concentrations average at 2.6 mg/L without any clear seasonal behavior, indicating that organic carbon is in equilibrium with NO_3^- availability (2.1 mg N/L, average value for the period 2018-2020). In fact, denitrification is an anaerobic respiration requiring organic carbon and NO_3^- in an approximate 1:1 ratio (Taylor and Townsend, 2010). When process substrates (i.e., NO_3^- and labile organic carbon) are not limiting, denitrification has a strong positive temperature dependence and is therefore sensitive to warming, as are all biogeochemical reactions controlled by microbial activities (de Klein et al., 2017; Velthuis and Veraart, 2022). This is consistent with the NO_3^- load time-series, which showed the most pronounced decline in summer and autumn, corresponding to the most marked increase in water temperature (~3.5°C and ~4°C in summer and autumn, respectively). Predicting the effects of climate change on denitrification in aquatic ecosystems is challenging because of the intertwined biogeochemical dynamics involved. Furthermore, experimental evidence on the temperature dependence of denitrification is sparse and highly variable between systems. However, a comprehensive synthesis of empirical and modeling results obtained in freshwater sediments has suggested that, in the range 15–25°C, denitrification rates may double upon a three-degree temperature rise (Veraart et al., 2011).

Nitrogen fate in rivers is not only affected by rising temperature, but other hydrological features depending on climate change, are also likely to impact the proximal drivers controlling N processing. Water warming leads to significantly greater N removal efficiency during summer low flow conditions, when denitrification and biological uptake effectively control N loads and prevent delivery to downstream waters due to longer water residence time and higher ratio of bioactive surface area to water volume (Birgand et al., 2007; Reisinger et al., 2016). For the Po River, a significant increase in water temperature in all seasons, together with an extension of the vegetative season length (i.e., an extended seasonal window of warm water temperatures) and prolonged durations of low flow periods, likely resulted in a longer residence time for NO_3^- and more opportunities for its removal in the river sediments along the lowland reaches. This evidence is supported by the inverse relationship between the number of warm days (i.e., days with water temperature above the long-term average) and the export of dissolved inorganic N forms in the spring-summer period (Appendix A, Fig. S5). It cannot be excluded that exceptional conditions of water scarcity and prolonged drought may partially disconnect rivers from floodplains, wetlands, and riparian ecosystems, reducing the extent of flooded areas and thus the possibility of reactive N removal and the denitrification capacity of the whole river system (Bernal et al., 2013; Cerco and Tian, 2021).

The negative relationship between water temperature and NH_4^+ loads in all seasons, except summer, suggests that warming may also have stimulated nitrification (Pina-Ochoa and Álvarez-Cobelas, 2006; Birgand et al., 2007). In the Po River, the water column is indeed generally well mixed, and the dissolved oxygen concentration is generally at or near 100% saturation, making the oxygen status of the surface sediment suitable to support coupled nitrification-denitrification (Gervasio et al., 2022a). This condition differs from that of other Mediterranean rivers which are experiencing declining oxygen levels correlated to upward trends of water temperatures (Diamantini et al., 2018). On the other hand, prolonged summer low flow conditions may promote the establishment of thermal and/or saline gradients and lead to partial or complete stratification, preventing the complete mixing of the water column and the NH_4^+ oxidation in the benthic compartment due to limited oxygen availability at the sediment-water interface (Gervasio et al., 2022b; Tarolli et al., 2023).

Despite the importance of bacterial denitrification in regulating N fluxes along the terrestrial-freshwater-marine continuum, the effect of ongoing hydrological variations and water temperature shifts on this process remains understudied. As data on the response of denitrification to temperature are usually obtained from microcosm experiments, it is challenging to forecast larger scale effects. Inferring how microbial communities will respond to gradual temperature increases, such as those occurring in aquatic ecosystems, is not entirely possible from short-term laboratory studies (Veraart et al., 2011; de Klein et al., 2017), making the outcome of global environmental change on N removal efficiency difficult to predict, despite the need to optimize future N budgets and management strategies. Watershed-scale studies have demonstrated a negative relationship between air temperature and N export to coastal zones (Schaefer and Alber, 2007; Salmon-Monviola et al., 2013; Wagena et al., 2018), suggesting that warming may lead to significantly higher denitrification efficiency across the landscape. Similarly, the results of the present work suggest that increased riverine denitrification associated with rising water temperatures may contribute to mitigate the N loads exported from Mediterranean catchments, with relevant implications to partially prevent coastal eutrophication.

3. Conclusions

The present study showed that for the Po River, downward trends in N export over the last three decades were correlated with upward trends in water temperature and an increasing number of warm days. The reduction of N loads can be seen as an unexpected consequence of climate change, enhancing rates of microbial denitrification in river sediments, with potential negative feedback on coastal eutrophication. In human-impacted watersheds, the study of the generation, transport, and transformation of nutrient loads is a key issue for the implementation of environmental policies to control eutrophication and protect coastal zones. Future scenarios of nutrient export from catchments must consider the simultaneous effects of hydrological changes and temperature increases that are already co-occurring. There is still a lack of scientific understanding of the net effects of climatic and hydrological extremes (e.g., dry summers or springs with unusually high temperatures) on the biogeochemistry of both freshwater and coastal ecosystems. It is crucial to investigate the combined effects of multiple stressors such as temperature, nutrient pulses following flood events, saline intrusion, on the self-depuration capacity and the balance between N removal and recycling processes in lowland stretches and deltas in order to predict how climate change will alter N fate in rivers. Furthermore, to fully understand how climate change will af-

fect eutrophication, it is necessary to incorporate the results of experimental studies on the intrinsic temperature response of key nutrient cycling processes into catchment-scale models.

Declaration of Competing Interest

The authors declare that they have no known competing financial interests or personal relationships that could have appeared to influence the work reported in this article.

Acknowledgments

This work was supported by the Consorzio di Bonifica Pianura di Ferrara (Ferrara Land Reclamation Consortium) as part of a collaboration aimed at defining management strategies to control eutrophication in the Po Delta. This research was also made possible thanks to funding from the Emilia-Romagna Region (General Directorate for Territorial and Environmental Care, Soil and Coast Protection and Land reclamation Service) in the framework of the project Post LIFE AGREE - Monitoring of the Valle di Gorino, Sacca di Goro, for the definition of a management plan in compliance with the Water Framework Directive. The authors are grateful to Dr. Emilio Viganò (A2A gencogas S.p.A.) for providing the time series of water temperature of the Po River and to Dr. Paolo Bronzi, President of the World Sturgeon Conservation Society, for valuable advice and contacts regarding the temperature data series.

Appendix A Supplementary data

Supplementary material associated with this article can be found, in the online version, at doi:10.1016/j.jes.2023.07.008.

References

Abily, M., Acuña, V., Gernjak, W., Rodríguez-Roda, I., Poch, M., Corominas, L., 2021. Climate change impact on EU rivers' dilution capacity and ecological status. Water Res. 199, 117166. doi:10.1016/j.watres.2021.117166.

Addinsoft, 2022. XLSTAT Statistical and Data Analysis Solution Paris, France. https://www.xlstat.com .

Antolini, G., Auteri, L., Pavan, V., Tomei, F., Tomozeiu, R., Marletto, V., 2016. A daily high-resolution gridded climatic data set for Emilia-Romagna, Italy, during 1961–2010. Int. J. Climatol. 36 (4), 1970–1986. doi:10.1002/joc.4473.

American Public Health Association (A.P.H.A.), American Water Works Association, Water Environment Federation, 2005. Standard Methods for the Examination of Water and Wastewater, 21st Ed. Washington DC.

APAT—IRSA/CNR. 2003. Analytical methods for water. Manuals and guidelines, 29/2003 (in Italian) https://www.isprambiente.gov.it/it/pubblicazioni/manuali-e-linee-guida/metodi-analitici-per-le-acque.

Appiotti, F., Krželj, M., Russo, A., Ferretti, M., Bastianini, M., Marincioni, F., 2014. A multidisciplinary study on the effects of climate change in the northern Adriatic Sea and the Marche region (central Italy). Regional Environ. Change 14 (5), 2007–2024. doi:10.1007/s10113-013-0451-5.

Arora, R., Tockner, K., Venohr, M., 2016. Changing river temperatures in northern Germany: trends and drivers of change. Hydrol. Processes 30 (17), 3084–3096. doi:10.1002/hyp.10849.

Artioli, Y., Friedrich, J., Gilbert, A.J., McQuatters-Gollop, A., Mee, L.D., Vermaat, J.E., et al., 2008. Nutrient budgets for European seas: a measure of the effectiveness of nutrient reduction policies. Mar. Pollut. Bull. 56 (9), 1609–1617. doi:10.1016/j.marpolbul.2008.05.027.

Baron, J.S., Hall, E.K., Nolan, B.T., Finlay, J.C., Bernhardt, E.S., Harrison, J.A., et al., 2013. The interactive effects of excess reactive nitrogen and climate change on aquatic ecosystems and water resources of the United States. Biogeochemistry 114, 71–92. doi:10.1007/s10533-012-9788-y.

Batool, M., Sarrazin, F.J., Attinger, S., Basu, N.B., Van Meter, K., Kumar, R., 2022. Long-term annual soil nitrogen surplus across Europe (1850–2019). Scientific Data 9 (1), 1–22. doi:10.1038/s41597-022-01693-9.

Battye, W., Aneja, V.P., Schlesinger, W.H., 2017. Is nitrogen the next carbon? Earth's Future 5 (9), 894–904. doi:10.1002/2017EF000592.

Beck, H.E., Zimmermann, N.E., McVicar, T.R., Vergopolan, N., Berg, A., Wood, E.F., 2018. Present and future Köppen-Geiger climate classification maps at 1-km resolution. Scientific Data 5 (1), 1–12. doi:10.1038/sdata.2018.214.

Bernal, S., von Schiller, D., Sabater, F., Martí, E., 2013. Hydrological extremes modulate nutrient dynamics in mediterranean climate streams across different spatial scales. Hydrobiologia 719 (1), 31–42. doi:10.1007/s10750-012-1246-2.

Birgand, F., Skaggs, R.W., Chescheir, G.M., Gilliam, J.W., 2007. Nitrogen removal in streams of agricultural catchments—a literature review. Crit. Rev. Environ. Sci. Technol. 37 (5), 381–487. doi:10.1080/10643380600966426.

Blaas, H., Kroeze, C., 2016. Excessive nitrogen and phosphorus in European rivers: 2000–2050. Ecol. Indic. 67, 328–337. doi:10.1016/j.ecolind.2016.03.004.

Cerco, C.F., Tian, R., 2021. Impact of wetlands loss and migration, induced by climate change, on Chesapeake Bay DO standards. JAWRA J. Am. Water Res. Ass. 58 (6), 958–970. doi:10.1111/1752-1688.12919.

Compton, J.E., Goodwin, K.E., Sobota, D.J., Lin, J., 2020. Seasonal disconnect between streamflow and retention shapes riverine nitrogen export in the Willamette River Basin. Oregon. Ecosyst. 23 (1), 1–17. doi:10.1007/s10021-019-00383-9.

Coppola, E., Verdecchia, M., Giorgi, F., Colaiuda, V., Tomassetti, B., Lombardi, A., 2014. Changing hydrological conditions in the Po basin under global warming. Sci. Total Environ. 493, 1183–1196. doi:10.1016/j.scitotenv.2014.03.003.

Costa, D., Sutter, C., Shepherd, A., Jarvie, H., Wilson, H., Elliott, J., et al., 2022. Impact of climate change on catchment nutrient dynamics: insights from around the world. Environ. Rev. 31 (1), 4–25. doi:10.1139/er-2021-0109.

Cozzi, S., Ibáñez, C., Lazar, L., Raimbault, P., Giani, M., 2018. Flow regime and nutrient-loading trends from the largest South European watersheds: Implications for the productivity of Mediterranean and Black Sea's Coastal Areas. Water 11 (1), 1. doi:10.3390/w11010001.

de Klein, J.J., Overbeek, C.C., Juncher Jørgensen, C., Veraart, A.J., 2017. Effect of temperature on oxygen profiles and denitrification rates in freshwater sediments. Wetlands 37, 975–983. doi:10.1007/s13157-017-0933-1.

de Wit, M., Bendoricchio, G., 2001. Nutrient fluxes in the Po basin. Sci. Total Environ. 273 (1-3), 147–161. doi:10.1016/S0048-9697(00)00851-2.

Diamantini, E., Lutz, S.R., Mallucci, S., Majone, B., Merz, R., Bellin, A., 2018. Driver detection of water quality trends in three large European river basins. Sci. Total Environ. 612, 49–62. doi:10.1016/j.scitotenv.2017.08.172.

Domeneghetti, A., Castellarin, A., Brath, A., 2012. Assessing

rating-curve uncertainty and its effects on hydraulic model calibration. Hydrol. Earth Syst. Sci. 16 (4), 1191–1202. doi:10.5194/hess-16-1191-2012.
Efthymiadis, D., Goodess, C.M., Jones, P.D., 2011. Trends in Mediterranean gridded temperature extremes and large-scale circulation influences. Natural Hazards Earth Syst. Sci. 11 (8), 2199–2214. doi:10.5194/nhess-11-2199-2011.
Fioravanti, G., Piervitali, E., Desiato, F., 2016. Recent changes of temperature extremes over Italy: an index-based analysis. Theor. Appl. Climatol. 123, 473–486. doi:10.1007/s00704-014-1362-1.
Formetta, G., Tootle, G., Therrell, M., 2022. Regional reconstruction of Po River Basin (Italy) streamflow. Hydrology 9 (10), 163. doi:10.3390/hydrology9100163.
Gervasio, M.P., Soana, E., Granata, T., Colombo, D., Castaldelli, G., 2022a. An unexpected negative feedback between climate change and eutrophication: higher temperatures increase denitrification and buffer nitrogen loads in the Po River (Northern Italy). Environ. Res. Lett. 17 (8). doi:10.1088/1748-9326/ac8497.
Gervasio, M.P., Soana, E., Vincenzi, F., Castaldelli, G., 2022b. An underestimated contribution of deltaic denitrification in reducing nitrate export to the coastal zone (Po River–Adriatic Sea, Northern Italy). Water 14 (3), 501. doi:10.3390/w14030501.
Glibert, P.M., 2017. Eutrophication, harmful algae and biodiversity—challenging paradigms in a world of complex nutrient changes. Mar. Pollut. Bull. 124 (2), 591–606. doi:10.1016/j.marpolbul.2017.04.027.
Goyette, J.O., Bennett, E.M., Maranger, R., 2019. Differential influence of landscape features and climate on nitrogen and phosphorus transport throughout the watershed. Biogeochemistry 142 (1), 155–174. doi:10.1007/s10533-018-0526-y.
Hannah, D.M., Garner, G., 2015. River water temperature in the United Kingdom: changes over the 20th century and possible changes over the 21st century. Prog. Phys. Geog. 39 (1), 68–92. doi:10.1177/0309133314550669.
Hardenbicker, P., Viergutz, C., Becker, A., Kirchesch, V., Nilson, E., Fischer, H., 2017. Water temperature increases in the river Rhine in response to climate change. Regional Environ. Change 17, 299–308. doi:10.1007/s10113-016-1006-3.
Helsel, D.R., Hirsch, R.M., Ryberg, K., Archfield, S., Gilroy, E., 2020. Statistical Methods in Water Resources Techniques and Methods 4 A3. USGS Tech. Methods 458. https://pubs.er.usgs.gov/publication/tm4A3.
Hill, A.R., 2023. Patterns of nitrate retention in agriculturally influenced streams and rivers. Biogeochemistry 163 (2), 155–183. doi:10.1007/s10533-023-01027-w.
Howarth, R., Swaney, D., Billen, G., Garnier, J., Hong, B., Humborg, C., et al., 2012. Nitrogen fluxes from the landscape are controlled by net anthropogenic nitrogen inputs and by climate. Front. Ecol. Environ. 10 (1), 37–43. doi:10.1890/100178.
IPCC, 2021. Climate Change 2021: The Physical Science Basis. Contribution of Working Group I to the Sixth Assessment Report of the Intergovernmental Panel on Climate Change. Cambridge University Press.
Jenny, J.P., Francus, P., Normandeau, A., Lapointe, F., Perga, M.E., Ojala, A., et al., 2016. Global spread of hypoxia in freshwater ecosystems during the last three centuries is caused by rising local human pressure. Global Change Biol. 22 (4), 1481–1489. doi:10.1111/gcb.13193.
Lenhart, H.J., Mills, D.K., Baretta-Bekker, H., Van Leeuwen, S.M., Van Der Molen, J., Baretta, J.W., et al., 2010. Predicting the consequences of nutrient reduction on the eutrophication status of the North Sea. J. Mar. Syst. 81 (1-2), 148–170. doi:10.1016/j.jmarsys.2009.12.014.
Li, X., Xu, Y.J., Ni, M., Wang, C., Li, S., 2023. Riverine nitrate source and transformation as affected by land use and land cover. Environ. Res. 222, 115380. doi:10.1016/j.envres.2023.115380.
Ludwig, W., Dumont, E., Meybeck, M., Heussner, S., 2009. River discharges of water and nutrients to the Mediterranean and Black Sea: major drivers for ecosystem changes during past and future decades? Prog. Oceanogr. 80 (3-4), 199–217. doi:10.1016/j.pocean.2009.02.001.
Malone, T.C., Newton, A., 2020. The globalization of cultural eutrophication in the coastal ocean: causes and consequences. Front. Marine Sci. 7, 670. doi:10.3389/fmars.2020.00670.
Marchina, C., Bianchini, G., Natali, C., Knöller, K., 2016. Geochemical and isotopic analyses on the Po delta water: insights to understand a complex riverine ecosystem. Rendiconti Lincei 27, 83–88. doi:10.1007/s12210-015-0465-7.
Marchina, C., Natali, C., Bianchini, G., 2019. The Po River water isotopes during the drought condition of the year 2017. Water 11 (1), 150. doi:10.3390/w11010150.
McCrackin, M.L., Harrison, J.A., Compton, J.E., 2014. Factors influencing export of dissolved inorganic nitrogen by major rivers: A new, seasonal, spatially explicit, global model. Global Biogeochem. Cycles 28 (3), 269–285. doi:10.1002/2013GB004723.
Meerhoff, M., Audet, J., Davidson, T.A., De Meester, L., Hilt, S., Kosten, S., et al., 2022. Feedback between climate change and eutrophication: revisiting the allied attack concept and how to strike back. Inland Waters, pp. 1–18. doi:10.1080/20442041.2022.2029317.
Moatar, F., Meybeck, M., 2005. Compared performances of different algorithms for estimating annual nutrient loads discharged by the eutrophic River Loire. Hydrol. Processes 19 (2), 429–444. doi:10.1002/hyp.5541.
Montanari, A., 2012. Hydrology of the Po River: looking for changing patterns in river discharge. Hydrol. Earth Syst. Sci. 16 (10), 3739–3747. doi:10.5194/hess-16-3739-2012.
Nava, V., Patelli, M., Rotiroti, M., Leoni, B., 2019. An R package for estimating river compound load using different methods. Environ. Modell. Software 117, 100–108. doi:10.1016/j.envsoft.2019.03.012.
Øygarden, L., Deelstra, J., Lagzdins, A., Bechmann, M., Greipsland, I., Kyllmar, K., et al., 2014. Climate change and the potential effects on runoff and nitrogen losses in the Nordic–Baltic region. Agricult., Ecosyst. Environ. 198, 114–126. doi:10.1016/j.agee.2014.06.025.
Palmeri, L., Bendoricchio, G., Artioli, Y., 2005. Modelling nutrient emissions from river systems and loads to the coastal zone: Po River case study, Italy. Ecol. Modell. 184 (1), 37–53. doi:10.1016/j.ecolmodel.2004.11.007.
Pettine, M., Patrolecco, L., Camusso, M., Crescenzio, S., 1998. Transport of carbon and nitrogen to the northern Adriatic Sea by the Po River. Estuarine Coastal Shelf Sci. 46 (1), 127–142. doi:10.1006/ecss.1997.0303.
Pina-Ochoa, E., Álvarez-Cobelas, M., 2006. Denitrification in aquatic environments: a cross-system analysis. Biogeochemistry 81 (1), 111–130. doi:10.1007/s10533-006-9033-7.
Plunge, S., Gudas, M., Povilaitis, A., 2022. Expected climate change impacts on surface water bodies in Lithuania. Ecohydrol. Hydrobiol. 22 (2), 246–268. doi:10.1016/j.ecohyd.2021.11.004.
Po River District Authority. 2021. Management Plan of the hydrographic district of the River Po. In Italian. https://pianoacque.adbpo.it/piano-di-gestione-2021/
Ptak, M., Sojka, M., Graf, R., Choiński, A., Zhu, S., Nowak, B., 2022. Warming Vistula River–the effects of climate and local conditions on water temperature in one of the largest rivers in Europe. J. Hydrol. Hydromech. 70 (1), 1–11. doi:10.2478/johh-2021-0032.
Ravazzani, G., Barbero, S., Salandin, A., Senatore, A., Mancini, M., 2015. An integrated hydrological model for assessing climate change impacts on water resources of the upper Po river basin. Water Resour. Manage. 29 (4), 1193–1215. doi:10.1007/s11269-014-0868-8.

Reisinger, A.J., Tank, J.L., Hoellein, T.J., Hall Jr, R.O., 2016. Sediment, water column, and open-channel denitrification in rivers measured using membrane-inlet mass spectrometry. J. Geophys. Res. 121 (5), 1258–1274. doi:10.1002/2015JG003261.

Ricci, F., Capellacci, S., Campanelli, A., Grilli, F., Marini, M., Penna, A., 2022. Long-term dynamics of annual and seasonal physical and biogeochemical properties: Role of minor river discharges in the North-western Adriatic coast. Estuarine Coastal Shelf Sci. 107902. doi:10.1016/j.ecss.2022.107902.

Romero, E., Ludwig, W., Sadaoui, M., Lassaletta, L., Bouwman, A.F., Beusen, A.H., et al., 2021. The Mediterranean region as a paradigm of the global decoupling of N and P between soils and freshwaters. Global Biogeochem. Cycles 35 (3). doi:10.1029/2020GB006874, e2020GB006874.

Rozemeijer, J., Noordhuis, R., Ouwerkerk, K., Pires, M.D., Blauw, A., Hooijboer, A., et al., 2021. Climate variability effects on eutrophication of groundwater, lakes, rivers, and coastal waters in the Netherlands. Sci. Total Environ. 771, 145366. doi:10.1016/j.scitotenv.2021.145366.

Salmon-Monviola, J., Moreau, P., Benhamou, C., Durand, P., Merot, P., Oehler, F., et al., 2013. Effect of climate change and increased atmospheric CO_2 on hydrological and nitrogen cycling in an intensive agricultural headwater catchment in western France. Clim. Change 120 (1–2), 433–447. doi:10.1007/s10584-013-0828-y.

Schaefer, S.C., Alber, M., 2007. Temperature controls a latitudinal gradient in the proportion of watershed nitrogen exported to coastal ecosystems. Biogeochemistry 85, 333–346. doi:10.1007/s10533-007-9144-9.

Seitzinger, S., Harrison, J.A., Böhlke, J.K., Bouwman, A.F., Lowrance, R., Peterson, B., et al., 2006. Denitrification across landscapes and waterscapes: a synthesis. Ecol. Appl. 16 (6), 2064–2090. https://doi.org/10.1890/1051-0761(2006)016[2064:DALAWA]2.0.CO;2

Seyedhashemi, H., Vidal, J.P., Diamond, J.S., Thiéry, D., Monteil, C., Hendrickx, F., et al., 2022. Regional, multi-decadal analysis on the Loire River basin reveals that stream temperature increases faster than air temperature. Hydrol. Earth Syst. Sci. 26 (9), 2583–2603. doi:10.5194/hess-26-2583-2022.

Sileika, A.S., Stålnacke, P., Kutra, S., Gaigalis, K., Berankiene, L., 2006. Temporal and spatial variation of nutrient levels in the Nemunas River (Lithuania and Belarus). Environ. Monit. Assess. 122 (1), 335–354. doi:10.1007/s10661-006-9186-9.

Soana, E., Bartoli, M., Milardi, M., Fano, E.A., Castaldelli, G., 2019. An ounce of prevention is worth a pound of cure: managing macrophytes for nitrate mitigation in irrigated agricultural watersheds. Sci. Total Environ. 647, 301–312. doi:10.1016/j.scitotenv.2018.07.385.

Sperna Weiland, F.C., Visser, R.D., Greve, P., Bisselink, B., Brunner, L., Weerts, A.H., 2021. Estimating regionalized hydrological impacts of climate change over europe by performance-based weighting of CORDEX projections. Front. Water 143. doi:10.3389/frwa.2021.713537.

Tarolli, P., Luo, J., Straffelini, E., Liou, Y.A., Nguyen, K.A., Laurenti, R., et al., 2023. Saltwater intrusion and climate change impact on coastal agriculture. PLOS Water 2 (4), e0000121. doi:10.1371/journal.pwat.0000121.

Taylor, P.G., Townsend, A.R., 2010. Stoichiometric control of organic carbon–nitrate relationships from soils to the sea. Nature 464 (7292), 1178–1181. doi:10.1038/nature08985.

Velthuis, M., Veraart, A.J., 2022. Temperature sensitivity of freshwater denitrification and N_2O emission–a meta-analysis. Global Biogeochem. Cycles doi:10.1029/2022GB007339, e2022GB007339.

Veraart, A.J., De Klein, J.J., Scheffer, M., 2011. Warming can boost denitrification disproportionately due to altered oxygen dynamics. PLoS One 6 (3), e18508. doi:10.1371/journal.pone.0018508.

Vezzoli, R., Mercogliano, P., Pecora, S., Zollo, A.L., Cacciamani, C., 2015. Hydrological simulation of Po River (North Italy) discharge under climate change scenarios using the RCM COSMO-CLM. Sci. Total Environ. 521, 346–358. doi:10.1016/j.scitotenv.2015.03.096.

Viaroli, P., Soana, E., Pecora, S., Laini, A., Naldi, M., Fano, E.A., et al., 2018. Space and time variations of watershed N and P budgets and their relationships with reactive N and P loadings in a heavily impacted river basin (Po river, Northern Italy). Sci. Total Environ. 639, 1574–1587. doi:10.1016/j.scitotenv.2018.05.233.

Wagena, M.B., Collick, A.S., Ross, A.C., Najjar, R.G., Rau, B., Sommerlot, A.R., et al., 2018. Impact of climate change and climate anomalies on hydrologic and biogeochemical processes in an agricultural catchment of the Chesapeake Bay watershed, USA. Sci. Total Environ. 637, 1443–1454. doi:10.1016/j.scitotenv.2018.05.116.

Withers, P.J.A., Jarvie, H.P., 2008. Delivery and cycling of phosphorus in rivers: a review. Sci. Total Environ. 400 (1-3), 379–395. doi:10.1016/j.scitotenv.2008.08.002.

Woolway, R.I., Sharma, S., Smol, J.P., 2022. Lakes in hot water: the impacts of a changing climate on aquatic ecosystems. Bioscience 72 (11), 1050–1061. doi:10.1093/biosci/biac052.

Yuan, Z., Jiang, S., Sheng, H., Liu, X., Hua, H., Liu, X., et al., 2018. Human perturbation of the global phosphorus cycle: changes and consequences. Environ. Sci. Technol. 52 (5), 2438–2450. doi:10.1021/acs.est.7b03910.

Zanchettin, D., Traverso, P., Tomasino, M., 2008. Po River discharges: a preliminary analysis of a 200-year time series. Clim. Change 89 (3), 411–433. doi:10.1007/s10584-008-9395-z.

Zheng, J., Cao, X., Ma, C., Weng, N., Huo, S., 2023. What drives the change of nitrogen and phosphorus loads in the Yellow River Basin during 2006-2017? J. Environ. Sci. 126, 17–28. doi:10.1016/j.jes.2022.04.039.

Appendix A Supplementary Data

Section 1

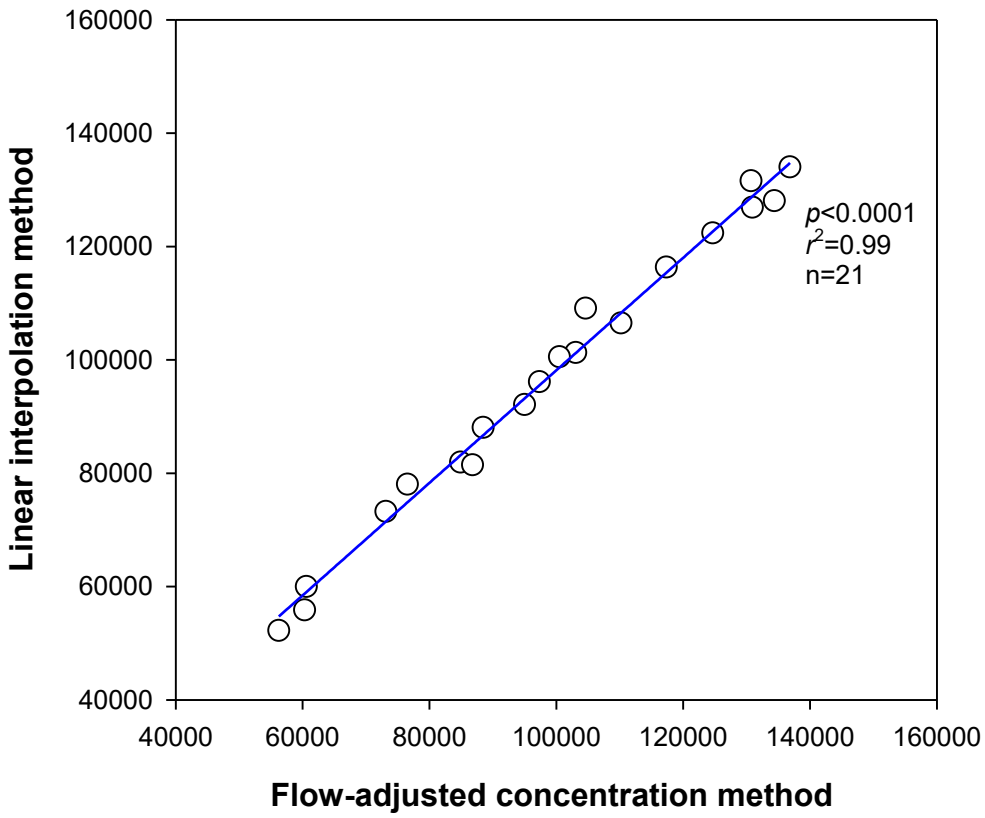

Figure S1: Correlation between annual NO_3^- loads at the closing section of the Po River basin (tons N/year, 2000–2020) calculated by the flow-adjusted concentration method and by the linear interpolation method.

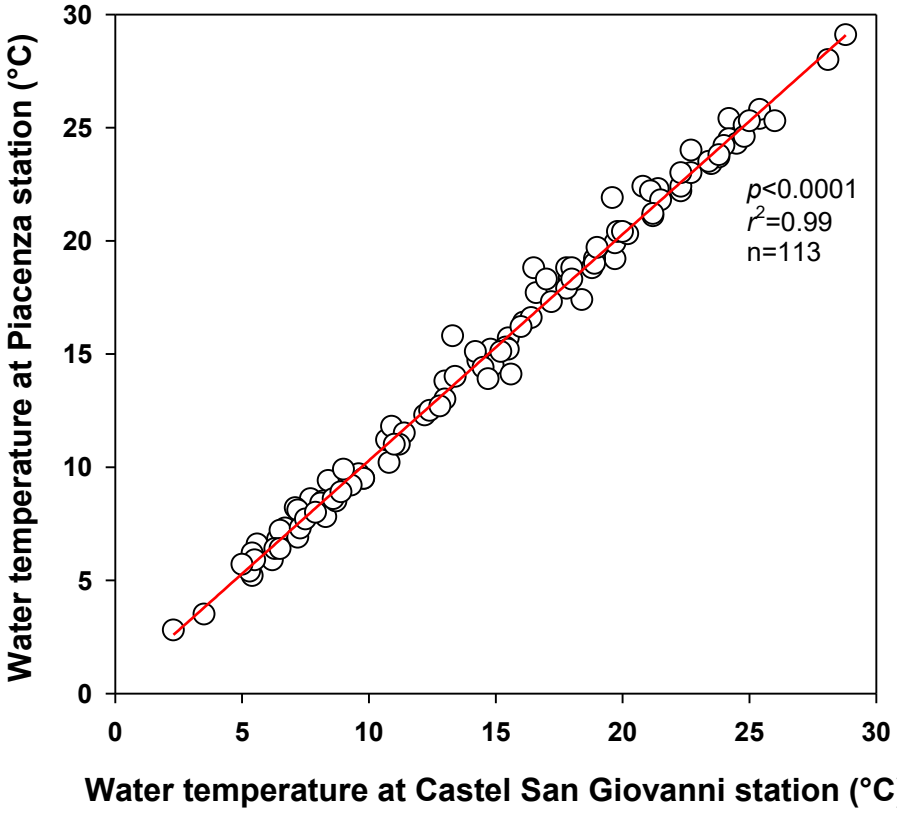

Figure S2: Relation between water temperature measured at Castel San Giovanni station and at Piacenza station. Data source: ARPAE (2000–2020; https://dati.arpae.it/group/acqua).

Section 2

Collection of census data

Statistics at the provincial level were obtained from the data warehouse of the National Institute of Statistics (ISTAT), published in the framework of the Annals of Agrarian Statistics (http://dati.istat.it/) and of the Annals of Resident Population (http://demo.istat.it/index.php). A total of 32 provinces (ranging in area from ~400 to ~6,900 km^2) were included, either wholly or partially within the catchment boundary. According to the official EU nomenclature for regional statistics elaborated by EUROSTAT (2015), Italian provinces correspond to the NUTS-3 territorial level. The statistical data were collected by consulting the printed volumes of the Annals for the years 1990 and 2000, and by web searches in the ISTAT data warehouse for the years 2010 and 2020. The values at the provincial level (of N and P loads from diffuse or point sources) were aggregated at the catchment scale by weighting, through GIS analysis (QGIS software, version 3.16), the values of each province based on the percentage of area included within the catchment boundaries.

Calculation of nutrient loads from diffuse sources (soil budget-SB)

Nutrient budgets in agricultural soils were calculated for the years 1990, 2000, 2010 and 2020, as follow:

$$SN - N = N_{Man} + N_{Fert} + N_{Fix} + N_{Dep} - N_{Harv} \quad (1)$$

$$SB - P = P_{Man} + P_{Fer} + P_{Dep} - P_{Harv} \quad (2)$$

Where:

N_{Man} and P_{Man} = N and P in livestock manure applied to agricultural soils

N_{Fert} and P_{Fert} = synthetic N and P fertilizers applied to agricultural soils

N_{Fix} = N_2 fixation by N fixing crops

N_{Dep} and P_{Dep} = atmospheric N and P deposition in agricultural soils

N_{Harv} and P_{Harv} = N and P export from agricultural soils with crop harvest

For each budget term, the type of data, equation and data sources are detailed below. Through a Monte Carlo analysis, an uncertainty has been attached to each budget term, obtained by propagating the errors in the coefficients used to calculate each specific item. The

uncertainty of the coefficients, expressed in terms of coefficient of variation (CV), was based on the best available information for the study area. Otherwise, values commonly used in watershed nutrient budgeting studies were assumed (Kroeze et al., 2003; Spiess, 2011; Cameira et al., 2019). It was assumed that all coefficients vary stochastically and independently around the mean with a normal probability distribution. For each simulation, a set of coefficients was randomly generated from probability distribution functions and a total of 1000 simulations were run.

N and P inputs from livestock manure were calculated from a) livestock density data (divided into 8 main categories and 30 subcategories according to species, age, and purpose), b) live weight of each livestock category and c) N and P excretion rates of each livestock category (DM 07/04/2006, Decree of the Italian Ministry of Agricultural and Forestry Policy on disciplinary agronomic use; Table S1). Provincial livestock data were obtained from the Annals of Agrarian Statistics (http://dati.istat.it/). For livestock excretion rates, CVs of 25% (cattle) and 10% (other livestock categories) were used (DM 07/04/2006, Decree of the Italian Ministry of Agricultural and Forest Policies on disciplinary agronomic use; Xiccato et al., 2005). It was assumed that manure was only used for spreading on arable land within the province where each farm was located.

N and P inputs (tons/year) from livestock manure were calculated as follows:

$$N_{Man}, P_{Man} = \sum_{livestock}(Exc \cdot LW \cdot N)/1000 \qquad (3)$$

Where:

Exc = N and P excretion rates of each livestock category (kg/ton live weight/year)

LW = live weight of each livestock category (tons)

N = livestock density for each category (N° of heads)

N and P inputs from synthetic fertilizers were estimated using official data on provincial-scale distribution retrieved from the Annals of Agrarian Statistics (http://dati.istat.it/) and converted into nutrient quantities using the average N and P content for each fertilizer type. The data included simple mineral N (calcium cyanamide, nitrates, ammonium sulphate, urea, and others N fertilizers), simple P fertilizers (simple superphosphate, triple superphosphate,

and other P fertilizers), compound mineral fertilizers (NP, NK, KP and NPK compounds), organic and organo-mineral fertilizers and soil amendments. It was assumed that the quantity distributed in each province corresponded to the quantity actually applied to the cropland in the same province. However, the data were cross-checked with the total nutrient demand calculated from the fertiliser application rates recommended for each crop by the Rural Development Programmes of the regions included in the Po catchment. A CV of 5% was assumed for the nutrient content of the fertiliser (Spiess, 2011).

N input from biological fixation was calculated from a) the area of each N-fixing crop type (alfalfa and soybean) and b) the areal rates of symbiotic N fixation. Biological N fixation rates were estimated by multiplying the production per unit area (i.e., yield) by the N uptake coefficient of harvested portion (Table S2), corrected by a multiplicative factor expressing the ratio of total biomass produced to harvested biomass. CVs of crop yield and N uptake coefficients were assumed to be 15% and 25%, respectively (Kroeze et al., 2003; Spiess, 2011). Values of 1.7 and 1.3 were used for alfalfa and soybean, respectively, according to Anglade et al. (2015). The provincial area and yield for each crop were obtained from the Annals of Agrarian Statistics (http://dati.istat.it/). According to the Rural Development Programme of the Regions belonging to the Po River basin, N fertilization is not allowed for N-fixing crops.

N input (tons N/year) from symbiotic fixation was calculated as follows:

$$N_{Fix} = \sum_{N-fixing\ crop}(Y \cdot Upt \cdot BGN \cdot UAA)/1000 \qquad (4)$$

where:

Y = yield of the harvest portion of each N-fixing crop (tons/ha)

BGN = factor expressing the ratio of the total biomass produced with respect to harvested biomass

Upt = N uptake coefficient of the harvest portion of N-fixing crop (kg N/ton)

UAA = surface of each N-fixing crop (ha)

Literature rates of 1–8 and 1–10 kg N/ha/year were uses for non-symbiotic N fixation in arable land and permanent crops, respectively (McKee and Eyre, 2000; Herridge et al., 2008; Butterbach-Bahl et al., 2011).

The spatialized mean of atmospheric deposition of oxidized N for the Po River basin varied between 8.5 (years 2010, 2020) and 9.5 kgN/ha/year (years 1990, 2000) according to the EMEP-Cooperative Programme for Monitoring and Evaluation of the Long-range Transmission of Air Pollutants in Europe (https://www.emep.int/). As conventionally done for N budget calculations at the watershed scale, only oxidized N species are considered, as deposition of reduced N species is likely to reflect local recycling, as NH_3 is short-lived in the atmosphere (Hong et al., 2012). The CV of N deposition was assumed to be 15% (Spiess, 2011). For P input from atmospheric deposition, an average value of 0.2 kg P/ha/year, representative of Northern Italy, was used (Mosello et al., 2002; Guieu et al., 2010; de Fommervault et al., 2015). N and P inputs from atmospheric deposition (tons/year) were calculated as follows:

$$N_{Dep}, P_{Harv} = A_{Dep} \cdot UAA_{tot} \qquad (5)$$

where:

A_{Dep} = areal values of atmospheric deposition of N and P (kg/ha/year)

UAA_{tot} = total agricultural surface (ha)

N and P outputs from crop harvest were calculated using a) the area of each crop type cultivated in the study area, b) N and P uptake coefficients, and c) the yield of the harvested portion of each crop (Table S2). For N-fixing crops, the N amount exported from agricultural land was assumed to be equal to the amount fixed in above-ground biomass. Provincial area and yield for each crop type were obtained from the Annals of Agrarian Statistics (http://dati.istat.it/). CVs of crop yield and nutrient uptake coefficients were assumed equal to 15% and 25%, respectively (Kroeze et al., 2003; Spiess, 2011; Cameira et al., 2019).

N and P outputs (tons/year) from crop harvest were calculated as follows:

$$N_{Harv}, P_{Harv} = \sum_{crop}(Y \cdot Upt \cdot UAA)/1000 \qquad (6)$$

where:

Y = yield of the harvest portion of each crop (tons/ha)

Upt = N and P uptake coefficients of the harvest portion of each crop (kg/ton)

UAA = surface of each crop (ha)

Calculation of nutrient loads from point sources (PS)

N and P loads from point sources were quantified using resident population data (Annals of Resident Population, http://demo.istat.it/index.php) and per capita production coefficients (12.5 g N/day, 1.8 g P/day; Bertanza and Boiocchi 2022) corrected for the percentage of sewerage systems connected to wastewater treatment plants-WTTPs (primary, secondary and tertiary treatment) and the corresponding depuration efficiency (Po river basin District Authority, 2015; https://pianoacque.adbpo.it/piano-di-gestione-2015/; Emilia-Romagna Region, 2017; https://datacatalog.regione.emilia-romagna.it/catalogCTA/) (Table S3).

Table S1: Livestock categories, live weights, and N and P excretion rates.

Category	Sub-category	Live weight (kg)	N excretion rate (kg N/ton live weight/year)	P excretion rate (kg P/ton live weight/year)
Cattle	cattle <1 year	220	67	18
	cattle 1-2 year: males	350	84	25
	cattle1-2 year: females	300	120	25
	cattle >2 years: males for reproduction	800	84	25
	cattle >2 years: heifers for breeding	600	120	25
	cattle >2 years: heifers for slaughtering	600	84	25
	cattle >2 years: dairy cows	600	138	35
	cattle >2 years: cows for meat and/or work	600	120	26
Buffaloes	buffalo calves	200	67	18
	famale buffaloes	600	138	35
	other buffaloes	300	84	25
Equidae	horses	350	69	26
	other (donkeys and mules)	200	69	26
Goats	goats	50	99	40
	other goats	25	99	40
Sheep	breeding females: dairy sheep	60	99	32
	breeding females: other sheep	50	99	32
	other sheep	35	99	32
Pigs	piglets < 20 kg	15	110	31
	pigs 20-50 kg	40	110	31
	pigs for fattening 50- 80 kg	65	110	31
	pigs for fattening 80- 110 kg	95	110	31
	pigs for fattening >110 kg	120	110	31
	males for reproduction	250	110	31
	sows	180	101	32
Poultry	broilers	1	250	68
	laying hens	1.9	230	94
	turkeys	6.5	167	68
Rabbits	breeding females	3.5	143	95
	other rabbits	1.7	143	95

Table S2: N and P uptake coefficients of the main crops (harvested portions) considered in the budget calculations.

Type	Crop	N uptake coefficient (kg N/ton)	P uptake coefficient (kg P/ton)
Cereals	common wheat and spelt	21.0	3.9
	durum wheat	22.8	3.9
	rye	19.3	3.1
	barley	18.1	3.1
	oats	19.1	2.6
	grain maize	14.9	3.1
	sorghum	15.9	3.1
	other cereals	18.0	3.1
Industrial crops	potato	4.2	0.4
	sugar beet	2.2	0.7
	rape and turnip rape	3.4	5.7
	sunflower	28.0	5.1
	soya beans	58.2	5.9
Fresh vegetables	tomato for processing	2.6	0.3
	other fresh vegetables	5.0	1.3
Temporary grassland	alfalfa	27.0	2.2
	other multi-annual temporary grass	21.5	2.4
	annual grass: green maize consumed directly	4.0	0.7
	annual grass: green maize for silage	4.0	0.7
	other monophytous annual grass, cereal	4.0	0.7
	other annual grass	26.0	1.3
Permanent grassland	meadows	19.7	3.9
	pastures	8.0	6.5
Permanent woody crops	vineyard	2.0	0.3
	apple-tree	0.6	0.1
	peach-tree	1.3	0.3
	apricot-tree	1.3	0.2
	pear-tree	0.6	0.1
	nectarine-tree	1.4	0.3
	kiwi-tree	1.5	0.2

Table S3: Percentage of resident population connected to wastewater treatment plants with primary, secondary, and tertiary treatments and correspondent nutrient removal efficiency.

year	Primary treatment (% of population)	Removal (%) in WTTPs with primary treatment		Secondary treatment (% of population)	Removal (%) in WTTPs with secondary treatment		Tertiary treatment (% of population)	Removal (%) in WTTPs with tertiary treatment	
		N	P		N	P		N	P
1990	50	15	20	50	60	58	0	72	58
2000	5	15	20	26	60	70	69	72	70
2010	3	15	20	27	60	70	70	72	70
2020	3	15	20	27	60	70	70	72	70

References

Anglade, J., Billen, G., Garnier, J., Makridis, T., Puech, T., Tittel, C. (2015). Nitrogen soil surface balance of organic vs conventional cash crop farming in the Seine watershed. Agricultural Systems, 139, 82-92. https://doi.org/10.1016/j.agsy.2015.06.006

Bertanza, G., Boiocchi, R. (2022). Interpreting per capita loads of organic matter and nutrients in municipal wastewater: A study on 168 Italian agglomerations. Science of The Total Environment, 819, 153236. https://doi.org/10.1016/j.scitotenv.2022.153236

Butterbach-Bahl, K., Gundersen, P., Ambus, P., Augustin, J., Beier, C., Boeckx, P., Dannenmann, M., Gimeno, B. S., Ibrom, A., Kiese, R., Kitzler, B., Rees, R., M., Smith, K., A., Stevens, C., Vesala, T. Zechmeister-Boltenstern, S. (2011) Nitrogen processes in terrestrial ecosystems. In The European Nitrogen Assessment: sources, effects, and policy perspectives (pp. 99-125). Cambridge University Press.

Cameira, M. R., Rolim, J., Valente, F., Faro, A., Dragosits, U., Cordovil, C. M. (2019). Spatial distribution and uncertainties of nitrogen budgets for agriculture in the Tagus River basin in Portugal–Implications for effectiveness of mitigation measures. Land Use Policy, 84, 278-293. https://doi.org/10.1016/j.landusepol.2019.02.028

De Fommervault, O. P., Migon, C., Dufour, A., d'Ortenzio, F., Kessouri, F., Raimbault, P., et al. (2015). Atmospheric input of inorganic nitrogen and phosphorus to the Ligurian Sea: Data from the Cap Ferrat coastal time-series station. Deep Sea Research Part I: Oceanographic Research Papers, 106, 116-125. https://doi.org/10.1016/j.dsr.2015.08.010

EUROSTAT - European Commission. Regions in the European Union. 2015. Nomenclature of territorial units for statistics NUTS 2013/EU-28. Manuals and guidelines. Luxemburgo, Publications Office of the European Union. http://ec.europa.eu/eurostat/web/products-manuals-and-guidelines/-/KS-GQ-14-006

Guieu, C., Loÿe-Pilot, M. D., Benyahya, L., Dufour, A. (2010). Spatial variability of atmospheric fluxes of metals (Al, Fe, Cd, Zn and Pb) and phosphorus over the whole Mediterranean from a one-year monitoring experiment: Biogeochemical implications. Marine Chemistry, 120(1-4), 164-178. https://doi.org/10.1016/j.marchem.2009.02.004

Herridge, D. F., Peoples, M. B., Boddey, R. M. (2008). Global inputs of biological nitrogen fixation in agricultural systems. Plant and soil, 311(1), 1-18. https://doi.org/10.1007/s11104-008-9668-3

Hong, B., Swaney, D. P., Mörth, C. M., Smedberg, E., Hägg, H. E., Humborg, C., et al. (2012). Evaluating regional variation of net anthropogenic nitrogen and phosphorus inputs (NANI/NAPI), major drivers, nutrient retention pattern and management implications in the multinational areas of Baltic Sea basin. Ecological Modelling, 227, 117-135. https://doi.org/10.1016/j.ecolmodel.2011.12.002

Kroeze, C., Aerts, R., van Breemen, N., van Dam, D., Hofschreuder, P., Hoosbeek, M., et al. (2003). Uncertainties in the fate of nitrogen I: An overview of sources of uncertainty illustrated with a Dutch case study. Nutrient Cycling in Agroecosystems, 66(1), 43-69. https://doi.org/10.1023/A:1023339106213

McKee, L. J., Eyre, B. D. (2000). Nitrogen and phosphorus budgets for the sub-tropical Richmond River catchment, Australia. Biogeochemistry, 50(3), 207-239. https://doi.org/10.1023/A:1006391927371

Mosello, R., Brizzio, M. C., Kotzias, D., Marchetto, A., Rembges, D., Tartari, G. (2002). The chemistry of atmospheric deposition in Italy in the framework of the National Programme for Forest Ecosystems Control (CONECOFOR). Journal of Limnology, 61(1s), 77-92. https://doi.org/10.4081/jlimnol.2002.s1.77

Spiess, E. (2011). Nitrogen, phosphorus and potassium balances and cycles of Swiss agriculture from 1975 to 2008. Nutrient Cycling in Agroecosystems, 91(3), 351-365. https://doi.org/10.1007/s10705-011-9466-9

Xiccato, G., Schiavon, S., Gallo, L., Bailoni, L., Bittante, G. (2005). Nitrogen excretion in dairy cow, beef and veal cattle, pig, and rabbit farms in Northern Italy. Italian Journal of Animal Science, 4(sup3), 103-111. https://doi.org/10.4081/ijas.2005.3s.103

Section 3

Table S4: Summary of statistical results from the trend analysis performed on nutrient load datasets. Values in bold are statistically significant at p=0.05. Arrows indicate significant increasing or decreasing trends.

Variable	*Period*	*Linear regression*	*Mann-Kendall*				*Pettitt test*		
		p-value	Kendall's tau	*p-value*	Sen's slope	Trend	K	*p-value*	Change point year
TN load	*Annual*	**0.0262**	**-0.266**	**0.0447**	**-1780.045**	↓	112	0.1036	2002
	Winter	0.5144	-0.088	0.5115	-170.710		56	0.619	2015
	Spring	0.2388	-0.207	0.1194	-423.409		90	0.364	2002
	Summer	**0.0280**	**-0.286**	**0.0310**	**-293.398**	↓	**140**	**0.0128**	**2002**
	Autumn	**0.0197**	**-0.261**	**0.0489**	**-852.509**	↓	108	0.1294	2000
Flow-normalized TN load	*Annual*	**0.0049**	**-0.360**	**0.0065**	**-703.853**	↓	**136**	**0.018**	**2010**
	Winter	**0.0093**	**-0.281**	**0.0340**	**-226.507**	↓	**144**	**0.0058**	**2010**
	Spring	**0.0005**	**-0.429**	**0.0012**	**-300.727**	↓	**124**	**0.0472**	**2006**
	Summer	0.8542	0.044	0.7498	8.362		66	0.9878	2016
	Autumn	**0.0013**	**-0.443**	**0.0008**	**-378.030**	↓	**170**	**0.0002**	**2009**
NO_3^- load	*Annual*	**0.0127**	**-0.310**	**0.0190**	**-1533.585**	↓	114	0.0832	2002
	Winter	0.5357	-0.059	0.6662	-115.265		54	0.5352	2015
	Spring	0.2179	-0.222	0.0950	-227.593		94	0.2898	2002
	Summer	**0.0090**	**-0.275**	**0.0373**	**-231.433**	↓	**138**	**0.0146**	**2002**
	Autumn	**0.0138**	**-0.300**	**0.0232**	**-705.060**	↓	108	0.1298	2000
Flow-normalized NO_3^- load	*Annual*	**0.0214**	**-0.271**	**0.0409**	**-639.659**	↓	**126**	**0.0368**	**2011**
	Winter	**0.0263**	-0.256	0.0533	-173.576		**150**	**0.0044**	**2010**
	Spring	**0.0035**	**-0.374**	**0.0046**	**-184.579**	↓	**128**	**0.0306**	**2006**
	Summer	0.4266	-0.054	0.6936	-18.165		58	0.6994	2006
	Autumn	**0.0014**	**-0.414**	**0.0017**	**-397.842**	↓	**162**	**0.0012**	**2009**
NH_4^+ load	*Annual*	**<0.0001**	**-0.571**	**<0.0001**	**-147.600**	↓	**198**	**<0.0001**	**2004**
	Winter	**<0.0001**	**-0.478**	**0.0003**	**-50.652**	↓	**196**	**<0.0001**	**2004**
	Spring	**0.0007**	**-0.468**	**0.0003**	**-27.055**	↓	**166**	**0.0008**	**2005**
	Summer	0.2384	-0.157	0.2373	-7.321		80	0.587	1999
	Autumn	**0.0007**	**-0.478**	**0.0003**	**-64.543**	↓	**174**	**0.0002**	**2005**
Flow-normalized NH_4^+ load	*Annual*	**<0.0001**	**-0.566**	**<0.0001**	**-118.324**	↓	**210**	**<0.0001**	**2005**
	Winter	**<0.0001**	**-0.556**	**<0.0001**	**-58.623**	↓	**202**	**<0.0001**	**2004**
	Spring	**0.0012**	**-0.448**	**0.0007**	**-22.822**	↓	**184**	**0.0002**	**2008**
	Summer	0.7373	-0.030	0.8365	1.089		72	0.8216	2009
	Autumn	**<0.0001**	**-0.576**	**<0.0001**	**-63.706**	↓	**194**	**<0.0001**	**2005**
TP load	*Annual*	0.0682	-0.202	0.1287	-95.631		80	0.5852	2014
	Winter	0.8924	-0.054	0.6936	-4.854		58	0.6926	2015
	Spring	0.4634	-0.162	0.2227	-24.331		72	0.811	2013
	Summer	**0.0138**	**-0.310**	**0.0190**	**-27.015**	↓	118	0.0642	2002
	Autumn	0.0719	-0.212	0.1108	-57.694		84	0.4936	2005
	Annual	0.1347	-0.123	0.3580	-27.297		82	0.524	2013
	Winter	0.3392	-0.148	0.2684	-8.644		104	0.1644	2009

Flow-normalized TP load	*Spring*	0.2462	-0.187	0.1595	-9.203	64	0.9208	1999
	Summer	0.2088	-0.217	0.1027	-10.335	78	0.6318	2013
	Autumn	0.3102	-0.128	0.3387	-16.583	84	0.4708	2013
PO_4^{3-} load	*Annual*	0.1594	-0.256	0.0533	-39.780	112	0.0976	2002
	Winter	0.4715	-0.157	0.2373	-6.159	64	0.9126	2015
	Spring	0.9853	0.000	1.000	-0.144	56	0.6054	1996
	Summer	0.3090	-0.217	0.1027	-7.174	118	0.0636	2002
	Autumn	0.1322	-0.335	0.1130	-20.511	110	0.1066	2000
Flow-normalized PO_4^{3-} load	*Annual*	0.6299	-0.143	0.2850	-14.531	114	0.0896	2008
	Winter	0.1447	-0.217	0.1027	-7.607	134	0.2360	2008
	Spring	0.6201	0.049	0.7215	1.240	50	0.3932	2015
	Summer	0.4445	0.049	0.7215	1.155	54	0.541	2018
	Autumn	0.4518	-0.069	0.613	-4.650	102	0.1736	2007

Table S5: Summary of statistical results from the trend analysis performed on air temperature datasets. Values in bold are statistically significant at p = 0.05. Arrows indicate significant increasing trends.

Variable	**Period**	**Linear regression**	**Mann-Kendall**				**Pettitt test**		
		***p*-value**	**Kendall 's tau**	***p*-value**	**Sen's slope**	**Trend**	**K**	***p*-value**	**Change point year**
Average air temperature	*Annual*	**0.0002**	**0.473**	**0.0003**	**0.049**	↑	**152**	**0.0036**	**2001**
	Winter	0.2255	0.148	0.2684	0.027		84	0.4738	2013
	Spring	**0.0280**	**0.335**	**0.0113**	**0.049**	↑	**128**	**0.0290**	**2002**
	Summer	**0.0006**	**0.438**	**0.0009**	**0.075**	↑	**152**	**0.0034**	**2002**
	Autumn	**0.0216**	**0.286**	**0.0310**	**0.050**	↑	114	0.0818	2001

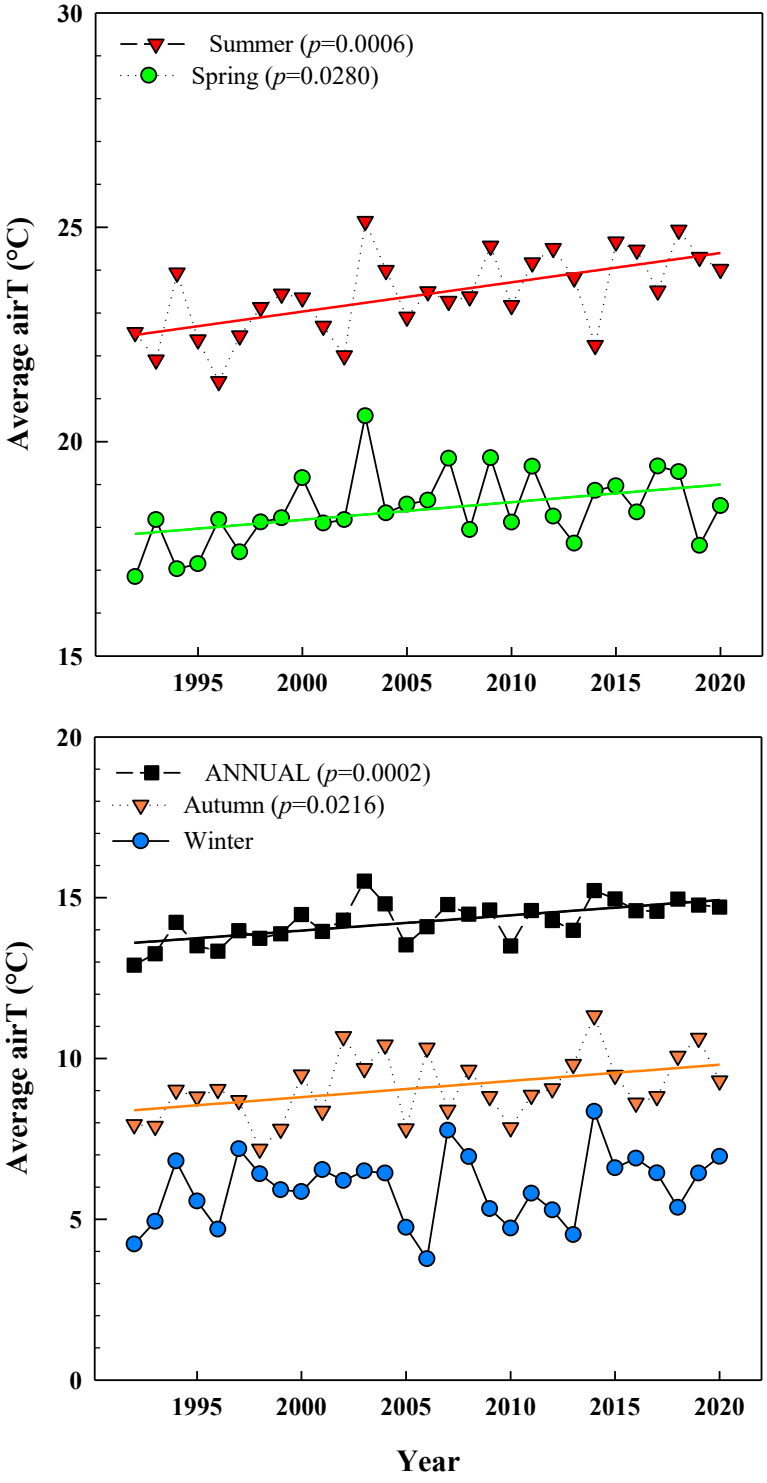

Figure S3: Temporal trends of average air temperature recorded at Piacenza station near the Po River course. Data source: ARPAE climatic "Eraclito" database (https://dati.arpae.it/dataset/erg5-eraclito).

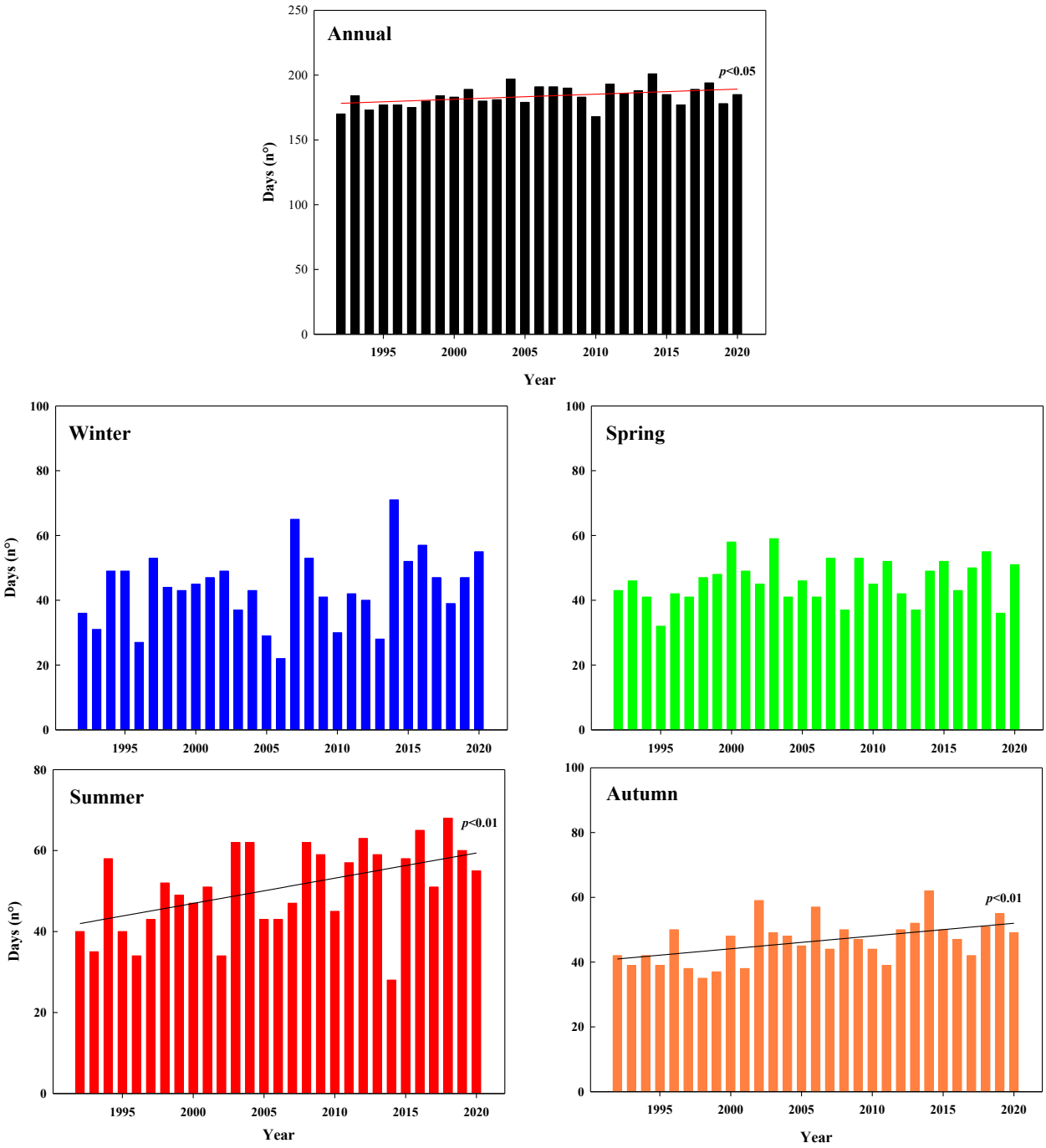

Figure S4: Number of days with air water temperature above the long-term average (1992–2020). Long-term average values calculated from daily measurements were 14.3°C, 6.0 °C, 18.4°C, 23.4°C, and 9.1°C for the annual, winter, spring, summer, autumn periods, respectively. Dashed lines show statistically significant trends.

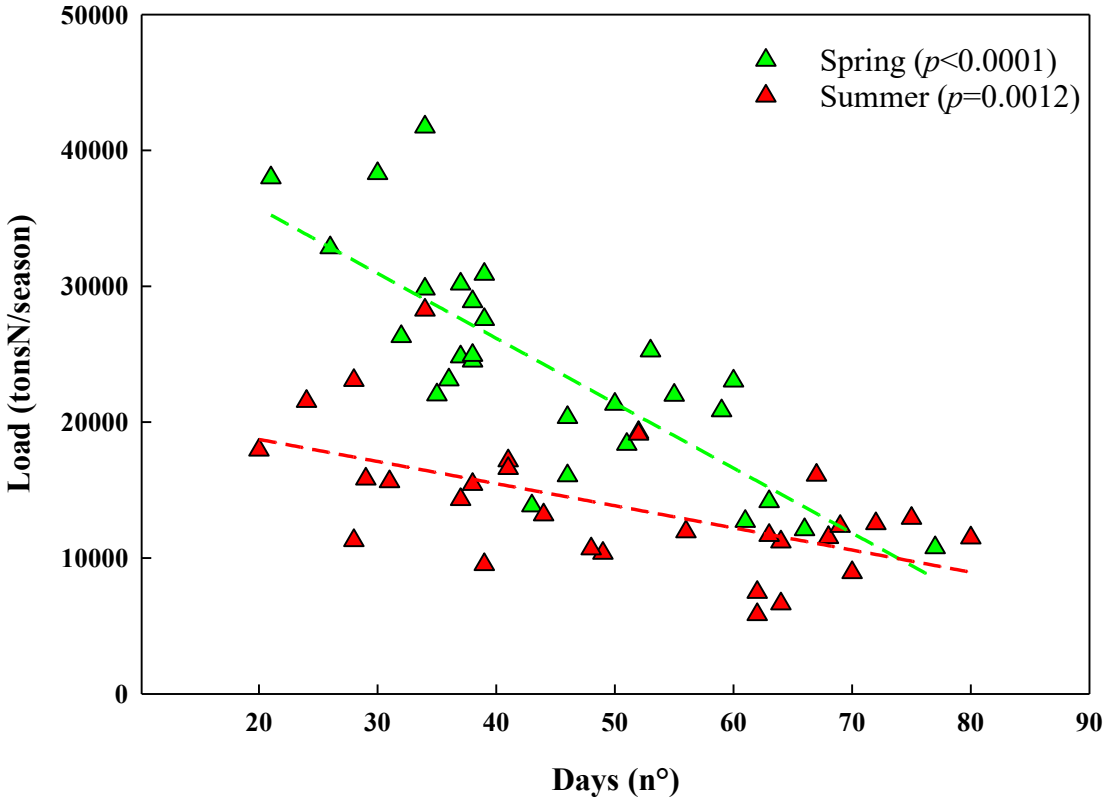

Figure S5: Correlation between the number of days with water temperature above the long-term average (1992–2020) and DIN (NO_3^-+NH_4^+) loads measured at the Po River closing section in spring and summer. Long-term average values calculated from daily measurements of water temperature were 17.8°C and 22.9°C for the spring and summer periods, respectively.

Paper II: Gervasio, M. P., Soana, E., Granata, T., Colombo, D., & Castaldelli, G. (2022). An unexpected negative feedback between climate change and eutrophication: higher temperatures increase denitrification and buffer nitrogen loads in the Po River (Northern Italy). *Environmental Research Letters*, 17(8), 084031. 10.1088/1748-9326/ac8497

ENVIRONMENTAL RESEARCH
LETTERS

OPEN ACCESS

RECEIVED
17 June 2022

ACCEPTED FOR PUBLICATION
27 July 2022

PUBLISHED
5 August 2022

LETTER

An unexpected negative feedback between climate change and eutrophication: higher temperatures increase denitrification and buffer nitrogen loads in the Po River (Northern Italy)

Maria Pia Gervasio[1], **Elisa Soana**[1,*], **Tommaso Granata**[2], **Daniela Colombo**[2] and **Giuseppe Castaldelli**[1]

[1] Department of Environmental and Prevention Sciences, University of Ferrara, Via Luigi Borsari 46, 44121 Ferrara, Italy
[2] CESI—Centro Elettrotecnico Sperimentale Italiano, via Rubattino 54, Milano 20134, Italy
[*] Author to whom any correspondence should be addressed.

E-mail: elisa.soana@unife.it

Keywords: nitrogen loads, eutrophication, climate change, water temperature, denitrification, Po River

Supplementary material for this article is available online

Abstract

Temperature is one of the most fundamental drivers governing microbial nitrogen (N) dynamics in rivers; however, the effect of climate change-induced warming on N processing has not been sufficiently addressed. Here, annual, and seasonal (spring and summer) N loads exported from the Po River watershed (Northern Italy), a worldwide hotspot of eutrophication and nitrate pollution, are investigated in relation to water temperature trends over the last three decades (1992–2019). Despite large inter-annual variations, from the early 1990s, the Po River experienced a significant reduction in total N loads (−30%) represented mainly by nitrate, although agricultural N surplus in croplands and other watershed conditions have remained constant. In parallel, the Po River water is steadily warming (+0.11 °C yr^{-1}, for average annual temperature) and the number of warm days is increasing (+50%, in the spring–summer period). The inverse relationship between water temperature and N loads strongly indicated that the higher temperatures have boosted the denitrification capacity of river sediments along the lowland reaches. Overall, over the last three decades, annual total N loads declined by around one-third due to a near 3 °C increase in temperature and this evidence was even more marked for the summer season (−45% for total N loads and +3.5 °C for temperature). Based on these observations, it is suggested that near-term effects of climate change, i.e. warming and an increase in the duration of low-flow periods in rivers, may have negative feedback on eutrophication, contributing to partially buffer the N export during the most sensitive period for eutrophication.

1. Introduction

Anthropogenic reactive nitrogen (N) inputs in agricultural watersheds have dramatically increased during the 20th century, with multiple detrimental environmental effects including water pollution, eutrophication, aquatic ecosystem functioning, biodiversity loss, and human health impacts [1–3]. The interaction between land use, hydroclimatic, and biogeochemical drivers over space and time mainly influences N use efficiency in croplands, runoff rates, and riverine N export from watersheds [4–6]. The amounts of N that reach coastal zones depend on an array of processes occurring across the landscape (e.g. crop uptake, leaching from the soil, nitrification, denitrification, etc) that are temperature- and precipitation-dependent. Thus, the alteration of the hydrological cycle and thermal regimes under climate change scenarios is expected to significantly affect both the magnitude and timing of N processing and delivery to inland waters and ultimately the sea [7–9]. Changes in precipitation frequency, intensity, and duration alter watershed hydrological cycles by emphasizing extreme hydrologic events (floods and droughts) and, consequently, the seasonality of N load generation and transport from land to aquatic ecosystems via runoff. Reductions in precipitation and higher evaporation rates are expected to decrease

discharge in summer, whereas higher winter rainfall or periods with short-term but heavy precipitation likely result in increased discharge and N leaching from agricultural areas outside the growing season [10, 11].

Studies on climate change and river water quality have almost exclusively focused on assessing the impact of altered hydrological regimes on runoff and nutrient loss from croplands and riverine transport. However, the impact of climate change on watershed biogeochemical cycles (N in particular) depends not only on changes in precipitation and runoff but also on water temperature changes. While trends in climatic variables (i.e. air temperature and precipitation) are well documented in many watersheds worldwide, studies concerning the trajectories of river water temperature are still limited due to the scarcity of long-term and high-resolution datasets. Thus, the effect of climate warming on the thermal regime and thus on microbial activity and N budget of river systems is still understudied [e.g. 12–14]. Warmer waters may stimulate, both directly and indirectly, the N-removal capacity of rivers, thereby reducing the amount of N transported to coastal zones. Denitrification, the anaerobic reduction of nitrate (NO_3^-) to N gas, is regarded as one of the main regulating ecosystem functions provided by rivers and is a crucial process that counteracts eutrophication [15, 16]. Like all microbial processes, denitrification is controlled by temperature, and higher water temperatures also enhance sediment oxygen demand and the extent of hypoxic or anoxic conditions in the benthic compartment [17, 18].

An interesting scientific question is how watersheds react to climate change with respect to N inputs to water bodies and the resulting timing of in-stream transformation, removal, and transport processes. For example, increasing water temperature induced by climate change, especially in summer, may strengthen the N-removal capacity of rivers, thereby attenuating the N loads transported to coastal zones during the most eutrophication-sensitive period. Studies targeting N budgets in watersheds and related N loads and processing in rivers are usually conducted on an annual scale [4, 6, 19]. Whilst annual N export is a useful indicator in temporal or comparative studies, is not sufficient for assessing eutrophication risk. The management of the timing and impacts of N export requires the detailed quantification of seasonal N loads, particularly in spring and summer when eutrophication potential is the highest in terminal water bodies [20, 21].

In the Mediterranean region, which is characterized by warm dry summers and wet winters, the impacts of climate change may be among the most severe worldwide [5, 22, 23]. The Po River basin (Northern Italy) is a worldwide hotspot of eutrophication and NO_3^- pollution and, as such, represents a useful study area that has been experiencing high flow variation and increased frequency and severity of air temperature anomalies and drought over the last few decades [19, 24–28]. Comprehensive studies have demonstrated a significant increase in both minimum and maximum temperature extremes in all seasons in Northern Italy, although the strongest warming trends have been detected from the early 1980s in summer, with an average rate of change of approximately 0.5 °C every 10 years together with an increasing frequency of heatwaves, which has resulted in a longer growing season [29–32].

In human-impacted watersheds, the study of N load formation, transport, and delivery is a key issue for implementing environmental policies aimed at protecting the coastal zones, with strong implications for productive sectors and urban wastewater management, and it must necessarily consider the climate change that is altering the inland waters. At present, it remains unknown whether climate change and water temperature affect in-stream N processing and transport in the Po river. To address this knowledge gap, for the first time, the present study explored the relationship between the Po River water temperature and N loads over the last three decades (1992–2019). The main hypothesis is that the occurrence of higher temperatures over longer periods boosts the sedimentary microbial processes responsible for N removal (i.e. nitrification and denitrification) and, thus, decreases N export to the Adriatic Sea, particularly during the spring and summer months, the most sensitive period for eutrophication.

2. Materials and methods

2.1. Study area

The Po River is the longest river in Italy, flowing eastward across Northern Italy for over 650 km (figure 1), and is also the largest river, with an average discharge of ∼1500 $m^3 s^{-1}$ at its closing section [33]. The Po drainage basin extends over an area of ∼75 000 km^2, a large portion of which constitutes the widest and most fertile lowland in Italy (∼47 000 km^2). The Po River is supported by both Alpine and Apennine's tributaries, fed mainly by snowmelt and rainfall, respectively, resulting in an annual flow regime that is characterized by two flood periods (in spring and late autumn) and two low-water periods (in summer and winter) [34]. The basin covers the transition zone between the sub-continental climate of Central Europe and the Mediterranean climate, with an average annual precipitation of approximately 1200 mm [35]. The Po River basin is densely urbanized and an intensely exploited area, accounting for 40% of Italy's gross domestic product and 35% of national agricultural production. With some of the highest rates of N losses to surface water and groundwater [19, 36, 37], this region is responsible for approximately two-thirds of the total nutrient inputs to the Northern Adriatic Sea [38–40].

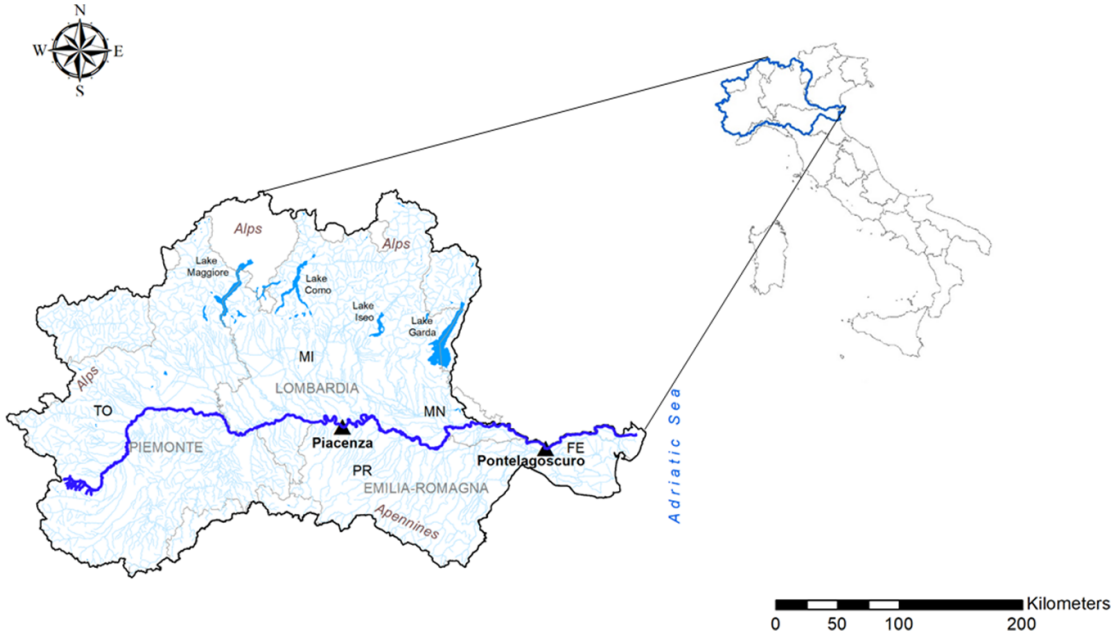

Figure 1. Map of the Po River basin and its hydrographic network. The blue line represents the main Po River course, and the two monitoring stations are indicated as black triangles. The borders of the Italian Regions are shown as gray lines with the following main cities indicated: Turin (TO), Milan (MI), Parma (PR), Mantua (MN), and Ferrara (FE).

2.2. Datasets of river water temperature

Accurate and continuous water temperature datasets, representative of the middle-lower reach of the Po River, were acquired from two monitoring stations, operated by energy companies, located at the cooling water intake of the power plants. Daily average water temperature data were recorded near the city of Piacenza (Emilia-Romagna Region, stream kilometer 330) at La Casella Power Station by the ENEL group (Italian multinational manufacturer and distributor of electricity and gas; www.enel.com/it/media/esplora/ricerca-foto/photo/2020/03/italia-centrale-la-casella) from 1992 to 2005, and at Piacenza Power Station by the A2A Life Company Group (www.a2a.eu/en/group) from 2006 to 2019, giving a complete dataset for the period 1992–2019. Water temperature measurements were carried out using resistance temperature detector (RTD) probes with platinum Pt100 resistance thermometers having a nominal resistance of 100 Ω at 0 °C defined according to IEC 751 (EN 60751) .Other sensor characteristics: measuring range 0–40 °C; accuracy ±0.1 °C at 0° C; 4-wire connection; signal conversion electronics with 4–20 mA output in measuring range 0 °C–40 °C. The validation procedure to reconstruct a continuous three-decade time series is reported in the supplementary material 1. From temperature daily data, the annual and seasonal trends in average values were analyzed for the spring (April–June) and summer (July–September) periods.

2.3. Calculation of riverine N loads

Monthly NO_3^- and ammonium (NH_4^+) loads and total nitrogen (TN) exported to the Adriatic Sea were calculated using discharge and concentration datasets for the study period (1992–2019) at the closing section of the Po River basin, which is conventionally located at Pontelagoscuro (44°53′19.34″N, 11°36′29.60″E) near the city of Ferrara (Emilia-Romagna Region; stream kilometer 586). Daily average discharge was acquired from the permanent records of a gauge operated by the Environmental Agency (ARPAE) of the Emilia-Romagna Region and retrieved from the 'Hydrological Annals—Second Part' published by ARPAE, the electronic versions of which are available on the Regional Open Data Portal (https://simc.arpae.it/dext3r/). Nitrogen species concentrations were obtained from fortnightly (or monthly) sampling campaigns carried out by ARPAE under the framework of the environmental monitoring program (https://dati.arpae.it/group/acqua). Sample collection and analysis were performed in accordance with standard methods and analytical protocols adopted by regional environmental agencies [41]. When not provided, TN concentrations were calculated from the concentrations of DIN ($NO_3^- + NH_4^+$) according to the formula $TN = 0.93 \times DIN + 0.75$ ($r^2 = 0.54$; $p < 0.001$), obtained by relating time series including simultaneous TN and DIN measurements.

Nutrient loads were calculated as the product of the daily discharge and nutrient concentration (measured fortnightly or monthly and interpolated to daily intervals) and aggregated into monthly means. The method employed for the monthly load calculation was based on the linear interpolation of concentration values between

two subsequent sampling events [42, 43], as follows (1):

$$L = k \cdot \sum_{j=1}^{n} C_j^{\text{int}} \cdot Q_j \quad (1)$$

where C_j^{int} is the daily N species concentration (g N m^{-3}) linearly interpolated between two measured samples, Q_j is the daily discharge (m^3 s^{-1}), n is the number of days in each month, and k is a conversion coefficient to take the recorded period into account (e.g. 365 d for annual loads). Seasonal load trends in the spring and summer periods (t N $season^{-1}$) were evaluated according to the following monthly clustering: April–June (spring) and July–September (summer). Annual loads (t N yr^{-1}) were computed by summing up all the monthly contributions. To validate the annual loads calculated by the interpolation concentration method, the obtained values were compared to those calculated by flow-adjusted concentration method. Flow-adjusted concentrations are commonly employed for assessing annual loads and are recommended in monitoring guidelines [44] and international conventions (e.g. OSPAR-Convention for the protection of the marine environment of the North-East Atlantic) [45], but they are not valid for calculating monthly (and thus seasonal) loads because the environmental monitoring quality programs typically carry out just one sampling per month. A very good correlation between the annual values calculated by the two methods was found ($r^2 = 0.99$, $p < 0.001$) and a discrepancy of about 5% on average (see supplementary material 2).

With the aim of assessing if long-term nutrient load trends might be mediated by the Po River water temperature trends, monthly flow-normalized loads (Ln) were calculated according to [46] to remove the effects of varying inter-annual hydrological conditions on N transport:

$$\text{Ln} = L \cdot Kh \quad (2)$$

where Kh (hydrological coefficient). The hydrological coefficient was obtained as the ratio of the long-term (period 1992–2019) average outflow of a specific month to the monthly outflow of a particular year. The annual normalized loads were computed by summing up the monthly normalized loads. Similarly, the seasonal normalized loads were calculated by summing up the normalized loads from April to June and from July to September, for spring and summer period, respectively.

2.4. Reconstruction of historical changes in diffuse and point N sources

Because the Po River basin is among the most agriculturally productive and densely populated areas in Italy, changes in agricultural practices and populations could result in changes in riverine N loading. The temporal evolution of diffuse and point N sources in the watershed was checked by collecting census data at an almost 10 year time interval for agricultural land occupied by different crop types and production systems, numbers of farmed animals, synthetic fertilizer application practices, and human population. Statistics were integrated in a N budgeting approach previously applied to several sub-basins of the Po River system [37, 47, 48]. Details regarding the data sources, computational methods, and uncertainty assessment of the diffuse and point N sources are presented in supplementary material 3.

2.5. Statistical analyses

Annual and seasonal time series of temperature, riverine N loads, and water flow were analyzed using parametric (linear regression) and non-parametric tests (Mann–Kendall, Sen's slope, and Pettitt's test). Pearson correlation analysis was used to investigate the relationship between temperature and riverine N loads. All statistical tests were performed using the software R (Core Team, 2021) with the *Kendall* package for the Mann–Kendall test and the *Trend* package [49] for the other analyses. The tested factors and trends were considered statistically significant at $p < 0.05$. Details of the statistical tests are presented in supplementary material 4.

3. Results and discussion

3.1. Nitrogen load trends

During the period 1992–2019, the annual TN loads at the closing section of the Po River basin showed a significant negative trend ($p < 0.05$, figure 2(a)), decreasing by nearly 33%, corresponding to a reduction of approximately 2000 t yr^{-1}. Depending on outflow variations linked to precipitation, the TN export varied greatly among years, ranging between ~68 000 t N yr^{-1} (2007 and 2017) and ~237 000 t N yr^{-1} (1996). As is commonly found in agricultural settings [15, 16], the nitrate load accounted, on average, for >75% (range = 62%–86%) of the TN load, whereas the contribution of NH_4^+ was comparatively minor (range = 1%–5%) (figure 2(a)). Compared to the early 1990s, the NO_3^- load declined over the study period by more than 30% ($p < 0.05$, figure 2(a)), showing inter-annual variations that coincided with those detected in the TN load. The highest annual NO_3^- export (~160 000 t yr^{-1}) occurred in 1996, while the lowest amount (~50 000 t N yr^{-1}) occurred in both 2007 and 2017. Over the study period, the annual NH_4^+ load decreased by approximately two-thirds ($p < 0.001$, figure 2(a)) from ~6300 t N yr^{-1} in the early 1990s to less than 2000 t N yr^{-1} in recent years. The hydrological conditions have also varied significantly during this period, although there has been no significant long-term trend in the annual outflow. For example, 2007 and 2017 were extremely dry, with outflow values 42%–45% lower than the

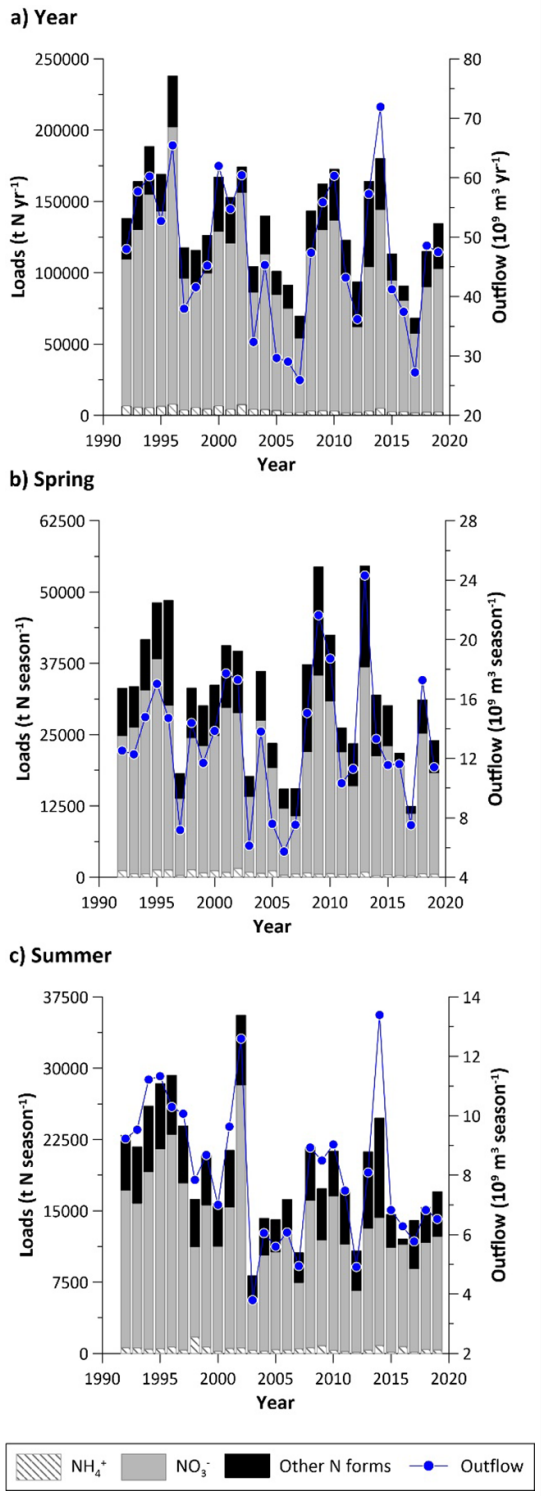

Figure 2. Temporal trends in nutrient loads (NH_4^+, NO_3^-, and other N forms) and outflow measured at the closing section of the Po River basin on an annual basis (panel (a)), in spring (panel (b)), and in summer (panel (c)). $NH_4^+ + NO_3^- +$ other N forms = TN. Note that the *Y*-axis differs between the panels.

long-term average and corresponding to lower N transport. Conversely, 2014 was an extremely wet year with an annual outflow >50% higher than the long-term average, and consequently higher N transport. In the Po River, early signals of climate change effects have been reported over the last three decades, when hydrological extremes have become progressively amplified [19, 33, 34], with large floods followed by persistent drought conditions [50, 51].

The trajectories of riverine N loads were not related to human pressures, productive sectors and the associated generation of N loads from diffuse and point sources. Indeed, the N balance across the croplands of the Po River basin revealed a steadily constant surplus during the 1990–2019 period, averaging ~180 kt N yr^{-1} (figure 3). The total N input during this period was estimated to exceed 600 kt N yr^{-1}, mostly derived by manure spreading (36%), synthetic fertilizers (33%) and biological fixation (26%). The total N output during the study period was estimated to exceed 430 kt N yr^{-1}, mainly associated with crop harvesting (74%). Total watershed N inputs to croplands showed a slight decline in 2010 (~14%) with respect to the previous two decades, but this was coupled to a decrease also in total N outputs (~15%) resulting, if the associated uncertainty is considered, in a net budget (i.e. surplus) not significantly different over the studied period. While the human population in the Po River basin has remained relatively constant over the last three decades at ~17 million, important legislative acts aimed at improving urban wastewater treatment plants (e.g. Directive 91/271/EEC) were followed by an appreciable reduction in the direct discharge of untreated or poorly treated domestic wastewater [28]. Nitrogen loads from point sources decreased by nearly 45% between 1990 and 2000 and then remained almost constant until 2019 (figure 3) and this may have been partly responsible for the clear decrease of riverine NH_4^+ loads. Despite this, the decrease was not in the order of magnitude to explain the decrease recorded for the riverine TN loads. Overall, over the entire investigated period, N loads from urban areas accounted for less than 5% of the total N input from diffuse agricultural sources. Since the early 1990s, NO_3^- pollution has become the main concern for surface water and groundwater in the Po River basin because the measures introduced by the European Directives for controlling widespread agricultural and livestock sources (i.e. 91/676/EEC, 2000/60/EC) have been largely ineffective [27, 52]. Recent studies have shown that in agricultural landscapes, artificial water bodies such as irrigation canals and drainage ditches may act as natural wetlands in terms of provision of biogeochemical services, i.e. the mitigation of N excess via denitrification [47, 53]. The capillary network of artificial waterways crossing the Po River plain was implemented over the centuries, from the Etruscan age to the 1960s, with multiple purpose, i.e. irrigation, drainage, and flood control [54–56]. It is reasonable to hypothesize that the N amount removed via denitrification by the whole canal network remained stable along the three decades analyzed in the present study and thus it is very

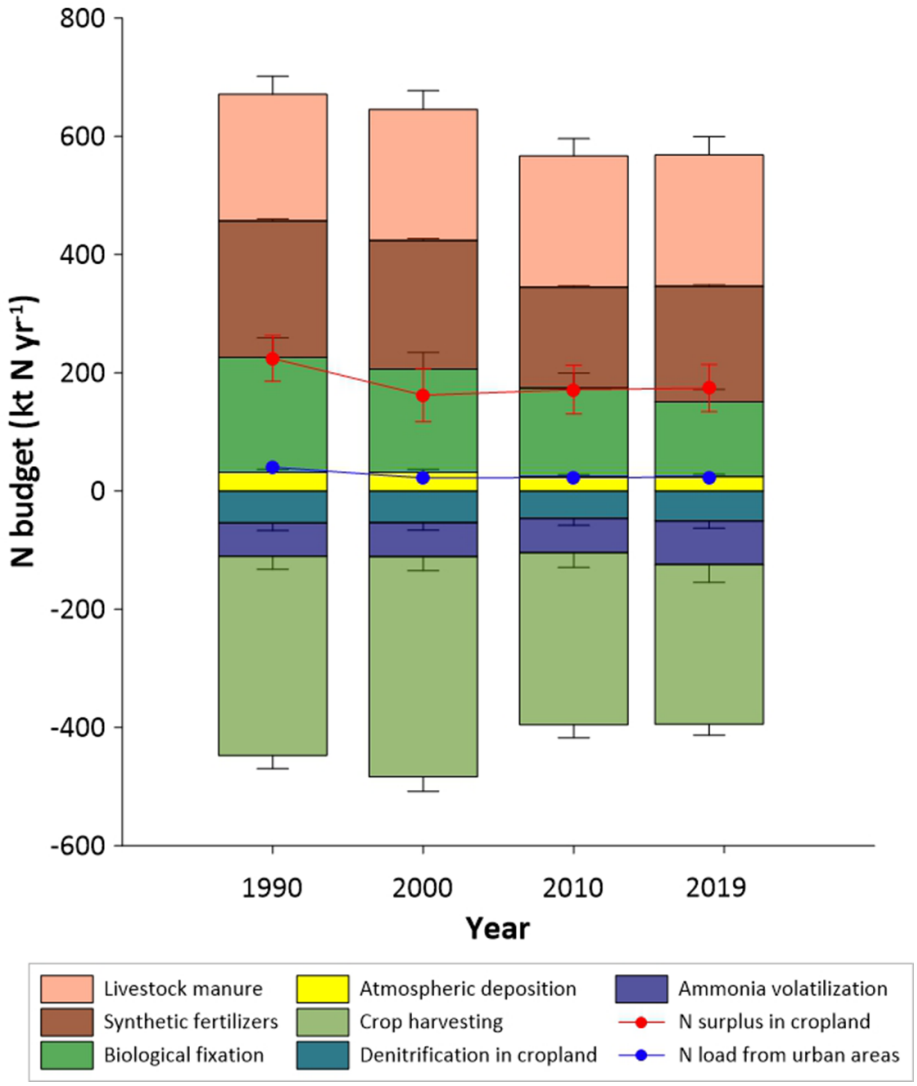

Figure 3. Decadal changes (1990–2019) in diffuse and point N sources (kt N yr^{-1}) in the Po River basin.

unlikely to explain the major reduction observed in the Po River NO_3^- loads, whose cause is to be found elsewhere.

Spring and summer nutrient loads represented on average 19%–24% and 13%–14% of the corresponding annual values, respectively (figures 2(b) and (c)). Summer TN and NO_3^- loads exhibited high inter-annual variations, ranging from ∼8000 (2003) to ∼3000 t N $season^{-1}$ (2002), and from ∼5500 (2003) to ∼27 600 t N $season^{-1}$ (2002), respectively. The analyzed dataset contained years with rather extreme summertime hydrological conditions; the summers of 2002 and 2014 were very wet, with outflow 56%–66% higher than the long-term summer average. In contrast, the summers of 2003 and 2007 were extremely dry, with outflow 39%–53% lower than the 1992–2019 average. The period from 2003 to 2007 was characterized by frequent and persistent summer drought that culminated in daily discharge frequently <300 $m^3\ s^{-1}$. Of the six most-prolonged drought events recorded during the last century, four occurred between 2003 and 2007, with the lowest daily discharge of ∼170 $m^3\ s^{-1}$ occurring in July 2006 [33, 57, 58]. The time series of summer loads exhibited a negative trend for TN and NO_3^- ($p < 0.01$, figure 2(c)), decreasing on average by 42%–47%, while a significant downward trend, if tested by linear regression, was not detected in spring when load variations among years were more erratic (figure 2(b)). Differently to TN and NO_3^-, NH_4^+ loads decreased by nearly 62% in spring ($p < 0.01$; figure 2(b)), whereas linear regression was no statistically significant in summer (figure 2(c)).

Summer outflow decreased by nearly 34% (1.3% per year), highlighting that drought events have been exacerbated during the more recent decades as previously demonstrated by hydrological studies [25, 33, 34]. The calculation of flow-normalized loads showed that the annual transport of TN, NO_3^-, and NH_4^+ at the Po River closing section decreased by 15%, 14%, and 61%, respectively, along the entire investigated period (figures 4(a), (d), and (g)). The

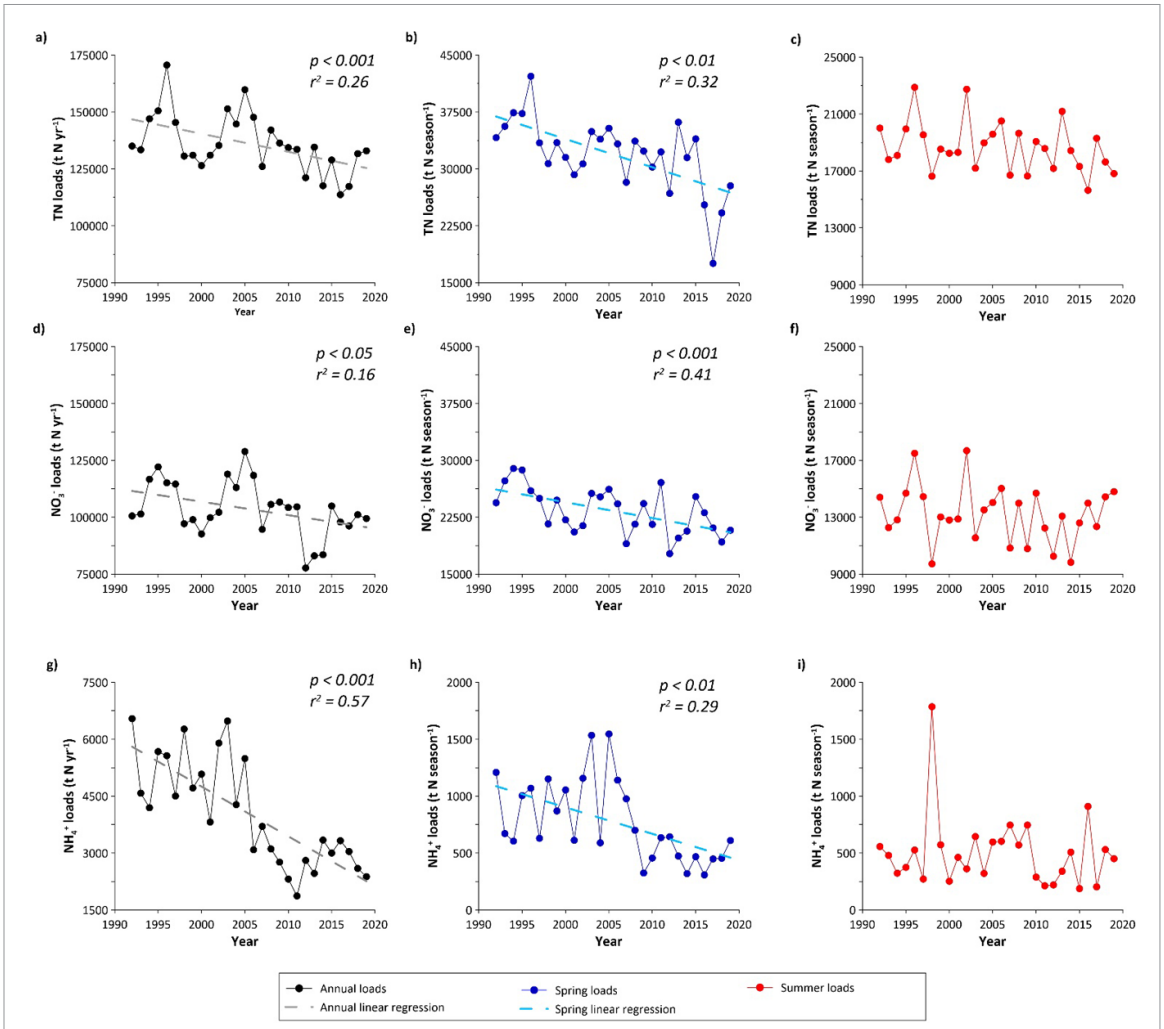

Figure 4. Temporal trends in flow-normalized N loads (TN, NO_3^-, and NH_4^+) measured at the closing section of the Po River basin on an annual basis (panels (a), (d), and (g)), in spring (panels (b), (e), and (h)), and in summer (panels (c), (f), and (i)). Note that the *Y*-axis differs between the panels. Dashed lines show statistically significant trends.

results of the Mann–Kendall and Sen's slope analyses on flow-normalized nutrient loads showed negative *Z* values, confirmed by a negative slope, indicating downward trends since 1992 both at the annual and seasonal scale (table 1). The Pettitt's test showed that the decline in seasonal nutrient loads began in 2006 (figures 4(b), (c), (e) and (f)), except for NH_4^+ for which trends began in 2008 for spring (figure 4(h)) and in 2009 for summer (figure 4(i)), resulting in annual loads started to decrease around 2010.

3.2. Water temperature trends

Significant positive trends in the annual, spring, and summer water temperature series of the Po River were identified for the 1992–2019 period (figure 5), as demonstrated by the positive Sen's slope values (table 1). The annual average temperature increased during this period by ∼3 °C, corresponding to an overall warming rate of 0.11 °C yr^{-1}, although the pattern of change showed two moments: the annual series from 1992 to 2002 were characterized by relative stability with an average temperature of 13.87 ± 0.22 °C and low inter-annual variability; while an abrupt increase occurred after 2002 with a slope of more than 0.18 °C yr^{-1} and high fluctuations among the years (average 15.88 ± 0.88 °C) (figure 5). The highest annual temperatures (up to ∼17 °C) were recorded in 2007 and 2015, 2 years marked by significant thermal (high air temperature) and meteorological (low precipitation) signals [26, 32]. Seasonally, the average spring and summer water temperatures increased by nearly 2 °C (0.07 °C yr^{-1}) and 3.5 °C (0.13 °C yr^{-1}) over the monitoring period, respectively (figures 5(b) and (c)), with the most marked warming trends and inter-annual variability starting in 2002 (table 1). These temperature increases resulted to be faster than the average increases observed in other large European and American rivers in temperate zones during similar periods [59, 60]. However, the present outcomes agree with previous studies indicating a major contribution to warming from the hottest period of the annual cycle with stronger positive trends for late spring–summer months and a significant advance of spring warming [61–65].

Meteorological stations located nearby the Po River course showed a significant positive trend for

Table 1. Results of the statistical analyses.

		Linear regression	Mann–Kendall			Sen's slope	Pettitt	
	Period	*p*-value	*p*-value	*S*	*Z*	*Q*	*K*	Year
Flow-normalized TN loading	Annual	0.001	<0.001	−132	−2.59	−744.77	134 316	2010
	Spring	0.001	<0.001	−170	−3.34	−326.40	33 282	2006
	Summer	—	<0.001	−74	−1.44	−66.61	20 519	2006
Flow-normalized NO_3^- loading	Annual	0.05	<0.001	−92	−1.80	−630.06	104 556	2011
	Spring	0.001	<0.001	−152	−2.98	−221.59	24 275	2006
	Summer	—	<0.001	−26	−0.49	−19.93	15 024	2006
Flow-normalized NH_4^+ loading	Annual	<0.001	<0.001	−214	−4.21	−126.44	5493	2005
	Spring	0.01	<0.001	−160	−3.14	−22.02	700	2008
	Summer	—	<0.001	−36	−0.69	−3.37	745	2009
Temperature	Annual	<0.001	<0.001	236	4.64	0.12	14.0	2002
	Spring	0.01	<0.001	160	3.14	0.09	17.1	2002
	Summer	<0.001	<0.001	192	3.77	0.14	21.1	2002
Outflow	Annual	—	<0.001	−62	−1.20	−0.39	60.45×10^9	2002
	Spring	—	<0.001	−122	−2.39	−0.14	12.60×10^9	2002
	Summer	0.05	<0.001	−20	−0.37	−0.03	17.29×10^9	2002

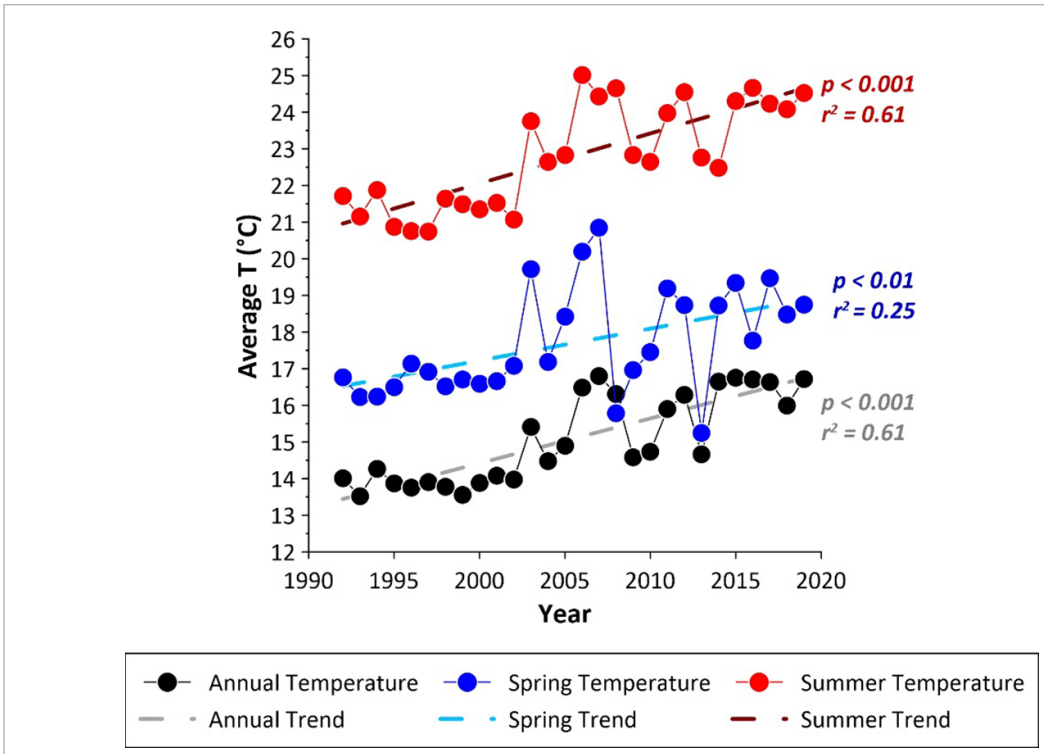

Figure 5. Annual (black line), spring (blue line), and summer (red line) average temperatures of the Po River water between 1992 and 2019. Dashed lines show statistically significant trends.

air temperature, recording an increase of about 2 °C in annual and summer average values and an increase of about 1 °C in spring average values over the last three decades (figures S2 and S3, supplementary material 1). The present data was confirmed by previous meteorological studies that have demonstrated how the air temperature in Po River basin has been affected by warming in the period 1952–2002, recording an increase of over 1 °C for average annual values [66] and detecting stronger positive anomalies in the mountain areas compared to the lowlands and the delta region [67]. Further studies have demonstrated an increase in annual maximum temperatures with linear and constant trends of about 0.5 °C every 10 year and predicted a raise of 3 °C–4 °C by the end of the last decade, as it happened [68] and an even higher temperature anomaly for the next decades [66].

Pettitt's test on the Po River water temperature highlighted a positive trend starting in 2002 (table 1) and this was consistent with the most marked increase in air temperature detected from the beginning of the 2000s (figure S3, supplementary material). Despite long-term increases in river water temperatures

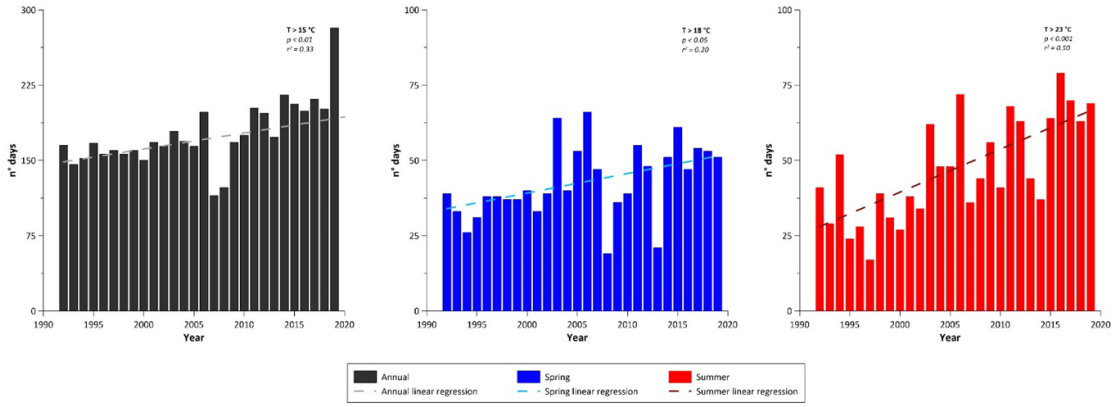

Figure 6. Numbers of days annually (black bars), in spring (blue bars), and in summer (red bars) having water temperature above the long-term average for the Po River (1992–2019). Long-term average values calculated from daily measurements were 15 °C, 18 °C, and 23 °C for the annual, spring, and summer periods, respectively. Dashed lines show statistically significant trends.

being correlated to increases in air temperatures, surprisingly, the warming trend of the Po River water was stronger than the atmosphere, when the latter is supposed to contribute to the warming of the former. These unusual data may be ascribed to the joint effect of rising air temperature and reduced outflow on river temperature trends [65].

In parallel to the upward temperature trends, the annual occurrence of warm days (i.e. the number of days with water temperatures above the long-term average) increased by more than 50% for both the spring and summer periods (figure 6). This condition was in agree with previous studies reporting, for the Mediterranean area, a significant increase of the days with warm temperature extremes [69–71], suggesting that the growing season length is increasing. The occurrence of warm days in summer is often related to low-flow conditions, as was the case for the period from 2003 to 2007, which was characterized by prolonged drought in the Po River basin. However, this has not been the case in the last decade, indicating that the Po River is becoming more sensitive and vulnerable to such extreme temperature events with ongoing climate change, as demonstrated for other large European rivers [64].

3.3. Negative feedback between climate change and eutrophication

The present outcomes demonstrated that the Po River water is steadily warming, with the number of warm days increasing over time and higher water temperatures corresponding to lower N loads during the entire spring–summer period, the time of year when the risk of coastal zone eutrophication is greatest [72, 73]. Indeed, highly significant negative ($p < 0.0001$) correlations were detected between average water temperature and monthly loads of TN and NO_3^- (figures 7(a)–(d)). When the temperature increased by 1 °C, TN and NO_3^- loads decreased by approximately 7% and 4% in summer and spring, respectively. A weaker but still significant negative correlation ($p < 0.05$) was also found between the average water temperature and monthly NH_4^+ loads in spring (figure 7(e)). The inverse relationship observed between temperature and TN loads (mainly NO_3^-) strongly indicates that the higher water temperatures recorded during the last few decades have stimulated NO_3^- removal via denitrification in the river sediments along the lowland reaches (figure 7). This likely act to partially buffer the eutrophication risk in the coastal waters. While several studies suggest that water temperature increases may alter the biodiversity and biological structure and functioning of rivers [59, 74], the resulting effects on ecosystem functions (i.e. N removal) and, ultimately, the regulation of ecosystem services (i.e. self-depuration capacity) remains unclear and warrant greater attention. Experimental laboratory studies have shown that warming boosts nitrification and denitrification rates alongside enzymatic reactions in freshwater sediments [17, 18, 75], but there is a lack of systematic research forecasting global warming effects on N cycling in rivers and expected changes in N loads [76]. When a suitable substrate, NO_3^-, and labile carbon are available, denitrification generally responds positively to increases in water temperature. At the closing section of the Po River, dissolved organic carbon during the spring–summer months average 1.8 mg l^{-1}, indicating that organic carbon is balanced with respect to NO_3^- availability (averaging 1.7 mg N l^{-1}, 1992–2019 period) according to a theoretical ratio of ∼1 based on denitrification stoichiometry [77]. The dissolved organic carbon concentrations in the lower reaches of the Po River tally with those measured in other agricultural rivers [78, 79], which demonstrates that denitrification is not likely limited by the organic carbon supply. Higher water temperatures decrease oxygen solubility and increase sediment oxygen respiration, thereby limiting the oxygen penetration depth and resulting in a synergistic indirect effect that strengthens

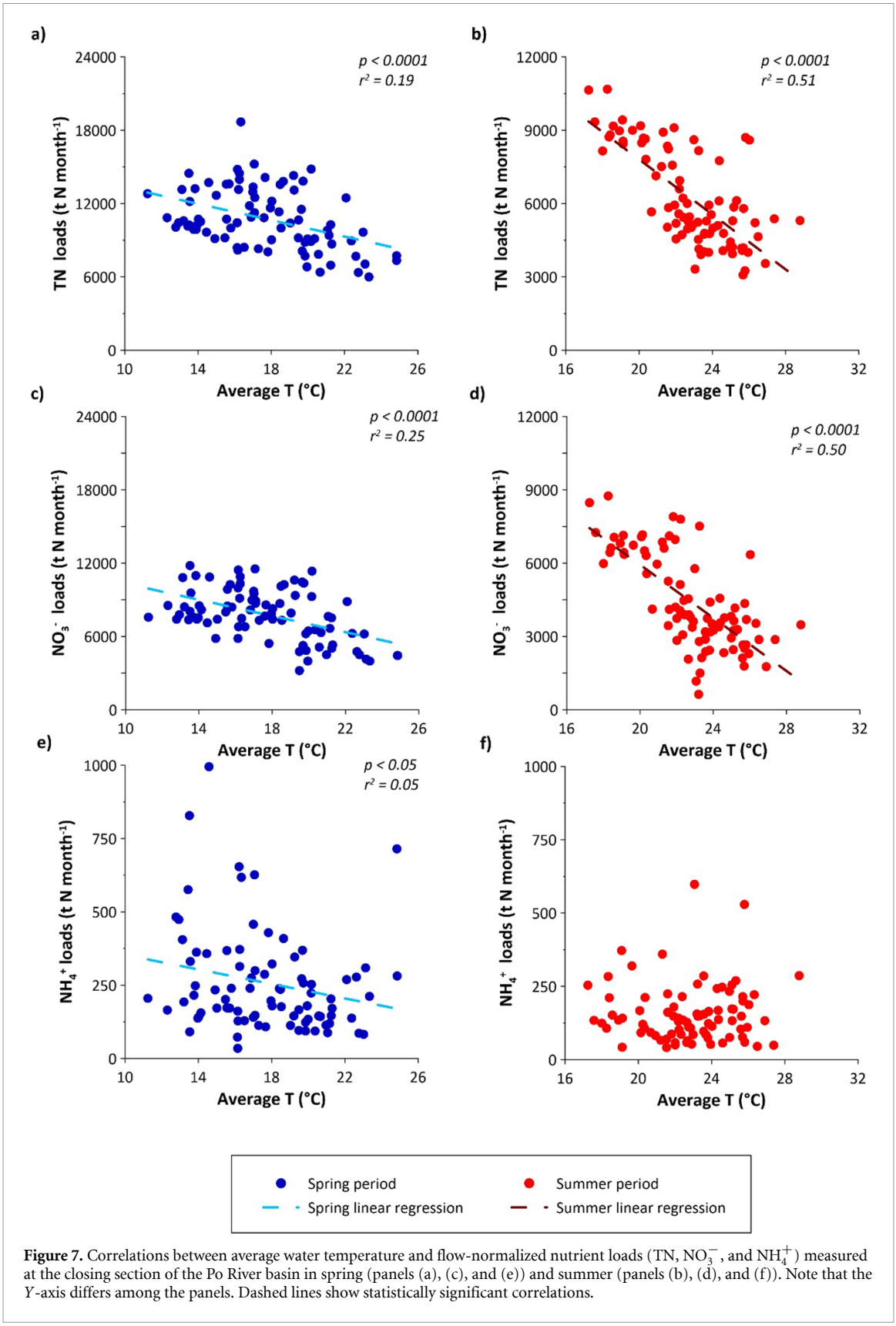

Figure 7. Correlations between average water temperature and flow-normalized nutrient loads (TN, NO_3^-, and NH_4^+) measured at the closing section of the Po River basin in spring (panels (a), (c), and (e)) and summer (panels (b), (d), and (f)). Note that the *Y*-axis differs among the panels. Dashed lines show statistically significant correlations.

the denitrification capacity [17, 75]. The inverse relationship between water temperature and NH_4^+ loads in spring also suggests that warming may stimulate nitrifying activity (figure 7(e)). Po River water column is indeed thoroughly mixed, thus dissolved oxygen concentrations are typically at or near 100% saturation, and the oxygenation of surface sediments is likely sufficient to support coupled nitrification–denitrification. However, as is widely reported, when water NO_3^- concentrations exceed 0.5 mg N l^{-1},

denitrification is expected to be fueled mainly by NO_3^- diffusing from the water column to the anoxic sediment layers [15, 16].

All biogeochemical NO_3^- dissimilative pathways, including denitrification and DNRA (dissimilatory NO_3^- reduction to NH_4^+), may be affected by water warming, both as a direct temperature effect on enzyme activity and as indirect temperature effect on sediment redox conditions (i.e. oxygen shortage because of decreased oxygen solubility or enhanced consumption rates). Organic carbon availability generally determines whether denitrification or DNRA will dominate in NO_3^- reduction, with organic enrichment and reducing (sulfidic) conditions under persistent stratification shifting NO_3^- reduction towards more pronounced DNRA, with internal NO_3^- recycling to NH_4^+ [80, 81]. However, this is not the case in the Po River where sediments are sandy and organic matter content is generally low [82]. Stimulation of DNRA by increased water temperature cannot be completely excluded, but this would have contributed to NH_4^+ accumulation in water, a condition not evidenced. On the contrary, the inverse relationship between water temperature and NH_4^+ loads suggested that warming might also have stimulated nitrifying activity as, in the Po River, the water column is constantly mixed and oxygen saturated, a condition favoring NH_4^+ consumption via nitrification–denitrification coupling. Despite direct measurements are still lacking, on the base of the evidence reported here, DNRA is likely a negligible pathway of N cycling in the Po River sediments.

The links between climate change and eutrophication are being debated and outcomes of many previous studies pointed towards an aggravation of eutrophication due to warming lentic water bodies [83]. Differently, warming and an increase in the duration of low-flow conditions might enhance the denitrification capacity of the river as a whole and partially reduce the risk of eutrophic conditions in the coastal zones. As temperatures are projected to increase in temperate regions over the coming decades, the present outcomes suggest an enhanced future denitrification, representing a natural way to counteract the harmful effects of eutrophication. Air temperatures are expected to rise across the entire Po River basin during all seasons and water temperatures will likely track this trend with the most significant changes occurring in summer alongside reductions in discharge [84]. A decrease in eutrophication phenomena in the Po River delta and nearby coastal zones may be expected, in the medium term, due to negative feedback between climate change and eutrophication in association with a potential water quality improvement.

4. Conclusions

The present study demonstrated that water temperature is a critical factor regulating N dynamics in rivers and water temperature increase associated with climate change may exert primary control on watershed-scale N export. The observed Po River temperature increase was likely associated with enhanced rates of microbial processes and more favorable conditions for denitrification and NO_3^- removal. Rivers are under pressure from eutrophication and warming, but an increased temperature-driven N dissipation capacity may ameliorate the quality of riverine water conveyed during the spring–summer period, partially preventing the degradation of coastal zones. As microbial communities drive key N cycle biogeochemical processes, understanding their response to climate change provides important insight into the river functioning regulation both now and in the future. Scenarios of in-stream N loads and export changes will benefit from further research into the relationships between climatic conditions and denitrification. The direct connection between climate warming and NO_3^- removal efficiency highlighted here demonstrates that differentiating climate change effects on denitrification during the spring and summer months is crucial for evaluating the N load delivery to the sea during those times of the year when the risk of eutrophication is greatest.

Data availability statement

The data that support the findings of this study are available upon reasonable request from the authors.

Acknowledgments

The research was developed within the research program ‘Origin and dynamics of the nutrient loadings delivered by the Po River and other basins flowing into the Adriatic Sea’ financed by the Po River District Authority. The authors are grateful to Dr Emilio Viganò (A2A gencogas S.p.A.) for providing water temperature dataset from Piacenza Power Station, to Dr Paolo Bronzi, President of the World Sturgeon Conservation Society, for precious advices and contacts relative to temperature data series, and to the Emilia-Romagna Agency for Environmental Protection for providing water quality data. Finally, the authors would like to thank Editage (www.editage.com) for English language editing.

Conflict of interest

The authors declare no conflict of interest.

Credit author contribution statements

Maria Pia Gervasio: investigation, formal analysis, writing—original draft preparation, visualization; Elisa Soana: conceptualization, methodology, investigation, writing—review and editing; Daniela Colombo: investigation; Tommaso Granata: investigation; Giuseppe Castaldelli: conceptualization, writing—review and editing, funding acquisition, supervision.

ORCID iDs

Maria Pia Gervasio https://orcid.org/0000-0003-1080-7759
Elisa Soana https://orcid.org/0000-0003-4656-5034
Giuseppe Castaldelli https://orcid.org/0000-0001-5954-1133

References

[1] Galloway J N, Townsend A R, Erisman J W, Bekunda M, Cai Z, Freney J R, Martinelli L A, Seizinger S P and Sutton M A 2008 Transformation of the nitrogen cycle: recent trends, questions and potential solutions *Science* **2008** 889–92
[2] Leip A *et al* 2015 Impacts of European livestock production: nitrogen, sulphur, phosphorus and greenhouse gas emissions, land-use, water eutrophication and biodiversity *Environ. Res. Lett.* **10** 115004
[3] Le Moal M *et al* 2019 Eutrophication: a new wine in an old bottle? *Sci. Total Environ.* **651** 1–11
[4] Howarth R, Swaney D, Billen G, Garnier J, Hong B, Humborg C, Johnes P, Mörth C M and Marino R 2012 Nitrogen fluxes from the landscape are controlled by net anthropogenic nitrogen inputs and by climate *Front. Ecol. Environ.* **10** 37–43
[5] Compton J E, Goodwin K E, Sobota D J and Lin J 2020 Seasonal disconnect between streamflow and retention shapes riverine nitrogen export in the Willamette River Basin, Oregon *Ecosystems* **23** 1–17
[6] Dupas R, Ehrhardt S, Musolff A, Fovet O and Durand P 2020 Long-term nitrogen retention and transit time distribution in agricultural catchments in western France *Environ. Res. Lett.* **15** 115011
[7] Jeppesen E *et al* 2011 Climate change effects on nitrogen loading from cultivated catchments in Europe: implications for nitrogen retention, ecological state of lakes and adaptation *Hydrobiologia* **663** 1–21
[8] Baron J S, Hall E K, Nolan B T, Finlay J C, Bernhardt E S, Harrison J A, Chan F and Boyer E W 2013 The interactive effects of excess reactive nitrogen and climate change on aquatic ecosystems and water resources of the United States *Biogeochemistry* **114** 71–92
[9] Ballard T C, Sinha E and Michalak A M 2019 Long-term changes in precipitation and temperature have already impacted nitrogen loading *Environ. Sci. Technol.* **53** 5080–90
[10] Øygarden L, Deelstra J, Lagzdins A, Bechmann M, Greipsland I, Kyllmar K, Povilaitis A and Iital A 2014 Climate change and the potential effects on runoff and nitrogen losses in the Nordic–Baltic region *Agric. Ecosyst. Environ.* **198** 114–26
[11] Yang X, Warren R, He Y, Ye J, Li Q and Wang G 2018 Impacts of climate change on TN load and its control in a River Basin with complex pollution sources *Sci. Total Environ.* **615** 1155–63
[12] Boulêtreau S, Salvo E, Lyautey E, Mastrorillo S and Garabetian F 2012 Temperature dependence of denitrification in phototrophic river biofilms *Sci. Total Environ.* **416** 323–8
[13] Boyacioglu H, Vetter T, Krysanova V and Rode M 2012 Modeling the impacts of climate change on nitrogen retention in a 4th order stream *Clim. Change* **113** 981–99
[14] McCrackin M L, Harrison J A and Compton J E 2014 Factors influencing export of dissolved inorganic nitrogen by major rivers: a new, seasonal, spatially explicit, global model *Glob. Biogeochem. Cycles* **28** 269–85
[15] Pina-Ochoa E and Álvarez-Cobelas M 2006 Denitrification in aquatic environments: a cross-system analysis *Biogeochemistry* **81** 111–30
[16] Birgand F, Skaggs R W, Chescheir G M and Gilliam J W 2007 Nitrogen removal in streams of agricultural catchments—a literature review *Crit. Rev. Environ. Sci. Technol.* **37** 381–487
[17] Veraart A J, de Klein J J and Scheffer M 2011 Warming can boost denitrification disproportionately due to altered oxygen dynamics *PLoS One* **6** e18508
[18] Tatariw C, Chapman E L, Sponseller R A, Mortazavi B and Edmonds J W 2013 Denitrification in a large river: consideration of geomorphic controls on microbial activity and community structure *Ecology* **94** 2249–62
[19] Viaroli P, Soana E, Pecora S, Laini A, Naldi M, Fano E A and Nizzoli D 2018 Space and time variations of watershed N and P budgets and their relationships with reactive N and P loadings in a heavily impacted river basin (Po River, Northern Italy) *Sci. Total Environ.* **639** 1574–87
[20] Romero E, Garnier J, Lassaletta L, Billen G, Le Gendre R, Riou P and Cugier P 2013 Large-scale patterns of river inputs in southwestern Europe: seasonal and interannual variations and potential eutrophication effects at the coastal zone *Biogeochemistry* **113** 481–505
[21] Yang J, Strokal M, Kroeze C, Chen X, Bai Z, Li H and Ma L 2021 Seasonal river export of nitrogen to Guanting and Baiyangdian Lakes in the Hai He Basin *J. Geophys. Res.* **126** e2020JG005689
[22] López-Moreno J I, Vicente-Serrano S M, Morán-Tejeda E, Lorenzo J, Kenawy A and Beniston M 2011 NAO effects on combined temperature and precipitation winter modes in the Mediterranean mountains: observed relationships and projections for the 21st century *Glob. Planet. Change* **77** 62–66
[23] Spinoni J, Barbosa P, de Jager A, McCormick N, Naumann G, Vogt J V, Magni D, Masante D and Mazzeschi M 2019 A new global database of meteorological drought events from 1951 to 2016 *J. Hydrol.: Reg. Stud.* **22** 100593
[24] Bozzola M and Swanson T 2014 Policy implications of climate variability on agriculture: water management in the Po River basin, Italy *Environ. Sci. Policy* **43** 26–38
[25] Appiotti F, Krželj M, Russo A, Ferretti M, Bastianini M and Marincioni F 2014 A multidisciplinary study on the effects of climate change in the northern Adriatic Sea and the Marche region (central Italy) *Reg. Environ. Change* **14** 2007–24
[26] Marchina C, Natali C, Fazzini M, Fusetti M, Tassinari R and Bianchini G 2017 Extremely dry and warm conditions in Northern Italy during the year 2015: effects on the Po River water *Rend. Lincei* **28** 281–90
[27] de Wit M and Bendoricchio G 2001 Nutrient fluxes in the Po basin *Sci. Total Environ.* **273** 147–61
[28] Palmeri L, Bendoricchio G and Artioli Y 2005 Modelling nutrient emissions from river systems and loads to the coastal zone: Po River case study, Italy *Ecol. Modelling* **184** 37–53
[29] Toreti A, Desiato F, Fioravanti G and Perconti W 2010 Seasonal temperatures over Italy and their relationship with low-frequency atmospheric circulation patterns *Clim. Change* **99** 211–27
[30] Fioravanti G, Piervitali E and Desiato F 2016 Recent changes of temperature extremes over Italy: an index-based analysis *Theor. Appl. Climatol.* **123** 473–86

[31] Free G et al 2021 Detecting climate driven changes in chlorophyll-a using high frequency monitoring: the impact of the 2019 European heatwave in three contrasting aquatic systems *Sensors* **21** 6242
[32] Brunetti M, Maugeri M, Monti F and Nanni T 2006 Temperature and precipitation variability in Italy in the last two centuries from homogenised instrumental time series *Int. J. Climatol. A* **26** 345–81
[33] Zanchettin D, Traverso P and Tomasino M 2008 Po River discharges: a preliminary analysis of a 200-year time series *Clim. Change* **89** 411–33
[34] Montanari A 2012 Hydrology of the Po River: looking for changing patterns in river discharge *Hydrol. Earth Syst. Sci.* **16** 3739–47
[35] Beck H E, Zimmermann N E, McVicar T R, Vergopolan N, Berg A and Wood E F 2018 Present and future Köppen-Geiger climate classification maps at 1-km resolution *Sci. Data* **5** 180214
[36] Eurostat 2012 Agri-environmental indicator—nitrate pollution of water p 389 (available at: https://ec.europa.eu/eurostat) (Accessed 31 July 2021)
[37] Musacchio A, Mas-Pla J, Soana E, Re V and Sacchi E 2021 Governance and groundwater modelling: hints to boost the implementation of the EU nitrate directive. The Lombardy Plain case, N Italy *Sci. Total Environ.* **782** 146800
[38] Ludwig W, Dumont E, Meybeck M and Heussner S 2009 River discharges of water and nutrients to the Mediterranean and Black Sea: major drivers for ecosystem changes during past and future decades? *Prog. Oceanogr.* **80** 199–217
[39] Blaas H and Kroeze C 2016 Excessive nitrogen and phosphorus in European rivers: 2000–2050 *Ecol. Indic.* **67** 328–37
[40] Grilli F et al 2020 Seasonal and interannual trends of oceanographic parameters over 40 years in the Northern Adriatic Sea in relation to nutrient loadings using the EMODnet chemistry data portal *Water* **12** 2280
[41] APAT—IRSA/CNR Metodi analitici per le acque. Manuali e linee guida 29/2003 (available at: www.irsa.cnr.it/Metodi.html)
[42] Moatar F and Meybeck M 2005 Compared performances of different algorithms for estimating annual nutrient loads discharged by the eutrophic River Loire *Hydrol. Process.* **19** 429–44
[43] Nava V, Patelli M, Rotiroti M and Leoni B 2019 An R package for estimating river compound load using different methods *Environ. Model. Softw.* **117** 100–8
[44] Po River District Authority. 2021. Management plan of the hydrographic district of the River Po In Italian (available at: https://pianoacque.adbpo.it/piano-di-gestione-2021/)
[45] Lenhart H J, Mills D K, Baretta-Bekker H, van Leeuwen S M, van der Molen J, Baretta J W and Wakelin S L 2010 Predicting the consequences of nutrient reduction on the eutrophication status of the North Sea *J. Mar. Syst.* **81** 148–70
[46] Sileika A S, Stålnacke P, Kutra S, Gaigalis K and Berankiene L 2006 Temporal and spatial variation of nutrient levels in the Nemunas River (Lithuania and Belarus) *Environ. Monit. Assess.* **122** 335–54
[47] Soana E, Bartoli M, Milardi M, Fano E A and Castaldelli G 2019 An ounce of prevention is worth a pound of cure: managing macrophytes for nitrate mitigation in irrigated agricultural watersheds *Sci. Total Environ.* **647** 301–12
[48] Pinardi M, Soana E, Bresciani M, Villa P and Bartoli M 2020 Upscaling nitrogen removal processes in fluvial wetlands and irrigation canals in a patchy agricultural watershed *Wetl. Ecol. Manage.* **28** 297–313
[49] McLeod A I 2011 Kendall: Kendall rank correlation and Mann-Kendall trend test. R package version 2.2. (available at: https://cran.r-project.org/web/packages/Kendall/index.html)
[50] Campanelli A, Grilli F, Paschini E and Marini M 2011 The influence of an exceptional Po River flood on the physical and chemical oceanographic properties of the Adriatic Sea *Dyn. Atmos. Oceans* **52** 284–97
[51] Marchina C, Natali C and Bianchini G 2019 The Po River water isotopes during the drought condition of the year 2017 *Water* **11** 150
[52] Martinelli G, Dadomo A, de Luca D A, Mazzola M, Lasagna M, Pennisi M, Pilla G, Sacchi E and Saccon P 2018 Nitrate sources, accumulation and reduction in groundwater from Northern Italy: insights provided by a nitrate and boron isotopic database *Appl. Geochem.* **91** 23–35
[53] Romero E, Garnier J, Billen G, Peters F and Lassaletta L 2016 Water management practices exacerbate nitrogen retention in Mediterranean catchments *Sci. Total Environ.* **573** 420–32
[54] Cencini C 1998 Physical processes and human activities in the evolution of the Po delta, Italy *J. Coast. Res.* **14** 775–93 (available at: www.jstor.org/stable/4298834)
[55] Marchetti M 2002 Environmental changes in the central Po Plain (Northern Italy) due to fluvial modifications and anthropogenic activities *Geomorphology* **44** 361–73
[56] Frascaroli F, Parrinello G and Root-Bernstein M 2021 Linking contemporary river restoration to economics, technology, politics, and society: perspectives from a historical case study of the Po River Basin, Italy *Ambio* **50** 492–504
[57] Ferrari I, Viglioli S, Viaroli P and Rossetti G 2006 The impact of the summer 2003 drought event on the zooplankton of the Po River (Italy) *Int. Vereinigung Theoretische Angew. Limnol.: Verh.* **29** 2143–9
[58] Giani M, Djakovac T, Degobbis D, Cozzi S, Solidoro C and Umani S F 2012 Recent changes in the marine ecosystems of the northern Adriatic Sea *Estuar. Coast. Shelf Sci.* **115** 1–13
[59] Kaushal S S, Likens G E, Jaworski N A, Pace M L, Sides A M, Seekell D, Belt K T, Secor D H and Wingate R L 2010 Rising stream and river temperatures in the United States *Front. Ecol. Environ.* **8** 461–6
[60] Hannah D M and Garner G 2015 River water temperature in the United Kingdom: changes over the 20th century and possible changes over the 21st century *Prog. Phys. Geogr.* **39** 68–92
[61] Langan S J, Johnston L, Donaghy M J, Youngson A F, Hay D W and Soulsby C 2001 Variation in river water temperatures in an upland stream over a 30-year period *Sci. Total Environ.* **265** 195–207
[62] Daufresne M, Roger M C, Capra H and Lamouroux N 2004 Long-term changes within the invertebrate and fish communities of the Upper Rhône River: effects of climatic factors *Glob. Change Biol.* **10** 124–40
[63] Floury M, Delattre C, Ormerod S J and Souchon Y 2012 Global versus local change effects on a large European river *Sci. Total Environ.* **441** 220–9
[64] Markovic D, Scharfenberger U, Schmutz S, Pletterbauer F and Wolter C 2013 Variability and alterations of water temperatures across the Elbe and Danube River Basins *Clim. Change* **119** 375–89
[65] Seyedhashemi H, Vidal J P, Diamond J S, Thiéry D, Monteil C, Hendrickx F, Maire A and Moatar F 2022 Regional, multi-decadal analysis on the Loire River basin reveals that stream temperature increases faster than air temperature *Hydrol. Earth Syst. Sci.* **26** 2583–603
[66] Ciccarelli N, von Hardenberg J, Provenzale A, Ronchi C, Vargiu A and Pelosini R 2008 Climate variability in north-western Italy during the second half of the 20th century *Glob. Planet. Change* **63** 185–95
[67] Pham H, Torresan S, Critto A and Marcomini A 2019 Alteration of freshwater ecosystem services under global change–a review focusing on the Po River basin (Italy) and the Red River basin (Vietnam) *Sci. Total Environ.* **652** 1347–65
[68] Tibaldi S, Cacciamani C and Pecora S 2010 The Po River in a changing climate *Biol. Ambient.* **24** 21–28
[69] Kostopoulou E and Jones P D 2005 Assessment of climate extremes in the Eastern Mediterranean *Meteorol. Atmos. Phys.* **89** 69–85
[70] Burić D, Luković J, Ducić V, Dragojlović J and Doderović M 2014 Recent trends in daily temperature extremes over

southern Montenegro (1951–2010) *Nat. Hazards Earth Syst. Sci.* **14** 67–72
[71] Efthymiadis D, Goodess C M and Jones P D 2011 Trends in Mediterranean gridded temperature extremes and large-scale circulation influences *Nat. Hazards Earth Syst. Sci.* **11** 2199–214
[72] Degobbis D, Precali R, Ivancic I, Smodlaka N, Fuks D and Kveder S 2000 Long-term changes in the northern Adriatic ecosystem related to anthropogenic eutrophication *Int. J. Environ. Pollut.* **13** 495–533
[73] Djakovac T, Degobbis D, Supić N and Precali R 2012 Marked reduction of eutrophication pressure in the northeastern Adriatic in the period 2000–2009 *Estuar. Coast. Shelf Sci.* **115** 25–32
[74] Jourdan J *et al* 2018 Effects of changing climate on European stream invertebrate communities: a long-term data analysis *Sci. Total Environ.* **621** 588–99
[75] de Klein J J, Overbeek C C, Jørgensen C J and Veraart A J 2017 Effect of temperature on oxygen profiles and denitrification rates in freshwater sediments *Wetlands* **37** 975–83
[76] Schaefer S C and Alber M 2007 Temperature controls a latitudinal gradient in the proportion of watershed nitrogen exported to coastal ecosystems *Biogeochemistry* **85** 333–46
[77] Tiedje J M 1988 Ecology of denitrification and dissimilatory nitrate reduction to ammonium *Biology of Anaerobic Microorganisms* ed A J B Zehnder (New York: Wiley) pp 179–244
[78] Holmes R M, Jones J B, Fisher S G and Grimm N B 1996 Denitrification in a nitrogen-limited stream ecosystem *Biogeochemistry* **33** 125–46
[79] Royer T V, Tank J L and David M B 2004 Transport and fate of nitrate in headwater agricultural streams in Illinois *J. Environ. Qual.* **33** 1296–304
[80] Scott J T, McCarthy M J, Gardner W S and Doyle R D 2008 Denitrification, dissimilatory nitrate reduction to ammonium, and nitrogen fixation along a nitrate concentration gradient in a created freshwater wetland *Biogeochemistry* **87** 99–111
[81] Nizzoli D, Carraro E, Nigro V and Viaroli P 2010 Effect of organic enrichment and thermal regime on denitrification and dissimilatory nitrate reduction to ammonium (DNRA) in hypolimnetic sediments of two lowland lakes *Water Res.* **44** 2715–24
[82] Viganò L *et al* 2003 Quality assessment of bed sediments of the Po River (Italy) *Water Res.* **37** 501–18
[83] Moss B *et al* 2011 Allied attack: climate change and eutrophication *Inland Waters* **1** 101–5
[84] Vezzoli R, Mercogliano P, Pecora S, Zollo A L and Cacciamani C 2015 Hydrological simulation of Po River (North Italy) discharge under climate change scenarios using the RCM COSMO-CLM *Sci. Total Environ.* **521** 346–58

Supplementary Materials 1

Datasets of air and water temperature

Po River water temperature was retrieved from the ARPAE (Regional Environmental Protection Agency of the Emilia-Romagna region) database (https://dati.arpae.it/group/acqua) for two stations belonging to the official monitoring network. The ARPAE Castel San Giovanni station (45°05'30.0"N, 9°26'44.2"E) is close to La Casella Power Station (less than 2 km), while the ARPAE Piacenza station (45°03'37.9"N, 9°42'19.9"E) is close to A2A Piacenza Power Station (less than 1.5 km). Water temperatures were obtained from monthly sampling campaigns carried out, the same day (within a few hours) for the two stations, under the framework of the ARPAE environmental monitoring program. Observation taken the same day at the two ARPAE stations were consistent. Due to the very good correlation (Fig. S1) and a discrepancy of less than 0.3°C, on average, between observations, we considered appropriate to combine the two datasets (from 1992 to 2005 for La Casella Power Station and from 2006 to 2019 for A2A Piacenza Power Station) to reconstruct a continuous three-decade time series.

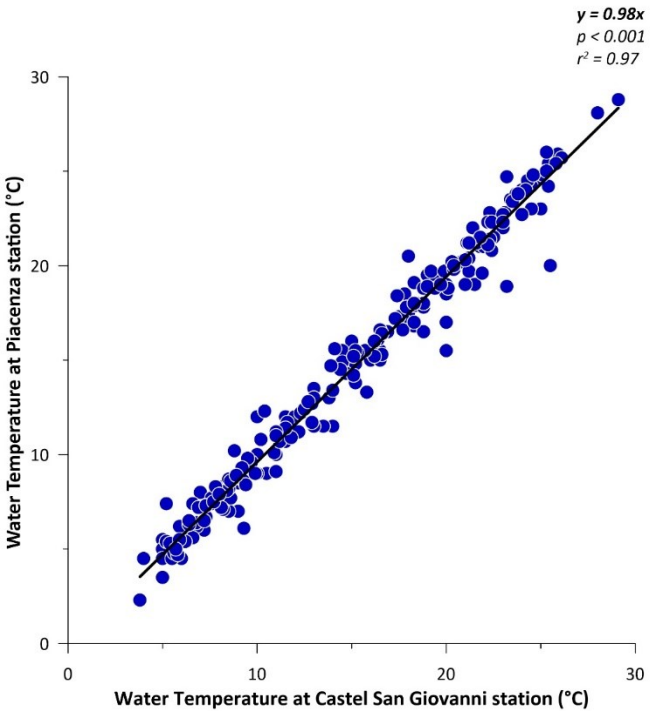

Figure S1: Correlation between water temperature measured at Castel San Giovanni station and Piacenza station. Black line shows statistically significant correlation; statistical data are

on the right top of the panel. Data source: ARPAE (1992-2019; https://dati.arpae.it/group/acqua).

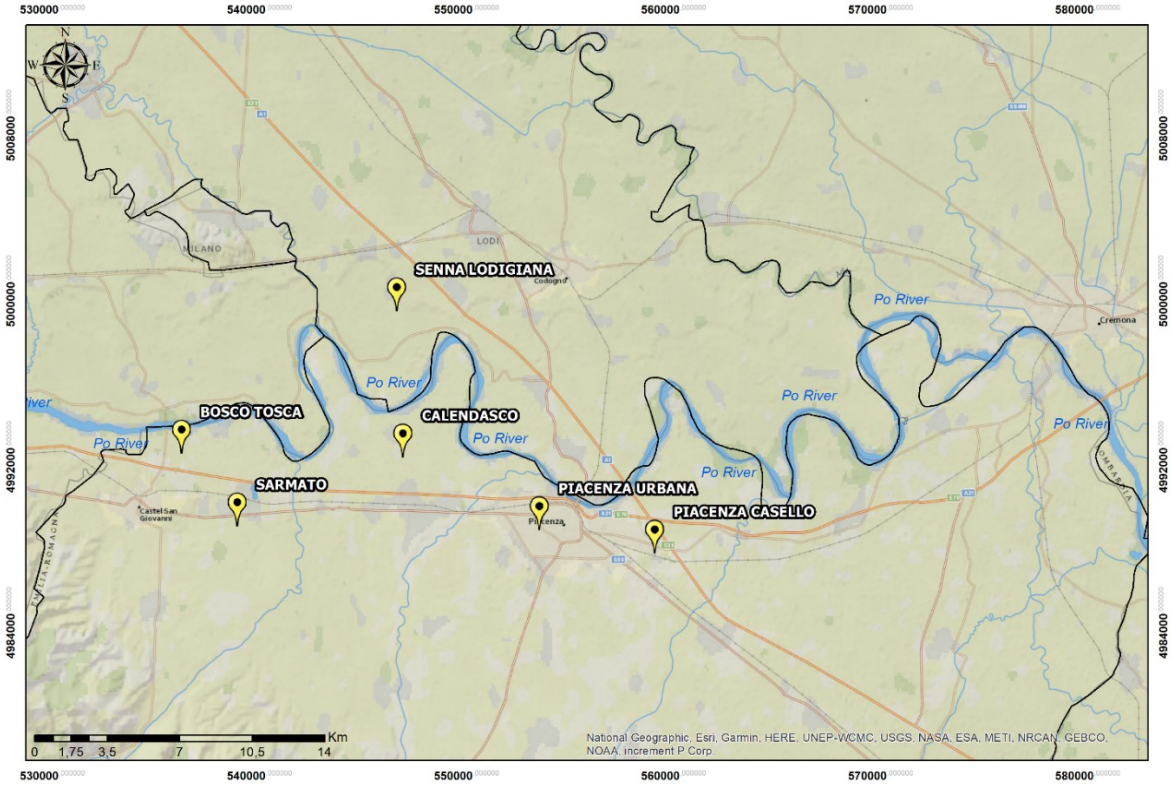

Figure S2: Map of six monitoring air stations of Eraclito (ARPAE climatic datasets) located near the city of Piacenza and the Po River course (modified from Basemap of ArcMap 10.2.2; source: Esri, Maxar, GeoEye, Earthstar Geographics, CNES/Airbus DS, USDA, USGS, AeroGRID, IGN, and the GIS User Community).

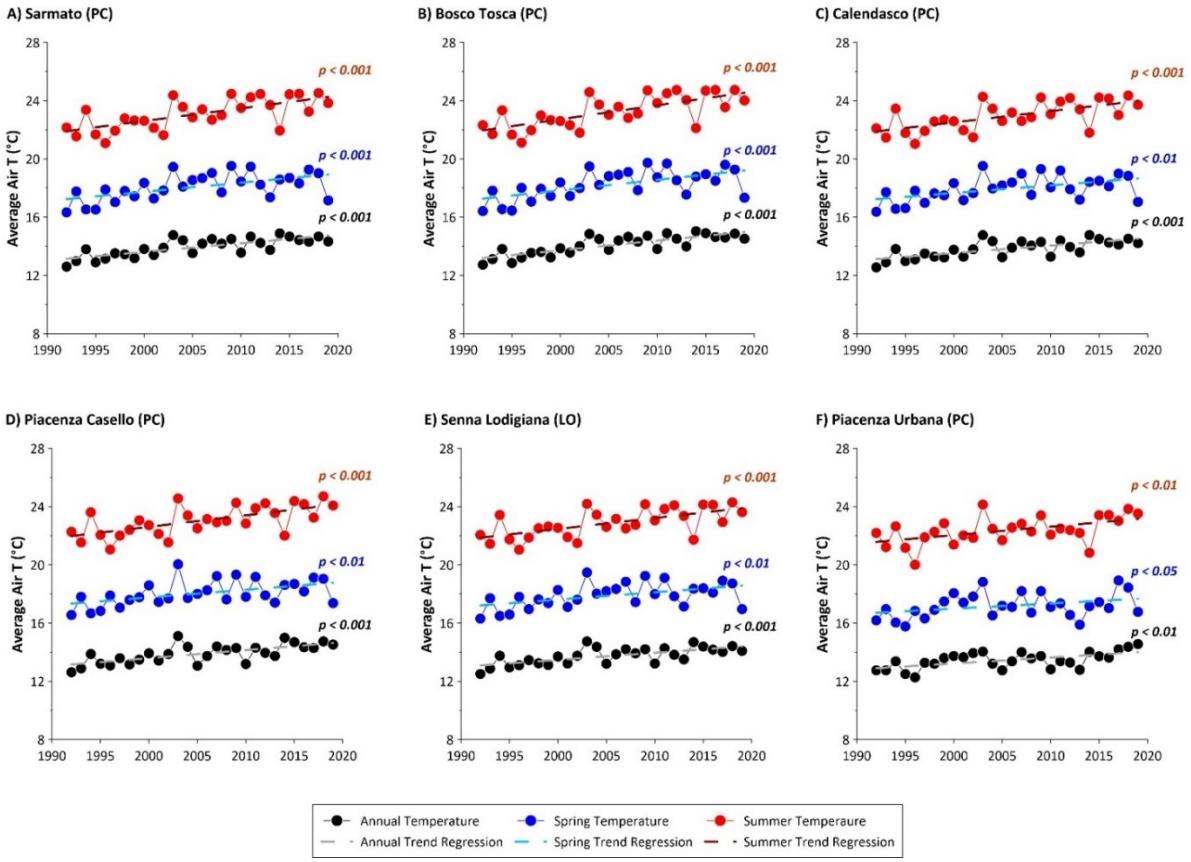

Figure S3: Temporal trend of annual, spring and summer average air temperature recorded at six monitoring stations near the city of Piacenza and the Po River course. Dashed lines show statistically significant trends. Data source: ARPAE climatic "Eraclito" database (https://dati.arpae.it/dataset/erg5-eraclito).

Supplementary Materials 2

Validation of annual riverine N load calculation

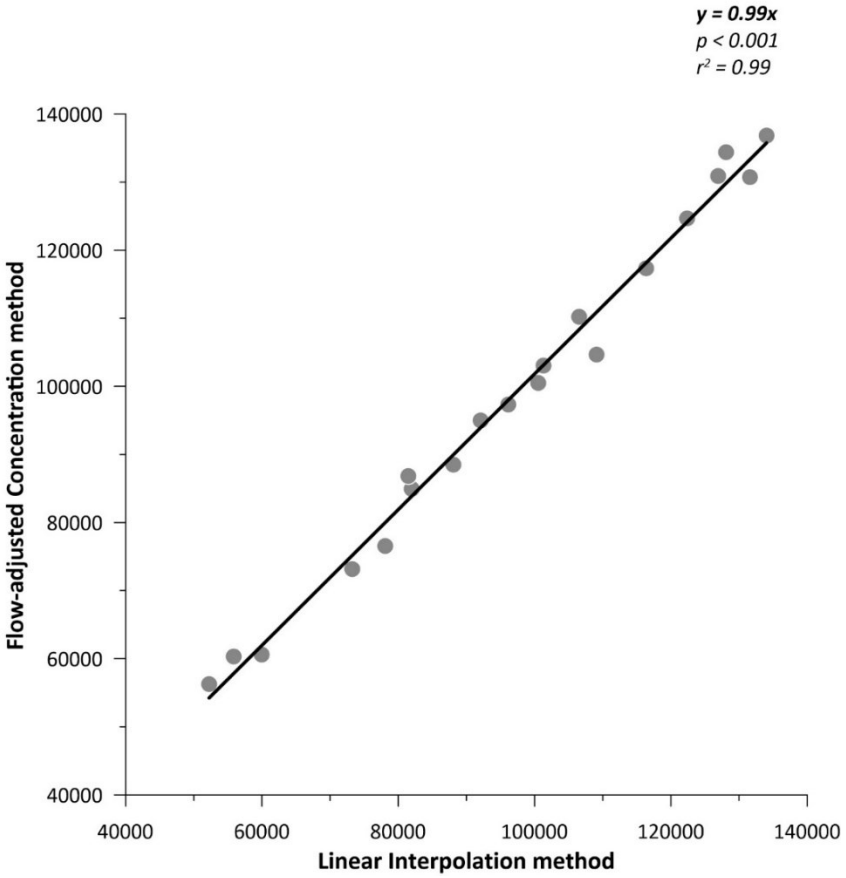

Figure S4: Correlation between annual nitrate loads calculated by the linear interpolation method and by flow-adjusted concentration method.

Supplementary Materials 3

Collection of census data

Statistics were retrieved, at the provincial scale, from the data warehouse of the National Institute of Statistics (ISTAT), published in the framework of the Annals of Agrarian Statistics (http://dati.istat.it/) and of the Annals of Resident Population (http://demo.istat.it/index.php). A total of 32 provinces (surface from ~400 to ~6900 km2), either totally or partially included within the basin boundary, were considered. According to the official EU division for regional statistics elaborated by EUROSTAT (2015; [1]), Italian provinces correspond to the NUTS-3 territorial level. The collection of statistical data was carried out through the consultation of printed volumes of Annals for the years 1990 and 2000 and through web searches in the ISTAT data warehouse for the years 2010 and 2019. Province-level N budgets were aggregated at the catchment scale by weighting, via GIS analysis (QGIS software, version 3.16), each province values based on the percentage of surface included within the watershed boundaries.

Calculation of N loads from diffuse sources

The N loads from diffuse sources were quantified by calculating the N balance across the agricultural lands (AL), accounting for the net difference between inputs (livestock manure, synthetic fertilizers, atmospheric deposition, and biological fixation) and outputs (crop harvest, ammonia volatilization, and denitrification) across the AL. Nitrogen budget was calculated for the years 1990, 2000, 2010 and 2019, as follow:

$$N\ budget\ =\ N_{Man}\ +N_{Fer}\ +\ N_{Fix}+N_{Dep}-N_{Harv}-N_{Vol}-N_{Den}$$

(1)

Where:

N_{Man} = livestock manure

N_{Fert} = synthetic fertilizer

N_{Fix} = N_2 fixation by N fixing crops

N_{Dep} = atmospheric deposition on AL

N_{Harv} = export from AL with crop harvest

N_{Vol} = ammonia volatilization in AL

N_{Den} = denitrification in AL

For each budget term, type of data, equation and data sources are detailed below. An uncertainty was associated to each budget term obtained by propagating the errors of the coefficients used to calculate each specific item. Uncertainty of the coefficients, expressed in term of coefficient of variation (CV), was based on the best available information for the investigated area. Otherwise, values commonly used in watershed nutrient budgeting studies were assumed [2; 3; 4].

N input from livestock manure was calculated by means of a) livestock density data (divided in 8 major categories and 30 sub-categories according to type, age, and purpose), b) live weight of each livestock category, and c) N excretion rate of each livestock category corrected for the N amount volatilised as NH_3 during animal housing and manure storage (DM 07/04/2006, decree of the Italian Ministry of Agricultural and Forest Policies about agronomic utilization disciplinary; Table S1). Livestock data at the provincial level were acquired from the Annals of Agrarian Statistics (http://dati.istat.it/). CVs of 25% (cattle) and 10% (other livestock categories) were used for livestock N excretion rates (DM 07/04/2006, decree of the Italian Ministry of Agricultural and Forest Policies about agronomic utilization disciplinary; [5]).

N input (t N yr^{-1}) from livestock manure was calculated as follows:

$$Man = \sum_{livestock}(Exc \cdot LW \cdot N) \cdot \frac{1}{1000} \quad (2)$$

where:

Exc = N excretion rate of each livestock category (kg N t^{-1} live weight yr^{-1})

LW = live weight of each livestock category (t)

N = livestock density for each category

N input from synthetic fertilizers was estimated using official data on provincial-scale distribution retrieved from the Annals of Agrarian Statistics (http://dati.istat.it/) and

converted into N amounts by means of the average N content for each fertilizer type. Data included simple mineral N fertilizers (calcium cyanamide, nitrates, ammonium sulphate, urea, and others N fertilizers), compound mineral fertilizers (NP, NK, and NPK compounds), organic and organo-mineral fertilizers and soil amendments. The assumption was that the quantity distributed in each province was equivalent to the quantity effectively applied on croplands of the same province. However, data was cross-checked with the total N demand calculated from the N fertilizer application rate recommended for each crop by the Rural Development Programs of the Regions included within the Po River catchment. CV of 5% was assumed for fertilizer N content [3].

N input from biological fixation was calculated by means of a) surface of each N-fixing crop type (alfalfa and soybean) and b) areal rates of symbiotic N fixation. Rates of biological N fixation were estimated by multiplying the production per unit of surface (i.e. yield) by the N uptake coefficient of the harvested portions (Table S2) corrected for a multiplicative factor expressing the ratio of total biomass produced to harvested biomass. CVs of crop yield and N uptake coefficients were assumed equal to 15% and 25%, respectively [2; 3]. According to Anglade et al. [6], a value of 1.7 and 1.3 was used for alfalfa and soybean, respectively. Provincial surface and yield for each crop type were retrieved from the Annals of Agrarian Statistics (http://dati.istat.it/). According to the Rural Development Program of the Regions belonging to the Po river basin, no N fertilization is allowed for N-fixing crops.

N input (t N yr^{-1}) from symbiotic fixation was calculated as follows:

$$Fix = \sum_{N-fixing\ crop}(Y \cdot Upt \cdot BGN \cdot UAA) \cdot \frac{1}{1000} \quad (3)$$

where:

Y = yield of the harvest portion of each N-fixing crop (t ha^{-1})

Upt = N uptake coefficient of the harvest portion of N-fixing crop (kg N t^{-1})

BGN = factor expressing the ratio of total biomass produced with respect to harvested biomass

UAA = surface of each N-fixing crop (ha)

Literature rates of 1-8 and 1-10 kg ha^{-1} yr^{-1} were adopted for non-symbiotic N fixation in arable land and permanent crops, respectively [7; 8; 9].

Spatialized average value of atmospheric oxidized N deposition for the Po River basin varied between 8.5 (years 2010, 2019) and 9.5 kg ha^{-1} yr^{-1} (years 1990, 2000) according to the EMEP-Co-operative Programme for Monitoring and Evaluation of the Long-range Transmission of Air Pollutants in Europe (https://www.emep.int/). As conventionally done for N budget calculations at the watershed scale, only the oxidized N species are considered, since the deposition of reduced N species likely reflects local recycling being NH_3 short-lived in the atmosphere [10]. CV of N deposition was assumed equal to 15% [3].

N output from crop harvest was calculated by means of a) surface of each crop type cultivated in the study area, b) N uptake coefficient and c) yield of the harvested portion of each crop (Table S2). For N-fixing crops, the N amount exported from agricultural land was assumed equal to that fixed in the above-ground biomass. As crop residues are usually left on the fields, N in crop residues was not accounted as an output in the budget. Provincial surface and yield for each crop type were retrieved from the Annals of Agrarian Statistics (http://dati.istat.it/). CVs of crop yield and N uptake coefficients were assumed equal to 15% and 25%, respectively [2; 3].

N output (t N yr^{-1}) from crop harvest was calculated as follows:

$$Harv = \sum_{crop}(Y \cdot Upt \cdot UAA) \cdot \frac{1}{1000} \quad (4)$$

where:

Y = yield of the harvest portion of each crop (t ha^{-1})

Upt = N uptake coefficient of the harvest portion of each crop (kg N t^{-1})

UAA = surface of each crop (ha)

Direct measurements of N losses to the atmosphere via ammonia volatilization and denitrification are still very limited for the Italian agriculture, in terms of national territory coverage, representativeness of the employed method, and type of fertiliser and application strategies tested [11; 12]. Thus, N outputs from ammonia volatilization and denitrification in

agricultural soils were estimated by published emission factors expressing the percentage loss of the supplied N, according to the budget methodology previously applied to other sub-basins of the Po River system [13; 14]. Ammonia volatilization factors of 5-60%, 1-30%, 2-10%, and 1-4% were associated to animal manure, urea plus ammonium sulphate, nitrates and other N fertilizers, respectively [12; 15]. About 60% of the volatilised ammonia was assumed to be re-deposited locally and only the remaining 40% was considered as a true N output from the agricultural system.

Nitrogen output from denitrification was assumed to be proportional to the total organic and chemical N application to AL and varied on average from 5 to 15% of the supplied N, spanning the main soil types of the study area, according to a review of a vast body of literature [14].

Calculation of N loads from point sources

Nitrogen load from point sources was quantified by employing resident population data (Annals of Resident Population, http://demo.istat.it/index.php) and per capita N production coefficient (12.5 g N d^{-1}; [16]) corrected for the percentage of sewage systems connected to wastewater treatment plants-WTTPs (primary, secondary and tertiary treatments) and the correspondent depuration efficiency (Po river basin District Authority, 2015; https://pianoacque.adbpo.it/piano-di-gestione-2015/; Emilia-Romagna Region, 2017; https://datacatalog.regione.emilia-romagna.it/catalogCTA/) (Table S3).

Table S1: Livestock categories, live weights, and N excretion rates.

Category	Sub-category	Live weight (kg)	N excretion rate (kg N t^{-1} live weight yr^{-1})
Cattle	cattle <1 year	220	67
	cattle 1-2 year: males	350	84
	cattle1-2 year: females	300	120
	cattle >2 years: males for reproduction	800	84
	cattle >2 years: heifers for breeding	600	120
	cattle >2 years: heifers for slaughtering	600	84
	cattle >2 years: dairy cows	600	138
	cattle >2 years: cows for meat and/or work	600	120
Buffaloes	buffalo calves	200	67
	famale buffaloes	600	138
	other buffaloes	300	84
Equidae	horses	350	69
	other (donkeys and mules)	200	69
Goats	goats	50	99
	other goats	25	99
Sheep	breeding females: dairy sheep	60	99
	breeding females: other sheep	50	99
	other sheep	35	99
Pigs	piglets < 20 kg	15	110
	pigs 20-50 kg	40	110
	pigs for fattening 50- 80 kg	65	110
	pigs for fattening 80- 110 kg	95	110
	pigs for fattening >110 kg	120	110
	males for reproduction	250	110
	sows	180	101
Poultry	broilers	1	250
	laying hens	1.9	230
	turkeys	6.5	167
Rabbits	breeding females	3.5	143
	other rabbits	1.7	143

Table S2: Nitrogen uptake coefficients of the main crops (harvested portions) considered in the calculation of N budget.

Type	Crop	N uptake coefficient (kg N ton^{-1})
Cereals	common wheat and spelt	21.0
	durum wheat	22.8
	rye	19.3
	barley	18.1
	oats	19.1
	grain maize	14.9
	sorghum	15.9
	other cereals	18.0
Industrial Crops	potato	4.2
	sugar beet	2.2
	rape and turnip rape	3.4
	sunflower	28.0
	soya beans	58.2
Fresh Vegetables	tomato for processing	2.6
	other fresh vegetables	5.0
Temporary grassland	alfalfa	27.0
	other multi-annual temporary grass	21.5
	annual grass: green maize consumed directly	4.0
	annual grass: green maize for silage	4.0
	other monophytous annual grass, cereal	4.0
	other annual grass	26.0
Permanent grassland	meadows	19.7
	pastures	8.0
Permanent woody crops	vineyard	2.0
	apple-tree	0.6
	peach-tree	1.3
	apricot-tree	1.3
	pear-tree	0.6
	nectarine-tree	1.4
	kiwi-tree	1.5

Table S3: Percentage of population connected to wastewater treatment plants with primary, secondary, and tertiary treatments and correspondent N removal efficiency.

year	Primary treatment (% of population)	N removal (%) in WTTPs with primary treatment	Secondary treatment (% of population)	N removal (%) in WTTPs with secondary treatment	Tertiary treatment (% of population)	N removal (%) in WTTPs with tertiary treatment
1990	50	15	50	60	0	72
2000	5	15	26	60	69	72
2010	3	15	27	60	70	72
2019	3	15	27	60	70	72

References

[1] EUROSTAT - European Commission. Regions in the European Union. 2015. Nomenclature of territorial units for statistics NUTS 2013/EU-28. Manuals and guidelines. Luxemburgo, Publications Office of the European Union. http://ec.europa.eu/eurostat/web/products-manuals-and-guidelines/-/KS-GQ-14-006

[2] Kroeze, C., Aerts, R., van Breemen, N., van Dam, D., Hofschreuder, P., Hoosbeek, M., deKlein, J., van der Hoek, K., Kros, H., van Oene, H., Oenema, O., Tietema, A., van der Veeren, R. & de Vries, W., (2003). Uncertainties in the fate of nitrogen I: An overview of sources of uncertainty illustrated with a Dutch case study. *Nutrient Cycling in Agroecosystems*, 66(1), 43-69. https://doi.org/10.1023/A:1023339106213

[3] Spiess, E. (2011) Nitrogen, phosphorus and potassium balances and cycles of Swiss agriculture from 1975 to 2008. *Nutrient Cycling in Agroecosystems*, 91(3), 351-365. https://doi.org/10.1007/s10705-011-9466-9

[4] Cameira, M. R., Rolim, J., Valente, F., Faro, A., Dragosits, U., & Cordovil, C. M. (2019). Spatial distribution and uncertainties of nitrogen budgets for agriculture in the Tagus river basin in Portugal–Implications for effectiveness of mitigation measures. *Land Use Policy*, 84, 278-293. https://doi.org/10.1016/j.landusepol.2019.02.028

[5] Xiccato, G., Schiavon, S., Gallo, L., Bailoni, L., Bittante, G. (2005). Nitrogen excretion in dairy cow, beef and veal cattle, pig, and rabbit farms in Northern Italy. *Italian Journal of Animal Science*, 4(3), 103-111. https://doi.org/10.4081/ijas.2005.3s.103

[6] Anglade, J., Billen, G., Garnier, J., Makridis, T., Puech, T., & Tittel, C. (2015). Nitrogen soil surface balance of organic vs conventional cash crop farming in the Seine watershed. *Agricultural Systems*, 139, 82-92. https://doi.org/10.1016/j.agsy.2015.06.006

[7] McKee, L. J., & Eyre, B. D. (2000). Nitrogen and phosphorus budgets for the sub-tropical Richmond River catchment, Australia. *Biogeochemistry,* 50(3), 207-239. https://doi.org/10.1023/A:1006391927371

[8] Herridge, D. F., Peoples, M. B., & Boddey, R. M. (2008). Global inputs of biological nitrogen fixation in agricultural systems. *Plant and Soil*, 311(1-2), 1-18. https://doi.org/10.1007/s11104-008-9668-3

[9] Butterbach-Bahl, K., Gundersen, P., Ambus, P., Augustin, J., Beier, C., Boeckx, P., Dannenmann, M., Gimeno, B. S., Ibrom, A., Kiese, R., Kitzler, B., Rees, R., M., Smith, K., A., Stevens, C., Vesala, T. & Zechmeister-Boltenstern, S. (2011) Nitrogen processes in terrestrial ecosystems. In The European Nitrogen Assessment: sources, effects and policy perspectives (pp. 99-125). *Cambridge University Press*. 10.1017/CBO9780511976988.009

[10] Hong, B., Swaney, D. P., Mörth, C. M., Smedberg, E., Hägg, H. E., Humborg, C., Howarth, R. W. & Bouraoui, F. (2012). Evaluating regional variation of net anthropogenic nitrogen and phosphorus inputs (NANI/NAPI), major drivers, nutrient retention pattern and management implications in the multinational areas of Baltic Sea basin. *Ecological Modelling,* 227, 117-135. https://doi.org/10.1016/j.ecolmodel.2011.12.002

[11] Arcara, P. G., Gamba, C., Bidini, D., & Marchetti, R. (1999). The effect of urea and pig slurry fertilization on denitrification, direct nitrous oxide emission, volatile fatty acids, water-soluble carbon and anthrone-reactive carbon in maize-cropped soil from the Po plain (Modena, Italy). *Biology and fertility of soils*, 29(3), 270-276. https://doi.org/10.1007/s003740050552

[12] Minoli, S., Acutis, M., & Carozzi, M. (2015). NH_3 emissions from land application of manures and N-fertilisers: a review of the Italian literature. *Italian Journal of Agronomy*, 3, 5-24.

[13] Soana, E., Racchetti, E., Laini, A., Bartoli, M., & Viaroli, P. (2011). Soil budget, net export, and potential sinks of nitrogen in the Lower Oglio River Watershed (Northern Italy). *CLEAN–Soil, Air, Water*, 39(11), 956-965. https://doi.org/10.1002/clen.201000454

[14] Castaldelli, G., Soana, E., Racchetti, E., Pierobon, E., Mastrocicco, M., Tesini, E., Fano, E.A., Bartoli, M. (2013). Nitrogen budget in a lowland coastal area within the Po river basin (Northern Italy): multiple evidences of equilibrium between sources and internal sinks. *Environmental Management*, 52(3), 567-580. 10.1007/s00267-013-0052-6

[15] Pan, B., Lam, S.K., Mosier, A., Luo, Y., Chen, D. (2016). Ammonia volatilization from synthetic fertilizers and its mitigation strategies: a global synthesis. *Agriculture, Ecosystems & Environment*, 232, 283-289. https://doi.org/10.1016/j.agee.2016.08.019

[16] Provini A, Galassi S, Marchetti R. 1998. *Applied Ecology*. Città Studi Edizioni, Torino (in Italian).

Supplementary Material 4

Statistical analyses

Linear regression test was applied to detect statistically significant temporal trends of water temperature, N loadings and water flow, and the correlation between water temperature and N loading. Linear regression lines were determined by the least-squares method. Data usually fit a straight line and if the slope is different from zero, the trend will be significant.

Mann-Kendall test [1; 2; 3] assumes the null hypothesis (H_0) of the absence of trend in the time series data over time, and the alternative hypothesis (H_1) of the existence of a trend. Statistics is calculated as:

$$S = \sum_{i=1}^{n-1} \sum_{j=i+1}^{n} sig\ (X_j - X_i) \quad (5)$$

$$VAR(S) = \frac{1}{10}\left[n(n-1)(2n+5) - \sum_{p=1}^{q} t_p\left(t_p - 1\right)\left(2t_p + 5\right)\right] \quad (6)$$

$$Z = \begin{cases} \frac{S-1}{\sqrt{VAR\ (S)}}\ if\ S > 0 \\ 0\ if\ S = 0 \\ \frac{S+1}{\sqrt{VAR\ (S)}}\ is\ S < 0 \end{cases} \quad (7)$$

where:

$$sig\ \left(X_j - X_i\right) = \begin{cases} +1\ if\ \left(X_j - X_i\right) > 0 \\ 0\ if\ \left(X_j - X_i\right) = 0 \\ -1\ if\ \left(X_j - X_i\right) < 0 \end{cases} \quad (8)$$

X_j and X_i are the time series observations in chronological order and n is the length of time series, tp is the number of ties for pth value, and q is the number of tied values. The Kendall Score (S) is the number of positive differences minus the number of negative differences; if S is a positive number, observations obtained later in time tend to be larger than observations

made earlier, opposite if *S* is a negative number. *VAR(S)* represents the variance of *S* and positive (negative) value of *Z* indicates that the data tend to increase (decrease) over the time.

The Sen's slope non-parametric test [4] was used to analyse the slope of the time series data (Q), as:

$$Q = \frac{X_i - X_j}{j - i} \tag{9}$$

where X_i and X_j indicate data value at time *j* and *i*, respectively. This method is applied as a support to Mann Kendall's test, to evaluate the magnitude of time series trend. Positive values indicate increasing trends and negative values indicate downward trends.

Pettitt test [5] identifies the existence of a changing point in the dataset: the null hypothesis (H_0) of the is that there is no change in the time series, while the alternative hypothesis (H_1) is that there is a shift in the central tendency. The non-parametric statistics is defined as:

$$K_T = max\left|U_{t,T}\right| \tag{10}$$

$$U_{t,T} = \sum_{i=1}^{t} \sum_{j=t+1}^{T} sgn(X_i - X_j) \tag{11}$$

and X_i and X_j are the value of the time series, and K_T indicates the position in the dataset where the change point is located.

References

[1] Mann, H. B. (1945). Nonparametric tests against trend. *Econometrica: Journal of the econometric society*, 245-259. https://doi.org/10.2307/1907187

[2] Kendall, M.G. (1975). *Rank Correlation Methods*, 4th edition, Charles Griffin, London.

[3] Gilbert, R. O. (1987). Statistical methods for environmental pollution monitoring. *John Wiley & Sons*.

[4] Sen, P. K. (1968). Estimates of the regression coefficient based on Kendall's tau. *Journal of the American statistical association*, 63(324), 1379-1389.

[5] Pettitt, A. N. (1979). A non-parametric approach to the change-point problem. *Journal of the Royal Statistical Society: Series C (Applied Statistics)*, 28(2), 126-135. https://doi.org/10.2307/2346729

Appendix II: One submitted article entitled: "*Contrasting effects of climate change on denitrification and nitrogen load reduction in the Po River (Northern Italy)*"

Paper III: Gervasio, M. P.*, Soana, E., Gavioli, A., Vincenzi, F., & Castaldelli, G. (under review). Contrasting effects of climate change on denitrification and nitrogen load reduction in the Po River (Northern Italy). Submitted to *Environmental Science and Pollution Research* (ESPR-D-24-04227).

Contrasting effects of climate change on denitrification and nitrogen load reduction in the Po River (Northern Italy)

Maria Pia Gervasio*, Elisa Soana, Anna Gavioli, Fabio Vincenzi, Giuseppe Castaldelli

Department of Environmental and Prevention Sciences, University of Ferrara, Via Luigi Borsari 46, Ferrara, 44121, Italy

e-mail: elisa.soana@unife.it; gvlnna@unife.it; fabio.vincenzi@unife.it; ctg@unife.it

*corresponding author: mariapia.gervasio@unife.it

Graphical abstract

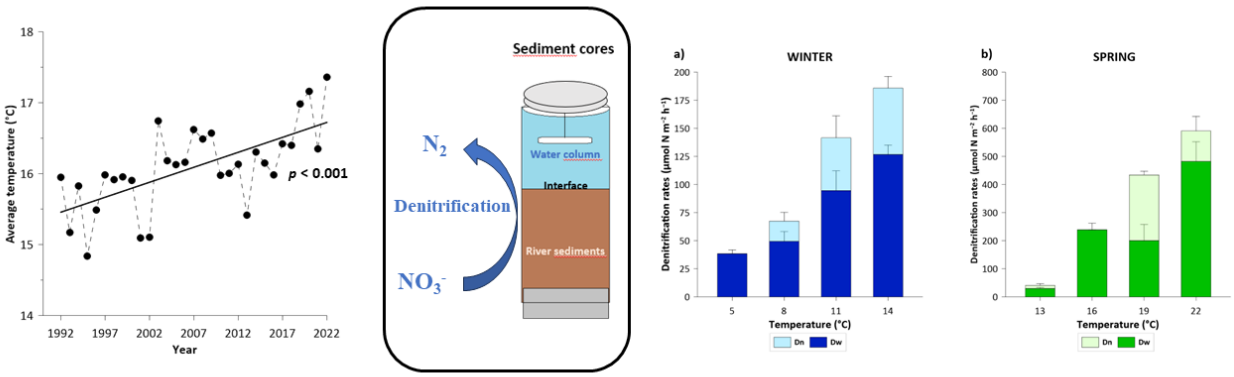

Abstract:

An increase in water temperature is one of the main factors that can potentially modify biogeochemical dynamics in rivers, such as the removal and recycling of nitrogen (N). This effect of climate change on N processing has not been described in the literature and deserves attention, as it may have unexpected impacts on eutrophication. Intact sediment cores were collected seasonally at the closing section of the Po River, the largest Italian river and one of the main N inputs to the Mediterranean Sea. Benthic oxygen fluxes, denitrification, and dissimilatory nitrate reduction to ammonium (DNRA) rates were measured via laboratory dark incubations. Different temperature treatments were set up for each season based on historical data and future predictions. Higher water temperatures enhanced sediment oxygen demand and the extent of hypoxic conditions in the benthic compartment, favoring anaerobic metabolism. Indeed, warming water temperature stimulated nitrate (NO_3^-) reduction processes, although NO_3^- and organic matter availability were found to be the main controlling factors shaping the rates between seasons. Denitrification was the main process responsible for NO_3^- removal, mainly supported by NO_3^- diffusion from the water column into the sediments, and was more favorable than N recycling via DNRA. The predicted increase in the Po River water temperature due to climate change may exert unexpected negative feedback on eutrophication by strongly controlling denitrification and contributing to partial buffering of N export in the lagoons and coastal areas, especially in spring.

Keywords: climate change, nitrogen, water temperature, denitrification, DNRA, Po River

1. Introduction:

Rivers are heavily affected by anthropogenic activities, particularly by nitrogen (N) input from agricultural sources, mostly in the form of nitrate (NO_3^-) (Lassaletta et al., 2009; Sutton et al., 2011). Nitrogen loads can affect the trophic state of rivers and, when delivered to terminal water bodies, fuel eutrophication triggering algal blooms in both transitional and coastal zones (Dodds, 2006; Glibert, 2017). The generation of N loads, their transport across land-river and river-sea interfaces, and eutrophication dynamics are strongly influenced by land use, river morphology, and hydrological and thermal conditions, all of which are subject to climate change (Hou et al., 2019; Romero et al., 2013; Tu, 2009).

Extreme meteorological events such as floods and droughts, which have increased in frequency in recent years, directly impact river discharge and the generation and delivery of nutrient loads to water bodies, transport dynamics within the hydrological network, and microbial processes of N transformation and removal (Abily et al., 2021; Zheng et al., 2023). Among microbial reactions occurring in sediments, denitrification, the anaerobic respiration that converts NO_3^- to di-nitrogen gas (N_2), the final product, and nitrite (NO_2^-) and nitrous oxide (N_2O), as intermediate products. Denitrification removes NO_3^- permanently and is the most important process supporting the self-depuration capacity of rivers (Hill, 2023; Piña-Ochoa and Álvarez-Cobelas, 2006; Seitzinger, 1988). An alternative microbial pathway for NO_3^- reduction is the dissimilatory nitrate reduction to ammonium (DNRA), which converts NO_3^- to ammonium (NH_4^+), using the same substrates as denitrification (NO_3^- and organic carbon). However, denitrification removes reactive N permanently from the aquatic ecosystem, whereas DNRA recycles it (Giblin et al., 2013).

River denitrification is controlled by several factors, such as oxygen concentration at the water-sediment interface, and the availability of NO_3^- and labile organic carbon (Ballard et al., 2019; Hu et al., 2023; Piña-Ochoa and Álvarez-Cobelas, 2006). One of the most important environmental drivers influencing denitrification is water temperature (De Klein et al., 2017; Veraart et al., 2011). Warming boosts denitrification alongside enzymatic reactions, but water temperature increase also has an impact on the process by regulating two of the aforementioned determinants

of denitrification, i.e., oxygen concentration and availability of labile organic matter (De Klein et al., 2017; Speir et al., 2023). Indeed, all biogeochemical NO_3^- dissimilatory pathways are affected by water warming, both as a direct effect of temperature on enzyme activity and an indirect effect on sediment redox conditions (Brin et al., 2017). In general, whether denitrification or DNRA dominates NO_3^- reduction depends on the availability of labile organic carbon in the sediments (Nizzoli et al., 2010; Aalto et al., 2021). Under climate change scenarios, a reduction in rainfall, runoff, and river flow is likely to lower NO_3^- concentrations (Oduor et al., 2023), thereby negatively affecting river denitrification. On the other hand, the expected increase in water temperature is likely to stimulate the process. Several studies have isolated the effect of temperature on denitrification through manipulative experiments (e.g., Silvennoinen et al., 2008; Velthuis and Veraart, 2022; Speir et al., 2023). Nevertheless, there is a lack of systematic research predicting the consequences of warming on the self-depuration capacity of large rivers, given their peculiar role in processing anthropogenic N inputs along the land-sea continuum.

The Po is the largest Italian river in terms of watershed extension and annual discharge at the closing section and is one of the major rivers in the Mediterranean region (Struglia et al., 2004). Its catchment is one of the most industrialized and intensively farmed catchments in the world (Moatti and Thiébault, 2016), making it a hotspot for NO_3^- pollution. The Po River contributes two-thirds of the total freshwater discharge and nutrient inputs conveyed to the Adriatic Sea (Grilli et al., 2020; Viaroli et al., 2018) and is the major basin for riverine N export to the Mediterranean Sea (Romero et al., 2021). In the last decades, the Po River basin was strongly affected by the increasing frequency of extreme events due to climate change (Appiotti et al., 2014; Coppola et al., 2014; Marchina et al., 2017). For example, rainfall in the basin and river discharge in 2022 were the lowest in historical records since 1961 (Montanari et al., 2023) and water temperature was the highest measured in the last two decades (Gervasio et al., 2023). Following these extreme hydrological and thermal conditions, experimental work was carried out on intact sediment cores sampled from the lower course of the Po River to measure benthic denitrification and DNRA rates. The aim of the present

study was to assess the seasonal effect of temperature and NO_3^- availability on the river buffering capacity against N pollution and eutrophication in the coastal zone.

2. Materials and methods

2.1. Study area

The Po River is the longest and most important Italian river, flowing from the Alps to the Adriatic Sea, with an average annual discharge of 1500 $m^3 s^{-1}$ at the Pontelagoscuro station, the basin closing section (Fig. 1; Zanchettin et al., 2008). The basin covers an area of approximately 71,000 km^2 across Italy, a quarter of the national territory. The river has more than 140 tributaries and a capillary network of artificial irrigation and drainage canals (Soana et al., 2019). The basin is subject to a mix of subcontinental and warm-temperature climates (the Mediterranean climate), which split the annual hydrological regime into two low-flow periods (winter and summer) and two recharging periods (spring and autumn) fed by snowmelt and rainfall (Coppola et al., 2014; Montanari, 2012; Ravazzani et al., 2015). In recent decades, the Po River basin has experienced the effects of climate change, with an increase in extreme storm events (Brunetti et al., 2004; Domeneghetti et al., 2015; Giambastiani et al., 2017), long drought periods, and water temperature warming (Gervasio et al., 2022; Bonaldo et al., 2023; Soana et al., 2023). The Po River crosses the Po Valley, the most fertile and extensively cultivated area in Italy, and is the main source of irrigation water for crops. Since the 1960s, the intensification of agriculture and livestock farming has made the Po River the main source of nutrient inputs to the North Adriatic Sea, triggering algal blooms during warm periods (Penna et al., 2004; Spillman et al., 2007).

2.2. Sampling activities and seasonal temperature gradients

Sediment cores were sampled in the Po River at Pontelagoscuro (red star in Fig. 1), the closing section of the basin (Ferrara, 44°53'16.9"N, 11°36'26.6"E), located 90 km from the main mouth to the Adriatic Sea, in winter (February), spring (May), summer (July), and autumn (November). Water column parameters (temperature, electrical

conductivity, and oxygen concentration) were measured *in situ* using a multiparametric probe (YSI Model 85-Handheld Dissolved Oxygen, Conductivity, Salinity and Temperature System, Yellow Springs, OH, USA) during the sampling days. Sampling, pre-incubation, and incubation were performed according to standardized protocols (Dalsgaard, T., 2000). The experimental design consisted of 25 intact sediment cores (plexiglass liners, internal diameter 4.5 cm, length 20 cm) for each seasonal sampling, five of which were randomly assigned to each of the four water temperature levels chosen and incubated in the dark to determine oxygen fluxes, denitrification, and DNRA rates. The remaining five cores were used for sediment characterization.

After collection, intact sediment cores were submerged in tanks with site water continuously aerated using aquarium pumps, and transported to the laboratory. Approximately 60 liters of bottom water were collected and brought to the laboratory for core maintenance, pre-incubation, and incubation. During each seasonal incubation, the temperature range was established from the historical temperature data of Po River (1992-2022), monitored monthly by the Regional Environmental Protection Agency of the Emilia – Romagna, Lombardy and Veneto Regions (ARPAE, ARPA of Lombardy Region, and ARPAV, respectively) in five sections covering the lower Po River stretch, before the Po River Delta, (Sermide, (S1), Stellata–Bondeno (S2), Pontelagoscuro, our sediment sampling site, Polesella (S3) and Serravalle (S4); indicated with black dots in Fig. 1). Four different temperatures were applied in each seasonal incubation, covering the following ranges: 5–14 °C in winter (January, February, March), 13–22 °C in spring (April, May, June), 21–30 °C in summer (July, August, September) and 9–18 °C in autumn (October, November, December) (Table 1). The minimum of each seasonal range corresponded to the seasonal minimum temperature measured in the Po River from the 1990s to the present, while the maximum of the ranges was established based on the maximum values expected in the near future owing to climate warming. In the period 2041-2070, air temperatures are expected to increase throughout the Po basin in all seasons, with positive anomalies of up to 3 °C (Vezzoli et al., 2015). Intermediate temperatures correspond to the most frequent seasonal mean temperatures over 30 years. The experimental

temperature in the incubation tanks was controlled using a thermostat (Fig. 2b) and continuously monitored during each incubation using a multi-parameter probe.

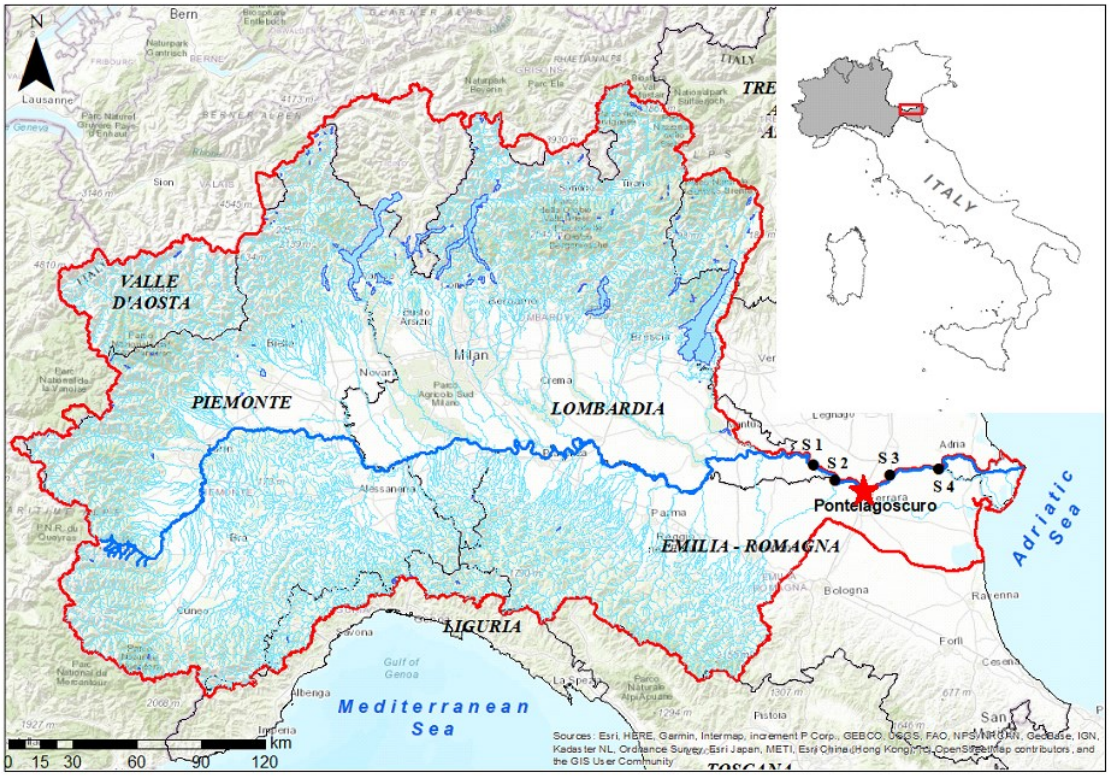

Fig. 1 Map of the Po River course (blue line) and its basin (bordered with red line and grey area on top) located in Northern Italy (modified by ArcGIS 10.8.2, ESRI). The red star indicates the sampling station in Pontelagoscuro. The black dots indicate the monitoring temperature stations belonging to the Regional Agency for Environmental Prevention of Emilia – Romagna, Lombardy and Veneto Regions: Sermide (S 1), Stellata - Bondeno (S 2), Polesella (S 3), and Serravalle (S 4), situated in province of Ferrara (Italy)

Table 1 Water temperature treatments applied to core incubations in each season (°C).

Season	T (°C)	T (°C)	T (°C)	T (°C)
Winter	5	8	11	14
Spring	13	16	19	22
Summer	21	24	27	30
Autumn	9	12	15	18

2.3. Seasonal incubation procedure

Each core was equipped with a rotating Teflon-coated magnet driven by an external magnet connected to a motor (40 rpm). Inside the cores, the magnet was suspended a few centimeters above the sediment-water interface to gently mix the water column while avoiding resuspension (Fig. 2a). To allow for acclimatization, each target temperature level was set in the early afternoon of the day before the start of incubation. According to standardized protocols (Dalsgaard, T., 2000; Owens and Cornwell, 2016), intact sediment cores were incubated in batch mode to measure benthic dark oxygen fluxes (sediment oxygen demand, SOD). Dark incubations were chosen to simulate *in situ* conditions, where light penetration is limited by turbidity and the benthic compartment is in the dark (Braga et al., 2017). The water in each tank was replaced with fresh water to maintain dissolved nutrient concentrations close to those *in situ*. Before the incubation of the benthic fluxes, O_2 was measured using a multiparametric probe inside each core. The water level in the tanks was lowered to a few centimeters below the top of the cores, and each liner was sealed with a plexiglass lid (Fig. 2a). The incubation time ranged between 1.5 and 4 h to maintain the O_2 concentration within 20% of the initial value (Table 2). At the end of the incubation period, the O_2 concentration in each core was measured in the same manner as that at the beginning. After the first incubation, the water in the tanks was replaced and the cores were submerged for approximately 2 h to stabilize the system. In the second incubation, the Isotope Pairing Technique (IPT; Nielsen, 1992) was applied to measure

the denitrification and DNRA rates. As in the first incubation, the water level in the tank was lowered to just below the top of the cores to isolate them. An aliquot of a stock solution of 15 mM $^{15}NO_3^-$ ($Na^{15}NO_3$, Sigma Aldrich, ≥98 atom% enrichment) was added to each core to obtain a final labelled NO_3^- enrichment of approximately 50%. Then, the cores were capped to start the IPT incubation. The NO_3^- concentrations were measured in each core before and after the addition of $^{15}NO_3^-$ to calculate the ^{14}N:^{15}N ratio in the NO_3^- pool. At the end of the incubation period, the entire sediment column was mixed with the water column to homogenize the dissolved N_2 pools in the water column and pore water. Slurry samples were transferred to glass-tight vials (12 mL, Exetainer®, Labco Limited, UK), flushing at least 3 times the vial volume, and fixed with 200 µL of 7 M $ZnCl_2$ to stop microbial activity. The IPT samples were analyzed for $^{29}N_2$ and $^{30}N_2$ using Membrane Inlet Mass Spectrometry (MIMS) (Bay Instruments, MD, USA; Kana et al., 1994).

An additional aliquot (30 mL) of the slurry from each core was used to determine the DNRA rate from the production of $^{15}NH_4^+$ (Gervasio et al., 2023; Magri et al., 2022). To determine the exchangeable NH_4^+ pool, the slurry was treated with 2 g of KCl (2 M), shaken for 30 min, and centrifuged (1800 rpm for 15 min). The supernatant was then filtered through Whatman GF/F glass fiber filters, stored in 20 mL-scintillation vials and frozen for subsequent analysis. Slurry samples were purged with air to eliminate $^{29}N_2$ and $^{30}N_2$ pools produced during IPT incubation, transferred to 12 mL-Exetainers and treated with an alkaline hypobromite solution to oxidize NH_4^+ to N_2 (Warembourg, 1993). After the oxidation procedure, the $^{29}N_2$ and $^{30}N_2$ concentrations were measured using MIMS.

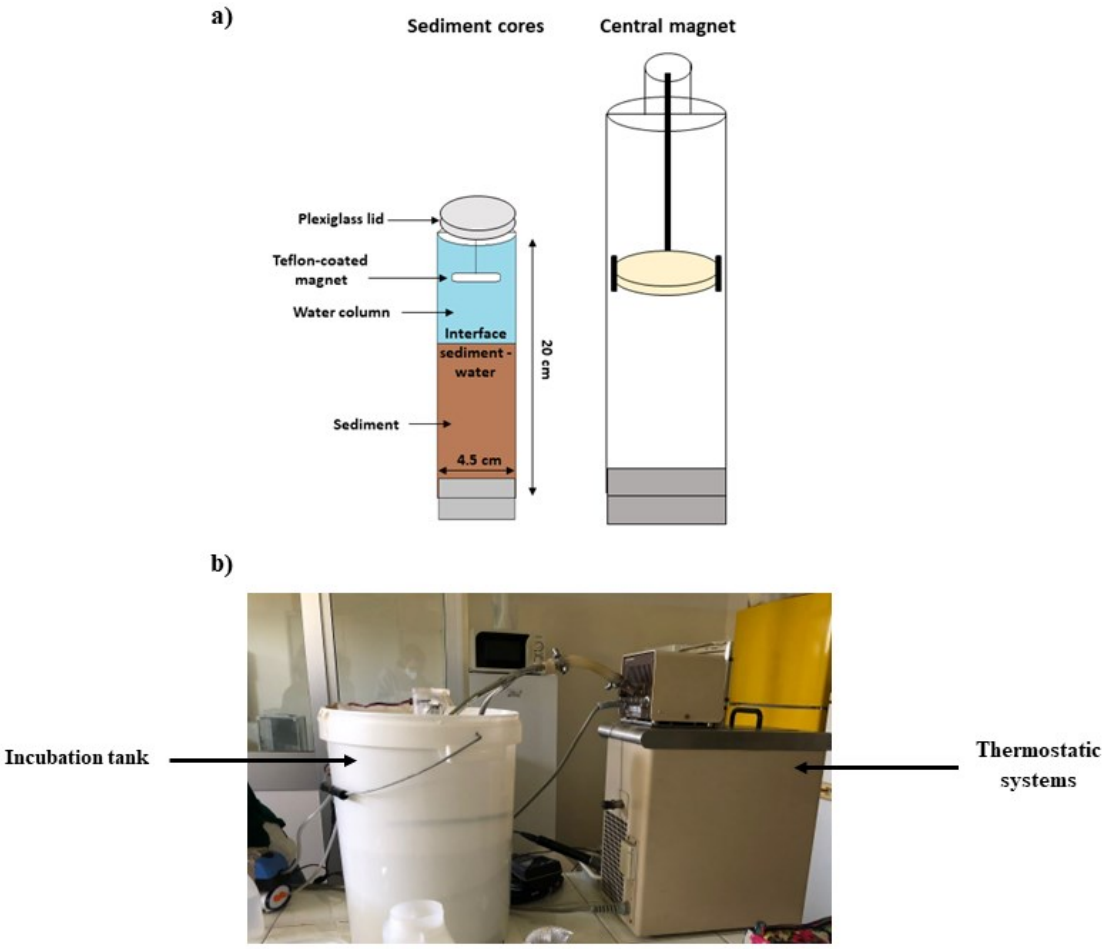

Fig. 2: a) Schematic representation of the incubation system with a central magnet and the example of sediment core situated in each tank; b) image of the incubation tank (on the left) connected to the thermostatic system (on the right) to regulate the experimental temperature for each seasonal incubation.

Table 2: Chemical (temperature, O_2, and NO_3^- concentrations) and physical conditions (organic matter content in river sediments) at Pontelagoscuro site during the four seasonal campaigns. Standard deviations are reported (±).

Seasons	Temperature (°C)	O_2 (mg L^{-1})	NO_3^- (µM)	NO_2^- (µM)	NH_4^+ (µM)	OM (%)
Winter	8	11.7	201 ± 0.5	2 ± 0.1	4 ± 1	1.6 ± 0.5
Spring	20	10.9	126 ± 6	1 ± 0.1	5 ± 1	0.6 ± 0.01
Summer	29	8.3	40 ± 3	1 ± 0.3	4 ± 1	0.4 ± 0.03
Autumn	14	10.2	190 ± 4	2 ± 0.5	0.2 ± 0	1.7 ± 0.4

2.4. Calculation of SOD, denitrification and DNRA rates

Hourly dark fluxes of O_2 (SOD, µmol O_2 m^{-2} h^{-1}) were calculated from the rate of change of concentrations with time according to the following equation (Owens and Cornwell, 2016):

$$\boldsymbol{SOD = \frac{(C_0 - C_f) \cdot V}{A \cdot t}} \quad (1)$$

Where C_0 and C_f (µM) are the O_2 concentrations at the beginning and end of incubation, respectively, A (m^2) is the area of the sediment core, V (L) is the water volume of the sediment core, and t (h) is the incubation time, which was different for each temperature in each seasonal experiment.

Denitrification rates (µmol N m^{-2} h^{-1}) were calculated on $^{29}N_2$ and $^{30}N_2$ production, as the equations below (Nielsen, 1992):

$$\boldsymbol{D_{15} = p29 + 2p30} \quad (2)$$

$$\boldsymbol{D_{14} = D_{15} \cdot \left(\frac{p29}{2p30}\right)} \quad (3)$$

where D_{15} is the denitrification rate of the added $^{15}NO_3^-$, D_{14} is the total denitrification rate of $^{14}NO_3^-$, and p29 and p30 are the production rates of $^{29}N_2$ and $^{30}N_2$, respectively. The total denitrification rate (Dtot) was divided into two components as follows:

$$\boldsymbol{D_{tot} = D_w + D_n} \quad (4)$$

$$\boldsymbol{D_w = \left(\frac{^{14}NO_3^-}{^{15}NO_3^-}\right) \cdot D_{15}} \quad (5)$$

$$\boldsymbol{D_n = D_{14} - D_w} \quad (6)$$

where Dw (µmol m^{-2} h^{-1}) is the denitrification rate of NO_3^- diffusing from the water column to the anoxic sediment layer, while Dn (coupled nitrification-denitrification; µmol N m^{-2} h^{-1}) is the denitrification rate of NO_3^- produced within the oxic sediment layer by nitrification.

DNRA rates were calculated according to (Risgaard-Petersen, N., & Rysgaard, S., 1995), as follows:

$$\boldsymbol{DNRA = pNH_4^+ \cdot \frac{D_{14}}{D_{15}}} \quad (7)$$

$$\boldsymbol{DNRA_w = \frac{^{14}NO_3^-}{^{15}NO_3^-} \cdot pNH_4^+} \quad (8)$$

$$\boldsymbol{DNRA_n = DNRA - DNRA_w} \quad (9)$$

where pNH_4^+ is the production of $^{15}NH_4^+$, DNRAw represents the direct DNRA of NO_3^- from the water column, and DNRAn is the DNRA rate coupled with nitrification.

2.5. Sediment characterization

The cores for sediment characterization were extracted and sliced into two layers: upper 0-1 cm and 1-2 cm sections. Aliquots from the two layers were rapidly homogenized and subsamples of 5 mL were collected using plastic syringes to determine their physical properties. Fresh sediments were dried at 50 °C to constant weight for 72 h and then they were set at 350 °C for 3 h into a muffle furnace. The dried samples were used to determine the organic matter content (OM, %) via weight loss during ignition.

2.6. Statistical analyses

Benthic fluxes of oxygen, denitrification, and DNRA rates were statistically analyzed using linear mixed effects (LME) to analyze differences in temperature and in seasons. The factor "season" is proxy for two variables that vary seasonally and interact in controlling denitrification. In the LME test, a random effect was applied to consider all replicate samples at each temperature. The sample size was equal in all tests. The statistical analyses were run in RStudio (RStudio-2023.06.0-421), using the *lme4* package. The focus of the test was to compare the differences in seasonal SOD, denitrification and DNRA rates by taking into account the fixed factors of season (winter, spring, summer and autumn) and different temperatures in each season, and the correlation between both factors. Moreover, Pearson's correlation was used to explore the relationship between water temperature and benthic oxygen fluxes.

3. Results

3.1. Historical water temperature of the Po River

Historical data on the Po River temperature, monitored at five stations along an 80-km stretch of the river centered on the section where the cores were taken (Pontelagoscuro), showed a gradual increase over the last decades (1992-2022). The upward trend was particularly marked in summer and autumn (nearly +5 °C; Fig. 3). Summer average temperature ranged from 22 (1996) to 27 °C (2022), showing a significant upward trend equivalent to a raise of 0.15 °C yr^{-1}. In autumn, the trend was similar in slope to summer (0.16 °C yr^{-1}), with values varying between 10 (1998) and 15 °C (2014). Although the average winter and spring temperature trends were not statistically significant, a slight increase was observed, with values ranging from 7 to 10 °C and from 17 to 20 °C, respectively.

Temporal trends in the minimum Po River water temperature were significant in all seasons except autumn. Minimum winter temperatures ranged from 3 to 7 °C and increased at a rate of 0.14 °C yr^{-1}, while spring values varied between 10 and 15 °C with an upward rate of 0.17 °C yr^{-1}. Finally, summer minimum temperatures ranged from

15 to 23 °C, showing the most pronounced warming signal (0.25 °C yr^{-1}). In contrast, the maximum temperatures did not show any significant trends in any season.

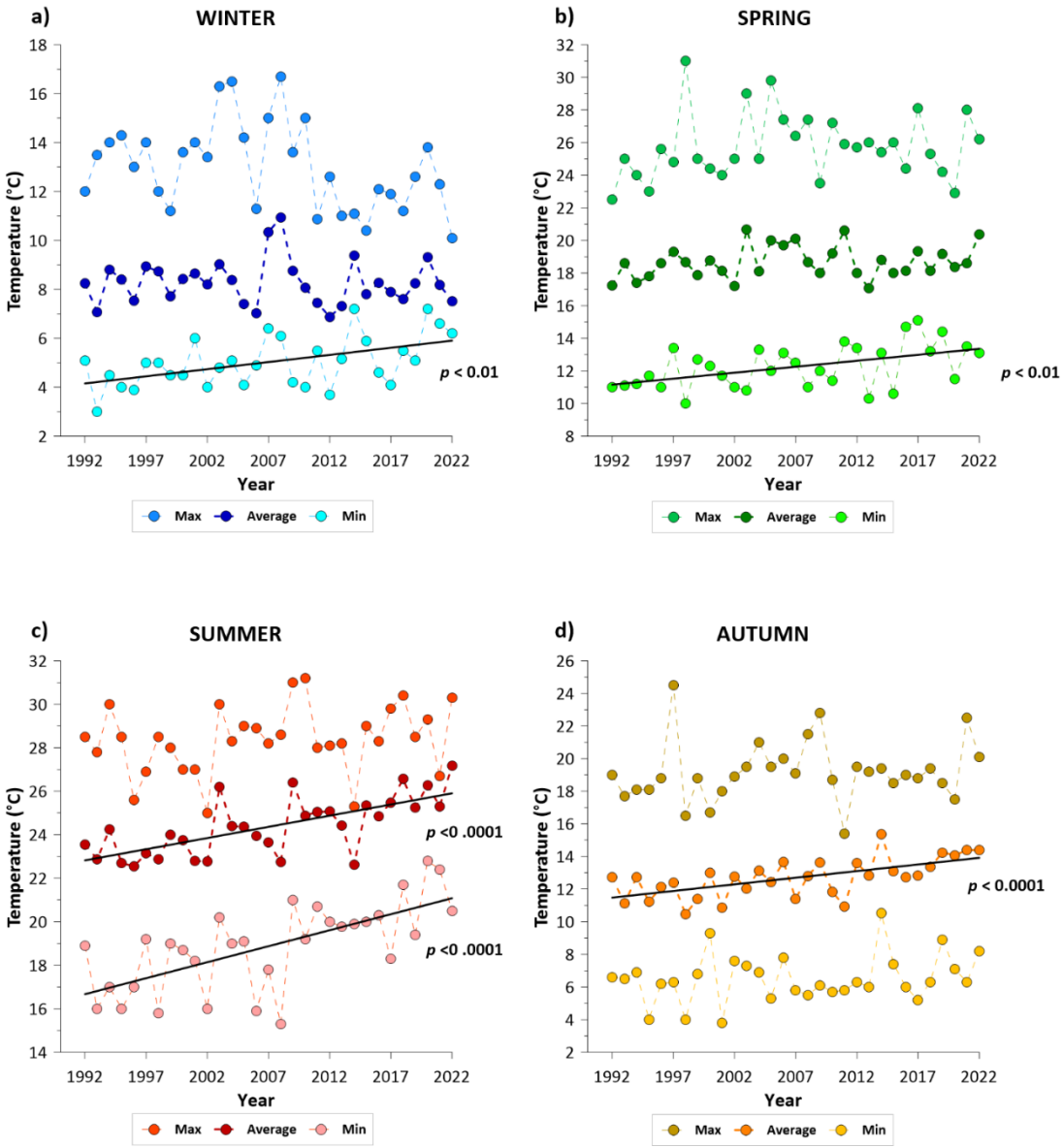

Fig. 3: Historical average, minimum, and maximum water temperatures (°C) of the Lower Po River since 1990's in each season, monitoring from Sermide to Serravalle section. Solid lines show significant trend. a) Winter: January – March period; b) spring: April – June period; c) summer: July – September period; d) autumn: October – December. Solid lines show statistically significant trends.

3.2. Oxygen fluxes

The oxygen concentration measured *in situ* during the four sampling campaigns ranged from 8.3 mg L^{-1} in summer, to 11.7 mg L^{-1} in winter, corresponding to approximately 100% saturation of the water column throughout the year (Table 2). The sediment oxygen demand increased with temperature in all seasonal incubations (Fig. 4). The average values in winter, spring, summer, and autumn were 561 ± 120, 799 ± 159, 1210 ± 116, and 389 ± 120 µmol O_2 m^{-2} h^{-1}, respectively. The raise along the temperature gradient averaged at 60 µmol O_2 m^{-2} h^{-1} $°C^{-1}$ in all seasons, except in spring when the highest SOD values were detected. The SOD in spring ranged from 453 ± 42 to 1186 ± 119 µmol O_2 m^{-2} h^{-1} at 13 and 22 °C, respectively, and increased along the temperature gradient with a raise of 82 µmol O_2 m^{-2} h^{-1} per degree. In summer incubation, SOD had the highest values due to the highest temperatures, from 936 ± 43 µmol O_2 m^{-2} h^{-1} at 21 °C to 1937 ± 86 µmol O_2 m^{-2} h^{-1} at 30 °C. On the contrary, the lowest values appeared during the autumn incubation, when SOD fluxes ranged between 156 ± 39 to 955 ± 84 µmol O_2 m^{-2} h^{-1} (at 9 and 18 °C, respectively). Finally, the winter SOD ranged from 323 ± 36 to 891 ± 62 µmol O_2 m^{-2} h^{-1} at 5 and 14 °C, respectively.

The results of the spring experiments were within the range of two extreme seasons: summer and winter. In fact, the SOD at the highest spring temperature had the same values as those of the summer SOD at the lowest temperature, and the lowest spring temperature had the same values as the highest winter temperature. The lowest values, - 156 ± 39 and 216 ± 23 µmol O_2 m^{-2} h^{-1}, were recorded during the autumn period at the first two temperatures tested, 9 and 12 °C, respectively, due to the low experimental temperature and initial O_2 concentration in situ (Table 2).

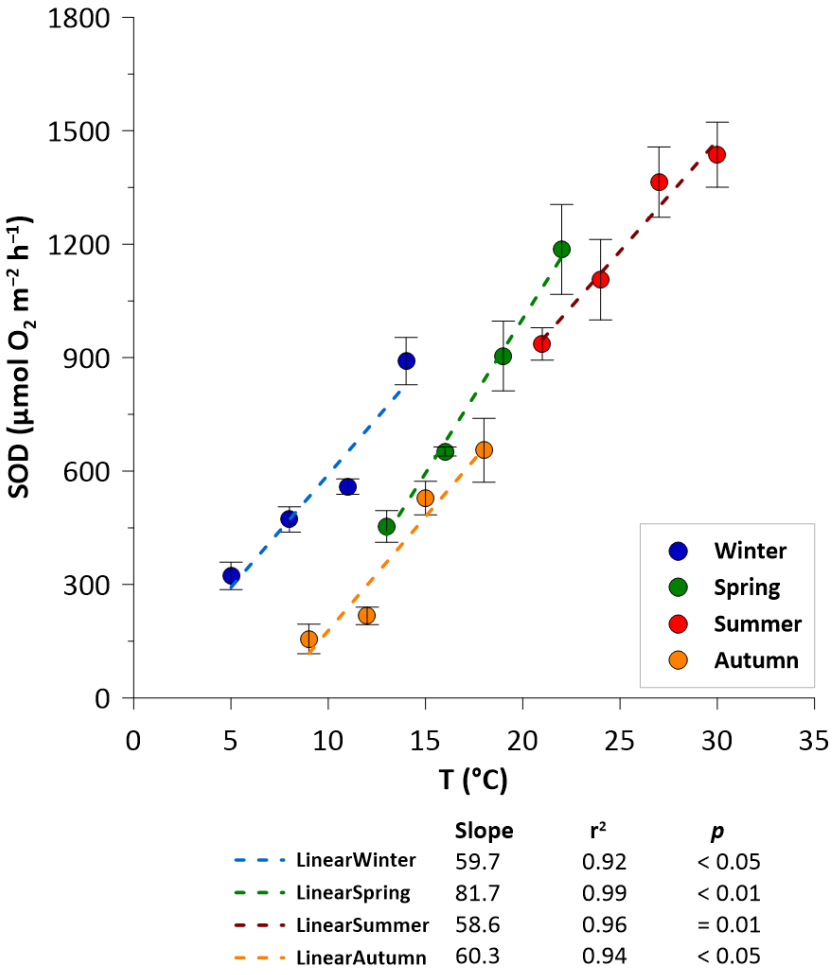

Fig. 4: Sediment oxygen demand (SOD, µmol O_2 m^{-2} h^{-1}) measured along the temperature gradients in the four seasons. Average values ± standard deviations are reported. Trend slopes, coefficient of determination (r^2), and *p-value* of linear regression models are reported at the bottom of the figure.

3.3. Denitrification and DNRA rates

Denitrification and DNRA rates showed wide seasonal variations related to both NO_3^- availability and temperature. Total denitrification rates increased along the experimental temperature gradient that was set in each season (Fig. 5). In winter, the total denitrification rates ranged from 38 ± 3 µmol N m^{-2} h^{-1} at 5 °C to 186 ± 16 µmol N m^{-2} h^{-1} at 14 °C, with a rise of 16 µmol N m^{-2} h^{-1} $°C^{-1}$. The highest rates were measured in spring incubation, increasing from 41 ± 5 to 591 ± 29 µmol N m^{-2} h^{-1} at 13 and 22 °C,

respectively, with a rise of 61 µmol N m^{-2} h^{-1} $°C^{-1}$. The summer rates increased from 14 ± 8 µmol N m^{-2} h^{-1} at 21 °C to 40 ± 5 µmol N m^{-2} h^{-1} at 30 °C, with a slightly increase, i.e. only 3 µmol N m^{-2} h^{-1} $°C^{-1}$ and, finally, the autumn denitrification rates ranged from 14 ± 5 to 49 ± 14 µmol N m^{-2} h^{-1} at 9 and 18 °C, respectively, with a raise of 4 µmol N m^{-2} h^{-1} $°C^{-1}$. Dw dominated Dn, accounting for an average of 76% of Dtot in the winter and spring incubations. In fact, in winter Dw ranged from 38 ± 3 to 127 ± 8 µmol N m^{-2} h^{-1} at 5 and 14 °C, respectively, while it showed the highest values in spring incubations, ranging from 30 ± 4 to 482 ± 70 µmol N m^{-2} h^{-1} at 13 and 22 °C, respectively. In contrast, in the summer incubations, Dw was systematically lower than Dn, representing an average of 31% of Dtot. During summer experiment, Dn increased along gradient temperature, ranging from 8 ± 3 to 32 ± 3 µmol N m^{-2} h^{-1} at 21 and 30 °C, respectively, while the same upward trend was not detected for Dw. Autumn Dw represented 95% of Dtot and increased along the temperature gradient, ranging from 13 ± 5 to 49 ± 15 µmol N m^{-2} h^{-1} at 9 and 18 °C, respectively. A strong denitrification response to temperature was observed, with an increase in the temperature gradient in all seasons ($p < 0.001$; Table 3). Statistical analysis showed a strong correlation between the N process and temperature in each season (Table 3), and the interaction between temperature and season was also significant, as the effect of temperature was evident in all seasons; nevertheless, the average rates differed among seasons (Table 3). In this case the main factor that influences the seasonal variability of conditions was NO_3^- availability, due to the variability of OM (%) content in the Po River sediments may be consider negligible (Table 3).

On average, the denitrification rates were one order of magnitude higher than those in the DNRA. DNRA increased along the temperature gradient in all seasons except winter, when the rates remained constant at the first three temperatures of the series (average 14 µmol N m^{-2} h^{-1}), increasing up to 31 ± 6 µmol N m^{-2} h^{-1} at the last one (14 °C). The highest DNRA rates were measured in spring, ranging from 11 ± 3 to 53 ± 24 µmol N m^{-2} h^{-1} at 13 and 22 °C, respectively. The rates in summer and autumn were very low in comparison to the other seasons (Fig. 6; note the difference in scale of the y-axis) and follow a significant linear increase with temperature, from 1 ± 0.7 to 10 ± 1

µmol N m^{-2} h^{-1}, at 21 and 30 °C, in summer, and from 1.3 ± 0.6 to 8 ± 1 µmol N m^{-2} h^{-1}, at 9 and 18 °C, in autumn, respectively.

In winter and spring, DNRAw increased along the temperature gradient (Fig. 6), representing an average of 77 and 64% of DNRAtot, respectively. In summer, DNRAw increased slightly along the temperature gradient but represented less than 30% of DNRAtot. Finally, in autumn, DNRAw increased along the temperature gradient and accounted for >95% of the DNRAtot.

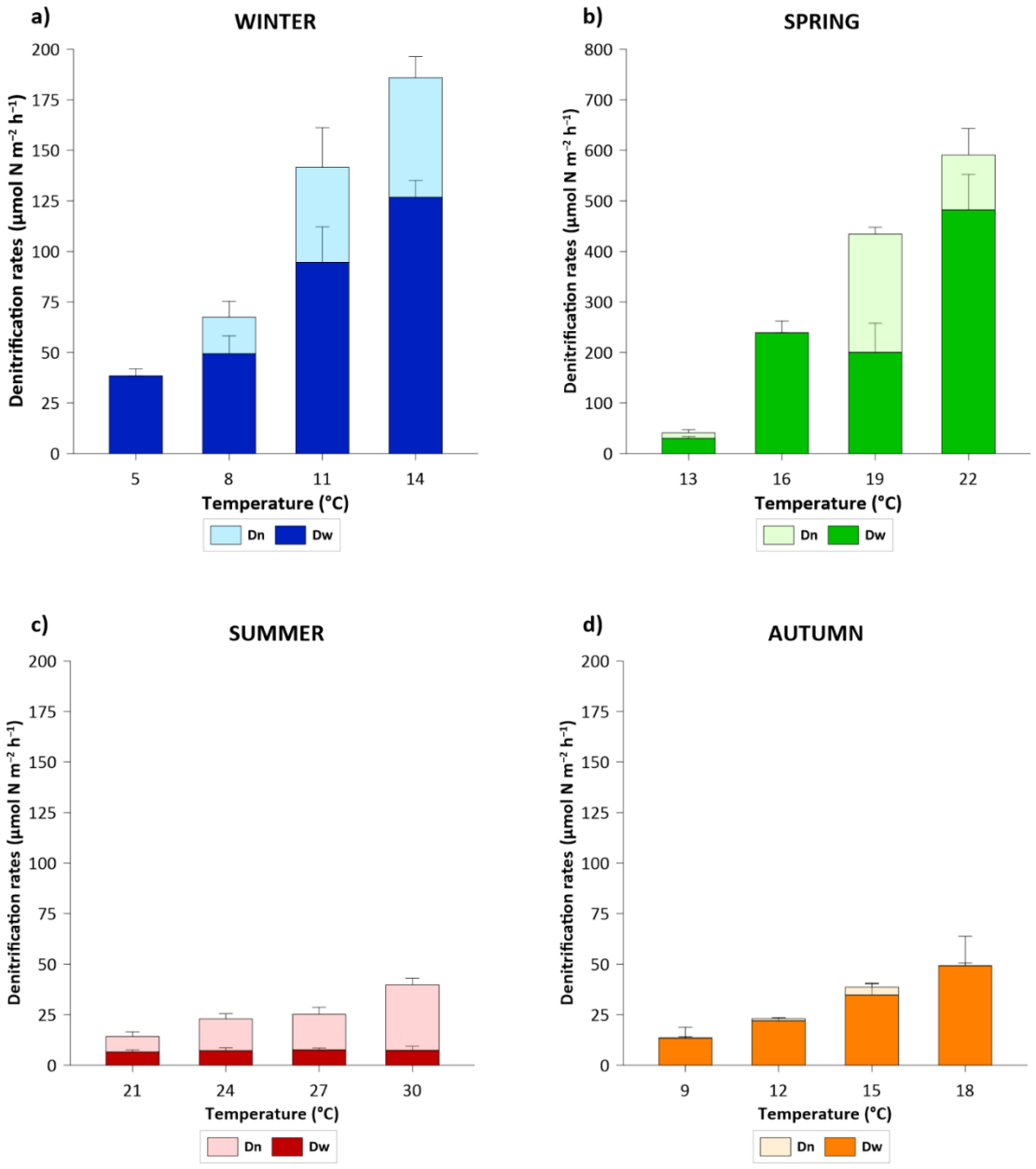

Fig. 5: Total denitrification rates (µmol N m^{-2} h^{-1}) splitted into Dw and Dn measured along the temperature gradients in the four seasons: a) winter; b) spring, c) summer; d) autumn (note the different scale of the y-axis). Average values ± standard deviations are reported.

Table 3: Results of the linear mixed-effects models on the effect of temperature, season, and their interaction with SOD, denitrification (Dw, Dn, and Dtot), and DNRA rates (DNRAw, DNRAn, and DNRAtot). Significant *p*-values (<0.05) are bolded.

Variable	**Temperature**		**Season**		**Temperature x Season**	
	F	***p***	**F**	***p***	**F**	***p***
SOD	548.8	**<0.0001**	24.9	**<0.0001**	1.3	0.2835
Dw	3.1	0.0809	79.3	**<0.0001**	26.5	**<0.0001**
Dn	5.1	**0.0264**	14.7	**<0.0001**	5.6	**0.0018**
Dtot	40.5	**<0.0001**	434.9	**<0.0001**	149.9	**<0.0001**
DNRAw	5.7	**0.0194**	12.9	**<0.0001**	0.7	0.5429
DNRAn	5.9	**0.0180**	8.7	**0.0001**	2.4	0.0729
DNRAtot	0.0	0.9627	18.0	**<0.0001**	2.3	0.0843

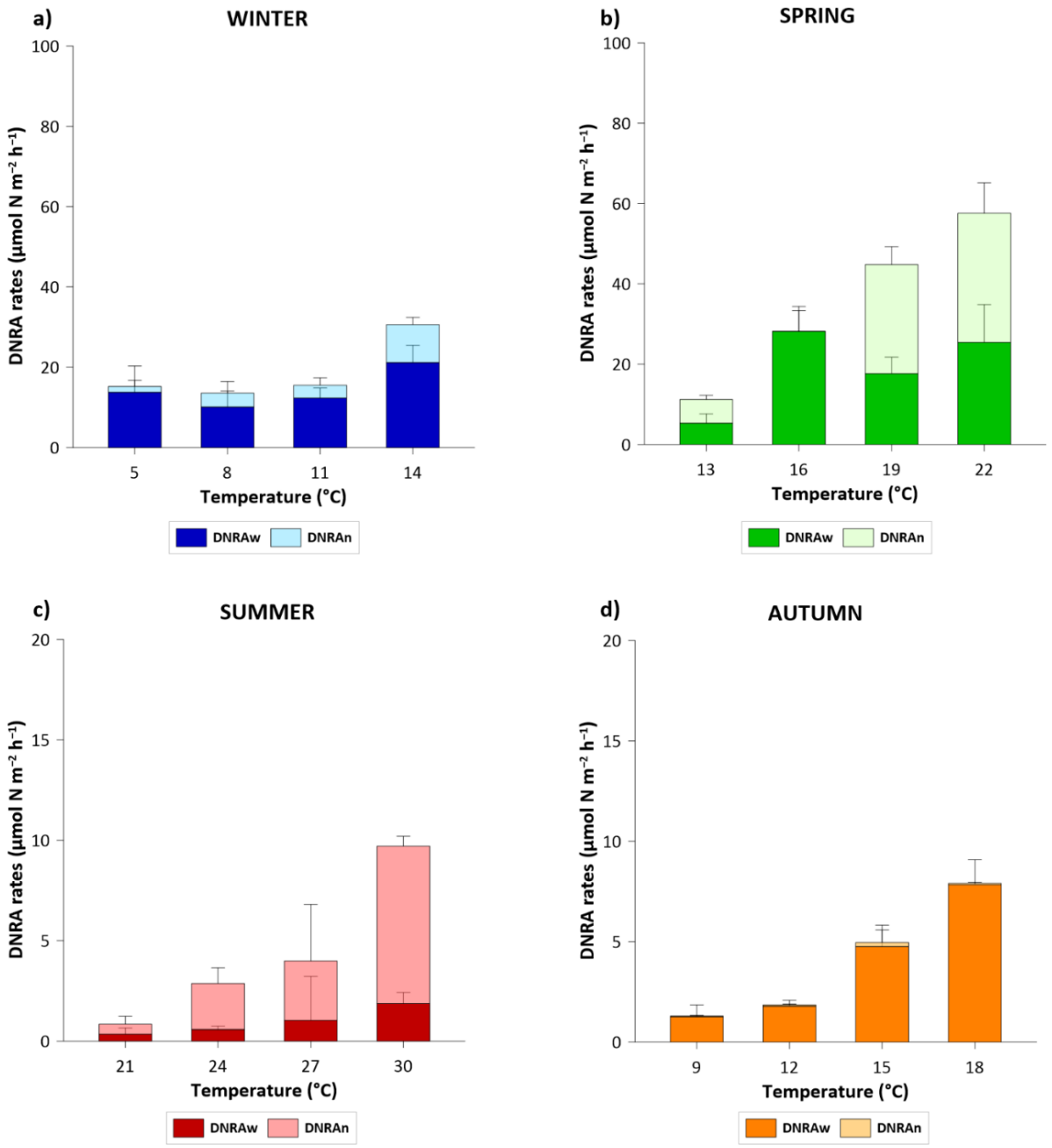

Fig. 6: Total dissimilatory nitrate reduction to ammonium (DNRA) rates (µmol N m^{-2} h^{-1}) splitted into DNRAw e DNRAn, measured along the temperature gradients in the four seasons: a) winter; b) spring, c) summer; d) autumn (note the different scale of the y-axis). Average values ± standard deviations are reported.

4. Discussion and conclusion

An increase in the water temperature of a river has several consequences. As water temperature increases, oxygen solubility and diffusion into the sediment decrease (Butcher and Covington, 1995; Rajesh and Rehana, 2022; Veraart et al., 2011; Muruganandam et al., 2023). Simultaneously, temperature warming stimulates sediment respiration rates and SOD, which in turn results in the vertical extension of the hypoxic-anoxic area within superficial sediments. Thus, this thicker anoxic sediment layer becomes suitable for denitrification because enzymes that sequentially reduce NO_3^- to N_2, i.e., NO_3^-, NO_2^-, NO and N_2O reductase, are inhibited by oxygen (Bonnett et al., 2013; Hobbs et al., 2013; Adouani et al., 2015).

In this study, denitrification responded positively to water warming, increasing along a temperature gradient in each season. There was a significant interaction between temperature and season (Table 3), indicating that the effect of temperature on denitrification was also dependent on other seasonal factors such as NO_3^- availability (Myrstener et al., 2016), which influenced the breakdown of total denitrification into Dw and Dn.

On average, increasing temperature and higher NO_3^- availability in the water column stimulate anaerobic processes, allowing the contribution of Dw to increase with respect to Dn (Dong et al., 2000). In fact, it has been widely reported that total denitrification rates are mainly supported by Dw when NO_3^- concentrations in the water column exceed 50 µM (Piña-Ochoa and Álvarez-Cobelas, 2006; Nizzoli et al., 2010; Racchetti et al., 2011), according to the winter and spring results. In winter, the total denitrification rates and, consequently, the Dw rates, were low owing to low temperatures, despite the high NO_3^- concentrations compared with the other seasons. In spring, the total denitrification and Dw rates were the highest owing to high temperatures and NO_3^- availability, followed by the same drift along the temperature gradient. In contrast, summer denitrification rates were limited by NO_3^- availability, despite high temperatures. The exceptionally low discharges that characterize the Po River (Montanari et al., 2023) led to a reduction in nutrient runoff from the basin (Cozzi et al., 2018; Viaroli et al., 2018) and consequently limited NO_3^- availability in water, resulting in a greater relevance of Dn compared to Dw, as previously reported also for deltaic system sediments (Gervasio et al., 2023).

Another exception occurred in autumn, when denitrification rates were low despite the water temperature and NO_3^- availability (Table 1, 2). However, although no specific measurements were made in this study, our results support the hypothesis that the sediment content of labile organic matter was lower in autumn than in other seasons as a result of a decrease in river primary productivity and sedimentation of labile phytoplanktonic material and an increase in lignocellulosic debris transport from the catchment after moderate rainfall in the week prior to sampling. The hypothesis was that the shift in the ratio of highly biodegradable autochthonous material to refractory lignocellulosic material from the catchment slowed heterotrophic bacterial metabolism in the sediment and, hence, NO_3^- reduction processes (Hu et al., 2019; Warneke et al., 2011). This hypothesis is supported by the low SOD flux measured in autumn (Fig. 4). SOD is strongly correlated with the availability of labile organic matter in river sediments, the mineralization of which primarily involves oxygen (Hargrave, 1972). Thus, oxygen consumption can be considered a proxy for mineralization rates (Seiter et al., 2005; Song et al., 2016). The low SOD in autumn at the same temperatures and with approximately the same sediment total organic matter content measured in spring, when the SOD was almost three times higher, highlights the role of organic matter quality (Myrstener et al., 2016) and variation throughout the year in the Po River.

Similar to denitrification, DNRA rates were temperature dependent in each seasonal experiment. According to Roberts et al. (2014), the total DNRA increased along the temperature gradient in each season, with the highest rates measured in the order of spring, winter, autumn, and summer. The two contributions of DNRA, that are DNRAw, and DNRAn, followed the same increase along the temperature gradient, with the exception of DNRAw in summer, owing to lower NO_3^- availability in the water column. In each season, DNRAw dominated DNRAn, except in summer, when the low water NO_3^- availability resulting from the extremely dry summer of 2022 resulted in higher DNRAn rates than DNRAw, although the total rates were the lowest measured throughout the year.

A previous study showed that DNRA outperforms denitrification in organic-rich brackish sediments of the Po River (Gervasio et al., 2023), with rates positively related

to the C/N ratio, as stimulated by labile carbon availability (Nizzoli et al., 2010). The sediments of the Po River were poor in organic matter in all seasons (Table 1), particularly the minimum values were measured in summer, highlighting the conditions under which DNRA is inhibited (Wei et al., 2020). These results contradict those of other studies showing that increasing temperatures can promote reducing conditions in the sediment by favoring DNRA over denitrification (Yin et al., 2002). In winter, the DNRA had similar values at three of the four experimental temperatures. This was due to the high O_2 availability in the water column of the Po River, which was thoroughly mixed and well-oxygenated in all seasons, especially in winter (Table 2) (Frascari et al., 2006). High oxygen availability, together with low sediment organic carbon and low SOD, likely led to the complete oxidation of the sandy sediments, limiting the activity of DNRA bacteria to micro-niches and resulting in low rates, which were unaffected by the experimental temperature increase (Kraft et al., 2014). Finally, in autumn, the DNRA rates were low despite NO_3^- availability (Table 2). This evidence is consistent with the hypothesis previously discussed for denitrification regarding the role of labile organic matter availability because DNRA and denitrification rely on the labile organic fraction of the total organic matter content in river sediments (Jiang et al., 2020; Guo et al., 2022; Jaiswal et al., 2023).

Overall, denitrification was found to be the main process responsible for the removal of NO_3^- from the Po River (Zhang et al., 2024), with a positive trigger by temperature increase, especially in spring when NO_3^- availability is maximal, as well as the risk of eutrophication in the Adriatic Sea. Instead, the temperature increase did not favor N recycling via DNRA to the extent that it exceeded denitrification, which generally occurs in sediments under strongly reducing conditions (Yuan et al., 2023). In the Po sediments, DNRA contributed on average of 13% of the total NO_3^- dissimilatory reduction, while most of the NO_3^- was permanently removed by denitrification, especially in autumn, when denitrification accounted for >90% of the total NO_3^- removal.

In conclusion, the direct link between water warming induced by climate change and denitrification positive response described in this study may have implications for

water quality improvement in the Adriatic Sea, due to the potential reduction of N loads especially in spring, when riverine nutrients trigger the most eutrophication.

The present outcomes suggest that recent increases in Po River water temperature could have increased the rate of NO_3^- loss via denitrification and ultimately caused the downward trends of N loads discharged to the Adriatic Sean observed in the last decades (Gervasio et al., 2022; Soana et al., 2023). Future studies should seek direct confirmation of this conclusion by scaling up to ecosystem scale experimental rates measured along water temperature gradients in sections characterized by different substrate availability (i.e., NO_3^- in the water column and organic matter in the sediments). Their multiple functional relationships make in fact the effects of climate change on rivers very complex to analyze and difficult to predict. Further investigations are needed to examine how other climatic factors such as reduced flow and extreme rainfall events may interact with temperature increases in terms of both the dynamics of nutrient load generation and nutrient export to the sea from temperate and Mediterranean basins. This is a key issue in the effective implementation of environmental policies to control eutrophication and protect coastal zones.

5. References

Aalto, S.L., Asmala, E., Jilbert, T., Hietanen, S., 2021. Autochthonous organic matter promotes DNRA and suppresses N2O production in sediments of the coastal Baltic Sea. Estuarine, Coastal and Shelf Science 255, 107369. https://doi.org/10.1016/j.ecss.2021.107369

Abily, M., Acuña, V., Gernjak, W., Rodríguez-Roda, I., Poch, M., Corominas, L., 2021. Climate change impact on EU rivers' dilution capacity and ecological status. Water Research 199, 117166. https://doi.org/10.1016/j.watres.2021.117166

Adouani, N., Limousy, L., Lendormi, T., Sire, O., 2015. N2O and NO emissions during wastewater denitrification step: Influence of temperature on the biological process. Comptes Rendus Chimie 18, 15–22. https://doi.org/10.1016/j.crci.2014.11.005

Appiotti, F., Krželj, M., Russo, A., Ferretti, M., Bastianini, M., Marincioni, F., 2014. A multidisciplinary study on the effects of climate change in the northern Adriatic Sea and the Marche region (central Italy). Reg Environ Change 14, 2007–2024. https://doi.org/10.1007/s10113-013-0451-5

Ballard, T.C., Sinha, E., Michalak, A.M., 2019. Long-Term Changes in Precipitation and Temperature Have Already Impacted Nitrogen Loading. Environ. Sci. Technol. 53, 5080–5090. https://doi.org/10.1021/acs.est.8b06898

Bonaldo, D., Bellafiore, D., Ferrarin, C., Ferretti, R., Ricchi, A., Sangelantoni, L., & Vitelletti, M. L. (2023). The summer 2022 drought: a taste of future climate for the Po valley (Italy)?. Regional Environmental Change, 23(1), 1. https://doi.org/10.1007/s10113-022-02004-z

Bonnett, S.A.F., Blackwell, M.S.A., Leah, R., Cook, V., O'Connor, M., Maltby, E., 2013. Temperature response of denitrification rate and greenhouse gas production in agricultural river marginal wetland soils. Geobiology 11, 252–267. https://doi.org/10.1111/gbi.12032

Braga, F., Zaggia, L., Bellafiore, D., Bresciani, M., Giardino, C., Lorenzetti, G., Maicu, F., Manzo, C., Riminucci, F., Ravaioli, M., Brando, V.E., 2017. Mapping turbidity patterns in the Po river prodelta using multi-temporal Landsat 8 imagery. Estuarine, Coastal and Shelf Science 198, 555–567. https://doi.org/10.1016/j.ecss.2016.11.003

Brin, L.D., Giblin, A.E., Rich, J.J., 2017. Similar temperature responses suggest future climate warming will not alter partitioning between denitrification and anammox in temperate marine sediments. Glob Change Biol 23, 331–340. https://doi.org/10.1111/gcb.13370

Brunetti, M., Buffoni, L., Mangianti, F., Maugeri, M., Nanni, T., 2004. Temperature, precipitation and extreme events during the last century in Italy. Global and Planetary Change 40, 141–149. https://doi.org/10.1016/S0921-8181(03)00104-8

Butcher, J.B., Covington, S., 1995. Dissolved-Oxygen Analysis with Temperature Dependence. J. Environ. Eng. 121, 756–759. https://doi.org/10.1061/(ASCE)0733-9372(1995)121:10(756)

Coppola, E., Verdecchia, M., Giorgi, F., Colaiuda, V., Tomassetti, B., Lombardi, A., 2014. Changing hydrological conditions in the Po basin under global warming. Science of The Total Environment 493, 1183–1196. https://doi.org/10.1016/j.scitotenv.2014.03.003

Cozzi, S., Ibáñez, C., Lazar, L., Raimbault, P., Giani, M., 2018. Flow Regime and Nutrient-Loading Trends from the Largest South European Watersheds: Implications for the Productivity of Mediterranean and Black Sea's Coastal Areas. Water 11, 1. https://doi.org/10.3390/w11010001

Dalsgaard, T., 2000. Protocol handbook for nitrogen cycling in estuaries: A project under the EU research programme: Marine Science and Technology (MAST III). Ministry of Environment and Energy,. Protocol handbook for nitrogen cycling in estuaries: A project under the EU research programme: Marine Science and Technology (MAST III). ISBN: 9788777725357.

de Klein, J.J.M., Overbeek, C.C., Juncher Jørgensen, C., Veraart, A.J., 2017. Effect of Temperature on Oxygen Profiles and Denitrification Rates in Freshwater Sediments. Wetlands 37, 975–983. https://doi.org/10.1007/s13157-017-0933-1

Dodds, W.K., 2006. Eutrophication and trophic state in rivers and streams. Limnol. Oceanogr. 51, 671–680. https://doi.org/10.4319/lo.2006.51.1_part_2.0671

Domeneghetti, A., Carisi, F., Castellarin, A., Brath, A., 2015. Evolution of flood risk over large areas: Quantitative assessment for the Po river. Journal of Hydrology 527, 809–823. https://doi.org/10.1016/j.jhydrol.2015.05.043

Dong, L., Thornton, D., Nedwell, D., Underwood, G., 2000. Denitrification in sediments of the River Colne estuary, England. Mar. Ecol. Prog. Ser. 203, 109–122. https://doi.org/10.3354/meps203109

Frascari, F., Spagnoli, F., Marcaccio, M., & Giordano, P. 2006. Anomalous Po River flood event effects on sediments and the water column of the northwestern Adriatic Sea. Climate Research, 31(2-3), 151-165. 10.3354/cr031151

Gervasio, M.P., Soana, E., Granata, T., Colombo, D., Castaldelli, G., 2022. An unexpected negative feedback between climate change and eutrophication: higher temperatures increase denitrification and buffer nitrogen loads in the Po River (Northern Italy). Environ. Res. Lett. 17, 084031. https://doi.org/10.1088/1748-9326/ac8497

Gervasio, M.P., Soana, E., Vincenzi, F., Magri, M., Castaldelli, G., 2023. Drought-Induced Salinity Intrusion Affects Nitrogen Removal in a Deltaic Ecosystem (Po River Delta, Northern Italy). Water 15, 2405. https://doi.org/10.3390/w15132405

Giambastiani, B.M.S., Colombani, N., Greggio, N., Antonellini, M., Mastrocicco, M., 2017. Coastal aquifer response to extreme storm events in Emilia-Romagna, Italy. Hydrol. Process. 31, 1613–1621. https://doi.org/10.1002/hyp.11130

Giblin, A., Tobias, C., Song, B., Weston, N., Banta, G., Rivera-Monroy, V., 2013. The Importance of Dissimilatory Nitrate Reduction to Ammonium (DNRA) in the Nitrogen Cycle of Coastal Ecosystems. oceanog 26, 124–131. https://doi.org/10.5670/oceanog.2013.54

Glibert, P.M., 2017. Eutrophication, harmful algae and biodiversity — Challenging paradigms in a world of complex nutrient changes. Marine Pollution Bulletin 124, 591–606. https://doi.org/10.1016/j.marpolbul.2017.04.027

Grilli, F., Accoroni, S., Acri, F., Bernardi Aubry, F., Bergami, C., Cabrini, M., Campanelli, A., Giani, M., Guicciardi, S., Marini, M., Neri, F., Penna, A., Penna, P., Pugnetti, A., Ravaioli, M., Riminucci, F., Ricci, F., Totti, C., Viaroli, P., Cozzi, S., 2020. Seasonal and Interannual Trends of Oceanographic Parameters over 40 Years in the Northern Adriatic Sea in Relation to Nutrient Loadings Using the EMODnet Chemistry Data Portal. Water 12, 2280. https://doi.org/10.3390/w12082280

Guo, Z., Su, R., Zeng, J., Wang, S., Zhang, D., Yu, Z., ... & Zhao, D. (2022). NosZI microbial community determined the potential of denitrification and nitrous oxide emission in

river sediments of Qinghai-Tibetan Plateau. Environmental Research, 214, 114138. https://doi.org/10.1016/j.envres.2022.114138

Hargrave, B.T., 1972. AEROBIC DECOMPOSITION OF SEDIMENT AND DETRITUS AS A FUNCTION OF PARTICLE SURFACE AREA AND ORGANIC CONTENT: DECOMPOSITION OF SEDIMENT AND DETRITUS. Limnol. Oceanogr. 17, 583–586. https://doi.org/10.4319/lo.1972.17.4.0583

Hill, A.R., 2023. Patterns of nitrate retention in agriculturally influenced streams and rivers. Biogeochemistry 163, 155–183. https://doi.org/10.1007/s10533-023-01027-w

Hobbs, J.K., Jiao, W., Easter, A.D., Parker, E.J., Schipper, L.A., Arcus, V.L., 2013. Change in Heat Capacity for Enzyme Catalysis Determines Temperature Dependence of Enzyme Catalyzed Rates. ACS Chem. Biol. 8, 2388–2393. https://doi.org/10.1021/cb4005029

Hou, C., Chu, M.L., Guzman, J.A., Acero Triana, J.S., Moriasi, D.N., Steiner, J.L., 2019. Field scale nitrogen load in surface runoff: Impacts of management practices and changing climate. Journal of Environmental Management 249, 109327. https://doi.org/10.1016/j.jenvman.2019.109327

Hu, J., Ouyang, W., Yang, Z., 2023. Impacts of extreme climate on nitrogen loss in different forms and pollution risk with the copula model. Journal of Hydrology 620, 129412. https://doi.org/10.1016/j.jhydrol.2023.129412

Hu, R., Zheng, X., Zheng, T., Xin, J., Wang, H., Sun, Q., 2019. Effects of carbon availability in a woody carbon source on its nitrate removal behavior in solid-phase denitrification. Journal of Environmental Management 246, 832–839. https://doi.org/10.1016/j.jenvman.2019.06.057

Jaiswal, D., Naaz, N., Gupta, S., Madhav, K., & Pandey, J. (2023). Diurnal oscillation in dissolved oxygen at sediment-water interface fuels denitrification-driven N removal in Ganga River. Journal of Hydrology, 619, 129301. https://doi.org/10.1016/j.jhydrol.2023.129301

Jiang, X., Gao, G., Zhang, L., Tang, X., Shao, K., & Hu, Y. (2020). Denitrification and dissimilatory nitrate reduction to ammonium in freshwater lakes of the Eastern Plain, China: Influences of organic carbon and algal bloom. Science of the Total Environment, 710, 136303. https://doi.org/10.1016/j.scitotenv.2019.136303

Kana, T.M., Darkangelo, Christina., Hunt, M.Duane., Oldham, J.B., Bennett, G.E., Cornwell, J.C., 1994. Membrane Inlet Mass Spectrometer for Rapid High-Precision Determination of N2, O2, and Ar in Environmental Water Samples. Anal. Chem. 66, 4166–4170. https://doi.org/10.1021/ac00095a009

Kraft, B., Tegetmeyer, H.E., Sharma, R., Klotz, M.G., Ferdelman, T.G., Hettich, R.L., Geelhoed, J.S., Strous, M., 2014. The environmental controls that govern the end product of bacterial nitrate respiration. Science 345, 676–679. https://doi.org/10.1126/science.1254070

Lassaletta, L., García-Gómez, H., Gimeno, B.S., Rovira, J.V., 2009. Agriculture-induced increase in nitrate concentrations in stream waters of a large Mediterranean catchment over 25years (1981–2005). Science of The Total Environment 407, 6034–6043. https://doi.org/10.1016/j.scitotenv.2009.08.002

Magri, M., Benelli, S., Castaldelli, G., Bartoli, M., 2022. The seasonal response of in situ denitrification and DNRA rates to increasing nitrate availability. Estuarine, Coastal and Shelf Science 271, 107856. https://doi.org/10.1016/j.ecss.2022.107856

Marchina, C., Natali, C., Fazzini, M., Fusetti, M., Tassinari, R., Bianchini, G., 2017. Extremely dry and warm conditions in northern Italy during the year 2015: effects on the Po river water. Rend. Fis. Acc. Lincei 28, 281–290. https://doi.org/10.1007/s12210-017-0596-0

Myrstener, M., Jonsson, A., & Bergström, A. K. (2016). The effects of temperature and resource availability on denitrification and relative N2O production in boreal lake sediments. Journal of Environmental Sciences, 47, 82-90. https://doi.org/10.1016/j.jes.2016.03.003

Moatti, J.-P., Thiébault, S. (Eds.), 2016. The Mediterranean region under climate change: A scientific update. IRD Éditions. https://doi.org/10.4000/books.irdeditions.22908

Montanari, A., 2012. Hydrology of the Po River: looking for changing patterns in river discharge. Hydrol. Earth Syst. Sci. 16, 3739–3747. https://doi.org/10.5194/hess-16-3739-2012

Montanari, A., Nguyen, H., Rubinetti, S., Ceola, S., Galelli, S., Rubino, A., Zanchettin, D., 2023. Why the 2022 Po River drought is the worst in the past two centuries. Sci. Adv. 9, eadg8304. https://doi.org/10.1126/sciadv.adg8304

Muruganandam, M., Rajamanickam, S., Sivarethinamohan, S., Reddy, M. K., Velusamy, P., Gomathi, R., ... & Munisamy, S. K. (2023). Impact of climate change and anthropogenic activities on aquatic ecosystem–A review. Environmental Research, 117233. https://doi.org/10.1016/j.envres.2023.117233

Nielsen, L.P., 1992. Denitrification in sediment determined from nitrogen isotope pairing. FEMS Microbiology Letters 86, 357–362. https://doi.org/10.1111/j.1574-6968.1992.tb04828.x

Nizzoli, D., Carraro, E., Nigro, V., Viaroli, P., 2010. Effect of organic enrichment and thermal regime on denitrification and dissimilatory nitrate reduction to ammonium (DNRA) in hypolimnetic sediments of two lowland lakes. Water Research 44, 2715–2724. https://doi.org/10.1016/j.watres.2010.02.002

Oduor, B.O., Campo-Bescós, M.Á., Lana-Renault, N., Casalí, J., 2023. Effects of climate change on streamflow and nitrate pollution in an agricultural Mediterranean watershed in Northern Spain. Agricultural Water Management 285, 108378. https://doi.org/10.1016/j.agwat.2023.108378

Owens, M.S., Cornwell, J.C., 2016. The Benthic Exchange of O_2, N_2 and Dissolved Nutrients Using Small Core Incubations. JoVE 54098. https://doi.org/10.3791/54098

Penna, N., Capellacci, S., Ricci, F., 2004. The influence of the Po River discharge on phytoplankton bloom dynamics along the coastline of Pesaro (Italy) in the Adriatic Sea. Marine Pollution Bulletin 48, 321–326. https://doi.org/10.1016/j.marpolbul.2003.08.007

Piña-Ochoa, E., Álvarez-Cobelas, M., 2006. Denitrification in Aquatic Environments: A Cross-system Analysis. Biogeochemistry 81, 111–130. https://doi.org/10.1007/s10533-006-9033-7

Racchetti, E., Bartoli, M., Soana, E., Longhi, D., Christian, R.R., Pinardi, M., Viaroli, P., 2011. Influence of hydrological connectivity of riverine wetlands on nitrogen removal via denitrification. Biogeochemistry 103, 335–354. https://doi.org/10.1007/s10533-010-9477-7

Rajesh, M., Rehana, S., 2022. Impact of climate change on river water temperature and dissolved oxygen: Indian riverine thermal regimes. Sci Rep 12, 9222. https://doi.org/10.1038/s41598-022-12996-7

Ravazzani, G., Barbero, S., Salandin, A., Senatore, A., Mancini, M., 2015. An integrated Hydrological Model for Assessing Climate Change Impacts on Water Resources of the Upper Po River Basin. Water Resour Manage 29, 1193–1215. https://doi.org/10.1007/s11269-014-0868-8

Risgaard-Petersen, N., & Rysgaard, S., 1995. Nitrate reduction in sediments and waterlogged soil measured by 15N techniques. Methods in applied soil microbiology. Academic Press Inc., London, United Kingdom.

Roberts, K.L., Kessler, A.J., Grace, M.R., Cook, P.L.M., 2014. Increased rates of dissimilatory nitrate reduction to ammonium (DNRA) under oxic conditions in a periodically hypoxic estuary. Geochimica et Cosmochimica Acta 133, 313–324. https://doi.org/10.1016/j.gca.2014.02.042

Romero, E., Garnier, J., Lassaletta, L., Billen, G., Le Gendre, R., Riou, P., Cugier, P., 2013. Large-scale patterns of river inputs in southwestern Europe: seasonal and interannual variations and potential eutrophication effects at the coastal zone. Biogeochemistry 113, 481–505. https://doi.org/10.1007/s10533-012-9778-0

Romero, E., Ludwig, W., Sadaoui, M., Lassaletta, L., Bouwman, A.F., Beusen, A.H.W., Apeldoorn, D., Sardans, J., Janssens, I.A., Ciais, P., Obersteiner, M., Peñuelas, J., 2021. The Mediterranean Region as a Paradigm of the Global Decoupling of N and P Between Soils and Freshwaters. Global Biogeochem Cycles 35. https://doi.org/10.1029/2020GB006874

Seiter, K., Hensen, C., & Zabel, M. (2005). Benthic carbon mineralization on a global scale. Global Biogeochemical Cycles, 19(1). https://doi.org/10.1029/2004GB002225

Seitzinger, S.P., 1988. Denitrification in freshwater and coastal marine ecosystems: Ecological and geochemical significance: Denitrification. Limnol. Oceanogr. 33, 702–724. https://doi.org/10.4319/lo.1988.33.4part2.0702

Silvennoinen, H., Liikanen, A., Torssonen, J., Stange, C. F., & Martikainen, P. J., 2008. Denitrification and N 2 O effluxes in the Bothnian Bay (northern Baltic Sea) river sediments as affected by temperature under different oxygen concentrations. Biogeochemistry, 88, 63-72. https://doi.org/10.1007/s10533-008-9194-7

Soana, E., Bartoli, M., Milardi, M., Fano, E.A., Castaldelli, G., 2019. An ounce of prevention is worth a pound of cure: Managing macrophytes for nitrate mitigation in irrigated

agricultural watersheds. Science of The Total Environment 647, 301–312. https://doi.org/10.1016/j.scitotenv.2018.07.385

Soana, E., Gervasio, M.P., Granata, T., Colombo, D., Castaldelli, G., 2023. Climate change impacts on eutrophication in the Po River (Italy): Temperature-mediated reduction in nitrogen export but no effect on phosphorus. Journal of Environmental Sciences S100107422300308X. https://doi.org/10.1016/j.jes.2023.07.008

Song, G., Liu, S., Zhu, Z., Zhai, W., Zhu, C., & Zhang, J., 2016. Sediment oxygen consumption and benthic organic carbon mineralization on the continental shelves of the East China Sea and the Yellow Sea. Deep Sea Research Part II: Topical Studies in Oceanography, 124, 53-63. https://doi.org/10.1016/j.dsr2.2015.04.012

Speir, S.L., Tank, J.L., Taylor, J.M., Grose, A.L., 2023. Temperature and carbon availability interact to enhance nitrous oxide production via denitrification in alluvial plain river sediments. Biogeochemistry 165, 191–203. https://doi.org/10.1007/s10533-023-01074-3

Spillman, C.M., Imberger, J., Hamilton, D.P., Hipsey, M.R., Romero, J.R., 2007. Modelling the effects of Po River discharge, internal nutrient cycling and hydrodynamics on biogeochemistry of the Northern Adriatic Sea. Journal of Marine Systems 68, 167–200. https://doi.org/10.1016/j.jmarsys.2006.11.006

Struglia, M.V., Mariotti, A., Filograsso, A., 2004. River Discharge into the Mediterranean Sea: Climatology and Aspects of the Observed Variability. River Discharge into the Mediterranean Sea: Climatology and Aspects of the Observed Variability 4740–4751. https://doi.org/10.1175/JCLI-3225.1

Sutton, M.A., Howard, C.M., Erisman, J.W., Billen, G., Bleeker, A., Grennfelt, P., van Grinsven, H., Grizzetti, B. (Eds.), 2011. The European Nitrogen Assessment: Sources, Effects and Policy Perspectives, 1st ed. Cambridge University Press. https://doi.org/10.1017/CBO9780511976988

Tu, J., 2009. Combined impact of climate and land use changes on streamflow and water quality in eastern Massachusetts, USA. Journal of Hydrology 379, 268–283. https://doi.org/10.1016/j.jhydrol.2009.10.009

Velthuis, M., Veraart, A.J., 2022. Temperature Sensitivity of Freshwater Denitrification and N_2O Emission—A Meta-Analysis. Global Biogeochemical Cycles 36. https://doi.org/10.1029/2022GB007339

Veraart, A.J., De Klein, J.J.M., Scheffer, M., 2011. Warming Can Boost Denitrification Disproportionately Due to Altered Oxygen Dynamics. PLoS ONE 6, e18508. https://doi.org/10.1371/journal.pone.0018508

Vezzoli, R., Mercogliano, P., Pecora, S., Zollo, A.L., Cacciamani, C., 2015. Hydrological simulation of Po River (North Italy) discharge under climate change scenarios using the RCM COSMO-CLM. Science of The Total Environment 521–522, 346–358. https://doi.org/10.1016/j.scitotenv.2015.03.096

Viaroli, P., Soana, E., Pecora, S., Laini, A., Naldi, M., Fano, E.A., Nizzoli, D., 2018. Space and time variations of watershed N and P budgets and their relationships with reactive N and P loadings in a heavily impacted river basin (Po river, Northern Italy). Science of The Total Environment 639, 1574–1587. https://doi.org/10.1016/j.scitotenv.2018.05.233

Warembourg, F.R., 1993. Nitrogen Fixation in Soil and Plant Systems, Academic Press Inc. ed. R Knowles and T H Black-burn, New York, NY, USA.

Warneke, S., Schipper, L.A., Matiasek, M.G., Scow, K.M., Cameron, S., Bruesewitz, D.A., McDonald, I.R., 2011. Nitrate removal, communities of denitrifiers and adverse effects in different carbon substrates for use in denitrification beds. Water Research 45, 5463–5475. https://doi.org/10.1016/j.watres.2011.08.007

Wei, H., Gao, D., Liu, Y., & Lin, X., 2020. Sediment nitrate reduction processes in response to environmental gradients along an urban river-estuary-sea continuum. Science of the Total Environment, 718, 137185. 10.1016/j.scitotenv.2020.137185

Yin, S.X., Chen, D., Chen, L.M., Edis, R., 2002. Dissimilatory nitrate reduction to ammonium and responsible microorganisms in two Chinese and Australian paddy soils. Soil Biology and Biochemistry 34, 1131–1137. https://doi.org/10.1016/S0038-0717(02)00049-4

Yuan, H., Cai, Y., Wang, H., Liu, E., & Zeng, Q., 2023. Impact of seasonal change on dissimilatory nitrate reduction to ammonium (DNRA) triggering the retention of nitrogen in lake. Journal of Environmental Management, 341, 118050. https://doi.org/10.1016/j.jenvman.2023.118050

Zanchettin, D., Traverso, P., Tomasino, M., 2008. Po River discharges: a preliminary analysis of a 200-year time series. Climatic Change 89, 411–433. https://doi.org/10.1007/s10584-008-9395-z

Zhang, Q., Huang, J., Zhang, J., Qian, R., Cui, Z., & Gao, J. (2024). Characterizing nitrogen dynamics and their response to sediment dredging in a lowland rural river. Journal of Hydrology, 628, 130479. https://doi.org/10.1016/j.jhydrol.2023.130479

Zheng, J., Cao, X., Ma, C., Weng, N., Huo, S., 2023. What drives the change of nitrogen and phosphorus loads in the Yellow River Basin during 2006-2017? Journal of Environmental Sciences 126, 17–28. https://doi.org/10.1016/j.jes.2022.04.039

Author contributions

Maria Pia Gervasio: investigation, formal analysis, writing original draft preparation, visualization; Elisa Soana: methodology, conceptualization, writing review and editing, supervision; Anna Gavioli: formal analysis; Fabio Vincenzi: investigation; Giuseppe Castaldelli: conceptualization, writing review and editing, funding acquisition, supervision.

Funding

This study was financially supported by the Consorzio di Bonifica Pianura di Ferrara (Ferrara Plain Reclamation Consortium) as part of a long-term collaboration aimed at defining management strategies to control eutrophication in the Po Delta region. This research was also made possible thanks to funding from the Emilia-Romagna Region (Hunting and Fisheries Division) in the framework of the project "Assessment and mapping of the productivity of the bivalve mollusc aquaculture in the Sacca di Goro lagoon and the coastal stretch from Lido di Volano to Lido delle Nazioni, Ferrara, Emilia-Romagna." The authors thank Prof. Marco Bartoli and Dr. Monia Magri (University of Parma, Italy) for their assistance with the DNRA measurements.

Conflict of interest statement

The authors declare no conflict of interest.

Appendix III: The impact of saline intrusion in the Po Delta on its capacity to dissipate N loads

Paper IV: Gervasio, M. P., Soana, E., Vincenzi, F., & Castaldelli, G. (2022). An Underestimated Contribution of Deltaic Denitrification in Reducing Nitrate Export to the Coastal Zone (Po River–Adriatic Sea, Northern Italy). *Water*, 14(3), 501. https://doi.org/10.3390/w14030501

water

MDPI

Article

An Underestimated Contribution of Deltaic Denitrification in Reducing Nitrate Export to the Coastal Zone (Po River–Adriatic Sea, Northern Italy)

Maria Pia Gervasio, Elisa Soana *, Fabio Vincenzi and Giuseppe Castaldelli

DiSAP—Department of Environmental and Prevention Sciences, University of Ferrara, Via L.Borsari 46, 44121 Ferrara, Italy; grvmrp@unife.it (M.P.G.); fabio.vincenzi@unife.it (F.V.); ctg@unife.it (G.C.)
* Correspondence: elisa.soana@unife.it

Abstract: In transitional environments, the role of sediments biogeochemistry and denitrification is crucial for establishing their buffer potential against nitrate (NO_3^-) pollution. The Po River (Northern Italy) is a worldwide hotspot of eutrophication. However, benthic N dynamics and the relevance of denitrification in its delta have not yet been described. The aim of the present study was to quantify the contribution of denitrification in attenuating the NO_3^- loading transported to the sea during summer. Benthic fluxes of dissolved inorganic nitrogen (N) and denitrification rates were measured in laboratory incubations of intact sediment cores collected, along a salinity gradient, at three sections of the Po di Goro, the southernmost arm of the Po Delta. The correlation between NO_3^- consumption and N_2 production rates demonstrated that denitrification was the main process responsible for reactive N removal. Denitrification was stimulated by both NO_3^- availability in the Po River water and organic enrichment of sediment likely determined by salinity-induced flocculation of particulate organic load, and inhibited by increasing salinity, along the river–sea gradient. Overall, denitrification represented a sink of approximately 30% of the daily N loading transported in middle summer, highlighting a previously underestimated role of the Po River Delta.

Keywords: denitrification; Po River; nitrate loading; eutrophication; river sediment

Citation: Gervasio, M.P.; Soana, E.; Vincenzi, F.; Castaldelli, G. An Underestimated Contribution of Deltaic Denitrification in Reducing Nitrate Export to the Coastal Zone (Po River–Adriatic Sea, Northern Italy). *Water* **2022**, *14*, 501. https://doi.org/10.3390/w14030501

Academic Editor: Qian Sun

Received: 9 December 2021
Accepted: 3 February 2022
Published: 8 February 2022

1. Introduction

Rivers draining agricultural and urban basins export high quantities of reactive nitrogen (N) causing eutrophication-related phenomena in the coastal zones. As the N availability in receiving water bodies increases, excessive algal growth is stimulated and the eventual organic matter results in bottom water anoxia and cascading effects such as biodiversity loss, and alterations in food web structure and function [1,2]. At the same time, riverine sediments are active sites for biogeochemical reactions, such as denitrification, which acts as a natural buffer against nitrate (NO_3^-) pollution [3,4]. Denitrification, the stepwise reduction of NO_3^- to nitrogen gas (N_2) under anaerobic conditions, is widely recognized as the dominant biogeochemical process responsible for permanent N removal in rivers and transitional environments [5–7]. Anammox, the anaerobic oxidation of ammonium, can also remove inorganic N by combining ammonium (NH_4^+) with nitrite (NO_2^-) and releasing N_2; however, its occurrence is generally irrelevant if compared to denitrification in freshwater sediments [8,9].

Spatially distributed global models have demonstrated that denitrification occurring in river networks may remove, on average, 20–50% of the total land-based N input, indicating they are important filters for the N loadings transported toward the sea and therefore play a considerable role in mitigating eutrophication effects [7,10]. Although the denitrification capacity of the river networks has been recognized, most studies on the regulation of denitrification have addressed headwater streams because of their intense water–streambed interactions (i.e., a high ratio between bioreactive surfaces and water

volumes), sustaining significant in-stream N retention [11,12]. The nitrate (NO_3^-) supply to the benthic compartment is mainly controlled by diffusion from the water column; thus, N loss may decline with increasing channel size and depth because of less contact and exchange, making the denitrification process progressively less effective [13]. However, lowland rivers, deltas, and estuaries of agricultural basins in temperate zones may be ideal sites for denitrification, showing the typical features of eutrophic environments, such as elevated NO_3^- concentrations in water, organic carbon availability, and favorable temperatures during the spring–summer period [7,14,15]. Conversely, salinity increase along the river–sea gradient has been demonstrated to inhibit the denitrification activity of the sediments [16,17].

In eutrophic deltas, reduced flow and water mixing during the summer, concomitant with the establishment of steep thermal and/or saline gradients, may lead to partial or full stratification. Under these conditions, discriminating the source of NO_3^- fueling sedimentary denitrification, from the water column or nitrified at the water/sediment interface, is crucial for understanding benthic N metabolism [10]. Moreover, hypoxic or anoxic conditions may be established more frequently in stratified bottom waters, where NH_4^+ released from the sediments is not oxidized to NO_3^- and may accumulate [18,19].

The Po River Basin (Northern Italy) is one of the most densely populated and agriculturally exploited areas in Europe and is a well-known hotspot of eutrophication and NO_3^- pollution. Although several studies have addressed the N cycle in a wide variety of aquatic ecosystems in the basin, such as drainage canals, wetlands, lakes, and brackish coastal lagoons (e.g., [20–23]), the fate of the Po River N loadings through the delta remains unknown as they are measured at the closure of the basin, which is approximately 60 km upstream from the delta and more than 90 km from the outlet into the Adriatic Sea. Determining the factors controlling denitrification in lowland rivers and deltas is a crucial step in efforts to protect coastal zones from eutrophication caused by N excess. The quantitative relevance of denitrification in attenuating in-stream N loading during the season most sensitive to eutrophication has not been well established.

The aims of the present study were (i) to measure benthic denitrification in the Po River branch, namely the Po di Goro, taken as a case study representative of the other deltaic branches; (ii) to study the effect of water stratification along a 30 km salinity gradient, from the full riverine reach to the mouth to the sea; and (iii) to assess the role of denitrification in buffering N loadings to the Adriatic Sea in summer, the most sensitive period for eutrophication.

2. Materials and Methods

2.1. Study Area

The study area was the southernmost arm of the Po River Delta, named Po di Goro River, crossing northeast Italy for over 48 km, marking the borderline between the Emilia-Romagna and Veneto regions (Figure 1) The average annual discharge of the Po di Goro accounts for approximately 5% of the Po River discharge measured at Pontelagoscuro, more than 90 km upstream of the main river mouth and conventionally considered the basin closing section [24]. The Po di Goro River is partly connected to the Goro lagoon in its lower reach till the mouth to the Adriatic Sea. The Sacca di Goro, a shallow coastal lagoon, has suffered in the past from eutrophication, macroalgal blooms followed by summer anoxia, dystrophic crises, and massive deaths of farmed mollusks [25]. Freshwater and saltwater stratification and partial mixing are typical summer phenomena in the terminal Po di Goro River [26]. In recent years, an increase in salt intrusion has been detected in the lower Po di Goro River. For instance, the monitoring network of the Regional Environmental Protection Agency of the Emilia-Romagna region (ARPAE) has evidenced in summer a mean saltwater intrusion of approximately 13 km from the mouth to the sea.

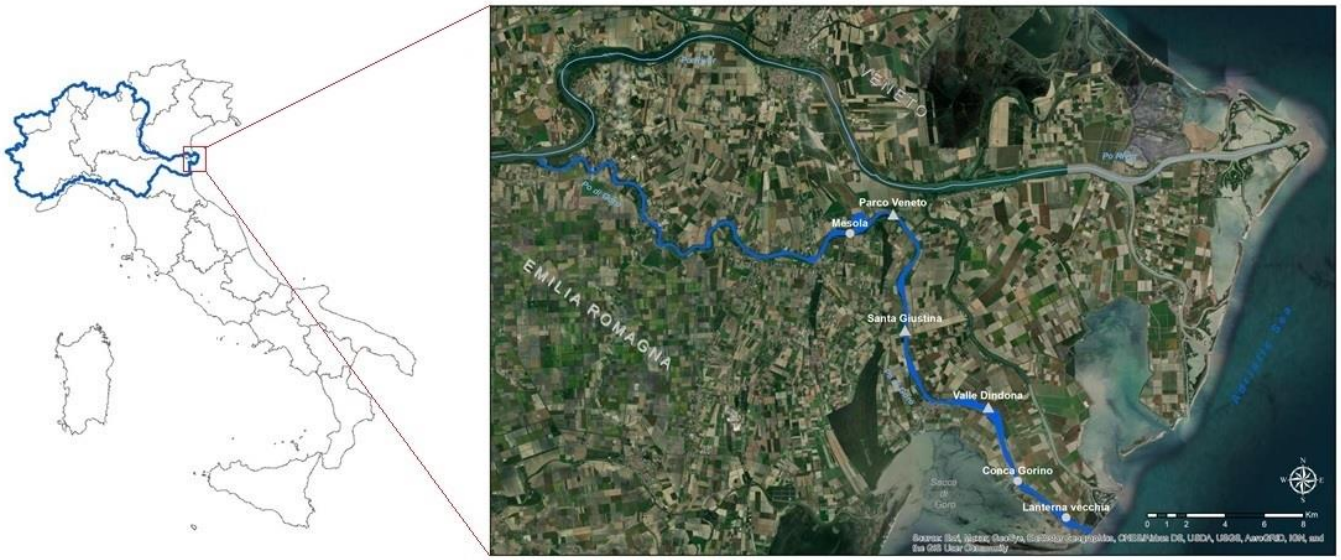

Figure 1. Study area. Location of the Po di Goro arm in Italy with the Po River Basin border reported in dark blue (map on the left). In the map on the right, the blue line represents the Po di Goro course and in light blue is indicated the Po River. Grey bubbles are the main study sites where sediment cores were sampled; while grey triangles indicate other monitoring stations along the Po di Goro (modified from basemap of ArcMap, ArcGIS 10.2.2., ESRI, Redlands, California).

In the present study, intact sediment cores were sampled in middle summer (end of July 2021) at three sections of the Po di Goro River along a salinity gradient: Mesola (M, 44°56′04.1″ N and 12°15′03.9″ E), Conca Gorino (G, 44°49′02.9″ N and 12°21′11.3″ E), and Lanterna Vecchia (LV, 44°47′59.0″ N and 12°23′00.3″ E), located 25, 5, and 1.5 km upstream, respectively, from the outlet into the Adriatic Sea (Figure 1; Table 1). The study area covered an overall surface of 7 km^2, and the three stations showed different characteristics. The M site was fully freshwater (340 µS cm^{-1}), the water column was thoroughly mixed, and the NO_3^- concentration (~90 µM) showed summer values typical of the terminal reach of the Po River [27]. At the bottom of G site, water was slightly saline, up to 11.2 ppt, while complete water stratification occurred at LV. In fact, in LV surface water, salinity was ~0.8 ppt and in depth ~18.1 ppt, due to salt intrusion from the Adriatic Sea. Nitrate availability decreased from ~60 µM to ~40 µM moving from G to LV (Table 1). During the sediment sampling campaign, profiles of physicochemical water variables (temperature, oxygen, electrical conductivity, and salinity) were monitored at different stations along the river course, demonstrating that freshwater conditions along the entire water depth extend from the M site to the location named Valle Dindona located approximately 5 km upstream from the G site.

Table 1. Features of the three sampling sites during the July campaign. Values of the bottom waters are reported.

Site	Distance from the Outlet (km)	Salinity (ppt)	NO_3^- (µM)	NH_4^+ (µM)	Total N (µM)
Mesola (M)	25	0.2	90	3	115
Conca Gorino (G)	5	11.2	59	13	122
Lanterna Vecchia (LV)	1.5	18.1	44	5	113

2.2. Sediment and Water Sampling

Measurements of sedimentary features, sediment oxygen demand, inorganic N fluxes (NO_3^-, NH_4^+, and N_2), and denitrification rates at the three sampling sites were performed in middle summer. Sampling and pre-incubation were performed according to standard-

ized procedures [28]. The experimental design consisted of the collection of seven intact sediment cores (plexiglass liners, internal diameter 4.5 cm, length 20 cm) at each site, of which five replicates were used for dark flux and denitrification measurements, and two replicates for sediment characterization. Only cores with visually undisturbed sediments and clear overlying water were used for further treatment. The sediment level of the collected intact cores was adjusted to approximately 9 cm on average, leaving an overlying water column of approximately 8 cm. Water column parameters (temperature, oxygen content, electrical conductivity, and salinity) were measured in situ with a multiparametric probe (YSI Model 85—Handheld Dissolved Oxygen, Conductivity, Salinity and Temperature System, YSI, Incorporated, Yellow Springs, OH, USA). After collection, the sediment cores were submerged in three different tanks with site water continuously aerated with aquarium pumps, and they were transported to the laboratory within a few hours. At each site, approximately 60 **L** of bottom water were collected using a Van Dorn bottle and brought to the laboratory for core maintenance, pre-incubation, and incubation periods.

2.3. Measurement of Benthic Fluxes and Denitrification Rates

In the laboratory, the sediment cores were maintained with the top open and aerated overnight in the dark. Each core was equipped with a Teflon-coated magnet, driven by a central magnet rotating at 40 rpm, which was suspended a few centimeters above the sediment surface to mix the water column while avoiding resuspension (Figure 2a,b). Water was stirred throughout the whole pre-incubation and incubation periods. Intact sediment cores were incubated in a batch mode according to standardized protocols developed for the measurement of benthic fluxes of gases and nutrients [28,29]. Incubations were performed in the laboratory at 25 °C, simulating the typical middle summer conditions in the Po River Delta. Dark fluxes of dissolved O_2 (SOD, sediment oxygen demand) and dissolved inorganic N (N_2, NO_3^-, NO_2^-, NH_4^+) across the water–sediment interface were quantified via start–end incubations lasting 2 h in order to maintain O_2 concentration within 20% of initial value [28]. Light penetration is generally very limited where the turbidity is high, such as in the Po River Delta; thus, the benthic compartment is assumed always to be in the dark. After overnight pre-incubation, five cores from each site were incubated in the dark. The water inside each tank was replaced with fresh water from each site in order to maintain near in situ dissolved nutrient concentrations. To initiate incubation, the water level in the tanks was lowered a few centimeters below the top of the cores and each liner was sealed with a rubber lid. Temperature and O_2 concentrations were measured with a multiparametric probe directly inside each core at the beginning and end of the incubation period. Simultaneously, water samples were collected from each core with a glass 60 mL syringe, filtered through Whatman GF/F glass fiber filters and transferred to polyethylene vials to analyze dissolved inorganic N compounds. In addition, samples for N_2:Ar were collected, transferred into 12 mL glass-tight vials (Exetainer, Labco, High Wycombe, UK) allowing abundant overflow, and preserved by adding 100 µL of 7 M $ZnCl_2$ to stop microbial activity. After the first incubation, the water in the tanks was replaced and the cores were submerged for approximately 1 h to stabilize. The isotope pairing technique (IPT [28,30]) was applied to measure denitrification rates on the same set of cores used for benthic flux determinations. At the beginning of the incubation, the water level in the tank was lowered just below the top of the cores, and aliquots of a stock solution of 15 mM $^{15}NO_3^-$ ($Na^{15}NO_3$, Sigma Aldrich) were added to the cores to obtain a final labelled NO_3^- enrichment of approximately 50%. The IPT incubation lasted 2 h from when the cores were capped. The NO_3^- concentrations were measured in each core before and after the addition of $^{15}NO_3^-$ to calculate the ^{14}N:^{15}N ratio in the NO_3^- pool. At the end of the incubation period, the entire sediment column was mixed with the water column to homogenize the dissolved N_2 pools in the water column and porewater. An aliquot of the slurry was transferred to a 12 mL Exetainer and fixed with 200 µL of 7 M $ZnCl_2$.

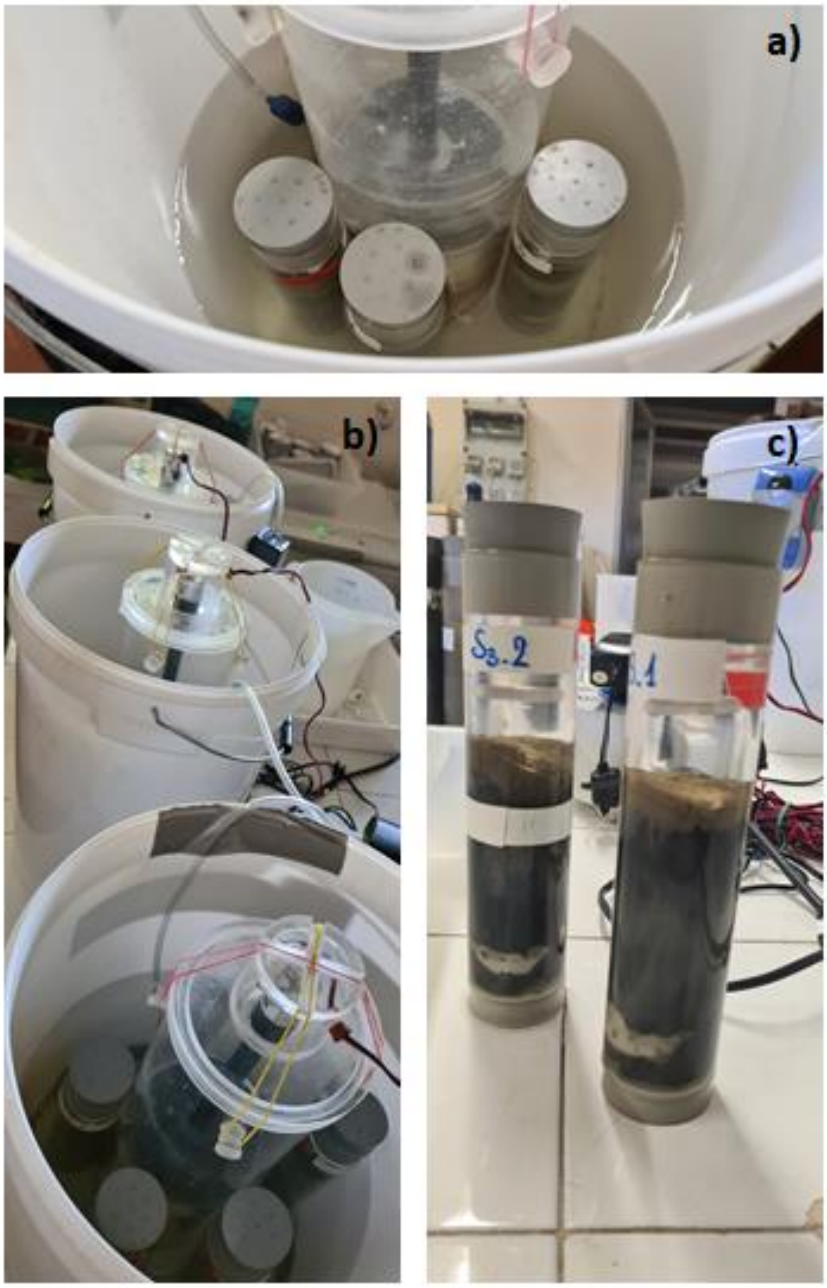

Figure 2. Laboratory design: (**a**) laboratory tank of one experimental site with sampling cores and central motor with mounted magnets to drive the individual magnetic stirrers within the cores; (**b**) experimental setup of the three sampling sites, consisting of five cores for each tank; (**c**) examples of sampling cores used for sediments characterization.

2.4. Analytical Methods, Calculation of Benthic Fluxes and Denitrification Rates

NO_2^- and NH_4^+ were analyzed via standard spectrophotometric methods using a Jasco V-550 spectrophotometer. NO_2^- was determined using sulfanilamide and N-(1-naphtyl)-ethylenediamine (detection limit 0.1 µM [31]). NH_4^+ was analyzed using salicylate and hypochlorite in the presence of sodium nitroprusside (detection limit 0.5 µM [32]). NO_3^- was analyzed using Technicon AutoAnalyser II (detection limit 0.4 µM [33]).

The N_2:Ar ratio (water samples from the incubation of benthic fluxes) and the abundance of $^{29}N_2$ and $^{30}N_2$ (slurry samples from the IPT incubation) were analyzed via membrane inlet mass spectrometry (MIMS) at the Laboratory of Aquatic Ecology, University of Ferrara (Bay instrument, MD, USA [34]). For MIMS analyses, the samples, after equilibra-

tion at 20 °C, were pumped through an under-vacuum gas-permeable silicone membrane. The extracted gases passed through (i) a liquid nitrogen cryogenic trap to remove carbon dioxide and water vapor, (ii) a copper reduction column controlled by a muffle furnace operating at 600 °C to remove oxygen, and finally (iii) a second liquid nitrogen trap before ionization and detection by a PrismaPlus quadrupole mass spectrometer [35,36]. The concentration of N_2 was calculated from the measured N_2:Ar ratio multiplied by the theoretical saturated Ar concentration at the sampling water temperature determined from gas solubility tables [37]. Benthic N_2 fluxes include coupled nitrification/denitrification and anammox. However, several studies showed that contribution of anammox to N_2 production in organic-rich freshwater ecosystems is generally negligible [3,38,39].

Dark fluxes were calculated from the rate of change in concentrations with time, according to the following equation [29]:

$$F_x = \frac{(C_0 - C_f) \cdot V}{A \cdot t}$$

where F_x (μmol m^{-2} h^{-1}) is the flux of a general compound, C_0 and C_f (μM) are the concentrations of the compound at the beginning and the end of incubation, respectively, V (L) is the water volume of the core, A (m^2) is the area of the sediment core, and t (h) is the time of incubation. Negative values indicate fluxes from the water column to the sediment, whereas positive values indicate fluxes from sediment to the water column.

Denitrification rates were calculated as described by [29]:

$$D_{15} = p29 + 2p30 D_{14} = D_{15} \cdot \left(\frac{p29}{2p30} \right)$$

where D_{15} is the denitrification rate of the added $^{15}NO_3^-$, D_{14} is the total denitrification rate of $^{14}NO_3^-$, and p29 and p30 are the production rates of $^{29}N_2$ and $^{30}N_2$, respectively. The denitrification of NO_3^- diffusing to the anoxic sediment layer from the water column (D_w) and the denitrification of NO_3^- produced within the oxic sediment layer by nitrification (Dn) were calculated according to [30]:

$$D_w = \frac{^{14}NO_3^-}{^{15}NO_3^-} \cdot D_{15} D_n = D_{14} - D_w$$

where $^{14}NO_3^-$ is the ambient nitrate and $^{15}NO_3^-$ is the labelled nitrate added to each core.

2.5. Sediment Characterization

The cores for sediment characterization (Figure 2c) were processed as follows. The upper 0–1 cm section was sliced, and rapidly homogenized and sediment subsamples of 5 mL were used to determine the physical properties. Bulk density was determined as the ratio of wet weight to volume. Porosity and water content (%) were determined from weight loss of a known fresh sediment volume, after drying at 50 °C to constant weight for 72 h. Finally, the dried samples (approximately 0.5 g) were placed into a muffle furnace at 350 °C for 3 h to quantify the organic matter content (OM, %), based on the weight loss by ignition.

2.6. Riverine N Loadings in the Po di Goro and Importance of NO_3^- Removal via Denitrification

Daily total N loadings transported by the Po di Goro River to the Adriatic Sea in the middle summer (July and August) months were calculated using official concentration and discharge datasets collected for the period 2014–2019. Nitrogen species concentrations were obtained by monthly sampling campaigns carried out at the Serravalle station (44°58′43.6″ N and 11°59′51.9″ E) in the framework of the ARPAE environmental monitoring program (https://dati.arpae.it/, accessed on 23 October 2021). The station is located on the main course of the Po River just before the diversion of the Po di Goro branch.

Sample collection and analysis were performed in accordance with standard methods and analytical protocols [40]. The daily average discharges of the Po River (Pontelagoscuro station, 44°53′19.34″ N and 11°36′29.60″ E) were acquired from the permanent records of a gauge operated by ARPAE. Discharge datasets were retrieved from the "Hydrological Annals—Second Part" published by ARPAE and available on the Regional Open Data Portal (https://simc.arpae.it/dext3r/, accessed on 23 October 2021). The discharge of the Po di Goro River was calculated as a function of the discharge measured at Pontelagoscuro by employing a predictive experimental equation obtained from data reviewed by the Environmental Agency of the Veneto Region (Supplementary Materials, Figure S1). Daily total N loadings were calculated by multiplying monthly concentrations by average monthly discharge and compared to the amount potentially removed by the entire sampled reach of the Po di Goro River obtained by scaling up the experimentally measured denitrification rates. The proportion of the N amount removed in the reach versus the total N loading entering that reach was considered as the denitrification efficiency.

2.7. Statistical Analysis

Differences among the three sampling sites in inorganic N fluxes, denitrification rates and SOD measured by core incubations were tested via one-way ANOVA and pairwise multiple comparisons of means (post hoc test, Tukey's test). Normality (Shapiro–Wilk test) and homoscedasticity (Levene's test) were examined, and all datasets fulfilled the requirements for parametric tests. Statistical analysis was performed using SigmaPlot 11.0 (Systat Software, Inc., San Jose, CA, USA), and the overall significance level was set at $p \leq 0.05$.

3. Results and Discussion

3.1. Factors Controlling NO_3^- Removal via Denitrification in the Po di Goro Sediments

Nitrate fluxes were always negative, indicating that consumption from the overlying bottom water occurred in the sediments of the Po di Goro River owing to benthic processes (Figure 3a). Nitrate removal rates differed among sampling sites (Table 1), with higher values at M and G sites (on average -402 ± 169 and -397 ± 193 μmol N m^{-2} h^{-1}, respectively) than at LV site (-83 ± 41 μmol N m^{-2} h^{-1}), reflecting a decrease in water NO_3^- availability along the river–sea gradient from the fully riverine reach (~90 μM) to the outlet into the Adriatic Sea (~40 μM). Similarly, the N_2 fluxes and Dtot and Dw rates were significantly different among the three sampling sites (Figure 3a, Table 2). The highest Dtot rates were measured at the M site and were almost equivalent to the rates of N_2 production and NO_3^- consumption (422 ± 99 and -424 ± 103 μmol N m^{-2} h^{-1}, respectively), exceeding, by a factor of four on average, the rates measured at LV, the site nearest to the sea. At LV, the lowest NO_3^- availability in the water resulted in the lowest rates of N_2 production and Dtot measured for the Po di Goro sediments. The post hoc Tukey's test showed significant differences in N fluxes (NO_3^- and N_2) and denitrification rates between M and LV and between G and LV sites, but not between M and G sites (Table 2).

Nitrate fluxes measured in single cores sampled from the Po di Goro River ranged between -640 μmol N m^{-2} h^{-1} and -48 μmol N m^{-2} h^{-1} and were highly correlated with both Dw rates ($p < 0.0001$) and N_2 effluxes ($p < 0.0001$) (Figure 3b,d; Table S2). The highest consumption of NO_3^- corresponded to the highest Dw rates and also to the maximum rates of N_2 production (Figure 3b,d). The generally good correlation between NO_3^- demand and N_2 effluxes detected in all the sampled sites demonstrated that denitrification was the main process responsible for reactive N removal and was quantitatively fueled by water column NO_3^-. Anammox cannot be excluded to occur and partially contribute to N_2 effluxes. However, studies measuring denitrification and anammox simultaneously in eutrophic and organic-rich freshwater ecosystems demonstrated that the contribution of anammox to the total N_2 production was generally <10% [3,38,39], and summer appeared to be a relatively unfavorable season for anammox bacterial growth [41].

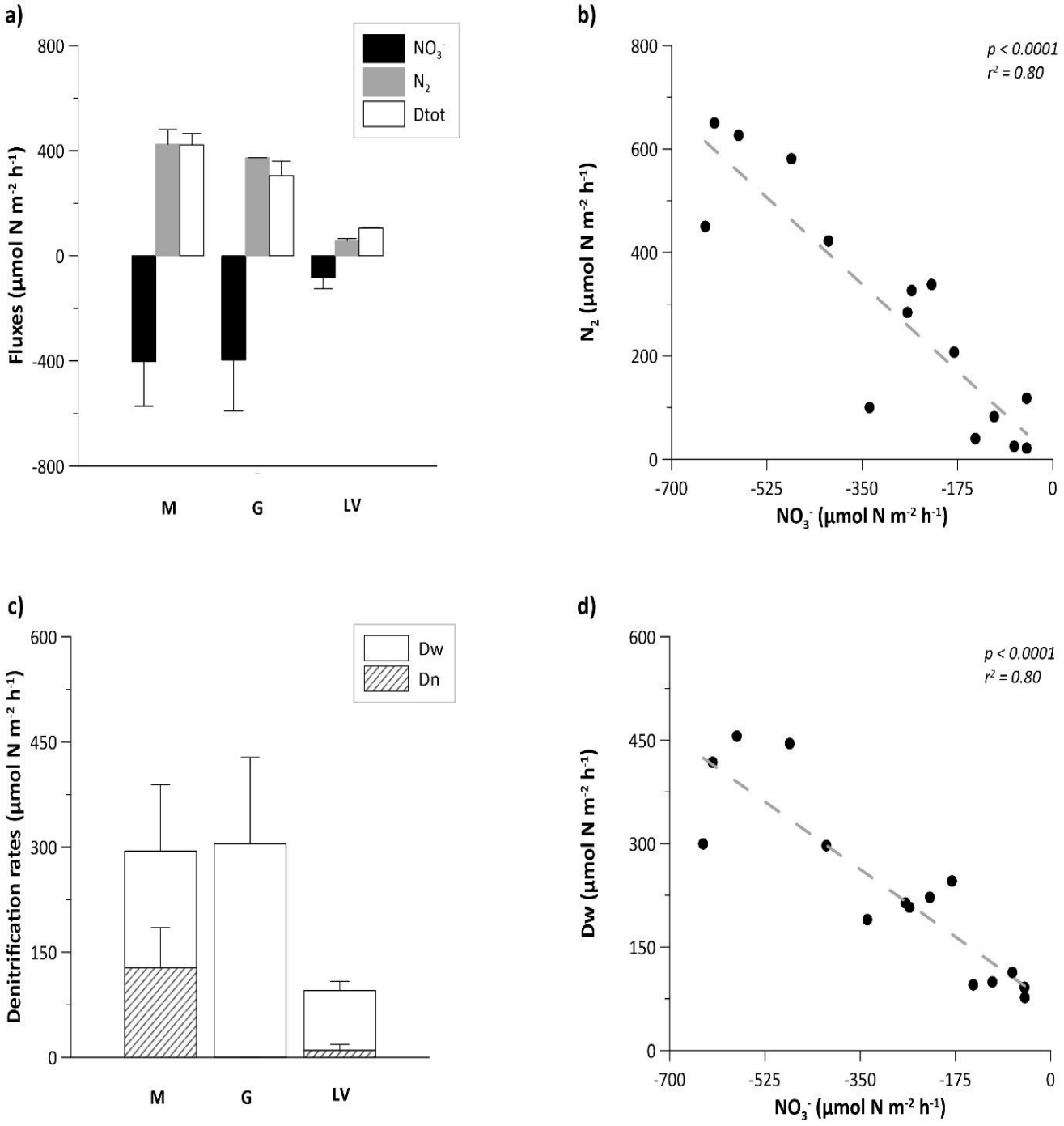

Figure 3. Benthic dark fluxes of inorganic N measured at the three sampling sites. (**a**) Fluxes of NO_3^- and N_2, and total denitrification (Dtot), (**b**) relation between fluxes of NO_3^- and N_2, (**c**) denitrification rates split into denitrification of water column NO_3^- (Dw, white bars) and denitrification coupled to nitrification in the sediment (Dn, hatched bars), (**d**) relation between fluxes of NO_3^- and Dw. In panels (**a**,**c**), average values ± standard deviations are reported, while graphs of panels (**b**,**d**) include single core measurements.

Table 2. Results of the one-way ANOVA and Tukey's test ($p < 0.05$). NS = not statistically significant).

Parameter	*p*	F	Turkey's Test
Dtot	<0.001	15.45	M vs. LV G vs. LV
Dw	<0.01	8.65	M vs. LV G vs. LV
NO_3^- flux	<0.01	7.37	M vs. LV G vs. LV
N_2 flux	<0.01	7.88	M vs. LV G vs. LV
NH_4^+ flux	NS	2.82	-
SOD	NS	0.68	-

In the Po di Goro sediment, denitrification was stimulated when NO_3^- availability in the water was greater (M) and the sediment richer in OM (G), whereas it was inhibited at the most saline site (LV). The highest rates measured at M and G reflected the occurrence of the three primary controls directly influencing denitrification, that is, availability of NO_3^- and organic carbon and anoxic environment. Nitrate and organic carbon availability, acting as terminal electron acceptor and electron supplier for denitrifying bacteria, respectively, are generally considered as the most important drivers determining the magnitude of denitrification [42]. The present outcomes were consistent with studies performed in a vast array of aquatic ecosystems demonstrating that high concentrations of NO_3^- and interstitially dissolved organic carbon, as well as low oxygen levels, in the overlying water enhance denitrification in summer [6,43]. Although NO_3^- concentrations decreased from M to G, the total denitrification rates were similar, likely resulting from a combination of factors, that is, the stimulating effect of higher sediment OM occurring at G (Table 3) together with the salinity-induced stratification. Low oxygen concentrations in the water column stimulate denitrification by reducing the distance for NO_3^- diffusion to encounter anoxic conditions in the sediment. The higher availability of labile OM occurring at G was likely a consequence of salinity-induced flocculation of the particulate organic load [44]. Sediment organic enrichment stimulates denitrification directly by providing an energy source for heterotrophic denitrifying bacteria, as well as indirectly, by fueling respiration that depletes dissolved oxygen in the benthic compartment [5,45]. A higher SOD value (~3100 μmol O_2 m^{-2} h^{-1}) appeared at G, indicating muddy–sandy sediments rich in OM (4.2%), while lower rates of oxygen consumption (~2700 μmol O_2 m^{-2} h^{-1}) were measured in sediments with lower organic enrichments (Table 3; Figure 4a; Table S2). No significant differences in SOD were observed among the sampling sites, but they overall resulted in a higher range of rates reported in the literature for freshwater eutrophic environments [21,46–48].

Table 3. Sediment characteristics at the three sampling sites of the Po di Goro River. Average values ± standard deviations are reported.

	M	G	LV
Typology	sandy	muddy–sandy	clay
Porosity	0.63 ± 0.08	0.64 ± 0.12	0.51 ± 0.04
Density (g/mL)	1.56 ± 0.17	1.14 ± 0.18	1.41 ± 0.32
OM (%)	2.00 ± 1.00	4.30 ± 0.40	1.80 ± 0.00

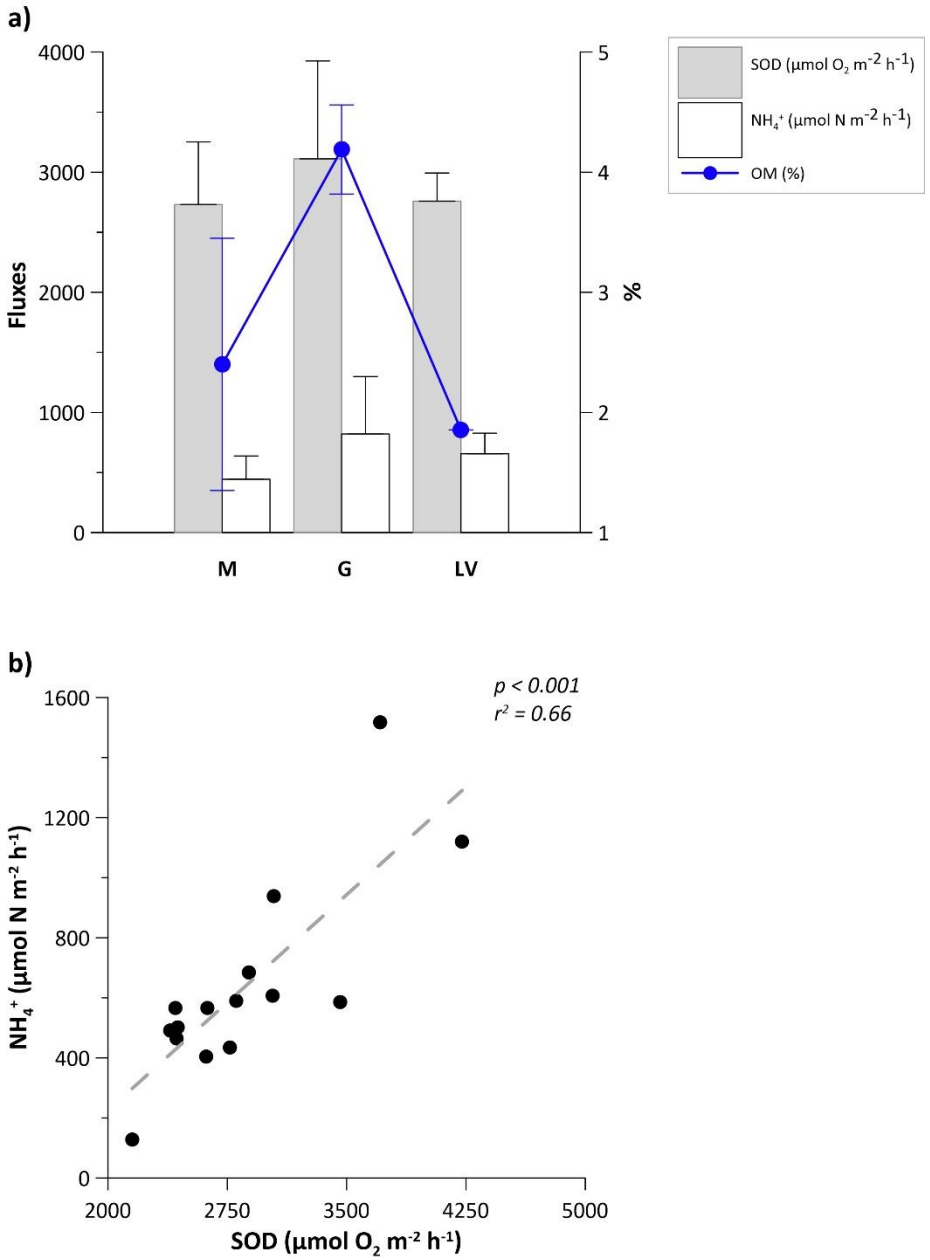

Figure 4. (**a**) Benthic dark fluxes of oxygen and NH_4^+ and sediment OM measured at the three sampling sites, (**b**) relation between dark oxygen fluxes and NH_4^+ fluxes. In panel (**a**), average values ± standard deviations are reported, while the graph of panel (**b**) includes single core measurements.

Denitrification supported by water column NO_3^- contributed mostly (70–100%) to total rates, as widely reported in the literature when water NO_3^- concentrations exceed 50−60 µM [10,21]. At all sites, sediments were simultaneously a net sink of water column NO_3^- but also a source of NH_4^+. Ammonium fluxes were always positive, indicating a production in the benthic compartment and a release to the overlying bottom water as a consequence of OM mineralization (Figure 4b; Table S2). The generally good correlation between NO_3^- and N_2 effluxes, and Dw rates (Figure 3) demonstrated that denitrification was the main process responsible for NO_3^- consumption. Dissimilatory nitrate reduction to ammonium (DNRA) cannot be excluded as a process contributing partially to NH_4^+ recycling from the sediment, especially in those sites with a higher ratio between sedimentary organic carbon and water column NO_3^-, such as G and LV. Previous studies have

demonstrated that reducing (sulfidic) conditions, such as those established in OM-rich sites, do favor DNRA over denitrification [48–50].

Denitrification coupled to nitrification was likely controlled by the limited oxygen availability at the sediment–water interface, preventing NH_4^+ oxidation, occurring as a consequence of water stratification, a typical summer condition of lowland canalized rivers and transitional environments [26,51,52]. At the G site, the bottom water was the dominant source of nitrate, accounting for 100% of the total amount required for denitrification. Here, the mineralization of the high OM content reduced the oxygen availability into the sediments, creating the anoxic conditions that prevented coupled nitrification–denitrification [48,53,54]. Conversely, coupled nitrification–denitrification was the highest at M (~130 μmol N m^{-2} h^{-1}, Figure 3c; Table S2), accounting for ~30% of the total denitrification rate, reflecting the thorough mixing of the water column and the oxygenation of the surface sediment. At the LV site, the denitrification rate was the lowest, because of the concomitant low water NO_3^- availability, increased salinity, and permanent stratification resulting in anoxic conditions in the benthic compartment. Salinity has been demonstrated to place physiological stress on bacterial communities, such as nitrifiers and denitrifiers [18]. In the sediments of transitional environments, the depletion of electron acceptors such as O_2 and NO_3^- generally leads to the dominance of sulphate reduction as a decomposition pathway accounting for a large part of the organic matter oxidation. Persistent anoxia is thus accompanied by a significant release of sulfide to the water column, a condition inhibiting nitrification and denitrification [55]. Organic enrichment and reducing conditions under persistent stratification may shift NO_3^- reduction towards more pronounced DNRA, with internal NO_3^- recycling to NH_4^+. Future research should address the concomitant measurement of denitrification and DNRA in deltaic environments to better understand the balance between N removal and N recycling processes.

3.2. Denitrification Rates in the Po di Goro: Comparison to the Literature and Relevance in Attenuating the Riverine N Loadings in Summer

The denitrification rates measured in the Po di Goro sediments were in line with those reported in the literature for estuarine and delta systems around the world with water temperatures > 20 °C (Table 4). The observed high spatial variability is typical of transitional zones where a multitude of factors are in a constant state of change, such as NO_3^- supply, rates of organic carbon sedimentation, and redox condition in the overlying water and surface sediments. The rates measured in this study for the freshwater site (M) were higher than the range of observations for nonsaline locations of other estuarine and delta systems (Table 4). This discrepancy is most likely due to the presence of a mixed NO_3^--rich water column which ensures a constant supply of NO_3^- to the benthic bioreactive surfaces where denitrification occurs. A combination of salinity-induced stratification and NO_3^- decrease plays a role in reducing the denitrification capacity along the river–sea gradient, as previously observed for other transitional environments [14,56].

In a worldwide hotspot of eutrophication and NO_3^- pollution, such as the Po River Basin, denitrification has been widely measured in several aquatic ecosystem types (e.g., wetlands, canals, lagoons, lakes), and its controlling factors diffusively investigated, resulting in the main process responsible for reactive N removal, especially in freshwater environments [20–22]. A comprehensive summary of denitrification measurements performed in the aquatic ecosystems of the Po River Basin during the summer period is presented in Figure 5. Details of the sampling locations and the main sediment and water features are reported in the Supplementary Material (Table S1). Summer denitrification was quite different among aquatic ecosystem types, with measured rates spanning along three orders of magnitude, i.e., from <2 to ~2000 μmol N m^{-2} h^{-1}. On average, the highest denitrification rates were found in aquatic environments tightly linked to the surrounding agricultural landscapes (connected wetlands and rivers), resulting in an increased availability of NO_3^- and labile organic carbon (Figure 5). The range of denitrification rates measured in the Po di Goro sediments overlapped with estimates of denitrification in

connected wetlands and rivers of the Po River Basin and was higher than those found in isolated wetlands, lakes, and coastal lagoons. Generally, denitrification rates were supported mainly by Dw in all aquatic ecosystems, with only the exception of lagoons, where sediment oxidation mediated by bioturbation contributes to stimulating coupled nitrification-denitrification [23].

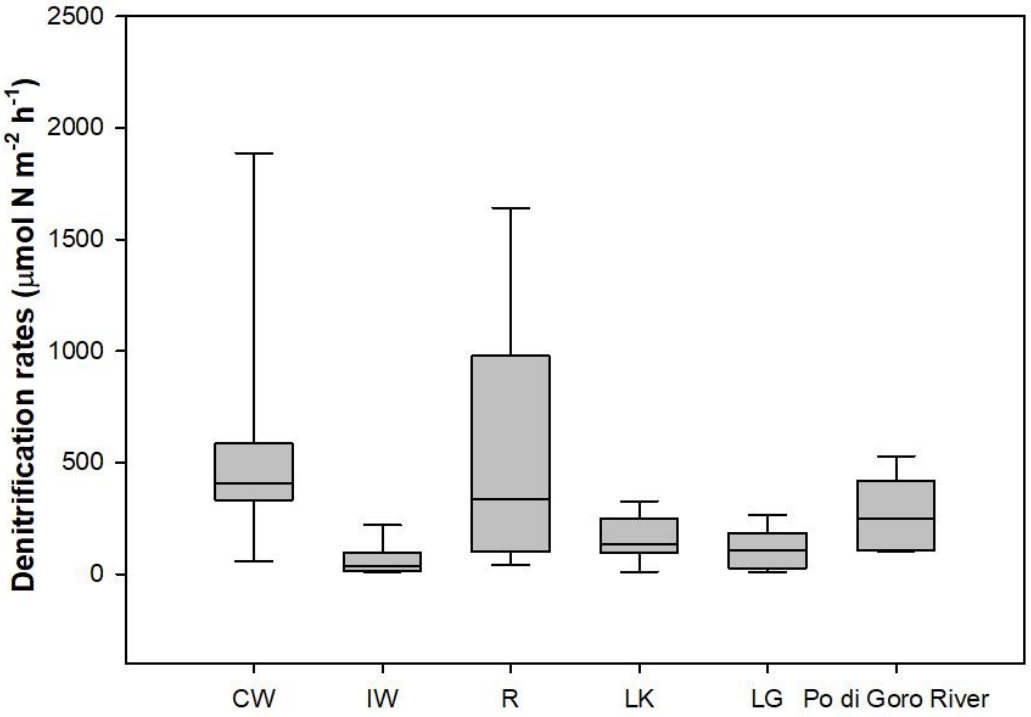

Figure 5. Boxplot on total denitrification rates measured during the period of highest temperature of the year in different aquatic ecosystems of the Po River Basin (CW, connected wetlands; IW, isolated wetlands; R, rivers; LK, lakes; LG, lagoons). The central horizontal line in the box is the median, the top and bottom boxes are 25th and 75th percentiles, and the whiskers are 10th and 90th percentiles. The employed datasets are reported in Table S1 (Supplementary Material).

Denitrification rates in the Po di Goro sediments can be addressed in a mass balance context to assess the relevance of the process at the whole-reach scale. Daily TN loadings transported by the Po di Goro River to the Adriatic Sea in middle summer varied between 1.6 and 4.8 t N day^{-1} according to different discharge values (13–35 m^3 s^{-1}) and NO_3^- was the dominant nitrogen form (on average 76–86% of TN). By extrapolating the total denitrification rates measured by sediment core incubations, the whole Po di Goro sampled reach (~7 km^2) was estimated to potentially dissipate by denitrification up to 0.94 ± 0.23 t N day^{-1}. Despite different drivers regulating denitrification at the three sampling sites, the present outcomes demonstrated that, in middle summer conditions, deltaic denitrification may remove a significant fraction, on average 28%, of the TN load transported by the Po di Goro to the Adriatic Sea, highlighting a previously underestimated role of the Po River terminal arms. Studies performed in several transitional environments around the world have estimated highly variable denitrification efficiency, contributing to removing from <10% to ~50% of the annual N loading (e.g., [57–59]). However, the rate at which this process occurs and how it affects the N supply to the coastal zones and the availability for primary producers is particularly important to address during summer periods when the eutrophication risk is higher. The present data suggest that the TN loadings, which are usually derived from river gauging above the tidal limit, overestimate, by nearly 30%, the real loadings reaching the Adriatic Sea in summer as they do not take into account the deltaic denitrification capacity. Quantitative information on N cycling in

deltaic sediments with high temporal and spatial resolution is needed to better understand how N loading from watersheds may affect eutrophication phenomena in the coastal zones.

Table 4. Total denitrification rates measured via isotope pairing technique in selected transitional environments (deltas and estuaries) around the world during the summer period. Main sediment and water features are reported for comparison with the results of this study. Standard deviations are reported.

Location	T (°C)	Salinity (‰)	NO_3^- (μM)	SOD (μmol O_2 m^{-2} h^{-1})	Dtot (μmol N m^{-2} h^{-1})	OM (%)	References
The Colne estuary (UK)	25	-	141	-	353 ± 37	-	[60]
Norsminde Fjord—shallow estuary (Denmark)	23	0.1–19.4	<1	-	106 ± 1	-	[61]
	23		2		153 ± 28		
Neuse River (North Carolina)	29	-	11	681 ± 88	8	-	[62]
	29		17	256 ± 177	73		
	26		24	647 ± 411	143		
	29		38	1187 ± 143	51		
	24.5		32	791 ± 136	19		
Wax Lake Delta (Louisiana)	30	0.1–0.4	58	1186 ± 143	41 ± 2	2	[15]
Barataria Bay (Louisiana)	30	0.1–0.4	45	1527 ± 451	42 ± 10	2	
Nueces River (Texas)	30	0.29	67	736 ± 2	27 ± 6	-	[63]
Corpus Christi Bay (Texas)	32.3	1.94	2	1077 ± 70	7 ± 1	-	
Thames estuary–Site 1 (UK)	-	2–32	611	3113 ± 184	4826 ± 395	4	[56]
Site 2	-	2–32	*	2884 ± 538	146 ± 28	2	
Site 3	-	2–32	*	5384 ± 186	140 ± 33	2	
Site 4	-	2–32	*	5486 ± 504	175 ± 55	3	
Site 5	-	2–32	*	4379 ± 914	462 ± 68	3	
Site 6	-	2–32	*	3680 ± 413	103 ± 9	1	
Wax Lake Delta (Louisiana)	27.3	0.2	64	1833	397	5	[64]
	19	0.2–0.4	98	1042 ± 0	115 ± 7	3	[14]
	22.2	0.2–0.4	102	1953 ±130	87 ± 5	6	
	21.2	0.2–0.4	82	3646 ± 130	230 ± 10	22	
Mildred Island (Suisun Delta, USA)	22.2	0.1	-	1160 ± 130	20	-	[19]
Franks (Suisun Delta, USA)	22	0.1	-	1490 ± 55	48 ± 3	-	
Big Break (Suisun Delta, USA)	21.5	0.1	-	1062 ± 32	21 ± 11	-	
Sherman Island (Suisun Delta, USA)	21	0.2	-	947 ± 98	71 ± 12	-	
Brown (Suisun Bay, USA)	21	0.4	-	1490 ± 250	53 ± 5	-	
Po di Goro (Mesola)	25	0.2	89	2731 ± 521	422 ± 99	2	This study
Po di Goro (Conca Gorino)	25	11.2	61	3111 ± 815	305 ± 123	4.3	
Po di Goro (Lanterna Vecchia)	25	18.1	71	2759 ± 234	105 ± 5	1.8	

* Nitrate concentration decreased along the river–sea gradient.

4. Conclusions

Benthic denitrification in the Po delta sediments was a net sink of N, which accounted for a significant reduction in TN loading to the coastal zone. These outcomes underscore the role of the terminal branches of the Po River delta, previously underestimated, as a buffering system as a whole, against summer N loadings and for the protection of coastal areas, right when eutrophication risk is the highest. Sedimentary regeneration of NH_4^+ was measured at all stations and partially counterbalanced N losses via denitrification. This positive

contribution to the generation of reactive N was unexpectedly high and requires further investigation. Knowledge of spatial and temporal variability and the relative importance of contrasting paths of the N cycle, such as denitrification and ammonia regeneration in deltaic sediments, is a key point for the definition of effective interventions to mitigating NO_3^- pollution and coastal eutrophication.

These preliminary findings need to be progressed both at the microscale (e.g., assessment of environmental drivers controlling benthic N dynamics) and at the whole-reach scale. Moreover, investigating the effects of increasing water temperature and saline intrusion on denitrification as consequences of global warming is of great interest for future studies on the buffering capacity against N loadings in deltaic ecosystems.

Supplementary Materials: The following are available online at https://www.mdpi.com/article/10.3390/w14030501/s1. Figure S1: Relation between the discharge (Q) of the Po River measured at Pontelagoscuro station and the percentage transported by the Po di Goro branch. Table S1: Total denitrification rates measured via isotope pairing technique in different aquatic ecosystems of the Po River Basin during the period of highest temperature of the year (CW, connected wetlands; IW, isolated wetlands; R, rivers; LK, lakes; LG, lagoons). Table S2: Summary of benthic fluxes and denitrification rates measured in the Po di Goro.

Author Contributions: Conceptualization, M.P.G., E.S. and G.C.; methodology, E.S. and G.C.; investigation, M.P.G., E.S., F.V. and G.C.; resources, F.V.; formal analysis, M.P.G.; writing—original draft preparation, M.P.G.; writing—review and editing, E.S. and G.C.; visualization, M.P.G.; funding acquisition, G.C.; supervision, G.C. All authors read and agreed to the published version of the manuscript.

Funding: This work was financially supported by the EU LIFE Project AGREE (coAstal laGoon long-teRm managEmEnt) (LIFE13 NAT/IT/000115), by the Po River District Authority within the research program "Origin and dynamics of the nutrient loadings delivered by the Po River and other basins flowing into the Adriatic Sea" and by the local water authority, Consorzio di Bonifica Pianura di Ferrara, within a collaboration aiming at defining management strategies for the control of eutrophication in the Po River Delta.

Data Availability Statement: Data collected by the Regional Environmental Protection Agency of the Emilia-Romagna region are available online at https://dati.arpae.it/ and https://simc.arpae.it/dext3r.

Acknowledgments: The authors would like to thank Marco Bartoli (University of Parma, Italy) for providing incubation devices, and Mattia Lanzoni and Luca Bellini for their help during the sampling campaign.

Conflicts of Interest: The authors declare no conflict of interest.

References

1. Glibert, P.M.; Harrison, J.; Heil, C.; Seitzinger, S. Escalating worldwide use of urea–a global change contributing to coastal eutrophication. *Biogeochemistry* **2006**, *77*, 441–463. [CrossRef]
2. Howarth, R.W.; Marino, R. Nitrogen as the limiting nutrient for eutrophication in coastal marine ecosystems: Evolving views over three decades. *Limnol. Oceanogr.* **2006**, *51*, 364–376. [CrossRef]
3. Zhou, S.; Borjigin, S.; Riya, S.; Terada, A.; Hosomi, M. The relationship between anammox and denitrification in the sediment of an inland river. *Sci. Total Environ.* **2014**, *490*, 1029–1036. [CrossRef]
4. Li, J.; Yu, S.; Qin, S. Removal capacities and environmental constrains of denitrification and anammox processes in eutrophic riverine sediments. *Water Air Soil Pollut.* **2020**, *231*, 1–16. [CrossRef]
5. Cornwell, J.C.; Kemp, W.M.; Kana, T.M. Denitrification in coastal ecosystems: Methods, environmental controls, and ecosystem level controls, a review. *Aquat. Ecol.* **1999**, *33*, 41–54. [CrossRef]
6. Piña-Ochoa, E.; Álvarez-Cobelas, M. Denitrification in Aquatic Environments: A Cross-system Analysis. *Biogeochemistry* **2006**, *81*, 111–130. [CrossRef]
7. Birgand, F.; Skaggs, R.W.; Chescheir, G.M.; Gilliam, J.W. Nitrogen removal in streams of agricultural catchments—A literature review. *Crit. Rev. Environ. Sci. Technol.* **2007**, *37*, 381–487. [CrossRef]
8. Zhu, G.; Wang, S.; Zhou, L.; Wang, Y.; Zhao, S.; Xia, C.; Wang, W.; Zhou, R.; Wang, C.; Jetten, M.S.M.; et al. Ubiquitous anaerobic ammonium oxidation in inland waters of China: An overlooked nitrous oxide mitigation process. *Sci. Rep.* **2015**, *5*, 1–10. [CrossRef]

9. Chen, H.; Zhang, B.; Yu, C.; Zhang, Z.; Yao, J.; Jin, R. The effects of magnetite on anammox performance: Phenomena to mechanisms. *Bioresour. Technol.* **2021**, *337*, 125470. [CrossRef]
10. Seitzinger, S.; Harrison, J.A.; Böhlke, J.K.; Bouwman, A.F.; Lowrance, R.; Peterson, B.; Tobias, C.; Drecht, G.V. Denitrification across landscapes and waterscapes: A synthesis. *Ecol. Appl.* **2006**, *16*, 2064–2090. [CrossRef]
11. Peterson, B.J.; Wollheim, W.M.; Mulholland, P.J.; Webster, J.R.; Meyer, J.L.; Tank, J.L.; Martì, E.; Bowden, W.B.; Valett, H.M.; Hershey, A.E.; et al. Control of nitrogen export from watersheds by headwater streams. *Science* **2001**, *292*, 86–90. [CrossRef]
12. Herrman, K.S.; Bouchard, V.; Moore, R.H. Factors affecting denitrification in agricultural headwater streams in Northeast Ohio, USA. *Hydrobiologia* **2008**, *598*, 305–314. [CrossRef]
13. Alexander, R.B.; Smith, R.A.; Schwarz, G.E. Effect of stream channel size on the delivery of nitrogen to the Gulf of Mexico. *Nature* **2000**, *403*, 758–761. [CrossRef] [PubMed]
14. Li, S.; Twilley, R.R. Nitrogen dynamics of inundated sediments in an emerging coastal deltaic floodplain in mississippi river delta using isotope pairing technique to test response to nitrate enrichment and sediment organic matter. *Estuaries Coasts* **2021**, *44*, 1899–1915. [CrossRef]
15. Upreti, K.; Rivera-Monroy, V.H.; Maiti, K.; Giblin, A.; Geaghan, J.P. Emerging wetlands from river diversions can sustain high denitrification rates in a coastal delta. *J. Geophys. Res. Biogeosci.* **2021**, *126*, e2020JG006217. [CrossRef]
16. Seo, D.C.; Yu, K.; Delaune, R.D. Influence of salinity level on sediment denitrification in a Louisiana estuary receiving diverted Mississippi River water. *Arch. Agron. Soil Sci.* **2008**, *54*, 249–257. [CrossRef]
17. Giblin, A.E.; Weston, N.B.; Banta, G.T.; Tucker, J.; Hopkinson, C.S. The effects of salinity on nitrogen losses from an oligohaline estuarine sediment. *Estuaries Coasts* **2010**, *33*, 1054–1068. [CrossRef]
18. Rysgaard, S.; Thastum, P.; Dalsgaard, T.; Christensen, P.B.; Sloth, N.P. Effects of salinity on NH_4^+ adsorption capacity, nitrification, and denitrification in Danish estuarine sediments. *Estuaries* **1999**, *22*, 21–30. [CrossRef]
19. Cornwell, J.C.; Glibert, P.M.; Owens, M.S. Nutrient fluxes from sediments in the San Francisco Bay Delta. *Estuaries Coasts* **2014**, *37*, 1120–1133. [CrossRef]
20. Pinardi, M.; Bartoli, M.; Longhi, D.; Viaroli, P. Net autotrophy in a fluvial lake: The relative role of phytoplankton and floating-leaved macrophytes. *Aquat. Sci.* **2011**, *73*, 389–403. [CrossRef]
21. Racchetti, E.; Bartoli, M.; Soana, E.; Longhi, D.; Christian, R.R.; Pinardi, M.; Viaroli, P. Influence of hydrological connectivity of riverine wetlands on nitrogen removal via denitrification. *Biogeochemistry* **2011**, *103*, 335–354. [CrossRef]
22. Castaldelli, G.; Soana, E.; Racchetti, E.; Vincenzi, F.; Fano, E.A.; Bartoli, M. Vegetated canals mitigate nitrogen surplus in agricultural watersheds. *Agric. Ecosyst. Environ.* **2015**, *212*, 253–262. [CrossRef]
23. Magri, M.; Benelli, S.; Bonaglia, S.; Zilius, M.; Castaldelli, G.; Bartoli, M. The effects of hydrological extremes on denitrification, dissimilatory nitrate reduction to ammonium (DNRA) and mineralization in a coastal lagoon. *Sci. Total Environ.* **2020**, *740*, 140169. [CrossRef] [PubMed]
24. Environmental Protection Agency of the Veneto Region. Distribution of Flows Among the Branches of the Po River and the outlets of the Po Delta Po: Historical Experiences and New Investigations During the 2011. Relation n° 2/12. In Italian. 2012. Available online: https://www.arpa.veneto.it/temi-ambientali/idrologia/approfondimenti/lidrologia-del-delta-del-po (accessed on 23 October 2021).
25. Viaroli, P.; Giordani, G.; Bartoli, M.; Naldi, M.; Azzoni, R.; Nizzoli, D.; Ferrari, I.; Comenges, J.M.Z.; Bencivelli, S.; Castaldelli, G.; et al. The sacca di Goro lagoon and an arm of the Po river. In *Estuaries*; Springer: Berlin/Heidelberg, Germany, 2006; pp. 197–232. [CrossRef]
26. Maicu, F.; Alessandri, J.; Pinardi, N.; Verri, G.; Umgiesser, G.; Lovo, S.; Turolla, S.; Paccagnella, T.; Valentini, A. Downscaling with an unstructured coastal-ocean model to the Goro Lagoon and the Po River Delta branches. *Front. Mar. Sci.* **2021**, *8*, 647781. [CrossRef]
27. Grilli, F.; Accoroni, S.; Acri, F.; Bernardi Aubry, F.; Bergami, C.; Cabrini, M.; Campanelli, A.; Giani, M.; Guicciardi, S.; Marini, M.; et al. Seasonal and interannual trends of oceanographic parameters over 40 years in the Northern Adriatic Sea in relation to nutrient loadings using the EMODnet Chemistry Data portal. *Water* **2020**, *12*, 2280. [CrossRef]
28. Dalsgaard, T.; Nielsen, L.P.; Brotas, V.; Viaroli, P.; Underwood, G.; Nedwell, D.; Sundback, K.; Rysgaard, S.; Miles, A.; Bartoli, M.; et al. *Protocol Handbook for NICE-Nitrogen Cycling in Estuaries: A Project under the EU Research Programme: Marine Science and Technology (MAST III)*; Ministry of Environment and Energy National Environmental Research Institute, Denmark© Department of Lake and Estuarine Ecology: Silkeborg, Denmark, 2000; pp. 1–62.
29. Owens, M.S.; Cornwell, J.C. The benthic exchange of O_2, N_2 and dissolved nutrients using small core incubations. *JoVE J. Vis. Exp.* **2016**, *114*, e54098. [CrossRef]
30. Nielsen, L.P. Denitrification in sediment determined from nitrogen isotope pairing. *FEMS Microbiol. Lett.* **1992**, *86*, 357–362. [CrossRef]
31. Golterman, H.L.; Clymo, R.S.; Ohnstand, M.A.M. Methods for physical and chemical analysis of fresh waters, I.B.P. In *Handbook Nr. 8*; Blackwell: Oxford, MS, USA, 1978.
32. Bower, C.E.; Holm-Hansen, T. A salicylate–hypochlorite method for determining ammonia in seawater. *Can. J. Fish. Aquat. Sci.* **1980**, *37*, 794–798. [CrossRef]

33. Armstrong, F.A.J.; Stearns, C.R.; Strickland, J.D.H. The measurement of upwelling and subsequent biological process by means of the Technicon Autoanalyzer® and associated equipment. In *Deep Sea Research and Oceanographic Abstracts*; Elsevier: Amsterdam, The Netherlands, 1967; Volume 14, pp. 381–389. [CrossRef]
34. Kana, T.M.; Darkangelo, C.; Hunt, M.D.; Oldham, J.B.; Bennett, G.E.; Cornwell, J.C. Membrane inlet mass spectrometer for rapid high-precision determination of N_2, O_2, and Ar in environmental water samples. *Anal. Chem.* **1994**, *66*, 4166–4170. [CrossRef]
35. Lunstrum, A.; Aoki, L.R. Oxygen interference with membrane inlet mass spectrometry may overestimate denitrification rates calculated with the isotope pairing technique. *Limnol. Oceanogr. Methods* **2016**, *14*, 425–431. [CrossRef]
36. Eyre, B.D.; Rysgaard, S.; Dalsgaard, T.; Christensen, P.B. Comparison of isotope pairing and N_2:Ar methods for measuring sediment denitrification—assumption, modifications, and implications. *Estuaries* **2002**, *25*, 1077–1087. [CrossRef]
37. Weiss, R.F. The solubility of nitrogen, oxygen and argon in water and seawater. In *Deep Sea Research and Oceanographic Abstracts*; Elsevier: Amsterdam, The Netherlands, 1970; Volume 17, pp. 721–735. [CrossRef]
38. Burgin, A.J.; Hamilton, S.K. Have we overemphasized the role of denitrification in aquatic ecosystems? A review of nitrate removal pathways. *Front. Ecol. Environ.* **2007**, *5*, 89–96. [CrossRef]
39. Koop-Jakobsen, K.; Giblin, A.E. Anammox in tidal marsh sediments: The role of salinity, nitrogen loading, and marsh vegetation. *Estuaries Coasts* **2009**, *32*, 238–245. [CrossRef]
40. APAT, IRSA/CNR. Analytical Methods for Water Analysis. 2003. Available online: https://www.isprambiente.gov.it/it/pubblicazioni/manuali-e-linee-guida/metodi-analitici-per-le-acque (accessed on 4 August 2021), ISBN 88-448-0083-7.
41. Hamersley, M.R.; Woebken, D.; Boehrer, B.; Schultze, M.; Lavik, G.; Kuypers, M.M. Water column anammox and denitrification in a temperate permanently stratified lake (Lake Rassnitzer, Germany). *Syst. Appl. Microbiol.* **2009**, *32*, 571–582. [CrossRef]
42. Wallenstein, M.D.; Myrold, D.D.; Firestone, M.; Voytek, M. Environmental controls on denitrifying communities and denitrification rates: Insights from molecular methods. *Ecol. Appl.* **2006**, *16*, 2143–2152. [CrossRef]
43. Dong, L.F.; Sobey, M.N.; Smith, C.J.; Rusmana, I.; Phillips, W.; Stott, A.; Nedwell, D.B. Dissimilatory reduction of nitrate to ammonium, not denitrification or anammox, dominates benthic nitrate reduction in tropical estuaries. *Limnol. Oceanogr.* **2011**, *56*, 279–291. [CrossRef]
44. Asmala, E.; Bowers, D.G.; Autio, R.; Kaartokallio, H.; Thomas, D.N. Qualitative changes of riverine dissolved organic matter at low salinities due to flocculation. *J. Geophys. Res. Biogeosci.* **2014**, *119*, 1919–1933. [CrossRef]
45. Rysgaard, S.; Christensen, P.B.; Nielsen, L.P. Seasonal variation in nitrification and denitrification in estuarine sediment colonized by benthic microalgae and bioturbating infauna. *Mar. Ecol. Prog. Ser.* **1995**, *126*, 111–121. [CrossRef]
46. Christensen, P.B.; Nielsen, L.P.; Sørensen, J.; Revsbech, N.P. Denitrification in nitrate-rich streams: Diurnal and seasonal variation related to benthic oxygen metabolism. *Limnol. Oceanogr.* **1990**, *35*, 640–651. [CrossRef]
47. Seitzinger, S.P. Linkages between organic matter mineralization and denitrification in eight riparian wetlands. *Biogeochemistry* **1994**, *25*, 19–39. [CrossRef]
48. Scott, J.T.; McCarthy, M.J.; Gardner, W.S.; Doyle, R.D. Denitrification, dissimilatory nitrate reduction to ammonium, and nitrogen fixation along a nitrate concentration gradient in a created freshwater wetland. *Biogeochemistry* **2008**, *87*, 99–111. [CrossRef]
49. Nizzoli, D.; Carraro, E.; Nigro, V.; Viaroli, P. Effect of organic enrichment and thermal regime on denitrification and dissimilatory nitrate reduction to ammonium (DNRA) in hypolimnetic sediments of two lowland lakes. *Water Res.* **2010**, *44*, 2715–2724. [CrossRef] [PubMed]
50. Jiang, X.; Gao, G.; Zhang, L.; Tang, X.; Shao, K.; Hu, Y. Denitrification and dissimilatory nitrate reduction to ammonium in freshwater lakes of the Eastern Plain, China: Influences of organic carbon and algal bloom. *Sci. Total Environ.* **2020**, *710*, 136303. [CrossRef] [PubMed]
51. Wang, X.; Hu, M.; Ren, H.; Li, J.; Tong, C.; Musenze, R.S. Seasonal variations of nitrous oxide fluxes and soil denitrification rates in subtropical freshwater and brackish tidal marshes of the Min River estuary. *Sci. Total Environ.* **2018**, *616*, 1404–1413. [CrossRef]
52. Yang, D.; Wang, D.; Chen, S.; Ding, Y.; Gao, Y.; Tian, H.; Chen, Z. Denitrification in urban river sediment and the contribution to total nitrogen reduction. *Ecol. Indic.* **2021**, *120*, 106960. [CrossRef]
53. Sigman, D.M.; Robinson, R.; Knapp, A.N.; Van Geen, A.; McCorkle, D.C.; Brandes, J.A.; Thunell, R.C. Distinguishing between water column and sedimentary denitrification in the Santa Barbara Basin using the stable isotopes of nitrate. *Geochem. Geophys. Geosyst.* **2003**, *4*, 1040. [CrossRef]
54. Dong, L.F.; Thornton, D.C.O.; Nedwell, D.B.; Underwood, G.J.C. Denitrification in sediments of the River Colne estuary, England. *Mar. Ecol. Prog. Ser.* **2000**, *203*, 109–122. [CrossRef]
55. Murphy, A.E.; Bulseco, A.N.; Ackerman, R.; Vineis, J.H.; Bowen, J.L. Sulphide addition favours respiratory ammonification (DNRA) over complete denitrification and alters the active microbial community in salt marsh sediments. *Environ. Microbiol.* **2020**, *22*, 2124–2139. [CrossRef]
56. Trimmer, M.; Nedwell, D.B.; Sivyer, D.B.; Malcolm, S.J. Seasonal benthic organic matter mineralisation measured by oxygen uptake and denitrification along a transect of the inner and outer River Thames estuary, UK. *Mar. Ecol. Prog. Ser.* **2000**, *197*, 103–119. [CrossRef]
57. Seitzinger, S.P. Denitrification in freshwater and coastal marine ecosystems: Ecological and geochemical significance. *Limnol. Oceanogr.* **1988**, *33*, 702–724. [CrossRef]
58. Nowicki, B.L.; Kelly, J.R.; Requintina, E.; Van Keuren, D. Nitrogen losses through sediment denitrification in Boston Harbor and Massachusetts Bay. *Estuaries* **1997**, *20*, 626–639. [CrossRef]

59. Fear, J.M.; Thompson, S.P.; Gallo, T.E.; Paerl, H.W. Denitrification rates measured along a salinity gradient in the eutrophic Neuse River Estuary, North Carolina, USA. *Estuaries* **2005**, *28*, 608–619. [CrossRef]
60. Ogilvie, B.; Nedwell, D.B.; Harrison, R.M.; Robinson, A.; Sage, A. High nitrate, muddy estuaries as nitrogen sinks: The nitrogen budget of the River Colne estuary (United Kingdom). *Mar. Ecol. Prog. Ser.* **1997**, *150*, 217–228. [CrossRef]
61. Nielsen, K.; Nielsen, L.P.; Rasmussen, P. Estuarine nitrogen retention independently estimated by the denitrification rate and mass balance methods: A study of Norsminde Fjord, Denmark. *Mar. Ecol. Prog. Ser.* **1995**, *119*, 275–283. [CrossRef]
62. Whalen, S.C.; Alperin, M.J.; Nie, Y.; Fischer, E.N. Denitrification in the mainstem Neuse River and tributaries, USA. *Fundam. Appl. Limnol.* **2008**, *171*, 249–261. [CrossRef]
63. Bernot, M.J.; Dodds, W.K.; Gardner, W.S.; McCarthy, M.J.; Sobolev, D.; Tank, J.L. Comparing denitrification estimates for a Texas estuary by using acetylene inhibition and membrane inlet mass spectrometry. *Appl. Environ. Microbiol.* **2003**, *69*, 5950–5956. [CrossRef]
64. Li, S.; Twilley, R.R.; Hou, A. Heterotrophic nitrogen fixation in response to nitrate loading and sediment organic matter in an emerging coastal deltaic floodplain within the Mississippi River Delta plain. *Limnol. Oceanogr.* **2021**, *66*, 1961–1978. [CrossRef]

Paper V: Gervasio, M. P., Soana, E., Vincenzi, F., Magri, M., & Castaldelli, G. (2023). Drought-Induced Salinity Intrusion Affects Nitrogen Removal in a Deltaic Ecosystem (Po River Delta, Northern Italy). *Water*, 15(13), 2405. https://doi.org/10.3390/w15132405

water

MDPI

Article

Drought-Induced Salinity Intrusion Affects Nitrogen Removal in a Deltaic Ecosystem (Po River Delta, Northern Italy)

Maria Pia Gervasio [1], Elisa Soana [1,*], Fabio Vincenzi [1], Monia Magri [2] and Giuseppe Castaldelli [1]

[1] DiSAP—Department of Environmental and Prevention Sciences, University of Ferrara, Via L. Borsari 46, 44121 Ferrara, Italy; grvmrp@unife.it (M.P.G.); fabio.vincenzi@unife.it (F.V.); ctg@unife.it (G.C.)
[2] Department of Chemistry, Life Sciences and Environmental Sustainability, University of Parma, Parco Area delle Scienze 33/A, 43124 Parma, Italy; monia.magri@unipr.it
* Correspondence: elisa.soana@unife.it

Abstract: In the summer of 2022, the Po River Delta (Northern Italy), a eutrophication hotspot, was severely affected by high temperatures, exceptional lack of rainfall and saline water intrusion. The effect of saline intrusion on benthic nitrogen dynamics, and in particular the N removal capacity, was investigated during extreme drought conditions. Laboratory incubations of intact sediment cores were used to determine denitrification and DNRA rates at three sites along a salinity gradient in the Po di Goro, an arm of the Po River Delta. Denitrification was found to be the main process responsible for nitrate reduction in freshwater and slightly saline sites, whereas DNRA predominated in the most saline site, highlighting a switch in N cycling between removal and recycling. These results provide evidence that salinity is a key factor in regulating benthic N metabolism in transitional environments. In a climate change scenario, salinity intrusion, resulting from long periods of low river discharge, may become an unrecognized driver of coastal eutrophication by promoting the dissimilatory nitrate reduction to ammonium and N recycling of bioactive nitrogen within the ecosystem, rather than its permanent removal by denitrification.

Keywords: saline intrusion; climate change; denitrification; DNRA; eutrophication; Po River Delta

Citation: Gervasio, M.P.; Soana, E.; Vincenzi, F.; Magri, M.; Castaldelli, G. Drought-Induced Salinity Intrusion Affects Nitrogen Removal in a Deltaic Ecosystem (Po River Delta, Northern Italy). *Water* **2023**, *15*, 2405. https://doi.org/10.3390/w15132405

Received: 4 May 2023
Revised: 16 June 2023
Accepted: 27 June 2023
Published: 29 June 2023

1. Introduction

Rivers draining highly exploited agricultural basins export large amounts of reactive nitrogen (N) to coastal waters, which may cause eutrophication in lagoonal and marine ecosystems [1–3]. In transitional environments, multiple biogeochemical reactions transform, temporarily retain, or permanently remove N species [4–7]. Sharp gradients of labile carbon, oxygen, salinity, and nutrients result in a continuously variable coupling among microbial reactions which, in turn, regulate N fate. Indeed, one of the most recognized ecosystem services of transitional environments is their ability to improve water quality, acting as biogeochemical filters that mitigate anthropogenic impacts on coastal environments by preventing excessive nutrient inputs [5,7].

Sediments are highly active sites for N cycling, especially for N removal through the coupled nitrification–denitrification process. Under favorable conditions, heterotrophic denitrification is the main sink for bioavailable N, resulting in its permanent N removal in the aquatic ecosystems via the reduction of N from nitrate (NO_3^-) to dinitrogen gas (N_2), which is released into the atmosphere [8–10]. Nitrification, the two-step chemoautotrophic oxidation of ammonium (NH_4^+) to nitrite (NO_2^-) and NO_3^-, provides oxidized substrates for denitrification [11]. The dissimilatory nitrate reduction to ammonium (DNRA), using the same substrates of denitrification (NO_3^- and organic carbon) can be an alternative microbial pathway for NO_3^- reduction. However, the first process removes the bioavailable N from the ecosystem, while the second recycles it [12]. Nitrification, denitrification and DNRA are functionally linked, and investigating their regulation drivers in coastal sediments is crucial to understanding the role of environmental stressor in the N biogeochemical processes.

The functioning of transitional environments is currently threatened by the interaction of eutrophication and climate change [13]. Climate change has been identified as one of the major challenges facing humanity in the 21st century, and the Mediterranean region is particularly vulnerable. Here, the IPCC Report (2022) [14] predicts a reduction in precipitation of up to 20% and an increase in the periodicity of droughts and extreme storm events [15,16]. By affecting the water temperature regime and the hydrodynamism of water masses, climate change not only shapes the timing and entity of N loads but may also affect their transformation and reduction in transitional environments, ultimately altering the capacity of these ecosystems to act as a natural N filters. Prolonged periods of elevated water temperature combined with low river discharge may increase water residence time, stratification, and saline intrusion and, hence, the extent of hypoxia or anoxia in bottom water and sediments [17–20]. Salinity, together with temperature and the availability of NO_3^- and organic carbon, is one of the main environmental factors regulating the partitioning between denitrification and DNRA. Therefore, saline intrusion caused by climate change may have a profound effect on N speciation and processing. In particular, salinity inhibits the activity of nitrifiers, thereby reducing the availability of NO_3^- for the denitrification process [21]. Conversely, DNRA has been shown to outcompete denitrification in organic-rich sediments during periods of summer saltwater intrusion [20,22,23] by enhancing NH_4^+ production. Thus, salinization can alter the dominant biogeochemical processes and the ability to provide the key ecosystem service of coastal N filtering [24].

The Po River Basin, an area of intense human activity with the fundamental role in the agricultural and industrial sectors in Italy, is a NO_3^- pollution hotspot, causing severe eutrophication in the north-western Adriatic coast. The Po Delta has recently been identified as a buffer zone for NO_3^- loads via denitrification during the summer season, the main sensitive period for eutrophication, due to the warm temperature [25]. However, this capacity may be threatened by climate change, the effects of which (e.g., increased frequency of droughts, temperature warming, and saline intrusion) have already been observed in the Po Basin over the last twenty years [25–27]. In particular, the extreme drought of spring and summer 2022 in the Po Delta determined a persistent saline intrusion along the branches of the Po River [27], which could alter the proportion of NO_3^- dissimilated by denitrification or by DNRA. The study of this partitioning of NO_3^- consumption, despite its great ecological importance, has not yet been adequately addressed.

The aim of the present study was to assess the effects of the summer saline intrusion of 2022 on the N cycling in the sediments of the Po Delta. Denitrification and DNRA rates were measured along a salinity gradient in the Po di Goro, the southernmost arm of the Po River and representative of the whole Po Delta and other transitional ecosystems increasingly affected by climate change-related phenomena.

2. Materials and Methods

2.1. Area of Study

The Po di Goro is the southernmost of the five branches of the Po River Delta, originating near the town of Serravalle (province of Ferrara) and marking the border between the Emilia-Romagna and Veneto regions as far as the Adriatic Sea (Figure 1). Its average summer discharge represents approximately 15% of the flow of the Po River, which is monitored at Pontelagoscuro (Ferrara, Italy) at the closing section of the Po River Basin [26]. The Po di Goro is one of the main freshwater inputs to the Sacca di Goro (26 km^2), the southernmost lagoon of the Po Delta, identified as the most important European site for the production of Manila clam. Since the 1980s, the lagoon has suffered from macroalgal blooms due to excessive nutrient loads, causing summer anoxic crises and dystrophic outbreaks [27].

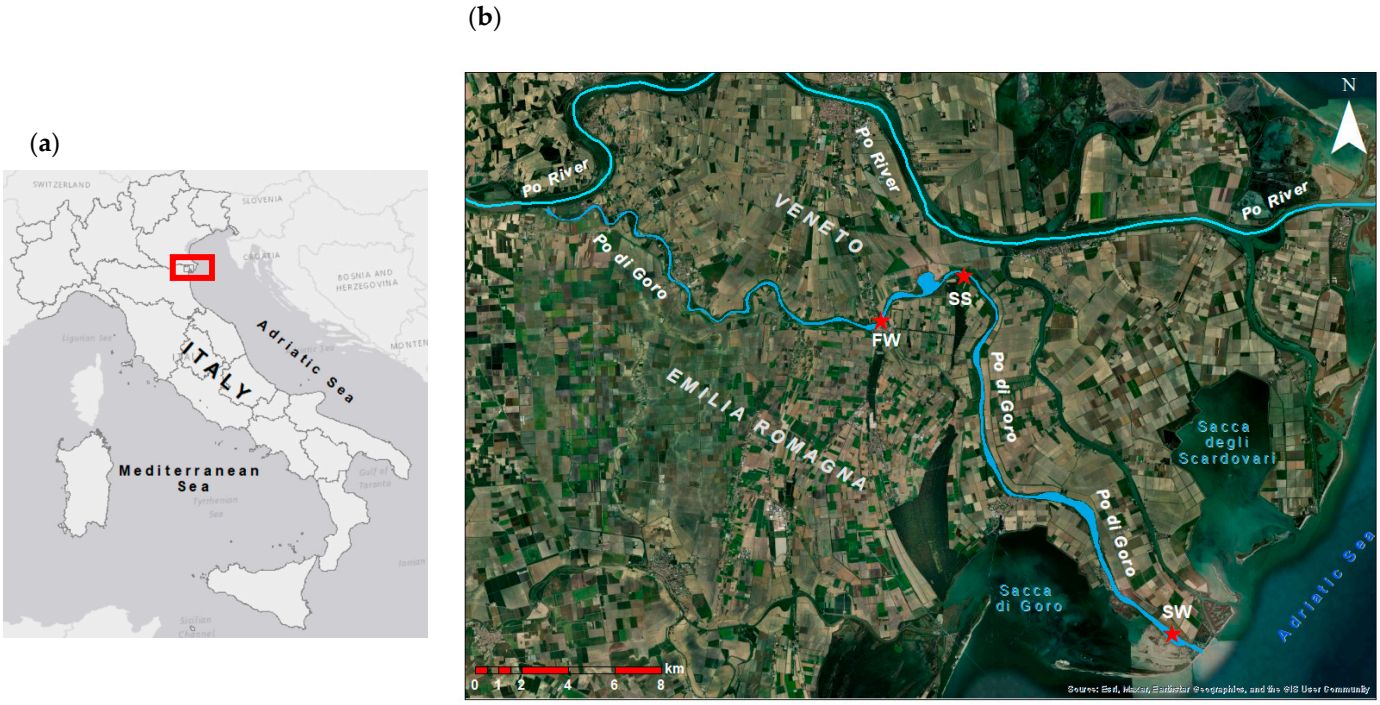

Figure 1. (**a**) The area of the study was situated in the Po River Delta (Northern Italy), indicated with a red square; (**b**) Po di Goro River and three sampling sites (red stars): freshwater site (FW), sightly saline site (SS), and saline water site (SW); (base map of ArcMap 10.8.2).

2.2. Sediment and Water Sampling

The sediment cores were taken on 28th June 2022, when the Po River was already in an extreme drought and the average water temperature (28 ± 1 °C) was significantly higher than in the previous summer (25 ± 0.5 °C) [7]. The lack of rainfall and the consequent reduction in the flow of the Po River caused a deep and persistent saline intrusion into the delta, extending the mixing zone between freshwater and seawater [28]. Three sampling sites (Figure 1) were selected on the basis of chemical parameters, in particular the salinity conditions along the vertical profile. The first station was located in Mesola (44°55′31.6″ N, 12°13′53.3″ E), 27 km upstream of the Po outlet, and was labeled as the freshwater site (FW). Here, the conductivity values were still typical of Po freshwater (approximately 400 µS cm^{-1} on the top; Figure 2). At the sightly saline site (SS; 44°56′32.8″ N, 12°16′41.8″ E), located 22 km upstream of the river mouth, the salinity profile showed values between 1.0 and 5.4 ppt from the surface to the bottom. The saline water site (SW; 44°47′59.0″ N, 12°23′00.3″ E) was located in a section 1.5 km upstream of the Po di Goro outlet.

The vertical profiles of the physical conditions (water temperature, oxygen, electrical conductivity, and salinity) were measured at the three sites using multiparametric probe (YSI ODO/CT), operated from the boat in the middle of the river section. The water samples from the sites were filtered and stored at −20 °C to be analyzed in the next two weeks. Intact sediment cores (Plexiglass liners, internal diameter: 4.5 cm, length: 20 cm) were collected from the boat using a hand corer and immediately immersed with site water in separate tanks corresponding to the sampling sites, continuously aerated with portable pumps, and transported to the laboratory. From each site, 50 L of bottom water were collected using a submerged pump for core maintenance during pre-incubation and incubation phases in laboratory. At each station, five intact sediment cores were used for dark flux and N process measurements and three replicates for sediment characterization. Cores stabilization and incubation were performed according to a standard protocol [29].

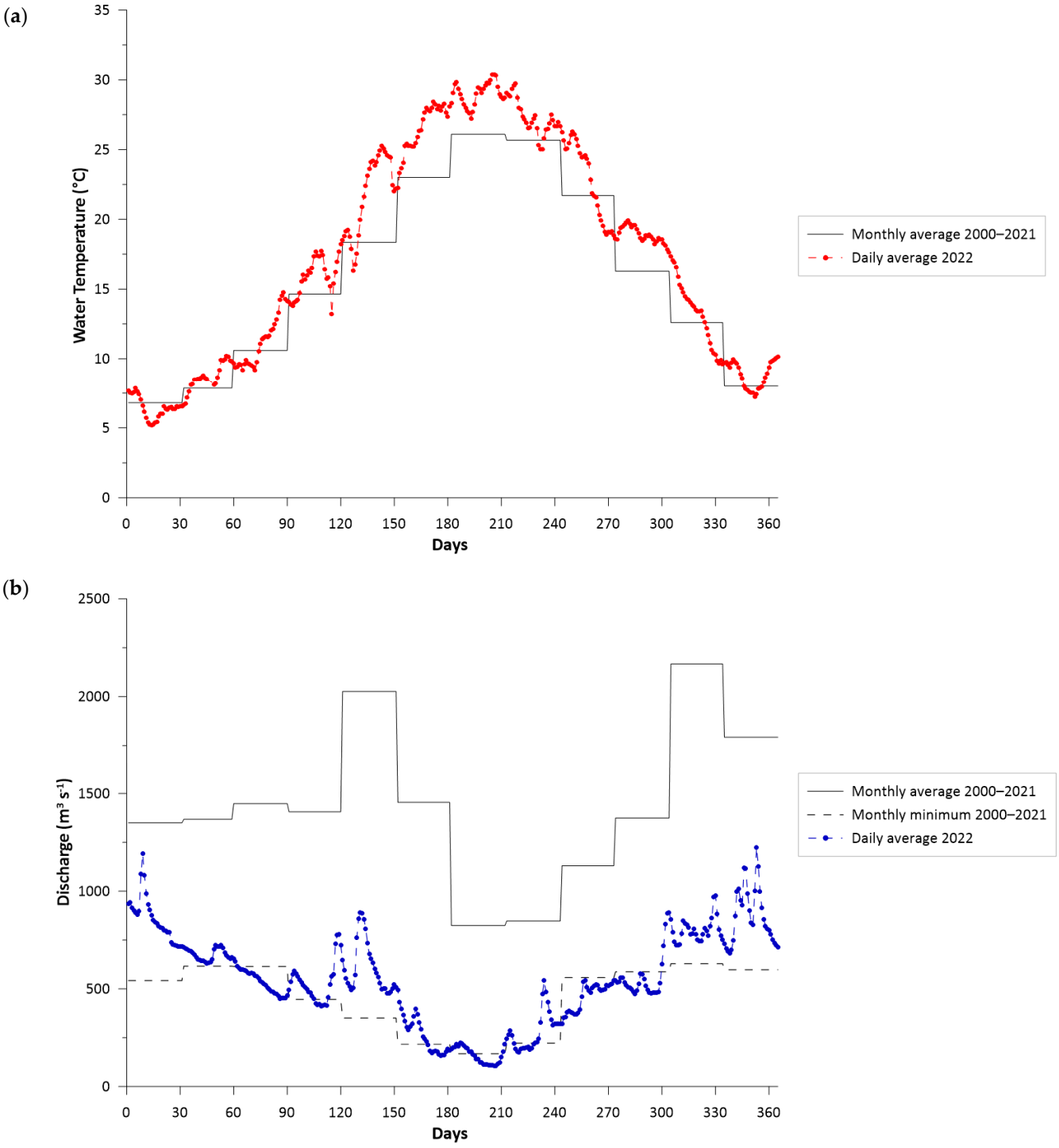

Figure 2. (**a**) Average daily water temperature of the Po River in 2022 at the basin closing section (Pontelagoscuro station) compared with the average monthly water temperature over the last 20 years; (**b**) average daily discharge in 2022 compared to the minimum and average monthly discharge over the last 20 years (data source: Environmental Protection Agency of the Emilia-Romagna Region, https://simc.arpae.it/dext3r/; accessed on 10 January 2023).

2.3. Benthic Flux Measurements and Sediment Characterization

Upon arrival at the laboratory, five sediment cores from each of the three sites were transferred to three separate tanks filled with unfiltered in situ water, submerged, and recirculated by the mean of a Teflon-coated magnetic bar rotating at 40 rpm, added a

few centimeters above the sediment surface, useful for mixing the core water column, avoiding resuspension. The cores were kept at in situ temperature (28 °C) by a thermostat connected to the tanks during the first night in laboratory. The next day, prior to the start of the incubation, the water tanks were replaced with water from each sampling site to maintain nutrient concentrations close to those in situ. At the start of incubation, the water in the tanks was removed to resubmerge the intact cores, and each core was closed with a gas-tight lid on the top.

Before and after the incubation, physical parameters such as temperature and oxygen concentration were measured directly inside the cores, using the same probe as the sampling probe, and water samples were taken from each core using a glass 60 mL syringe, filtered thought Whatman GF/F glass fiber filters (pore size: 0.45 µm), transferred to 20 mL polyethylene scintillation vials, and frozen before the determination of dissolved inorganic N concentrations (NO_3^-, NO_2^-, and NH_4^+). Dark incubation was applied for 2 h to keep the variation of the O_2 concentration within 20% of the initial value throughout the incubation [29]. Dark conditions were imposed to reproduce the in situ benthic conditions of the Po di Goro, always in darkness, as the depth ranged from 3 to 6 m, and the light penetration was limited by phytoplanktonic high turbidity. In the following days, water samples were analyzed according to standard protocols. The nitrate was analyzed with a Technicon AutoAnalyser II (detection limit: 0.4 µM [30]); NO_2^- was determined with sulfanilamide and N-(1-naphtyl)-ethylenediamine (detection limit: 0.1 µM [31]) using a Jasco V-550 double-beam spectrophotometer at 541 nm; and NH_4^+ was analyzed using salicylate and hypochlorite in the presence of sodium nitroprusside (detection limit: 0.5 µM [32]) and determined with the same spectrophotometer at 640 nm. The concentrations of the solutes together with the incubation time were used to calculate the dark fluxes (F_x, µmol m^{-2} h^{-1}) at the sediment–water interface, according to Equation (1):

$$F_x = \frac{(C_t - C_0) \cdot V}{A \cdot t} \quad (1)$$

where C_0 (µM) is the concentrations of the species at the beginning of the incubation, C_t is the concentrations of the same species at the end of incubation, V (L) is the water column volume present in each core, A (m^2) is the sediment surface, and t (h) is the incubation time. The negative values describe the net consumption of species from the water column to the sediment, and positive values indicate the net production, so the fluxes are determined from the sediment to the water column (net production).

Three additional cores from each sampling site were used to determine the physical properties of the sediments. The porosity and water content (%) were determined using the wet weight loss method. The upper 0–2 cm layer (divided into two parts: 0–1 and 1–2 cm layers) was cut from each core, and after being homogenized using a spatula, a sub-sample of 5 mL was collected using cut-off syringes and dried for 72 h at 50 °C; the samples were then transferred to a muffle furnace at 350 °C for 3 h to quantify the organic matter content (OM, %) using the same weight loss method.

2.4. Measurement of Denitrification and DNRA Rates

At the end of the first incubation, the water was replaced with the water of sampling site and the intact cores were resubmerged for approximately 1 h to stabilize before the following incubation. Then, the water level in the tank was lowered again and the isotope pairing technique (IPT [33]) was applied to measure the denitrification rates. An aliquot of a 15 mM $^{15}NO_3^-$ stock solution ($Na^{15}NO_3^-$, Sigma Aldrich, USA) was added in the water column of each core to achieve a final ^{15}N atomic % enrichment of at least ~50%. Water samples were collected in each core before and after the addition of $^{15}NO_3^-$ to calculate the ^{14}N:^{15}N ratio in the NO_3^- pool. As in the first incubation, the cores were sealed with a gas-tight lid on the top and incubated for 2 h in the dark. At the end of the incubation, in each core the sediment and water phases were gently mixed to homogenize the N_2 pools dissolved in the aqueous phase and in the pore water. From each core, an

aliquot of the slurry was transferred to a 12 mL glass-tight vial (Exetainer®, Labco Limited, UK), fixed with 200 µL of 7 M $ZnCl_2$ to stop microbial activity and kept refrigerated with the upside down orientation until the analysis in the following days. The water samples were analyzed using a Membrane Inlet Mass Spectrometer equipped with a copper reduction column maintained at 600 °C (MIMS, Bay Instrument, MD, USA [34]) to determine the abundance of $^{29}N_2$ and $^{30}N_2$. The denitrification rates were calculated using Equations (2) and (3), as follows [33]:

$$D_{15} = p29 + 2p30 \quad (2)$$

$$D_{14} = D_{15} \cdot \left(\frac{p29}{2p30} \right) \quad (3)$$

where D_{15} is the denitrification rate of the labeled $^{15}NO_3^-$, and D_{14} is the total denitrification rate; p29 and p30 are the production rate of $^{29}N_2$ and $^{30}N_2$, respectively.

The total denitrification rate (Dtot) was calculated as the sum of Dw (i.e., the denitrification of NO_3^- diffusing from the water column to the sediment) and Dn (i.e., the denitrification of NO_3^- produced in the superficial oxic sediment by nitrification). The rates were calculated according to the following equations [33] and expressed in µmol N m^{-2} h^{-1}.

$$D_{tot} = D_w + D_n \quad (4)$$

$$D_w = \frac{^{14}NO_3^-}{^{15}NO_3^-} \cdot D_{15} \quad (5)$$

$$D_n = D_{14} - D_w \quad (6)$$

The denitrification efficiency (DE, %) is the ratio between the denitrification and the total fluxes of inorganic N from the sediment, both in ionic (NO_3^- + NO_2^- + NH_4^+) and gaseous (N_2) form, calculated according to Equation (7) [35]:

$$DE = \frac{Dtot}{(DIN + Dtot)} \cdot 100 \quad (7)$$

where DIN (µmol N m^{-2} h^{-1}) is the sum of inorganic N fluxes (NO_3^- + NO_2^- + NH_4^+) directed from the sediment to the water column (effluxes), and Dtot is the total efflux of N_2 from the sediment.

After IPT incubation, an additional aliquot (30 mL) of the sediment slurry was sampled from each core to determine the DNRA rates from the production of $^{15}NH_4^+$, according to the procedure reported by Magri et al. [36]. Briefly, the slurry was treated with 2 g of KCl (2 M) in 50 mL falcon tubes to determine the exchangeable ammonium pool, comprehensive of the $^{15}NH_4^+$ fraction. The samples were shaken for 30 min, centrifuged (1800 rpm for 15 min), filtered (Whatman GF/F glass fiber filters, pore size: 0.45 µm), transferred into 20 mL scintillation vials and frozen. At the time of the analyses, the samples were diluted (1:5) and air-purged for 10 min to eliminate $^{29}N_2$ and $^{30}N_2$ pools generated during the IPT incubation. A 12 mL aliquot of each purged sample was transferred to Exetainers, and a volume of 200 µL of alkaline hypobromite solution was added to oxidize NH_4^+ to N_2 [37]. After oxidation, the $^{29}N_2$ and $^{30}N_2$ concentrations were determined using MIMS. The total DNRA rates (µmol N m^{-2} h^{-1}) were calculated according to [38] as the DNRA of NO_3^- from the water column (DNRAw; µmol N m^{-2} h^{-1}) and the DNRA coupled to nitrification (DNRAn; µmol N m^{-2} h^{-1}), according to the Equations (8)–(10), as follows:

$$DNRA = p^{15}NH_4^+ \cdot \frac{D_{14}}{D_{15}} \quad (8)$$

$$DNRA_w = \frac{^{14}NO_3^-}{^{15}NO_3^-} \cdot p^{15}\,NH_4^+ \quad (9)$$

$$DNRA_n = DNRA - DNRA_w \quad (10)$$

where $p^{15}NH_4^+$ is the production of $^{15}NH_4^+$.

2.5. Statistical Analysis

One-way ANOVA and pairwise multiple comparisons of the means (post hoc and Tukey's test) were used to determine the difference in the N fluxes, denitrification and DNRA rates among the three sampling sites. The Shapiro–Wilk and Levene's tests were used to check whether the data had a normal distribution and to determine the homogeneity of the variance, respectively. The statistical analysis, with the significance level set at $p < 0.05$, was performed using Sigma Plot 14.5 (Systat Software, Inc., San Jose, CA, USA).

3. Results and Discussion

3.1. The Summer Drought of 2022

The spring and summer months of 2022 will be remembered for the severe drought that affected large areas of Europe, combined with long and intense heat waves that spread from the Iberian Peninsula to Northern and Central Europe, also affecting Italy [39]. In particular in the north of Italy, the dry conditions were a result of low snow accumulation in the Alps during the winter and early spring of 2021–2022, similar to the year 2015 [40], and a persistent lack of precipitation in late spring and early summer [28], combined with early heat waves in May and June. According to Italian reports, the period from May to July 2022 was indicated as the warmest months in the recent decades, although other summers were just as dry, such as in the years 2003 and 2009 [41]. This critical period was confirmed by water temperature and discharge data for the Po River (Figure 3), measured throughout the whole of 2022 at the basin's closing section. The water temperature was steadily higher than the 2000–2021 average monthly values, with the maximum discrepancy recorded in the second half of May (+5 °C) and an average positive anomaly of 2.5 °C throughout the summer and until mid-autumn. The Po River was enduring an exceptional hydrological drought, with an average discharge deficit of approximately 60% during the whole of 2022 (Figure 3). The daily river discharge was particularly low during June–August, at or below the historical minimum of the last twenty years. The most negative monthly anomaly at the closing section occurred in July when the discharge was approximately 30% below the historical minimum for 2000–2021, which occurred in July 2006 [42]. The water shortage lasted until August, when the hydrological situation improved after some storms, although the flow remained below typical seasonal values. The critical reduction in the river discharge led to a significant intrusion of the deep and persistent saline wedge during late spring and summer in the Po Delta, extending along the Po di Goro branch for a maximum length of approximately 35 km from the mouth [43], more than the 15 km of saline intrusion in Po di Goro during the summer of 2017. In particular, the slightly saline site (SS) was identified at a greater distance from the Po di Goro outlet compared to the previous year [7].

The in situ conditions were different for the three sites, in particular the salinity varied along the Po di Goro River, starting from 1.5 mg L^{-1} in the bottom of the FW site to 30.1 mg L^{-1} in the SW site, and also along the vertical profile in each sampling site (Figure 3a). The FW site showed homogeneity of water, while the SS and SW sites showed an increase in the saline concentrations from the surface to the bottom water, highlighting the water stratification. Moreover, the water stratification was also confirmed with the vertical profile of the concentration of oxygen (Figure 3b). As can be seen, the oxygen concentration was distributed equally in the FW site, indicating the continued mixing in of the freshwater systems of the Po River, different from the other sites. The SS and SW sites showed a reduction in the oxygen concentrations along the vertical profile, in particular for

the SS site, where the concentrations reduced down to 2.9 mg L^{-1} at the bottom (Table 1). The sampling sites were different also in the composition and physical properties of the surface sediments: sandy and low organic matter (OM, %) at the FW site, muddy–sandy and with high organic matter at the SS site, and mostly clay at the SW site; the highest porosity was found at the SS and SW sites (Table 2).

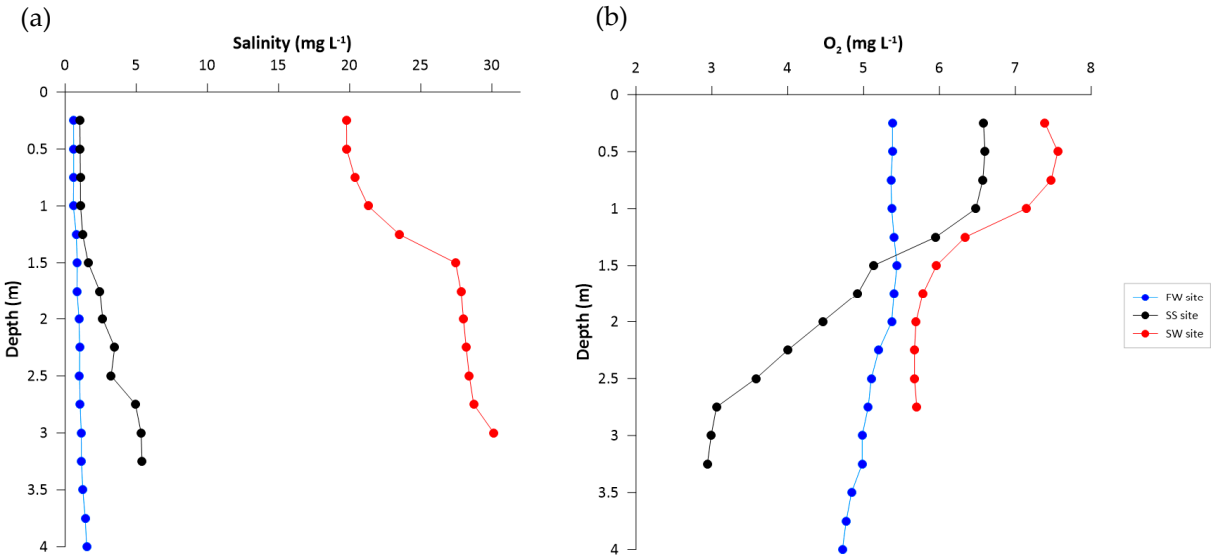

Figure 3. Vertical profiles of (**a**) salinity (ppt) and (**b**) O_2 concentration (mg O_2 L^{-1}) at the three sampling stations on the day of sampling.

Table 1. Oxygen concentrations, N nutrient availability, and salinity conditions at the three sampling stations during the experimental campaign in situ.

Site	Distance from the Outlet (km)	O_2 (mg L^{-1})	Salinity (mg L^{-1})	NO_3^- (µM)	NH_4^+ (µM)	N_{tot} (µM)
FW	25	4.7	1.5	39	14	107
SS	22	2.9	5.4	40	23	118
SW	1.5	5.8	30.1	11	3	68

Table 2. Typology, porosity, density (g mL^{-1}), and organic matter content (OM) in sediments at the three sampling sites of Po di Goro River. Average values and standard deviations are reported.

	FW	SS	SW
Typology	Sandy	Muddy–Sandy	Clay
Porosity	0.47 ± 0.12	0.65 ± 0.02	0.62 ± 0.05
Density (g mL^{-1})	1.80 ± 0.11	1.47 ± 0.04	1.56 ± 0.05
OM (%)	1.00	3.9	1.90

3.2. Benthic N Fluxes along the Salinity Gradient

Because of the low spring rainfall and Po flows, nitrate concentrations were generally low in summer 2022, decreasing from ~40 µM at the FS to the very low value of ~10 µM at the most downstream station SW (Table 1). This decrease along with the increasing salinity gradient is not surprising and is mainly due to a mixed contribution of removal processes along the river and dilution with seawater. In all three stations, sediment–water fluxes of oxidized N species (NO_3^- + NO_2^-) were negative, indicating that consumption prevailed over production in the sediments of the Po di Goro River, and the removal rates depended on the availability of NO_3^- in the overlying bottom water. The rates of NO_x^- consumption (with NO_3^- always representing >95% of NO_x^-) decreased significantly with the increasing salinity ($p < 0.05$, Table 3) along the river–sea gradient, from

FW (-245 ± 36 µmol N m^{-2} h^{-1}) to SS (-154 ± 31 µmol N m^{-2} h^{-1}) and to the more marine station SW (-70 ± 23 µmol N m^{-2} h^{-1}). A good agreement was found between the NO_x^- removal rates and the N_2 production rates, but the latter were always slightly higher on average, suggesting that denitrification was not only fueled by the diffusion of NO_3^- from the water column into the sediment (Figure 4).

Table 3. One-way ANOVA and Tukey's test results ($p < 0.05$; NS = not statistically significant).

Parameter	*p*	F	Tukey's Test
NO_x^- flux	<0.05	5.6	FW vs. SW
NH_4^+ flux	NS	0.9	-
Dtot	<0.001	30.9	FW vs. SW SS vs. SW
Dw	<0.001	47.1	FW vs. SS SS vs. SW FW vs. SW
Dn	<0.01	15.1	FW vs. SW SS vs. SW
DNRAtot	<0.05	4.9	SS vs. SW
DNRAw	NS	4.1	-
DNRAn	NS	2.5	-

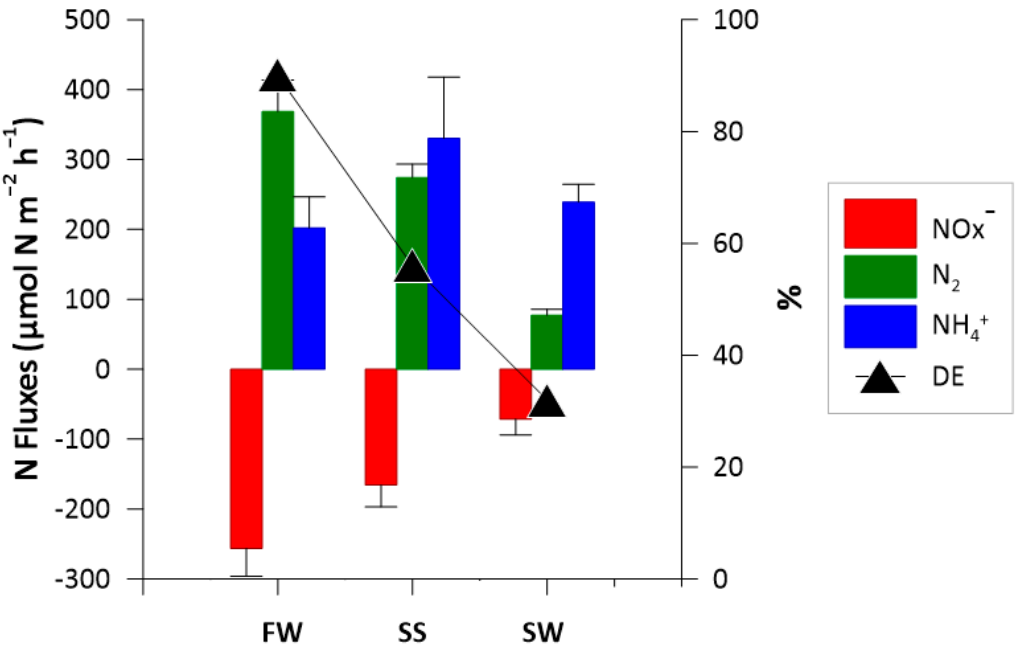

Figure 4. Benthic dark fluxes of NO_x^- (NO_3^- + NO_2^-), NH_4^+, total denitrification (N_2), and denitrification efficiency (DE, black triangle) at the three sampling sites. The average values and standard deviations are reported.

The denitrification rates decreased along the salinity gradient ($p < 0.001$, Table 3), likely due to the cumulative effect of the NO_3^- availability, which decreased progressively downstream (Table 1), and the bottom water oxygen concentration, which was high at the well-mixed freshwater station FW, low at the stratified intermediate station SS, and again high at the stratified saline station SW (Figure 2), influencing the N availability along the vertical profile. The denitrification rates were the highest at the FW station (368 ± 45 µmol N m^{-2} h^{-1}), where NO_3^- was more available (~30 µM), and there was continuous freshwater mixing [44]. The intermediate station had almost the same NO_3^- concentration (Table 1), but the denitrification rates were lower (274 ± 19 µmol N m^{-2} h^{-1}), likely due to the onset of water stratification, affecting the diffusion of NO_3^- in water

column. The Dtot was not significantly different between the FW and SS sites, but it was significantly higher in both the FW and SS than in the SW station, according to Tukey's test (Table 3). The lowest oxygen concentration measured in the bottom water at SS station was probably because of the sediment OM content, which was the highest at this site (Table 2), and its mineralization. Here, the high organic matter content was due to the flocculation of the particulate organic load induced by the mixing of salt and fresh water, which caused the riverine organic carbon to form sinking aggregates [45,46]. The most downstream station (SW) had the lowest denitrification rates (77 ± 9 μmol N m^{-2} h^{-1}), likely due to the lowest NO^{3-} concentration (Table 1), water column stratification and high oxygen concentration in the bottom water (Figure 2). Bacterial communities, such as nitrifiers and denitrifiers, have been shown to be physiologically stressed by salinity. In addition, when other electron acceptors, such as NO_3^- and O_2, are limited, saltwater intrusion promotes sulphate reduction, leading to sulphide accumulation, which directly inhibits nitrification and denitrification [47,48].

At all sampling sites, the NH_4^+ fluxes were positive, indicating a higher production than consumption (Figure 4) and systematically higher than the corresponding N_2 production rate. Although not significant (Table 3), the release of NH_4^+ was slightly higher at the SS site, where the sediment organic matter concentration was higher (~4%) than at the other two stations. The denitrification efficiency was approximately 90% at FW, indicating that the sediments lost N mostly as N_2, while it decreased to 32% at the most downstream station, where the sediments tended to be sources of inorganic N ions that were recycled to the water column. The marked decrease in DE at the site closer to the Po di Goro outlet has a very important ecological consequence.

3.3. Denitrification and DNRA Rates

At the FW station, Dtot was 368 ± 45 μmol N m^{-2} h^{-1}, decreasing to 274 ± 19 μmol N m^{-2} h^{-1} and 77 ± 9 μmol N m^{-2} h^{-1} at the SS and SW stations, respectively. At the FW station, Dw was still 55% of Dtot, while because of the extreme drought condition, water column stratification and, thus, reduced NO_3^- supply from the water column, Dw was a lower fraction of the total, 35% and 48% of Dtot at the SS and SW stations, respectively. Both availability of NO_3^- in the water column and oxygen concentration regulated the partitioning of the total rates into Dw and Dn [9]. In the freshwater site, the denitrification was mostly supported by the nitrate present in the water column (Dw~65%), while the contributions of Dw and Dn were almost equal at the SW site (Figure 5), which was confirmed by Tukey's test (Table 3), which highlighted a difference in Dw among the three sampling sites, while the differences in Dn appeared between FW and SW or SS and SW but not between FW and SS. The Dn rates strongly decreased at SW likely due to the occurrence of salinity-induced sulphidic conditions inhibiting the nitrification process [28,49] and the loss of NO_3^- via coupled nitrification–denitrification [50].

DNRA process was always detected, but the rates at the first two sites were one order of magnitude lower than the corresponding denitrification rates. In fact, denitrification consistently outperformed DNRA in freshwater and slightly saline sites, while the two processes were almost equally important in the more saline site. While denitrification along the salinity gradient to the sea decreased ($p < 0.001$), DNRA increased ($p < 0.05$), with the highest DNRA rate measured at the SW site (116 ± 29 μmol N m^{-2} h^{-1}) (Figure 5, Table 3), followed by the FW and SS sites (55 ± 9 and 27 ± 8 μmol N m^{-2} h^{-1}, respectively), and significant statistical differences appeared between SS and SW, according to the post hoc Tukey's test (Table 3). The DNRA rates were slightly higher than the denitrification rates at SW, suggesting that saline conditions may favor DNRA over denitrification [6]. Nevertheless, DNRAw was slightly higher than DNRAn at the FW and SS sites (56% and 68% of DNRAtot, respectively), while at SW site the DNRAn was higher than the DNRAw, due to limited NO_3^- availability in the water column (65 ± 4 and 50 ± 8 μmol N m^{-2} h^{-1}, respectively).

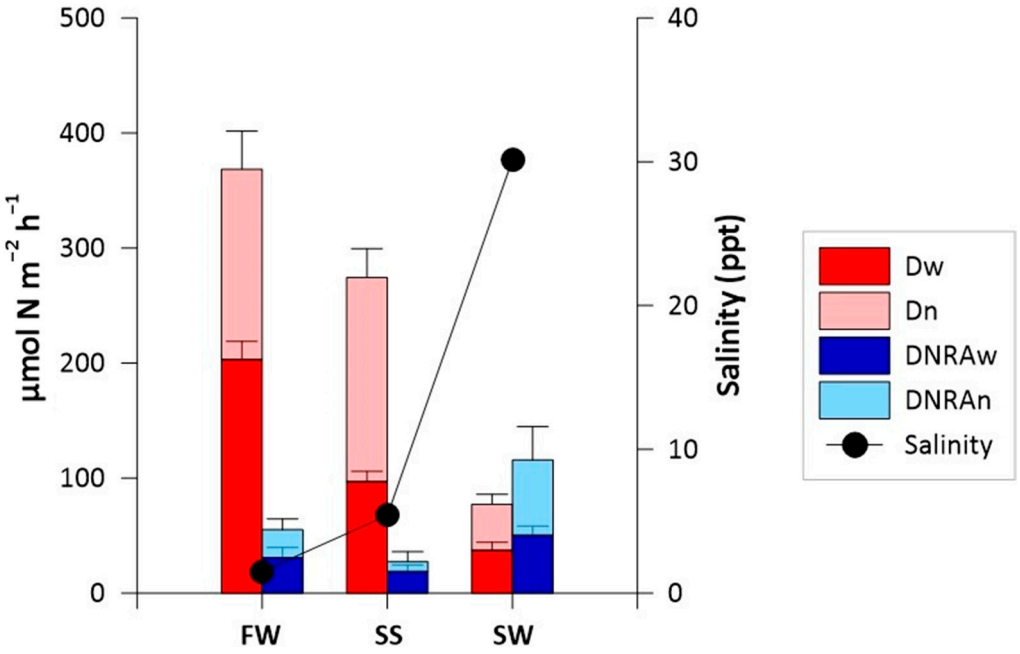

Figure 5. Denitrification and DNRA rates measured at the three sampling stations along the salinity gradient (black dots). The fraction of the two processes supported by NO_3^- from the water column (Dw and DNRAw) and the fraction portion coupled to nitrification (Dn and DNRAn) are also shown. The data are reported as the means and standard deviations.

Denitrification was the dominant pathway for NO_3^- reduction in freshwater and slightly saline conditions, outperforming DNRA by an average factor of 7. DNRA was low at the FW and SS stations, and the consumption of NO_3^- by the DNRA process, calculated as the percentage ratio of the DNRA:NO_3^- flux, was 14% and 11%, respectively. At the SW station, the DNRA:NO_3^- flux ratio increased to 74%, likely due to the decrease in the NO_3^- concentration and the higher salinity conditions which favor NO_3^- reduction to NH_4^+ [6,51,52]. According to several authors [10,52,53], DNRA is favored over denitrification at high salinity conditions, low NO_3^- availability, and where the presence of sulphide inhibits coupled nitrification–denitrification [47,54].

The DNRA rates measured in the Po River Delta are in line with rates obtained in other aquatic ecosystems of the Po River Basin (lakes and lagoons) and in other brackish environments in summer (Table 4) [36,55]. This comparison (Table 4) confirms that the DNRA process was stimulated by saline conditions; in fact, the higher rates occurred in Goro Lagoon (Italy) and in Plum Island Sound estuary (Massachusetts) [55,56], where the salinity was 28‰ and 25‰, respectively. Moreover, DNRA rates increased along the NO_3^- availability gradient and when sediments were more OM rich, such as in the Goro Lagoon [55].

Table 4. Total denitrification and DNRA rates measured in other aquatic ecosystems of the Po River Basin (lakes and lagoons) and in selected freshwater and brackish environments during summer around the world. The rates are expressed as the average values ± standard deviations. Water and sediment features are reported for comparison.

Location	T (°C)	Salinity (‰)	NO_3^- (μM)	OM (%)	DNRAtot (μmol N m^{-2} h^{-1})	Dtot (μmol N m^{-2} h^{-1})	Reference
Pit Lake Ca' Stanga—Hypolimnetic Sediments (Italy)	6.5	-	202	1 *	7 ± 4	163 ± 12	[57]
Pit Lake Verde—Hypolimnetic Sediments (Italy)	12.5		102	2 *	4 ± 1	31 ± 5	
Goro Lagoon—Site Giralda (Italy)	23	5	32	2 *	48	217	[36]
	21.7	7	79	7	65 ± 11	152 ± 36	[55]
			105		45 ± 11	290 ± 94	
			236		62 ± 8	414 ± 123	
			437		59 ± 11	377 ± 65	
			874		74 ± 8	472 ± 50	
			1722		108 ± 23	631 ± 51	
Goro Lagoon—Site Gorino (Italy)	25	28	23	0.24 *	35	72	[36]
	22.5	16	61	9	176 ± 14	290 ± 58	[55]
			113		127 ± 17	399 ± 94	
			226		241 ± 102	690 ± 109	
			462		150 ± 11	713 ± 36	
			871		334 ± 65	1077 ± 225	
			1725		235 ± 42	1304 ± 196	
Baltic Sea—Site A	6	10	1.3	-	0.15	40	[58]
Baltic Sea—Site B		12	0.5		0.67	22	
Baltic Sea—Site C		10	0.9			0.13	
Curonian Lagoon—Baltic Sea (Sediments)	22	0.3	1	13 *	2 ± 1	0.95 ± 0.06	[59]
Plum Island Sound Estuary—Coastal Sediments (Massachusetts, USA)	23	22		-	13 ± 2	26 ± 0.6	[60]
Plum Island Sound Estuary—Tidal Creek (Massachusetts, USA)	24	25	7	-	20 ± 5	27 ± 2	[56]

Note: * Organic carbon.

In the Po di Goro arm, the maximum saline intrusion was recorded in August and reached 38 km upstream from the mouth [61]. Extending the denitrification rates presented here to the river stretch affected by saline intrusion, the N dissipation capacity via denitrification of the entire Po di Goro arm was estimated to be reduced by 33% of the value measured in June. This simulation highlights the need to gather further information on saline intrusion and the relative effects on denitrification and DNRA and, hence, on N load dissipation vs. recycling, induced by extreme drought conditions, which may have relevant impacts on nutrient availability and eutrophication in coastal ecosystems.

4. Conclusions

Global warming affects aquatic ecosystems in terms of N cycling and nutrient availability. The drought observed in the summer of 2022 decreased the Po River discharge, also reducing N loads and N availability in the delta. At the same time, low discharge caused an extensive saline intrusion in most of the Po River Delta, which by the end of June had already reached sections ~30 km upstream of the Adriatic Sea.

The present results show that global warming and reduced precipitation are altering nitrogen cycling in transitional ecosystems, decreasing denitrification and nitrate removal and increasing DNRA and NH_4^+ release from sediments. Prolonged drought and saline water intrusion, by favoring DNRA over denitrification (i.e., N recycling rather than removal) may have negative effects on coastal eutrophication in the spring and summer

seasons, reducing the effectiveness of transitional environments to remove nitrogen and increasing N export to the sea.

DNRA is still one of the least understood N cycling processes in aquatic ecosystems. The results presented here are the first quantification of denitrification and DNRA in the Po Delta and indicate that drought and saline intrusion may regulate benthic N dynamics, N load speciation, and eutrophication in coastal ecosystems. Further studies are needed to clarify the specific role of extreme meteorological conditions on aquatic ecosystems and biogeochemical processes, including the effects of multiple drivers, such as NO_3^- and organic carbon availability, as well as sediment sulphide concentrations, and why they will become more important as extreme conditions worsen because of climate change.

Author Contributions: Conceptualization, M.P.G., E.S. and G.C.; methodology, E.S., M.M., F.V. and G.C.; investigation, M.P.G., E.S., F.V., M.M. and G.C.; resources, F.V.; formal analysis, M.P.G. and M.M.; writing—original draft preparation, M.P.G.; writing—review and editing, E.S., M.M. and G.C.; visualization, M.P.G.; funding acquisition, G.C. and E.S.; supervision, G.C. All authors have read and agreed to the published version of the manuscript.

Funding: This work was financially supported by the Emilia-Romagna Region (project Post LIFE AGREE—"Monitoring of the Valle di Gorino, Sacca di Goro, for the definition of a management plant in line with the Water Framework Directive") and by the local water authority, Consorzio di Bonifica Pianura di Ferrara, within a collaboration aimed at defining management strategies for the control of eutrophication in the Po River Delta.

Data Availability Statement: Data will be made available upon request.

Acknowledgments: The authors would like to thank Mattia Lanzoni and Luca Bellini for their help during the sampling campaign.

Conflicts of Interest: The authors declare no conflict of interest.

References

1. Dugdale, R.C.; Wilkerson, F.P.; Hogue, V.E.; Marchi, A. The Role of Ammonium and Nitrate in Spring Bloom Development in San Francisco Bay. *Estuar. Coast. Shelf Sci.* **2007**, *73*, 17–29. [CrossRef]
2. Howarth, R.W. Coastal Nitrogen Pollution: A Review of Sources and Trends Globally and Regionally. *Harmful Algae* **2008**, *8*, 14–20. [CrossRef]
3. Kroeze, C.; Bouwman, L.; Seitzinger, S. Modeling Global Nutrient Export from Watersheds. *Curr. Opin. Environ. Sustain.* **2012**, *4*, 195–202. [CrossRef]
4. Cornwell, J.C.; Kemp, W.M.; Kana, T.M. Denitrification in coastal ecosystems: Methods, environmental controls, and ecosystem level controls, a review. *Aquat. Ecol.* **1999**, *33*, 41–54. [CrossRef]
5. Santoro, A.E. Microbial Nitrogen Cycling at the Saltwater–Freshwater Interface. *Hydrogeol J.* **2010**, *18*, 187–202. [CrossRef]
6. Zhou, Z.; Ge, L.; Huang, Y.; Liu, Y.; Wang, S. Coupled Relationships among Anammox, Denitrification, and Dissimilatory Nitrate Reduction to Ammonium along Salinity Gradients in a Chinese Estuarine Wetland. *J. Environ. Sci.* **2021**, *106*, 39–46. [CrossRef]
7. Gervasio, M.P.; Soana, E.; Vincenzi, F.; Castaldelli, G. An Underestimated Contribution of Deltaic Denitrification in Reducing Nitrate Export to the Coastal Zone (Po River–Adriatic Sea, Northern Italy). *Water* **2022**, *14*, 501. [CrossRef]
8. Tiedje, J.M.; Sexstone, A.J.; Myrold, D.D.; Robinson, J.A. Denitrification: Ecological Niches, Competition and Survival. *Antonie Van Leeuwenhoek* **1983**, *48*, 569–583. [CrossRef]
9. Piña-Ochoa, E.; Álvarez-Cobelas, M. Denitrification in Aquatic Environments: A Cross-System Analysis. *Biogeochemistry* **2006**, *81*, 111–130. [CrossRef]
10. Burgin, A.J.; Hamilton, S.K. Have We Overemphasized the Role of Denitrification in Aquatic Ecosystems? A Review of Nitrate Removal Pathways. *Front. Ecol. Environ.* **2007**, *5*, 89–96. [CrossRef]
11. Heil, J.; Vereecken, H.; Brüggemann, N. A Review of Chemical Reactions of Nitrification Intermediates and Their Role in Nitrogen Cycling and Nitrogen Trace Gas Formation in Soil: Chemical Reactions of Nitrification Intermediates in Soil. *Eur. J. Soil Sci.* **2016**, *67*, 23–39. [CrossRef]
12. Scott, J.T.; McCarthy, M.J.; Gardner, W.S.; Doyle, R.D. Denitrification, Dissimilatory Nitrate Reduction to Ammonium, and Nitrogen Fixation along a Nitrate Concentration Gradient in a Created Freshwater Wetland. *Biogeochemistry* **2008**, *87*, 99–111. [CrossRef]
13. Xia, R.; Zhang, Y.; Critto, A.; Wu, J.; Fan, J.; Zheng, Z.; Zhang, Y. The Potential Impacts of Climate Change Factors on Freshwater Eutrophication: Implications for Research and Countermeasures of Water Management in China. *Sustainability* **2016**, *8*, 229. [CrossRef]

14. Pörtner, H.-O.; Roberts, D.C.; Tignor, M.; Poloczanska, E.S.; Mintenbeck, K.; Alegría, A.; Craig, M.; Langsdorf, S.; Löschke, S.; Möller, V. (Eds.) *IPCC, 2022: Climate Change 2022: Impacts, Adaptation and Vulnerability. Contribution of Working Group II to the Sixth Assessment Report of the Intergovernmental Panel on Climate Change*; Cambridge University Press: Cambridge, UK; New York, NY, USA, 2022; p. 3056.
15. Gao, X.; Giorgi, F. Increased Aridity in the Mediterranean Region under Greenhouse Gas Forcing Estimated from High Resolution Simulations with a Regional Climate Model. *Glob. Planet. Change* **2008**, *62*, 195–209. [CrossRef]
16. Carvalho, D.; Pereira, S.; Silva, R.; Rocha, A. Aridity and Desertification in the Mediterranean under EURO-CORDEX Future Climate Change Scenarios. *Clim. Change* **2022**, *174*, 28. [CrossRef]
17. Howarth, R.W.; Swaney, D.P.; Butler, T.J.; Marino, R. Rapid Communication: Climatic Control on Eutrophication of the Hudson River Estuary. *Ecosystems* **2000**, *3*, 210–215. [CrossRef]
18. Feyen, L.; Dankers, R. Impact of Global Warming on Streamflow Drought in Europe. *J. Geophys. Res.* **2009**, *114*, D17116. [CrossRef]
19. Statham, P.J. Nutrients in Estuaries—An Overview and the Potential Impacts of Climate Change. *Sci. Total Environ.* **2012**, *434*, 213–227. [CrossRef]
20. Osborne, R.I.; Bernot, M.J.; Findlay, S.E.G. Changes in Nitrogen Cycling Processes Along a Salinity Gradient in Tidal Wetlands of the Hudson River, New York, USA. *Wetlands* **2015**, *35*, 323–334. [CrossRef]
21. Xie, R.; Rao, P.; Pang, Y.; Shi, C.; Li, J.; Shen, D. Salt Intrusion Alters Nitrogen Cycling in Tidal Reaches as Determined in Field and Laboratory Investigations. *Sci. Total Environ.* **2020**, *729*, 138803. [CrossRef]
22. Giblin, A.E.; Weston, N.B.; Banta, G.T.; Tucker, J.; Hopkinson, C.S. The Effects of Salinity on Nitrogen Losses from an Oligohaline Estuarine Sediment. *Estuaries Coasts* **2010**, *33*, 1054–1068. [CrossRef]
23. Marchant, H.K.; Lavik, G.; Holtappels, M.; Kuypers, M.M.M. The Fate of Nitrate in Intertidal Permeable Sediments. *PLoS ONE* **2014**, *9*, e104517. [CrossRef]
24. Herbert, E.R.; Boon, P.; Burgin, A.J.; Neubauer, S.C.; Franklin, R.B.; Ardón, M.; Hopfensperger, K.N.; Lamers, L.P.M.; Gell, P. A Global Perspective on Wetland Salinization: Ecological Consequences of a Growing Threat to Freshwater Wetlands. *Ecosphere* **2015**, *6*, art206. [CrossRef]
25. Gervasio, M.P.; Soana, E.; Granata, T.; Colombo, D.; Castaldelli, G. An Unexpected Negative Feedback between Climate Change and Eutrophication: Higher Temperatures Increase Denitrification and Buffer Nitrogen Loads in the Po River (Northern Italy). *Environ. Res. Lett.* **2022**, *17*, 084031. [CrossRef]
26. Bellafiore, D.; Ferrarin, C.; Maicu, F.; Manfè, G.; Lorenzetti, G.; Umgiesser, G.; Zaggia, L.; Levinson, A.V. Saltwater Intrusion in a Mediterranean Delta Under a Changing Climate. *J. Geophys. Res. Ocean.* **2021**, *126*, e2020JC016437. [CrossRef]
27. Viaroli, P.; Giordani, G.; Bartoli, M.; Naldi, M.; Azzoni, R.; Nizzoli, D.; Ferrari, I.; Comenges, J.M.Z.; Bencivelli, S.; Castaldelli, G.; et al. The Sacca Di Goro Lagoon and an Arm of the Po River. In *Estuaries*; Wangersky, P.J., Ed.; The Handbook of Environmental Chemistry; Springer: Berlin/Heidelberg, Germany, 2005; Volume 5H, pp. 197–232; ISBN 978-3-540-00270-3.
28. Bonaldo, D.; Bellafiore, D.; Ferrarin, C.; Ferretti, R.; Ricchi, A.; Sangelantoni, L.; Vitelletti, M.L. The Summer 2022 Drought: A Taste of Future Climate for the Po Valley (Italy)? *Reg. Environ. Change* **2023**, *23*, 1. [CrossRef]
29. Dalsgaard, T.; Nielsen, L.P.; Brotas, V.; Viaroli, P.; Underwood, G.; Nedwell, D.; Sundback, K.; Rysgaard, S.; Miles, A.; Bartoli, M.; et al. *Protocol Handbook for NICE-Nitrogen Cycling in Estuaries: A Project under the EU Research Programme: Marine Science and Technology (MAST III)*; Ministry of Environment and Energy National Environmental Research Institute: Denmark; Department of Lake and Estuarine Ecology: Silkeborg, Denmark, 2000; pp. 1–62.
30. Armstrong, F.A.J.; Stearns, C.R.; Strickland, J.D.H. The Measurement of Upwelling and Subsequent Biological Process by Means of the Technicon Autoanalyzer®and Associated Equipment. In *Deep Sea Research and Oceanographic Abstracts*, 1967th ed.; Elsevier: Amsterdam, The Netherlands; Volume 14.
31. Golterman, H.L.; Clymo, R.S.; Ohnstand, M.A.M. *Methods for Physical and Chemical Analysis of Fresh Waters, I.B.P.*; Blackwell: Oxford, MS, USA, 1978; Volume 8.
32. Bower, C.E.; Holm-Hansen, T. A Salicylate–Hypochlorite Method for Determining Ammonia in Seawater. *Can. J. Fish. Aquat. Sci.* **1980**, *37*, 794–798. [CrossRef]
33. Nielsen, L.P. Denitrification in Sediment Determined from Nitrogen Isotope Pairing. *FEMS Microbiol. Lett.* **1992**, *86*, 357–362. [CrossRef]
34. Kana, T.M.; Darkangelo, C.; Hunt, M.D.; Oldham, J.B.; Bennett, G.E.; Cornwell, J.C. Membrane Inlet Mass Spectrometer for Rapid High-Precision Determination of N2, O2, and Ar in Environmental Water Samples. *Anal. Chem.* **1994**, *66*, 4166–4170. [CrossRef]
35. Eyre, B.; Ferguson, A. Comparison of Carbon Production and Decomposition, Benthic Nutrient Fluxes and Denitrification in Seagrass, Phytoplankton, Benthic Microalgae- and Macroalgae-Dominated Warm-Temperate Australian Lagoons. *Mar. Ecol. Prog. Ser.* **2002**, *229*, 43–59. [CrossRef]
36. Magri, M.; Benelli, S.; Bonaglia, S.; Zilius, M.; Castaldelli, G.; Bartoli, M. The Effects of Hydrological Extremes on Denitrification, Dissimilatory Nitrate Reduction to Ammonium (DNRA) and Mineralization in a Coastal Lagoon. *Sci. Total Environ.* **2020**, *740*, 140169. [CrossRef]
37. Warembourg, F.R. *Nitrogen Fixation in Soil and Plant Systems*; R Knowles and T H Black-burn; Academic Press Inc.: New York, NY, USA, 1993.
38. Risgaard-Petersen, N.; Rysgaard, S. Nitrate Reduction in Sediments and Waterlogged Soil Measured by 15N Techniques. In *Methods in Applied Soil Microbiology*; Academic Press Inc.: London, UK, 1995.

39. Toreti, A.; Masante, D.; Acosta Navarro, J.; Bavera, D.; Cammalleri, C.; De Felice, M.; de Jager, A.; Di Ciollo, C.; Hrast Essenfelder, A.; Maetens, W.; et al. *Drought in Europe July 2022: GDO Analytical Report*; Publications Office of the European Un-Ion: Luxembourg, 2022.
40. Marchina, C.; Natali, C.; Fazzini, M.; Fusetti, M.; Tassinari, R.; Bianchini, G. Extremely Dry and Warm Conditions in Northern Italy during the Year 2015: Effects on the Po River Water. *Rend. Fis. Acc. Lincei* **2017**, *28*, 281–290. [CrossRef]
41. Chatzidaki, E.; Vecchi, A. *Estate 2022: Presente e Futuro Si Toccano*; Ecoscienza—ARPAE: Bologna, Italy, 2022.
42. Montanari, A. Hydrology of the Po River: Looking for Changing Patterns in River Discharge. *Hydrol. Earth Syst. Sci.* **2012**, *16*, 3739–3747. [CrossRef]
43. Autorità di Bacino Distrettuale del Fiume Po. *Osservatorio Permanente Sugli Utilizzi Idrici Del Distretto Idrografico Del Fiume Po*; Autorità di Bacino Distrettuale del Fiume Po: Parma, Italy, 2022.
44. Maicu, F.; De Pascalis, F.; Ferrarin, C.; Umgiesser, G. Hydrodynamics of the Po River-Delta-Sea System. *J. Geophys. Res. Ocean.* **2018**, *123*, 6349–6372. [CrossRef]
45. Sholkovitz, E.R. Flocculation of Dissolved Organic and Inorganic Matter during the Mixing of River Water and Seawater. *Geochim. Et Cosmochim. Acta* **1976**, *40*, 831–845. [CrossRef]
46. Asmala, E.; Bowers, D.G.; Autio, R.; Kaartokallio, H.; Thomas, D.N. Qualitative Changes of Riverine Dissolved Organic Matter at Low Salinities Due to Flocculation: Riverine DOM Flocculation. *J. Geophys. Res. Biogeosci.* **2014**, *119*, 1919–1933. [CrossRef]
47. Neubauer, S.C.; Piehler, M.F.; Smyth, A.R.; Franklin, R.B. Saltwater Intrusion Modifies Microbial Community Structure and Decreases Denitrification in Tidal Freshwater Marshes. *Ecosystems* **2019**, *22*, 912–928. [CrossRef]
48. Ardón, M.; Morse, J.L.; Colman, B.P.; Bernhardt, E.S. Drought-Induced Saltwater Incursion Leads to Increased Wetland Nitrogen Export. *Glob. Chang. Biol.* **2013**, *19*, 2976–2985. [CrossRef]
49. Æsøy, A.; Ødegaard, H.; Bentzen, G. The Effect of Sulphide and Organic Matter on the Nitrification Activity in a Biofilm Process. *Water Sci. Technol.* **1998**, *37*, 115–122. [CrossRef]
50. Joye, S.B.; Hollibaugh, J.T. Influence of Sulfide Inhibition of Nitrification on Nitrogen Regeneration in Sediments. *Science* **1995**, *270*, 623–625. [CrossRef]
51. Lisa, J.A.; Song, B.; Tobias, C.R.; Hines, D.E. Genetic and Biogeochemical Investigation of Sedimentary Nitrogen Cycling Communities Responding to Tidal and Seasonal Dynamics in Cape Fear River Estuary. *Estuar. Coast. Shelf Sci.* **2015**, *167*, A313–A323. [CrossRef]
52. Kraft, B.; Tegetmeyer, H.E.; Sharma, R.; Klotz, M.G.; Ferdelman, T.G.; Hettich, R.L.; Geelhoed, J.S.; Strous, M. The Environmental Controls That Govern the End Product of Bacterial Nitrate Respiration. *Science* **2014**, *345*, 676–679. [CrossRef] [PubMed]
53. King, D.; Nedwell, D.B. The Influence of Nitrate Concentration upon the End-Products of Nitrate Dissimilation by Bacteria in Anaerobic Salt Marsh Sediment. *FEMS Microbiol. Lett.* **1985**, *31*, 23–28. [CrossRef]
54. An, S.; Gardner, W. Dissimilatory Nitrate Reduction to Ammonium (DNRA) as a Nitrogen Link, versus Denitrification as a Sink in a Shallow Estuary (Laguna Madre/Baffin Bay, Texas). *Mar. Ecol. Prog. Ser.* **2002**, *237*, 41–50. [CrossRef]
55. Magri, M.; Benelli, S.; Castaldelli, G.; Bartoli, M. The Seasonal Response of in Situ Denitrification and DNRA Rates to Increasing Nitrate Availability. *Estuar. Coast. Shelf Sci.* **2022**, *271*, 107856. [CrossRef]
56. Koop-Jakobsen, K.; Giblin, A.E. The Effect of Increased Nitrate Loading on Nitrate Reduction via Denitrification and DNRA in Salt Marsh Sediments. *Limnol. Oceanogr.* **2010**, *55*, 789–802. [CrossRef]
57. Nizzoli, D.; Carraro, E.; Nigro, V.; Viaroli, P. Effect of Organic Enrichment and Thermal Regime on Denitrification and Dissimilatory Nitrate Reduction to Ammonium (DNRA) in Hypolimnetic Sediments of Two Lowland Lakes. *Water Res.* **2010**, *44*, 2715–2724. [CrossRef]
58. Bonaglia, S.; Klawonn, I.; De Brabandere, L.; Deutsch, B.; Thamdrup, B.; Brüchert, V. Denitrification and DNRA at the Baltic Sea Oxic-Anoxic Interface: Substrate Spectrum and Kinetics: Denitrification and DNRA at the Oxic-Anoxic Interface. *Limnol. Oceanogr.* **2016**, *61*, 1900–1915. [CrossRef]
59. Broman, E.; Zilius, M.; Samuiloviene, A.; Vybernaite-Lubiene, I.; Politi, T.; Klawonn, I.; Voss, M.; Nascimento, F.J.A.; Bonaglia, S. Active DNRA and Denitrification in Oxic Hypereutrophic Waters. *Water Res.* **2021**, *194*, 116954. [CrossRef]
60. Murphy, A.E.; Bulseco, A.N.; Ackerman, R.; Vineis, J.H.; Bowen, J.L. Sulphide Addition Favours Respiratory Ammonification (DNRA) over Complete Denitrification and Alters the Active Microbial Community in Salt Marsh Sediments. *Environ. Microbiol* **2020**, *22*, 2124–2139. [CrossRef]
61. Po River Basin District Authority. *Monthly Bullettin of the Permanent Observatory on Water Uses in the Po River District (August 2022)*; Autorità di Bacino Distrettuale del Fiume Po: Parma, Italy, 2022.